Regulation and function of the mitochondrial protease HtrA2 / Omi in the control of cell death

Kristina Klupsch

A thesis submitted toward the degree of

Doctor of Philosophy

February 2007

CANCER RESEARCH UK

Signal Transduction Laboratory,
Cancer Research UK – London Research Institute,
44 Lincoln's Inn Fields, London.

UCL

Department of Biochemistry and Molecular Biology,
University College London,
Gower Street, London.

ProQuest LLC
789 East Eisenhower Parkway
P.O. Box 1346
Ann Arbor, MI 48106-1346

Declaration

I, Kristina Klupsch, confirm that the work presented in this thesis is my own. Where information has been derived from other sources, I confirm that this has been indicated in the thesis.

London, February 2007

Abstract

The serine protease HtrA2 is released from mitochondria following apoptotic stimuli. Once in the cytosol, HtrA2 has been implicated in promoting cell death by a caspase-dependent and –independent mechanism. However, mice lacking expression of HtrA2 show no evidence of reduced rates of cell death. On the contrary, loss of HtrA2 causes mitochondrial dysfunction leading to a neurodegenerative disorder with parkinsonian features. This suggests that the protease function of HtrA2 in the mitochondria, and not its pro-apoptotic action in the cytosol, is critical. Mammalian HtrA2 is therefore likely to function *in vivo* in a manner similar to its bacterial homologues, which are involved in protection against cell stress.

The bacterial DegS homologue senses unfolded proteins, activating a proteolytic cascade leading to induction of stress response genes. Transcriptional profiling of wild type and HtrA2 knockout (KO) cells identified the stress-inducible transcription factor CHOP being differentially regulated when mitochondrial stress was triggered. CHOP up-regulation was found in HtrA2 KO mouse brains but not in other tissues. Transcriptional profiling of brain tissue revealed a number of putative ATF4 target genes being up-regulated in HtrA2 KO, among these CHOP. Promoter analysis identified a C/EBP-ATF composite site in the majority of the genes within this signature. Therefore, loss of HtrA2 might impact on nuclear gene expression specifically in brain, subverting normal cellular homeostasis leading to disease.

In humans, point mutations in HtrA2 are a susceptibility factor for Parkinson's disease (PD) resulting in partial loss of proteolytic activity. Affinity purification shows that the mitochondrial kinase PINK1 interacts with HtrA2. PINK1 mutations are associated with the PARK6 PD susceptibility locus. HtrA2 is phosphorylated in a PINK1-dependent manner at residues adjacent to positions found mutated in PD patients. Phosphorylation of HtrA2 and thereby modulation of its proteolytic activity seems necessary for the function of HtrA2 in the mitochondria contributing to increased resistance of cells to mitochondrial stress.

Acknowledgements

Firstly, I would like to thank my supervisor, Julian Downward, for giving me the opportunity to work in his laboratory, for his support, advice and patience and also for giving me the freedom to develop and explore my own ideas.

In particular, I would like to thank Miguel Martins for his invaluable advice, encouragement and enthusiasm that have helped and shaped the progress of this work. Very special thanks go to Helene Plun-Favreau for support and discussions, shared experiments, and a lot of fascination for the proteins at centre-stage of this thesis. I would also like to thank Dave Hancock for giving feed-back and providing an incomparable source of knowledge.

Thanks to all the other past and present members of the Signal Transduction Laboratory and beyond – Thomas, Barbara, Julie, Caro, Pat, Michy, Surbhi, Megan, Justin, Charlie, Michael, Tony, Patrick, Olivier, Sophie, Subham, Boon Tin, Oona and Almut – for scientific and social contributions which have made the past years very enjoyable.

I would like to thank the staff of the research services, especially Phil East and Simon Tomlinson in the Bioinformatics Group, Stuart Pepper and Yvonne Hey in the GeneChip Service, Derek Davies and Ayad Eddaoudi in the FACS Laboratory, and David Frith in the Protein Analysis Laboratory. In addition, I would like to thank Cancer Research UK for providing funding and an excellent research environment, and the Boehringer Ingelheim Fonds for building a great network with other students and for providing support as well as funding.

Special thanks go to the people who have enriched my time in London and all the friends everywhere else. Especially, I would like to thank Johannes for his steadfast support and patience, Sarah for being a great friend, and Angi for providing a warm welcome and a lot of enthusiasm for living in London.

Finally, I would like to thank my parents for their constant support and encouragement, helping me through difficult times, and making everything possible.

Table of Contents

List of Figures

List of Tables

Abbreviations

AARE	amino acid response element
AFU	arbitrary fluorescence unit
AIF	apoptosis-inducing factor
APP	amyloid β precursor protein
ATF	activating transcription factor
BH	Bcl-2 homology
BiP	also known as Grp78, glucose-regulated protein, 78kDa
BIR	baculovirus IAP repeat
bp	base pair
bZIP	basic leucine zipper
C/EBP	CCAAT/enhancer binding protein
CARD	caspase recruitment domain
CBP	calmodulin binding protein
cDNA	complementary DNA
CHOP	C/EBP homologous protein
CRE	cAMP response element
cRNA	complementary RNA
C-terminal	carboxy-terminal
DA	dopamine
DAT	dopamine transporter
DCS	donor calf serum
DED	death effector domain
DMEM	Dulbecco's modified Eagle medium
DTT	dithiothreitol
eIF2α	eukaryotic translation initiation factor 2α
ER	endoplasmic reticulum
ERSE	ER stress response element
ES cell	embryonic stem cell
FACS	fluorescence activated cell sorting
FBS	foetal bovine serum
FDR	false discovery rate
F12	Ham's nutrient mixture

GCN2	general control non-derepressible-2
GFAP	glial fibrillary acidic protein
Grp94	glucose-regulated protein, 94kDa
GSEA	gene set enrichment analysis
GSH	glutathione
H&E	haematoxylin-eosin
Het	heterozygous
HisRS	histidyl-tRNA synthetase
HRI	haem-regulated inhibitor
HRP	horseradish peroxidase
h / hrs	hour / hours
HtrA	high temperature requirement A
IAA	iodoacetamide
IAP	Inhibitor of Apoptosis
IBM	IAP-binding motif
IEF	isoelectric focussing
IGFBP	insulin growth factor binding domain
IRE1	inositol-requiring protein 1
IPTG	isopropyl-β-D-1-thiogalactopyranoside
kb	kilo base
kDa	kilo Dalton
KLH	keyhole limpet hemacyanin
KI	kazal-protease inhibitor
KO	knockout
MAP-2	microtubule-associated protein-2
MEF	mouse embryonic fibroblast
Mnd2	motor neuron degeneration 2
MPP+	1-methyl-4-phenylpyridinium
MPTP	1-methyl-4-phenyl-1,2,3,4-tetrahydropyridine
mtDNA	mitochondrial DNA
MTS	mitochondrial targeting sequence
MTT	3-[4,5-dimethylthiazol-2-yl]-2,5-diphenyl tetrazolium bromid
NAC	N-acetyl-L-cysteine

NRSE	nutrient-sensing response element
N-terminal	amino-terminal
o/n	over night
OMP	outer membrane porin
P	post-natal day
PARK	Parkinson's disease-locus
PCR	polymerase chain reaction
PD	Parkinson's disease
PDZ	protein/discs-large protein/zonula
PERK	PKR-like ER kinase
PGK-neo cassette	phosphoglycerate kinase (promoter)-neomycin cassette
P-HtrA2	phospho-S142 HtrA2
PI	propidium iodide
PINK1	PTEN-induced putative kinase 1
PKR	protein kinase RNA-activated
PS1	Presenilin 1
PVDF	polyvenylfluoridine
RING	really interesting new gene
RMA	robust multi-chip average
ROS	reactive oxygen species
RT	room temperature
RT qPCR	reverse transcriptase quantitative real-time PCR
S1P and S2P	site 1 and site 2 protease
SCN	severe congenital neutropenia
SDS-PAGE	sodium dodecyl sulfate polyacrylamide gel electrophoresis
SNpc	substantia nigra pars compacta
SS	signal sequence
SV40LT	SV40 large T antigen
TEM	transmission electron microscopy
TEV	tobacco etch virus
TF	transcription factor
TM	transmembrane domain
TSS	transcriptional start site

uORF	upstream open reading frame
UPR	unfolded protein response
UPS	ubiquitin proteasome system
UTR	untranslated region
WT	wild type
XBP-1	X-box binding protein 1
$\Delta\psi m$	mitochondrial membrane potential
2D DIGE	fluorescence 2D difference gel electrophoresis
4OH-Tx	4-hydroxy-tamoxifen
6-OHDA	6-hydroxydopamine

1 Chapter 1: Introduction

1.1 Apoptosis, programmed cell death

Programmed cell death, also known as apoptosis, is an essential mechanism in the removal of cells during development and in homeostasis of multi-cellular organisms in order to control cell number. During vertebrate life, most newly formed but unwanted lymphocytes in the thymus undergo apoptosis. Apoptosis also plays an important role in a variety of diseases, including cancer, autoimmune diseases and many neurodegenerative disorders.

The process of controlled killing by activation of an intracellular death programme was first described in 1972, when Kerr and co-workers observed that large numbers of cells die after hormone withdrawal from hormone-dependent tumours (Kerr et al. 1972). Cells undergoing apoptosis show characteristic morphological changes, including cell shrinkage, plasma membrane blebbing, DNA fragmentation and chromatin condensation which eventually result in disassembly of the cell into membrane-enclosed vesicles, termed apoptotic bodies. These are then recognised and eliminated by phagocytes or neighbouring cells without the release of intracellular components, thereby preventing an inflammatory response. At the cell surface phosphatidyl-serine is externalised, which promotes recognition of the apoptotic cell for phagocytosis (Homburg et al. 1995; Martin et al. 1995). In contrast, cells that die by an uncontrolled process, termed necrosis, swell and the organelles lose their integrity. The plasma membrane ruptures and the intracellular contents are released, which can elicit a damaging inflammatory response.

The first genetic evidence for apoptosis came from studies using *Caenorhabditis elegans*: during somatic development, apoptosis normally occurs in 131 cells resulting in an adult worm with 959 cells. This made *C. elegans* a model organism for studying the core components of the cell death machinery (for review (Meier et al. 2000)).

1.1.1 Caspases, central executioners of apoptosis

Studies in *C. elegans* led to the identification of genes required for apoptosis, the *ced* genes. One of them was called *ced-3* and loss-of-function mutations in *ced-3* resulted in

survival of all 131 doomed cells (Ellis and Horvitz 1986). CED-3 is the prototype of a family of cysteine proteases, termed caspases, with specificity for aspartic acid residues carboxy-terminal (C-terminal) to the cleavage site in their substrates (Yuan et al. 1993). Caspases are highly conserved throughout evolution. They are synthesised as enzymatically inert zymogens composed of three domains: an N-terminal pro-domain, a large domain containing the active site cysteine and a C-terminal small domain (for review (Earnshaw et al. 1999)). The pro-domain is separated from the large domain by an aspartate cleavage site. The large and the small domains are separated by a linker region harbouring one or two aspartate cleavage sites. Based on their structural and functional differences the apoptotic caspases can be divided into two groups. The first group comprises caspases with large pro-domains which are involved in the initiation of the apoptotic response and are therefore named initiator caspases. Two types of protein-protein interaction motifs have been identified in their pro-domains: capsase-8 and -10 each contain two death effector domains (DED), while caspase-2 and -9 contain caspase recruitment domains (CARD). These domains enable them to bind adaptor molecules containing similar domains, a process which is required for their activation. The second group of caspases comprises caspases with short pro-domains such as caspase-3 and -7. They are activated by the initiator caspases and are therefore termed effector caspases.

Caspases are ubiquitously expressed in most cells, however, as zymogens they exhibit low intrinsic enzymatic activity. Upon a pro-apoptotic stimulus, pro-caspases are activated by proteolytic cleavage either through an autocatalyic process or through other caspases. A first proteolytic cleavage in the linker region divides the pro-caspase into a large and a small caspase subunit and a second cleavage removes the N-terminal pro-domain. The active caspases are heterotetramers composed of two identical small and two identical large subunits with two active sites.

Currently, two major pathways are described by which different initiator pro-caspases can be activated. One is dependent on a cell surface stimulus and therefore termed the extrinsic pathway: the apoptotic signal is transduced through the binding of an extra-cellular death ligand to its death receptor, such as CD95, TRAIL-R1 or TRAIL-R2 (Ashkenazi and Dixit 1998). This results in the activation of pro-caspase-8, which is mediated by recruitment to the adaptor protein FADD (Figure 1-1A). The other major

pathway for pro-caspase activation occurs via intrinsic stimuli as a consequence of cellular stress such as irradiation, cytotoxic drugs, and growth factor withdrawal. This involves release of cytochrome c from mitochondria which is required for activation of the adaptor protein bound initiator caspase-9 (Figure 1-1B). Once initiator caspases are activated, they target and activate effector caspases such as caspase-3 and -7, thereby initiating a complex amplification cascade.

1.2 Cellular substrates of caspases

Once active, caspases can cleave a variety of intra-cellular substrates, including structural components, protein kinases and components of the DNA repair machinery. This results in inhibition of cellular survival pathways and destruction of cell structure and commitment to cell death (for review (Earnshaw et al. 1999)).

Another important feature of apoptosis is the disassembly of the nucleus. The inhibitor of the nuclease CAD (ICAD) is cleaved by caspase-3 (Liu et al. 1997), leading to activation of DNA fragmentation and nuclear chromatin condensation (Enari et al. 1998). Mediators of DNA repair, such as PARP, DNA-PKs and hsRAD51 are among the earliest proteins to be cleaved in the apoptotic cell, which prevents DNA repair allowing accumulation of fragmented DNA. Cleavage of major structural nuclear proteins, including the laminins, are essential for disassembling the nuclear structure required for nuclear shrinkage (Rao et al. 1996).

1.2.1 Formation of the apoptosome

Cytochrome c release from mitochondria into the cytosol plays a crucial role in the amplification of apoptotic signals. Cytochrome c is essential for the intrinsic initiation of a caspase cascade by causing formation of the apoptosome (for review (Green and Reed 1998; Desagher and Martinou 2000)). Normally, cytochrome c is located in the mitochondrial intermembrane space, where it serves an essential function in the respiratory chain. During apoptosis, cytochrome c release from the mitochondria leads to oligomerisation with the adaptor protein Apaf-1. In the presence of ATP, this leads to conformational changes, which unmask the CARD domain of Apaf-1. Via CARD-CARD interaction, pro-caspase-9 is recruited into this protein complex (Li et al. 1997), forming the apoptosome (Cain et al. 1999). Aggregation of pro-caspase-9 facilitates its

autoactivation, which then leads to activation of downstream caspases, such as effector caspase-3 and -7. In the absence of an apoptosis signal, the CARD of Apaf-1 is not exposed and therefore unable to bind to pro-caspase-9.

Besides cytochrome c, other proteins are released from the mitochondria during apoptosis. Smac and HtrA2 are released from the intermembrane space, and their function will be discussed later. Apoptosis-inducing factor (AIF) and endonuclease G are released after a cell has committed to die and their release is dependent on post-mitochondrial caspase activity (Arnoult et al. 2003). AIF was initially described as a pro-apoptotic protein to function as a protease and flavoprotein (Susin et al. 1996; Susin et al. 1999), however, mice deficient for AIF die during embryogenesis without an over-abundance of cells (Joza et al. 2001), and mice hypomorph for AIF are more sensitive to induction of apoptosis rather than showing increased resistance (Klein et al. 2002). Endonuclease G mediates nucleosomal DNA fragmentation during apoptosis (Li et al. 2001).

1.2.2 Bcl-2 proteins

There is a large body of evidence that release of mitochondrial proteins is controlled by members of the Bcl-2 family. Over time, a large number of Bcl-2 family members have been identified, which can be divided into three groups based on structural and functional differences. Members of group I, such as Bcl-2 and Bcl-XL are anti-apoptotic. They contain four short conserved Bcl-2 homology (BH) domains and a C-terminal hydrophobic sequence, which localises the proteins predominantly to the outer surface of the mitochondria, but also to the endoplasmic reticulum (ER) membrane and outer nuclear membrane (Krajewski et al. 1993; Akao et al. 1994). In contrast, members of group II and III have pro-apoptotic activity (for review (Adams and Cory 1998)). Members of group II, including Bax and Bak, are similar in structure to Bcl-2 and Bcl-XL. They also contain the C-terminal hydrophobic tail, but only three BH domains. Group III consists of a large and diverse group of proteins including Bid, Bad and Bim, whose only common feature is the presence of a BH3 domain. These BH3-only proteins are essential initiators of apoptosis (Huang and Strasser 2000).

Pro-apoptotic Bcl-2 members were found to localise to the cytosol or cytoskeleton prior to a death signal. Upon an apoptotic stimulus they are activated and translocate to the

mitochondria, where they can dimerise with and neutralise Bcl-2 or Bcl-XL and induce cytochrome c release (for review (Desagher and Martinou 2000)). The principal mechanism by which Bcl-2 family proteins regulate apoptosis is by controlling cytochrome c release from the mitochondria. Once the apoptotic process gets past the mitochondria, Bcl-2 and Bcl-XL have no protective effect (Moriishi et al. 1999).

1.2.3 Inhibitor of Apoptosis proteins

Inhibitor of Apoptosis (IAP) proteins were first discovered in baculovirus through their ability to inhibit apoptosis of insect cells upon viral infection (Clem et al. 1991; Bump et al. 1995; Uren et al. 1998). They were found to suppress caspase activation and apoptosis induced by a variety of stimuli, including TNF, CD95L/FasL, staurosporine, etoposide and growth factor withdrawal (for review (Salvesen and Duckett 2002)). The human members of the IAP family, X-linked IAP (XIAP), cIAP1, cIAP2, neuronal IAP (NIAP), ILP2, ML-IAP, Survivin and Bruce contain one to three BIR (baculovirus IAP-repeat) motifs. Some IAP members also contain additional protein-protein interaction domains, such as a RING and a CARD domain. IAPs appear to inhibit apoptosis through direct interaction with caspases. XIAP, which is the most potent inhibitor, can specifically bind and inhibit caspase-3, -7 and -9 *in vitro*, thereby blocking the apoptotic process (Deveraux et al. 1997; Deveraux et al. 1998). The RING domain, which recruits E2 ubiquitin-conjugating enzymes, mediates ubiquitylation and destruction of IAP interacting proteins as well as IAPs themselves by the 26S proteasome (Yang et al. 2000).

On activation, caspases are proteolytically processed between their large and small subunits as a result of either autocatalytic processing following dimerisation or the activity of upstream proteases. For caspase-3, -7 and -9, the newly generated N-terminus of the small subunit constitutes an IAP-binding motif (IBM) which is characterised by an alanine at position P1. The IBM is then bound by the IBM-interaction grove in the BIR2 (caspase-3, -7) or BIR3 (caspase-9) domain of XIAP. In addition, a peptide strand preceding the BIR2 domain stretches across the catalytic cleft of caspase-3 and -7, leading to tight inhibition of their catalytic activity (Sun et al. 1999). In addition to interaction of the IBM of caspase-9 with the BIR3 domain of XIAP, a helix immediately after the BIR3 domain binds to the dimer interface of the

caspase, thereby preventing it from dimerising and becoming catalytically active (Sun et al. 2000; Shiozaki et al. 2003). Intriguingly, those elements of XIAP required for caspase inhibition are not conserved among other mammalian IAPs (for review (Eckelman et al. 2006)). Therefore, it seems that XIAP is the only mammalian IAP that directly inhibits caspase activity, and the mechanism by which the other mammalian IAPs attenuate apoptosis is less clear.

1.2.4 IAP antagonists

In *D. melanogaster*, the cytoplasmic IAP antagonists Reaper, Grim, HID, Sickle and Jafrac2 promote apoptosis by interacting with the BIR domains of IAPs through their N-terminal IBMs, thereby excluding active caspases from these complexes (Abrams 1999; Goyal et al. 2000; Christich et al. 2002; Srinivasula et al. 2002; Tenev et al. 2002; Wing et al. 2002). Initially, two mammalian proteins with N-terminal IBMs have been identified: Smac (also known as DIABLO) (Du et al. 2000; Verhagen et al. 2000; Ekert et al. 2001) and HtrA2 (also known as Omi) (Suzuki et al. 2001; Hegde et al. 2002; Martins et al. 2002; van Loo et al. 2002; Verhagen et al. 2002). They appear to be able to act through a mechanism similar to the Reaper family proteins in flies by interacting with the BIR domains of mammalian IAPs through their N-terminal IBMs. Concomitantly, other proteins were identified to contain IBMs and many are able to antagonise XIAP inhibition of caspase-3 *in vitro* (Hegde et al. 2003; Verhagen et al. 2007). In mammalian cells, apoptotic stimuli result in the release of Smac and HtrA2 from the mitochondrial intermembrane space into the cytosol, along with other apoptosis regulatory molecules such as cytochrome c, AIF and endonuclease G (van Loo et al. 2002). Since IAPs are localised in the cytosol, the release of Smac and HtrA2 will result in displacement of IAPs from caspases and loss of their suppressive effect on caspase activity.

1.2.5 Identification of HtrA2 as a Reaper-related protein

HtrA2 is synthesised as a 49kD precursor containing a mitochondrial targeting sequence at its N-terminus (amino acids 1-31), which gets cleaved off upon translocation into the mitochondrial matrix. Further, HtrA2 possesses a central serine protease domain (amino acids 166-342) and a C-terminal PDZ binding domain (amino acids 364-445) (Figure 1-2A). Following import into mitochondria, HtrA2 is anchored

into the inner mitochondrial membrane through an N-terminal transmembrane domain. In addition, this enzyme also exists in the intermembrane space of mitochondria as a more abundant non-anchored form that results from cleavage C-terminal of the transmembrane domain. Processing of HtrA2 was thought to occur through autoproteolytic cleavage, and *in vitro* HtrA2 can process itself (Seong et al. 2004). However, mice with proteolytically inactive HtrA2 show that the mutant HtrA2 was correctly processed into the mature form *in vivo* (Jones et al. 2003), suggesting that processing of HtrA2 into the mature form is probably catalysed by other mitochondrial proteases. The 36kD mature HtrA2 (amino acids 134-458) exposes an IBM at the newly generated N-terminus, and gets released into the cytosol following an apoptotic stimulus.

HtrA2 was the second mitochondrial protein identified to bind to XIAP (Suzuki et al. 2001; Hegde et al. 2002; Martins et al. 2002; van Loo et al. 2002; Verhagen et al. 2002). Binding of HtrA2 to IAPs suppresses their inhibitory activity towards caspases. This binding results in the increase of the proteolytic activity of HtrA2 (Martins et al. 2003) and has also been reported to cause proteolytic degradation of bound IAPs (Srinivasula et al. 2003; Yang et al. 2003). HtrA2 has therefore been proposed to be a pro-apoptotic protein analogous to the Reaper family proteins that removes the protective effect of IAPs and thus potentiates the ability of cytochrome c to trigger caspase activation (Martins et al. 2002; van Loo et al. 2002; Wolf and Green 2002; van Gurp et al. 2003). To achieve a complete antagonism of XIAP-mediated survival by HtrA2, both its IBM and its protease activity were required, as mutations at either the N-terminal alanine of the IBM (A134) or the catalytic serine (S306) reduced its potency to promote cell death (Verhagen et al. 2002). Interaction of the N-terminus of mature HtrA2 with the BIR2 and BIR3 domains of XIAP is responsible for the caspase-dependent death induced by HtrA2. Mutation of alanine 134 to glycine in HtrA2 abolishes the IBM and prevents interaction with XIAP causing cell death that is independent of caspase activation (Verhagen et al. 2002), therefore mediating cell death through its own serine protease activity (Suzuki et al. 2001; Hegde et al. 2002).

At the commencement of this work, mice with deleted HtrA2 genes had just been generated. These mice showed a severe phenotype and died early during development. Although the severity of the phenotype of the HtrA2 deficient mice suggested a crucial

role for this protease, it was unclear if this was due to an apoptotic defect or an essential role for HtrA2 in the mitochondria of healthy cells. In contrast, deletion of the other mammalian Reaper homologue Smac in mice has no detectable effect other than relatively slow activation of caspase-3 *in vitro* (Okada et al. 2002). Little else is known about the function of Smac and close homologues have not been characterised in non-mammalian species. Similarly, mice deleted for the broadly expressed IAP family member XIAP show no abnormal phenotype (Harlin et al. 2001). It is possible that IAPs and their antagonists play relatively minor roles in the regulation of apoptosis in mammals, unlike in flies. Alternatively, the high degree of redundancy amongst IAPs, and possibly also IBM-containing proteins, may make their *in vivo* function hard to analyse by single gene deletion experiments.

1.3 HtrA2 belongs to the HtrA family of serine proteases

HtrA2 belongs to the HtrA family of serine proteases, which is conserved across eukaryotic and prokaryotic species (Clausen et al. 2002). Initially, mammalian HtrA2 was identified as a homologue of the *Escherichia coli* protein HtrA (also known as DegP), and was reported to be up-regulated in conditions of cellular stress such as ischemia-reperfusion, heat shock, and ER stress (Faccio et al. 2000; Gray et al. 2000). However, whereas bacterial DegP protease possesses two PDZ (protein/discs-large protein/zonula) domains and forms a hexamer (Krojer et al. 2002), bacterial DegS protease is structurally closer to mammalian HtrA2 in that it has a similar domain structure with only one PDZ domain and forms a trimer (Li et al. 2002; Wilken et al. 2004) (Figure 1-2B and Figure 1-3B, C and D).

HtrA2 is the only member of the family of four mammalian HtrA proteases that has been found in the mitochondria and the only one that has been shown to be processed to reveal a Reaper-like N-terminal IBM. HtrA1 and HtrA3 are reported to be secreted from cells (Hu et al. 1998; Nie et al. 2003; Tocharus et al. 2004), the same seems to be the case for HtrA4. Neither of those three possesses a TM domain, but instead their sequences are characterised through a signal sequence (SS) found at the N-terminus, followed by an insulin growth factor binding domain (IGFBP) and a kazal-protease inhibitor (KI) domain (Figure 1-2B).

1.3.1 HtrA2 structure and regulation of its protease activity

The crystal structure of mature HtrA2 revealed a trimeric structure mediated exclusively by the serine protease domains. In addition, mutational analysis demonstrated that monomeric HtrA2 mutants are unable to induce cell death and are deficient in protease activity (Li et al. 2002). In the crystal structure, the PDZ domains are oriented inwards and cover the catalytic centre of the protease (Figure 1-3A and B). The peptide-binding pocket of the PDZ domain is buried in the intimate interface between the PDZ and the protease domains. Interestingly, the topology of the PDZ domain of HtrA2 exhibits a circular permutation, which has been observed only in bacterially derived PDZ-like sequences (Liao et al. 2000). Thus, the evolutionary conservation is manifested in both primary sequence and three-dimensional fold. The N-terminal IBM is flexible in solution and disordered in the HtrA2 crystals (Figure 1-3A). However, in contrast to Smac, the N-termini of the three HtrA2 monomers are close to each other (Figure 1-3B), potentially having an adverse effect on IAP binding.

Peptide library screening determined the primary sequence specificity for HtrA2 proteolytic activity, indicating that the protease favours cleavage following aliphatic residues (Martins et al. 2003), similar to its bacterial homologues DegP (Jones et al. 2002) and DegS (Walsh et al. 2003). Secondary preferences of HtrA2 include basic residues at the P2 and P3 positions as well as small residues at P1' and aromatic residues at P2'. The optimal cleavage peptide was determined as IRRV-SYSF, this substrate can be used *in vitro* to monitor HtrA2 activity (Martins et al. 2003). It is likely that this specificity at least partly determines the choice of sites selected by HtrA2 within a target protein. However, the selection of target proteins may also be dependent on which proteins are bound by the PDZ domain of HtrA2 and thus brought into proximity with the activated protease domain. Binding selectivity of the PDZ domain of HtrA2 was shown to favour a C-terminal valine or isoleucine, preceded by three residues rich in tyrosine and phenylalanine or large aliphatic groups (Martins et al. 2003; Gupta et al. 2004).

Mutational studies demonstrated that the PDZ domain dampens the proteolytic and cytotoxic potential of HtrA2 (Li et al. 2002; Martins et al. 2003). Activation of HtrA2 protease activity can be accomplished through heat shock, interactions with the PDZ

domain, or binding of XIAP to its IBM (Figure 1-4) (Martins et al. 2003). All of these are thought to cause conformational changes leading to opening of the PDZ domain and enabling access to the catalytic centre. Interestingly, the proteolytic activity of DegP is induced at elevated temperatures (Spiess et al. 1999), similarly HtrA2 activity is increased following transient heat shock. Peptides binding to the PDZ domains of DegS and DegP were also characterised to activate their proteolytic activity (Jones et al. 2002; Walsh et al. 2003).

1.3.2 *E. coli* DegP can function as a chaperone or protease

DegP is an essential protein in the *E. coli* periplasm and it is necessary for oxidative, thermo, and osmotic tolerance. DegP protects cells by degrading damaged or denatured proteins generated during heat or chemical stress (Pallen and Wren 1997). Such damaged proteins would otherwise form aggregates that are highly toxic to cells. DegP homologues in a number of pathogenic bacteria have been shown to be virulence factors, helping bacteria survive within the host cell in part by degrading periplasmic proteins damaged by the host's oxidative defence system (Pedersen et al. 2001). Several years ago, an unusual property of *E. coli* DegP was reported. It appears that the enzyme acts to chaperone unfolded proteins, possibly contributing to their re-folding, and degrades them only at high temperatures, when the amount of unfolded proteins in the cell is greatly increased (Spiess et al. 1999). Therefore, DegP exhibits chaperone function at normal temperature and protease function at high temperature.

In contrast to mammalian HtrA2, bacterial DegP protease possesses two PDZ domains and does not contain a transmembrane domain (TM) (Figure 1-2B). Whereas HtrA2 is active as a trimer, DegP forms a hexameric structure (Figure 1-3B and D). Another striking difference between HtrA2 and DegP in the environments of their active sites emerged from the crystal structures. The proteolytic domains are typical of trypsin-like proteases with a classical aspartate-histidine-serine catalytic triad located in a crevice between two β-barrel lobes. In HtrA2, the proteolytic active sites are in an active conformation poised for catalysis (Li et al. 2002). In contrast, in the inactive conformation, the catalytic centre of DegP is sterically blocked by a trio of loops from the surrounding protein, and the catalytic triad is distorted away from an active configuration (Krojer et al. 2002). Once DegP is active as a protease, it cleaves

substrates which are transiently or globally denatured. DegP exhibits preference for aliphatic amino acids at position P1 similar to mammalian HtrA2, however in contrast to HtrA2, DegP does not show preference for any specific amino acid at the P1' position of its substrate (Kolmar et al. 1996).

1.3.3 *E. coli* DegS is involved in the periplasmic stress response

Interestingly, another bacterial member of the HtrA family of serine proteases, DegS, acts as sensor for unfolded proteins in the periplasm (Walsh et al. 2003). DegS, like mammalian HtrA2, possesses only one PDZ domain (Figure 1-2B), and it is anchored into the inner bacterial cell membrane facing the periplasmic space (Figure 1-5). Unfolded proteins activate DegS by binding to its PDZ domain, thereby relieving its inhibitory effect. Activated DegS initially cleaves the anti-sigma factor RseA, an inner membrane protein that, together with RseB, sequesters the transcriptional regulator σ^E at the cytoplasmic face of the inner membrane. The first cleavage of RseA through DegS allows a second cleavage by the membrane-embedded metalloprotease RseP (also known as YaeL) (Alba et al. 2002; Kanehara et al. 2002). This releases the transcriptional regulator σ^E from its sequestering complex with the cytosolic domain of RseA, thereby allowing σ^E to associate with the core RNA polymerase, enabling transcription of genes encoding periplasmic chaperones, folding catalysts, proteases and proteins involved in cell wall biogenesis (Figure 1-5). Interestingly, DegP is among the genes induced through σ^E-mediated transcription (Erickson and Gross 1989). In this envelope stress response the activation of DegS is the first decisive step in the proteolytic cascade, and is tightly controlled by the association of unassembled outer membrane porins (OMPs) via a conserved YXF motif located at their C-termini (Walsh et al. 2003). Crystal structures of OMPs show that in the fully assembled state this motif is buried and therefore cannot bind to DegS. Thus, the exposure of the YXF motif of OMPs signals folding stress, leading to activation of DegS and up-regulation of the downstream envelope stress response genes.

DegS crystallised as a trimer, where the protease domains form the core and the PDZ domains protrude outwards, creating a funnel-like arrangement (Wilken et al. 2004). In this structure, the active sites of the protease domains are not blocked by the PDZ domains. However, structural alignments to several serine proteases indicate that the

catalytic site of DegS in this crystal is in an inactive state. An active conformation was obtained when the crystals were soaked with an activating peptide resembling the C-terminus of OMPs (Figure 1-3C). The peptide was bound in a pocket of the PDZ domain close to the interface with the protease domain. Association of the activator peptide results in several important conformational changes in the protease domain. Most noticeably, the flexible loop L3, protruding from the protease domain was displaced from its previous location in the inactive form and was stabilised by a contact to the OMP peptide. Upon peptide association, several residues in the active site involved in substrate binding and catalysis, previously blocked or distorted in inactive DegS, become accessible for substrate binding and correctly aligned for catalysis (Wilken et al. 2004).

Structural comparison of DegS and HtrA2 clearly indicates that the active site of HtrA2 is present in a non-functional state. There is no oxyanion hole and most likely no proper catalytic triad. Consistently, some active site loops of HtrA2 align better to the inactive than to the active form of DegS. Since the position of the PDZ domain in the HtrA2 crystal structure was strongly influenced by crystal packing constraints (Li et al. 2002), in solution, the PDZ domain of HtrA2 might function similarly as in DegS, trapping the flexible loop L3. Upon a proper stimulus, the PDZ domain might reorient, thereby releasing L3, which in turn triggers adjustment of the activation domain yielding a functional active site. In the PDZ deletion mutant of HtrA2, which exhibited increased proteolytic activity (Li et al. 2002; Martins et al. 2003), loop L3 probably cannot be fixed in the domain interface and thus activates the protease.

Activation of DegP should require larger conformational changes than in DegS and HtrA2. In its chaperone conformation, the DegP protease was observed in a completely inactive state and the active site loops L1 and L2 are severely distorted and attain different conformations. For example the turn structure of loop L1 that sets up the oxyanion hole is pre-formed in DegS and HtrA2, while it is entirely absent in DegP. However, similar to DegS and HtrA2, DegP can be allosterically activated by specific peptides that bind to its PDZ domains (Jones et al. 2002) and has a flexible loop L3 that is wedged between protease and PDZ domains (Krojer et al. 2002; Kim et al. 2003).

Taken together, the known protective stress response activities of the bacterial HtrA2 homologues, DegP and DegS, thus appear to be very different from the proposed pro-apoptotic, Reaper-like action of mammalian HtrA2. Whether HtrA2 exerts a similar function in mammals is unclear, however, the high level of similarity between the bacterial proteases and mammalian HtrA2 may suggest that they do indeed share similar functions.

1.4 Proteins binding to and cleaved by HtrA2

Since HtrA2 was discovered in 2000 (Faccio et al. 2000; Gray et al. 2000), several binding partners and substrates for its proteolytic activity have been reported. First of all, HtrA2 was reported to bind to XIAP and mediate its proteolytic degradation (Suzuki et al. 2001; Hegde et al. 2002; Martins et al. 2002; van Loo et al. 2002; Verhagen et al. 2002; Srinivasula et al. 2003; Yang et al. 2003).

Amyloid β, a principle component of the cerebral plaques found in the brains of patients with Alzheimer's disease, was found to bind to the C-terminal region containing the PDZ domain of HtrA2 by yeast two-hybrid assay (Park et al. 2004), however, the production or degradation of Amyloid β was not directly altered by HtrA2 (Liu et al. 2005). Subsequently, HtrA2 was shown to bind to the amyloid β precursor protein (APP), which partially localises to mitochondria. APP was cleaved *in vitro* and *in vivo* by HtrA2, resulting in the C161 fragment of APP (amino acids 535-695) (Park et al. 2006). Presenilins are important determinants of γ-secretase activity responsible for proteolytic cleavage of APP. The C-terminal tail of Presenilin 1 (PS1) was reported to bind to the PDZ domain of HtrA2 and increase its proteolytic activity, and it was suggested that PS1 may regulate HtrA2 proteolytic activity after its release from the mitochondria during apoptosis (Gupta et al. 2004).

The anti-apoptotic protein ped/pea-15 was shown to interact with HtrA2 during apoptosis when HtrA2 was released into the cytosol. HtrA2 was implied in degradation of ped/pea-15 during apoptosis, and this degradation could be inhibited by the HtrA2 inhibitor Ucf-101 (Cilenti et al. 2003; Trencia et al. 2004).

Bruce, a giant IAP, was reported to interact with HtrA2. Bruce ubiquitylated and facilitated proteasomal degradation of HtrA2, conversely, HtrA2 was capable of cleaving Bruce (Sekine et al. 2005).

WARTS, a tumour suppressor and mitotic regulator was shown to bind to HtrA2's PDZ domain, enhancing its proteolytic activity (Kuninaka et al. 2005). Subsequently, WARTS was identified to be a substrate for HtrA2 potentially leading to inhibition of G1/S phase progression (Kuninaka et al. 2006).

Peroxiredoxin 1 (Prdx1, also known as Pag) is a cytosolic protein involved in the redox regulation of the cell. During oxidative stress Prdx1 expression is induced, which causes apoptosis. Prdx1 was shown to bind to the PDZ domain of HtrA2 once released from the mitochondria and thereby modulate the proteolytic activity of HtrA2 (Hong et al. 2006). All of the proteins interacting with or cleaved by HtrA2 discussed so far are cytosolic proteins or, in the case of APP and PS1, proteins mainly localised to cellular membranes such as plasma, ER, and perinuclear membranes. Only during apoptosis, when HtrA2 is released from the mitochondria, can an interaction between these proteins and HtrA2 take place, suggesting that the increase in HtrA2 proteolytic activity mediated by binding to its PDZ domain or the degradation of some of these proteins might be necessary for apoptosis.

Interestingly, one mitochondrial protein, HAX-1, was shown to interact with HtrA2, and this interaction involved both the PDZ and the catalytic domain of HtrA2 (Cilenti et al. 2004). HAX-1 has been reported to be an anti-apoptotic protein (Suzuki et al. 1997; Sharp et al. 2002), and its protein levels decreased when cells where stimulated with an apoptotic trigger (Cilenti et al. 2004). Degradation of HAX-1 could be prevented with the HtrA2-specific inhibitor Ucf-101 (Cilenti et al. 2004). However, the specificity of this inhibitor was thrown into doubt recently (Klupsch and Downward 2006), suggesting that HtrA2 possibly interacts with HAX-1, but HtrA2 probably does not degrade it. Nevertheless, HAX-1 to date is the only mitochondrial protein shown to bind to HtrA2. Recently, mutations in the HAX-1 gene were identified to cause autosomal recessive severe congenital neutropenia (SCN) (Klein et al. 2007), a primary immunodeficiency syndrome associated with increased apoptosis in myeloid cells.

1.5 Cellular stress pathways

Eukaryotic cells recognise and process diverse stress signals to elicit programmes of gene expression that are designed to remediate cellular damage, or alternatively induce apoptosis. In the following sub-chapters, an overview about cellular stress pathways is given. This does naturally not comprise all stress pathways but a selection of pathways and molecules whose understanding is beneficial for readers of this thesis.

1.5.1 The unfolded protein response (UPR)

The accumulation of misfolded proteins in the ER activates a protective signalling cascade termed the unfolded protein response (UPR). Proximal transducers of the mammalian UPR, which include PERK (Shi et al. 1998; Harding et al. 1999), IRE1 (Tirasophon et al. 1998; Wang et al. 1998), and ATF6 (Haze et al. 1999), are all ER-localised transmembrane proteins (Figure 1-6A). Under non-stressed conditions, they are kept in an inactive monomeric state by binding to the ER chaperone BiP (also called Grp78). During ER stress, misfolded proteins accumulate in the ER, and BiP is dissociated from the luminal domains of these sensor proteins, leading to their activation (Bertolotti et al. 2000; Shen et al. 2002). For ATF6, dissociation from BiP allows its translocation to the Golgi, where its cytosolic domain encoding a transcription factor (TF), is cleaved by the site 1 (S1P) and site 2 (S2P) proteases (Ye et al. 2000). The liberated ATF6 then migrates to the nucleus, where it directly binds to and activates the consensus ER stress response element (ERSE) found in the promoters of various UPR targets including TFs XBP-1 and CHOP, and ER chaperones like BiP and Grp94 (Yoshida et al. 1998; Yoshida et al. 2000). For IRE1, dissociation from BiP leads to its dimerisation and activation of the cytosolic kinase domain, which in turn stimulates an endoribonuclease activity located at its C-terminus. Activated IRE1 recognises and cleaves two specific stem loop sequences in the XBP-1 mRNA, which are then ligated, resulting in a larger XBP-1 protein (spXBP-1) due to a resulting frameshift (Shen et al. 2001; Calfon et al. 2002). Spliced XBP-1 encodes a TF that binds and transactivates the same ERSE site *in vitro* as ATF6, however, not all ATF6 and XBP-1 targets are shared (Yoshida et al. 2003). In the case of PERK, BiP dissociation during UPR activation leads to oligomerisation and activation of its cytosolic kinase domain. Activated PERK phosphorylates eIF2α, leading to an immediate, yet transient protein synthesis inhibition (Harding et al. 2000). Unlike

ATF6 and IRE1 activation, which are specific to ER stress, the downstream consequences of PERK activation are shared with other cellular stress responses including amino acid deprivation, infection with double-stranded RNA viruses, haem deficiency and oxidative stress (Figure 1-6B) (reviewed in (Wek et al. 2006)). Therefore, the mammalian ER stress response can be divided into two main branches: one that is downstream of both ATF6 and IRE1/XBP-1 and is specific to ER stress, and another that is downstream of PERK and is shared by other cellular stresses that lead to phosphorylation of eIF2α.

1.5.2 eIF2α kinases and translational control

An important contributor to stress adaptation is a family of protein kinases that phosphorylate the α subunit of eIF2, which leads to general inhibition of protein synthesis. Yeast cells possess only one eIF2α kinase, whereas mammalian cells have four different kinases, namely PERK, PKR, HRI and GCN2, suggesting that the targets of these pathways are important in a generalised stress response. In mammals, each of the four eIF2α kinases contains unique regulatory regions that recognise a different set of stress conditions (Figure 1-6B). PERK activation by misfolded proteins in the ER reduces the load on the protein folding and degradation apparatus in the organelle (Harding et al. 1999). PKR activation by double-stranded RNA shuts down the host's protein synthesis machinery, interfering with viral infections (Clemens and Elia 1997). HRI is activated by haem deprivation, matching haemoglobin synthesis with iron availability (Chen and London 1995), as well as oxidative and heat stresses in erythroid tissues (Lu et al. 2001). In cells deprived of nutrients, activation of mammalian GCN2 conserves scarce amino acids for use in essential metabolic processes and is activated by elevated levels of uncharged tRNAs (Berlanga et al. 1999; Sood et al. 2000). Interestingly, GCN2 is also activated by other stresses that are not directly related to nutritional deprivation, including proteasome inhibition (Jiang and Wek 2005) and UV irradiation (Deng et al. 2002). Phosphorylation of eIF2α impedes recycling of eIF2α to its active GTP-bound form, and the accompanying reduction in the levels of eIF2α–GTP reduces global (cap-dependent) translation, allowing cells to conserve resources and to initiate a reconfiguration of gene expression to effectively manage stress conditions. This reduction in global protein synthesis is concomitant with induced translation of selected mRNAs, such as those encoding the bZIP (basic leucine zipper)

TF ATF4 (Harding et al. 2000). Enhanced ATF4 expression involves two uORFs (upstream open reading frames) located in the 5′-leader of the ATF4 mRNA that facilitate its translation in response to eIF2α phosphorylation. Elevated levels of ATF4 lead to induction of additional bZIP TFs, ATF3 (Jiang et al. 2004) and CHOP (Fawcett et al. 1999; Harding et al. 2000), which together induce a programme of gene expression important for cellular remediation and apoptosis. The phosphorylation of eIF2α and downstream events are shared with the UPR pathway (Figure 1-6A and B).

1.5.3 CHOP and Herp are regulated by the ER stress-specific as well as the shared branch of the UPR

CHOP (C/EBP homologous protein, also called Gadd153 or Ddit3) is a member of the C/EBP family of bZIP TFs that are critical for the regulation of various aspects of cellular differentiation and function in multiple tissues. CHOP is ubiquitously expressed at low levels in proliferating cells, but when cells are exposed to stressful stimuli the expression of CHOP is increased (for review (Oyadomari and Mori 2004)). CHOP has been implicated as a mediator of apoptosis in the contexts of both ER stress (Matsumoto et al. 1996; Zinszner et al. 1998; Kawahara et al. 2001; Maytin et al. 2001; Gotoh et al. 2002) and oxidative stress (Guyton et al. 1996; Mengesdorf et al. 2002). CHOP has a dual role in the regulation of cellular gene expression: as an inhibitor of the binding of C/EBP to classical C/EBP target genes (Ron and Habener 1992) and as an activator of genes that have CHOP-C/EBPβ-binding sites (Ubeda et al. 1996). Several genes downstream of CHOP, induced by ER stress (Wang et al. 1998; Sok et al. 1999) or mitochondrial stress (Zhao et al. 2002), have been identified to contain this CHOP-C/EBPβ-binding sequence. In addition, CHOP interacts with TFs of the AP-1 family such as JunD, c-Jun and c-Fos, and has been reported to activate transcription of their target genes (Ubeda et al. 1999).

CHOP is one of the UPR target genes that has been shown to be dually regulated by both the ER stress-specific and the shared branches of the UPR (Ma et al. 2002). The CHOP promoter contains both ERSEs and a C/EBP-ATF composite site, through which these two branches act, respectively. Deletion of either element from a CHOP promoter construct leads to a decrease in its transcriptional activity (Ma et al. 2002). TFs ATF6 and XBP-1 can bind to ERSEs *in vitro*, and ATF6 over-expression leads to

CHOP induction in cells (Yoshida et al. 2000). The TF ATF4 binds to the C/EBP-ATF composite site and stimulates CHOP expression in response to various cellular stress conditions (Fawcett et al. 1999; Ma et al. 2002).

Herp, an ER localised protein with an N-terminal ubiquitin-like domain is another UPR target that is, like CHOP, dually regulated by both the shared and the ER stress-specific branches of the UPR pathway (Ma and Hendershot 2004). ATF6 can transactivate the Herp gene through the ERSEI and II sites present in its promoter (Kokame et al. 2001). In addition, during both amino acid deprivation and ER stress, eIF2α phosphorylation causes ATF4 induction, which then directly binds to and transactivates the C/EBP-ATF composite site in the Herp promoter (Ma and Hendershot 2004). Therefore, although Herp is an ER localised protein, it can be induced by cellular stress conditions that are not thought to affect the ER.

The convergence of two signalling branches of the ER stress response upon a single target is a conserved feature of the UPR, which suggests there could be additional targets that are regulated this way. Since the activation of stress-specific eIF2α kinases and their common downstream target ATF4 is well-conserved among various cellular stress conditions, the ability of this pathway to transactivate the CHOP and Herp promoters ensures that these genes are also induced during other stresses that do not involve ATF6 cleavage, XBP-1 splicing, and ERSE activation (Figure 1-6B). These dually regulated targets are activated to a much higher level during ER stress than with other cytosolic stresses like hypoxia (Price and Calderwood 1992), amino acid deprivation (Marten et al. 1994), and oxidative stress (Harding et al. 2000).

1.5.4 ATF3 is induced by multiple stresses

The TF ATF3 has been reported to be induced by a variety of stresses (for review (Hai and Hartman 2001)). Up-reguation of ATF3 appears to correlate with cellular injury and probably leads to detrimental outcomes. The list of conditions that induce ATF3 is long: In animal experiments, the signals include ischemia, ischemia coupled with reperfusion, wounding, axotomy, toxicity, and seizure; in cultured cells, the signals include cytokines, genotoxic agents such as UV, activators of JNK signalling, microtubule binding agents, proteasome inhibitors, homocysteine, hydrogen peroxide,

ER stress, viral proteins, and nerve growth factor depletion.

The increase in ATF3 expression following amino acid deprivation or ER stress was demonstrated to occur by mechanisms requiring the eIF2α kinases GCN2 and PERK respectively (Jiang et al. 2004). The ATF3 promoter contains an ATF/CRE site and a C/EBP-ATF composite site (Liang et al. 1996; Wolfgang et al. 2000) and ATF4 was shown to bind to the latter in response to amino acid limitation (Pan et al. 2007), leading to the induction of ATF3. Its name is slightly misleading and reflects the history of discovery, because ATF3 is more homologous to the Fos proteins (members of the AP-1 family) (Meyer and Habener 1993) rather than to other members of the ATF family of TFs. Homodimers of ATF3 are transcriptional repressors, however, heterodimeric complexes of ATF3 with AP-1 family members have been demonstrated to function as transcriptional activators. CHOP, in addition to being a target gene of ATF3 (Wolfgang et al. 1997; Fawcett et al. 1999), also dimerises with ATF3 and induces transcription (Hai and Hartman 2001).

Taken together, the ER stress response and the stress pathways leading to activation of eIF2α kinases overlap partially through the activation of PERK during ER stress. Therefore, some of the genes induced by ER stress, like CHOP, Herp and ATF3, can also be induced by other stresses unrelated to ER stress (Figure 1-6B). In the case of CHOP and Herp, the ER stress-specific branch (ATF6, IRE1/XBP-1) as well as the shared branch (PERK-eIF2α/ATF4) can lead to their induction. ATF3 expression is not up-regulated by the ER stress-specific branch, however, ATF4 induction by eIF2α kinases is activating ATF3 expression. In addition, other stresses like oxidative stress and activation of p38 MAP kinase signalling modulate ATF3 expression (Lu et al. 2007), and some of these have also been implicated in the activation of CHOP, although their mechanism has not been studied extensively (Kultz et al. 1998). In addition, CHOP has been reported to be modulated through phosphorylation by p38 or casein kinase 2, leading to activation or inhibition of its transcriptional activity, respectively (Wang and Ron 1996; Ubeda and Habener 2003).

1.6 Parkinson's disease

Parkinson's disease (PD), first described by James Parkinson in 1817, is a chronically progressive neurodegenerative disease, affecting at least 1% of the population over the age of 65, rising to 4-5% over 85 years of age. The aetiology of this disease is likely due to combinations of environmental and genetic factors. The main clinical phenotype of PD is parkinsonism, a movement disorder that is characterised by resting tremor, rigidity, postural instability, bradykinesia (slowness of movement) and in extreme cases akinesia (absence of movement) (Fahn 2003). At the morphological and anatomical level, PD is characterised by degeneration of the neural connection between the substantia nigra (SN) and the striatum, two brain regions essential for normal motor function. The striatum receives its dopaminergic input from neurons of the substantia nigra pars compacta (SNpc) via this nigrostriatal pathway. Progressive degeneration of the nigrostriatal dopaminergic pathway results in profound striatal dopamine deficiency, leading to the described motor deficiencies. Often, PD affected brains show appearance of Lewy bodies (protein aggregates) within the surviving dopaminergic neurons. Initially, patients respond well to dopamine replacement therapy but treatment is effective for only a limited period and fails to halt disease progression.

1.6.1 Mitochondrial dysfunction in Parkinson's disease

Mitochondrial dysfunction has long been implicated in the pathogenesis of PD (Figure 1-8). Evidence first emerged following the accidental exposure of drug abusers to 1-methyl-4-phenyl-1,2,3,4-tetrahydropyridine (MPTP) – an environmental toxin that results in an acute and irreversible parkinsonian syndrome (Langston et al. 1983). The active metabolite of MPTP, the 1-methyl-4-phenylpyridinium ion (MPP+) is an inhibitor of complex I of the respiratory chain and a substrate for the dopamine transporter (DAT). It therefore accumulates in dopaminergic neurons, where it confers toxicity and neuronal death through complex I inhibition (Nicklas et al. 1985). This has many deleterious consequences, including increased oxidative stress and decreased ATP production, which causes increased intracellular calcium concentration, excitotoxicity and nitric oxide related cellular damage. Subsequently, administration of MPTP to mice was shown to lead to the development of parkinsonism (Sedelis et al. 2001). Crucially, a biochemical link between MPTP toxicity and idiopathic PD was established when complex I deficiency was reported in the SN, skeletal muscle and

platelets of patients with PD ((Schapira et al. 1989), for review (Orth and Schapira 2002)). In line with this, chronic administration of rotenone in rats can produce a progressive model of parkinsonism (Betarbet et al. 2000; Sherer et al. 2003). In contrast to MPTP, which accumulates selectively in dopaminergic neurons, chronic exposure to rotenone can produce mild but systemic complex I inhibition. When a degenerative lesion results, it is selective to the nigrostriatal system, indicative of the vulnerability of this neuronal population to oxidative stress. Furthermore, intracerebral administration of the neurotoxin 6-hydroxydopamine (6-OHDA) provides an acute animal model for PD (for review (Bove et al. 2005)). The neurotoxicity of 6-OHDA is believed to be related to production of reactive oxygen species (ROS) and inhibition of complex I activity, which probably induce destruction of SN neurons. In addition, mitochondrial involvement and dysfunction has also been reported in numerous studies on the genes associated with familial PD (see 1.6.3).

1.6.2 Activation of the UPR in Parkinson's disease models

Studies linking activation of the UPR and PD use neurotoxins to model the disease process both in cell culture and *in vivo* (Ryu et al. 2002; Holtz and O'Malley 2003; Silva et al. 2005). Compounds, such as 6-OHDA and MPTP or its active derivative, MPP+, induce oxidative stress and impair mitochondrial respiration and energy metabolism. Studies with cultured neuronal cells, including dopaminergic neurons, showed that these compounds trigger activation of the UPR and induce a number of genes. Gene profiling revealed that both ER chaperones and other components of the UPR such as the TF CHOP were up-regulated in exposed cells, in addition to the phosphorylation of the ER stress kinases, IRE1 and PERK, leading to increased ATF4 translation. These changes were specific for the two PD mimetics and also rotenone, a mitochondrial inhibitor that causes degeneration of dopaminergic neurons, but not with other agents (Ryu et al. 2002). However, there were some unexpected differences in the magnitude and pattern of gene responses induced by 6-OHDA and MPP+ (Holtz and O'Malley 2003). The transcriptional changes induced by MPP+ treatment were subtle compared to the strong response elicited by stimulation with 6-OHDA. Furthermore, 6-OHDA led to the induction of ER chaperones and other genes that are associated with the ER stress-specific branch of the UPR, but MPP+ did not. However, both, 6-OHDA and MPP+ caused transcriptional up-regulation of a set of genes that are induced

downstream of the shared branch of the UPR, as most of these genes were described previously to be induced in response to ER stress dependent on the presence of ATF4 (Figure 1-6B) (Harding et al. 2003). Experiments carried out using neuronal cultures from PERK gene deleted mice revealed an increased sensitivity of the cells against treatment with 6-OHDA (Ryu et al. 2002). This suggests that neurons lacking PERK were unable to mount a proper UPR and are more vulnerable to 6-OHDA. It also supports the notion that an early UPR response may be neuroprotective for the dopaminergic neurons, while sustained activation of the UPR leads to an up-regulation of gene products that induce cell death. Thus it seems to be the shared branch of the UPR that is central in the response to treatment with such neurotoxins. In addition, stresses leading to activation of eIF2α kinases other than ER stress might turn out to be important in the development of PD.

1.6.3 Genetic forms of Parkinson's disease

Genetic mutations identified in familial parkinsonism are relatively rare, accounting for only 5-10% of the overall PD population. However, identification of the genes associated with familial PD have recently provided new tools to implicate and understand the molecular pathways affected (Table 1-1). In the past decade, recessively inherited loss-of-function mutations in Parkin, DJ-1 and PINK1 were found to cause early-onset PD. In contrast, dominantly inherited, gain-of-function mutations in α-synuclein and LRRK2 result in more typical late-onset PD (for review (Farrer 2006)).

1.6.3.1 Parkin, an E3 ligase

Mutations in Parkin are thought to impair its E3 ubiquitin protein ligase activity and result in improper targeting of substrates for proteasomal degradation, and may lead to subsequent neurotoxic accumulation. A number of substrates have been reported including Pael, a rare glycosylated form of α-synuclein and a subunit of the aminoacyl-tRNA synthetase complex (for review (Farrer 2006)). Some studies have localised Parkin to the ER, where it has been shown to have a neuroprotective role against ER stress (Takahashi et al. 2003). In addition, Parkin might have a role in maintaining mitochondrial function. It has been localised to the outer mitochondrial membrane, and ubiquitylation can also mediate the insertion of proteins into the outer mitochondrial

membrane (Zhaung and McCauley 1989).

1.6.3.2 DJ-1, involved in oxidative stress protection

DJ-1 is a member of the ThiJ/PfpI family of molecular chaperones which are induced during oxidative stress. The protein exists predominantly as a dimer localised to mitochondria, and mutations are thought to cause PD via impaired oxidative stress protection (Bonifati et al. 2003; Zhang et al. 2005). In mammalian cells exposed to an oxidative stressor, such as H_2O_2, DJ-1 undergoes an acidic shift in pI by modifying its cysteine residues, which quench ROS and protect cells against stress-induced death. Ablation of DJ-1 function in mice leads to increased sensitivity to MPTP treatment (Kim et al. 2005).

1.6.3.3 PINK1, a mitochondrial kinase

PINK1 was originally identified to be transcriptionally up-regulated by the tumour suppressor PTEN in cancer cells, however, PINK1 has not been shown to exhibit any effects on PTEN-dependent cell phenotypes (Unoki and Nakamura 2001). In addition, it was reported that Pink1 mRNA is reduced in ovarian tumour samples from patients (Unoki and Nakamura 2001). Furthermore, PINK1 mRNA was found to be increased in tumour cell lines with high metastatic potential (Nakajima et al. 2003).

PINK1 encodes a ubiquitously expressed 581 amino acid protein, which consists of an N-terminal MTS, a highly conserved serine/threonine kinase domain and a C-terminal autoregulatory domain. Initially, three pedigrees were described with identified mutations: a G309D point substitution in one family and a truncation mutation (W437X) in two additional families (Valente et al. 2004). Subsequently, several studies have described other point mutations or truncations (Hatano et al. 2004; Rogaeva et al. 2004; Rohe et al. 2004; Bonifati et al. 2005; Li et al. 2005). The reported mutations do not show any obvious clustering within the gene, and most are distributed throughout the kinase domain with a subset located in the N-terminal region between the MTS and the kinase domain (Figure 1-7). As the kinase domain is the only functional domain in PINK1 and the site of most of the mutations, disruption of the kinase activity is the most probable disease mechanism. However, studies showing PINK1 kinase activity in *in vitro* autophosphorylation assays are relatively weak (Beilina et al. 2005; Silvestri et

al. 2005; Sim et al. 2006). Furthermore, these assays are too crude to distinguish any significant functional effects of the mutations on kinase activity. Some functional data has been obtained from indirect assays, which show that loss of PINK1 adversely affects mitochondrial function and cell viability under stress. Mitochondrial membrane potential $\Delta\psi m$ and levels of cell death were measured in a neuroblastoma cell line over-expressing G309D PINK1 after exposure to an exogenous source of cellular stress, MG-132, a proteasome inhibitor. Cells over-expressing G309D PINK1 had significantly reduced $\Delta\psi m$ compared with the wild type and increased levels of cell death following exposure to stress, but not under basal conditions. Moreover, cells over-expressing wild type PINK1 had higher $\Delta\psi m$ and lower levels of cell death than cells transfected with vector alone (Valente et al. 2004). Consistent with these results, over-expression of wild type PINK1 was subsequently shown to reduce the release of cytochrome c from mitochondria under basal conditions and staurosporine-induced stress. Significantly, two PINK1 mutations, E240K and L489P, were shown to abrogate the protective effect (Petit et al. 2005). Finally, the L347P mutation decreases the half-life of PINK1 from approximately 2hrs to 30min, which supports the idea that loss of PINK1 function might contribute to PD (Beilina et al. 2005).

In *Drosophila melanogaster*, loss of PINK1 leads to defects in mitochondrial function resulting in male sterility, apoptotic muscle degeneration and minor loss of dopamine neurons (Clark et al. 2006; Park et al. 2006; Yang et al. 2006). A similar phenotype has been characterised for Parkin loss-of-function mutants of *D. melanogaster* (Greene et al. 2003). Interestingly, over-expression of Parkin in PINK1 deficient flies rescues their phenotype, but over-expression of PINK1 in Parkin deficient flies does not (Clark et al. 2006; Park et al. 2006; Yang et al. 2006). Thus, PINK1 appears to function upstream of Parkin in a common pathway.

1.6.3.4 HtrA2, a mitochondrial protease

Recently, two point-mutations were identified in the coding sequence of HtrA2. A mutation of G399S located in the PDZ domain was found in four patients with sporadic PD, and a polymorphism at A141S close to the mature N-terminus of the protein was found at higher frequencies in patients with PD (Strauss et al. 2005). Both mutations are predicted to affect regulation of the proteolytic activity of HtrA2, thereby

modulating cell death. At the cellular level, the mutations have been demonstrated to increase susceptibility to stress, as shown by decreased mitochondrial membrane potential after exposure to staurosporine. Subsequently, the HtrA2 gene has been designated as the Parkinson's disease-13 (PARK13) locus.

1.6.3.5 ATP13A2, a lysosomal ATPase

ATP13A2 encodes for a P-type ATPase that transports cations and other substrates across membranes (Schultheis et al. 2004). Whereas the wild type protein is located in the lysosome of transiently transfected cells, the unstable truncated mutants were retained in the ER and degraded by the proteasome, potentially inducing ER stress (Ramirez et al. 2006).

1.6.3.6 UCHL1, a ubiquitin hydrolase

UCHL1 has been associated with familial PD, but the genetic evidence for its pathogenicity is weak as only a single mutation has been identified in one family (Leroy et al. 1998). UCHL1 functions as a ubiquitin hydrolase, recycling polymeric ubiquitin to its monomeric form.

1.6.3.7 α-synuclein, component of Lewy bodies

α-synuclein is a protein that is expressed throughout the brain and has potential roles in learning, synaptic plasticity, vesicle dynamics and dopamine synthesis (Lotharius and Brundin 2002; Sidhu et al. 2004). The gene encoding α-synuclein was the first gene to be linked to familial PD. Several multiplications and three missense mutations have been described to be dominantly inherited, gain-of-function mutations (for review (Farrer 2006)). Given that α-synuclein assumes a fibrillar β-pleated sheet structure in Lewy bodies in PD and related α-synucleinopathies (Spillantini et al. 1998), the leading hypothesis for its pathogenicity is the formation of toxic aggregates. α-synuclein has been shown to bind synaptic vesicles, and protofibrils can form pores that could lead to permeabilisation of the vesicle membranes, thereby releasing excess dopamine into the cytosol (Lashuel et al. 2002). Formation of protofibrils is enhanced and stabilised by dopamine quinones derived from the oxidation of dopamine, and this could account for the selective toxicity of α-synuclein in the substantia nigra (Conway et al. 2001). There is accumulating evidence for a close relationship between α-

synuclein and oxidative damage. Over-expression of mutant α-synuclein sensitises neurons to oxidative stress and damage by dopamine and mitochondrial toxins such as MPTP and 6-hydroxydopamine (6-OHDA), resulting in increased protein carbonylation and lipid peroxidation *in vitro* and *in vivo* (Tabrizi et al. 2000).

1.6.3.8 LRRK2, leucine-rich repeat kinase 2

Mutations in LRRK2 have only recently been identified (Zimprich et al. 2004). Strikingly, they account for 0.5–2.0% of cases of sporadic PD and 5% of familial PD. In Ashkenazi Jews and North African Arab populations this mutation might even account for 18–30% of PD cases, therefore LRRK2 is the gene most frequently associated with familial PD (for review (Farrer 2006)). LRRK2 encodes a complex multi-domain protein that consists of N-terminal leucine-rich repeats, a GTPase domain, a MAPKKK and C-terminal WD40 repeats. LRRK2 mutations increase its kinase activity (West et al. 2005; Gloeckner et al. 2006). It might be associated with the outer mitochondrial membrane and can bind Parkin. In addition, over-expression of mutant LRRK2 was sufficient to induce neuronal degeneration in mouse primary cortical neurons (Smith et al. 2005).

1.6.4 Common themes in Parkinson's disease

The diverse causes of PD may be related mechanistically (Figure 1-8). As expected, normal mitochondrial activity may be affected by environmental chemicals, mitochondrial DNA polymorphisms (Schapira 2006) and nuclear genes (see 1.6.3). Less expected are the findings that α-synuclein over-expression and inactivation of Parkin can also cause mitochondrial dysfunction (Beal 2004; Palacino et al. 2004). A common by-product of many types of mitochondrial impairment is increased production of ROS, and this may be the source of the oxidative damage found in PD brains. Inhibition of mitochondrial complex I leads to increased production and aggregation of α-synuclein (Sherer et al. 2002). In dopaminergic neurons, aggregation may be promoted by dopamine metabolites and, perhaps, by the formation of highly reactive dopamine-quinones. The latter can form adducts with proteins, such as α-synuclein (Conway et al. 2001), cross-link them, and facilitate their aggregation. In addition to aberrant protein modification, dopamine oxidation can affect mitochondrial function (Berman and Hastings 1999) and increase oxidative stress. Inhibition of

complex I can also impair the ubiquitin proteasome system (UPS), apparently by yielding ROS that cause oxidative damage to proteins, perhaps including the components of proteasomes (Shamoto-Nagai et al. 2003). The normal versions of DJ-1 and PINK1 seem to protect against oxidative stress, but the mutant proteins associated with PD do not (Petit et al. 2005; Zhang et al. 2005). Studies using *D. melanogaster* mutants demonstrate that PINK1 might function upstream of Parkin and therefore be linked in a common pathway (Clark et al. 2006; Park et al. 2006; Yang et al. 2006). Furthermore, Parkin has been localised to the ER, where it has been shown to have a neuroprotective role against ER stress (Takahashi et al. 2003), and oxidative stress was demonstrated to activate the UPR (Holtz et al. 2006). The ER and proteasome system are intimately linked, since proteins targeted for degradation in the ER are exported into the cytosol to be further processed by the UPS. However, when misfolded proteins accumulate in the ER, the UPR is activated. Therefore, disturbance of any of the two, UPR or UPS, will impact on the other.

Thus, although there seem to be multiple, divergent causes of PD, yet the pathogenesis of this disease appears to be converging on common mechanisms – mitochondrial impairment, oxidative stress, and protein mishandling, all of which are tightly linked.

1.7 Outline of subsequent chapters

Apoptosis plays an essential role in metazoan development and tissue homeostasis. Apart from their function in respiration, during apoptosis mitochondria integrate a variety of cellular stress stimuli. In most cases apoptotic insults are translated into the release of pro-apoptotic factors from mitochondria into the cytosol and nucleus, resulting in the organised demise of the cell. One of these proteins is the serine protease HtrA2. The role of HtrA2 *in vivo* is examined in Chapter 3 by studying mice lacking HtrA2. The phenotype of these animals and cells derived from them do not support a pro-apoptotic function for HtrA2 *in vivo*, but rather suggest the opposite, a protective role for HtrA2. Cells lacking HtrA2 exhibit increased sensitivity to some death stimuli and mice deficient for HtrA2 develop a parkinsonian syndrome. Interestingly, HtrA2 shows homology to bacterial proteases involved in a stress response pathway leading to the attractive hypothesis that mammalian HtrA2 may exert its protective function by signalling in a mitochondrial stress response pathway. In Chapter 4, transcriptional

changes resulting from loss of HtrA2 are investigated, leading to characterisation of a stress signature in brain tissue of HtrA2 deficient animals. Subsequently, the mitochondrial kinase PINK1 is identified as a novel binding partner of HtrA2 in Chapter 5. PINK1-dependent phosphorylation of HtrA2 appears to regulate HtrA2 protease activity, placing PINK1 upstream of HtrA2.

Figure 1-1. Extrinsic and intrinsic apoptotic pathways.

Apoptosis can be initiated through either extrinsic or intrinsic apoptotic signalling pathways. **(A)** Activation of the extrinsic pathway is triggered by ligation of death receptors and results in formation of the DISC complex, activation of caspase-8 and subsequently of effector caspases leading to apoptosis. Bid cleavage by caspase-8 provides cross-talk with the mitochondrial pathway. **(B)** Activation of the intrinsic (mitochondrial) pathway is triggered by BH3-only proteins and results in Bax-mediated mitochondrial dysfunction, leading to the release of cytochrome c, activation of the apoptosome caspase-9 complex and then effector caspases leading to apoptosis. Release of Reaper-like proteins such as Smac and HtrA2 from the mitochondria lead to inhibition of IAPs. Figure taken from (Igney and Krammer 2002).

Figure 1-1

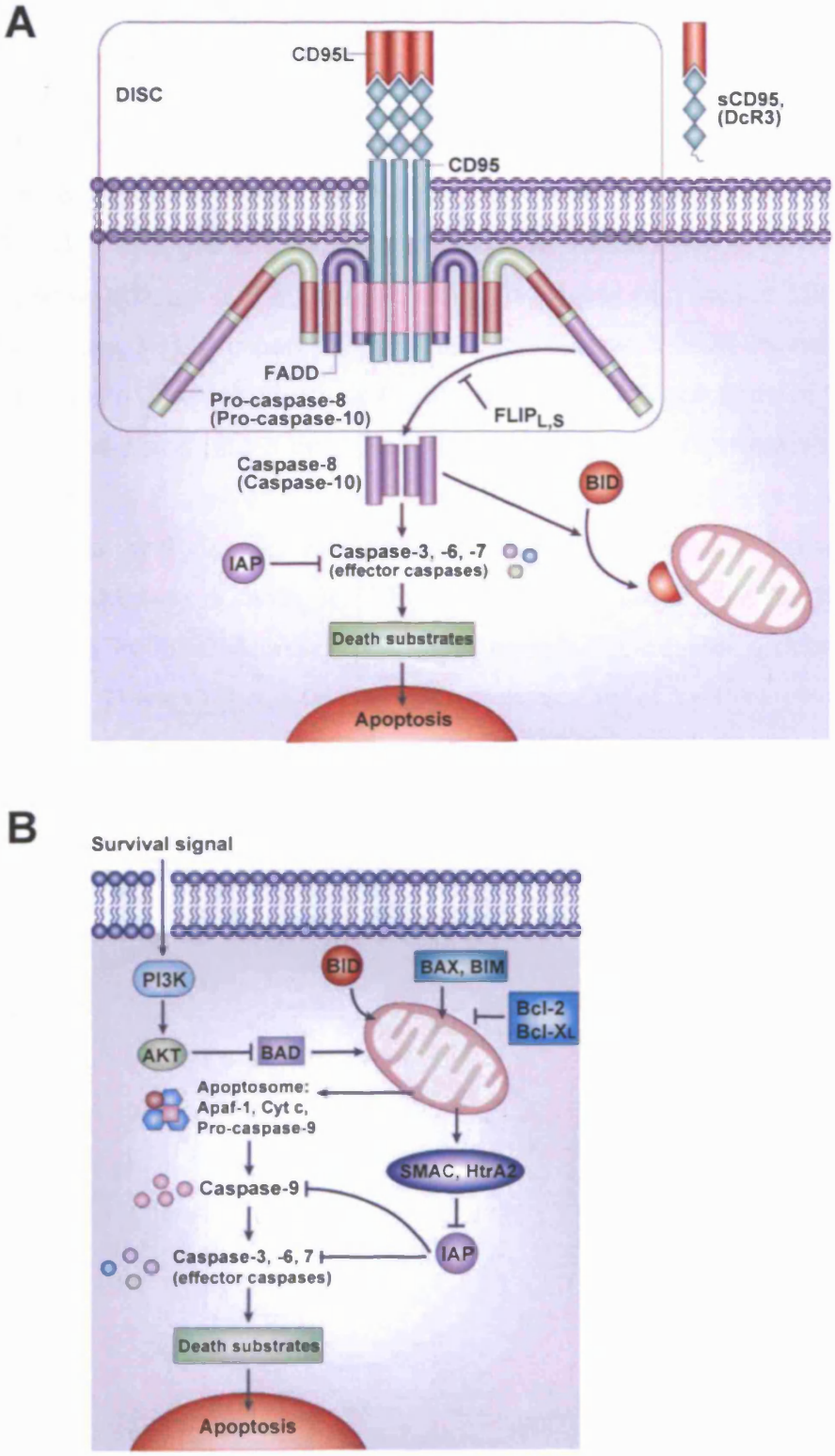
A
CD95L
DISC
sCD95,
(DcR3)
CD95
FADD
Pro-caspase-8
(Pro-caspase-10)
FLIP$_{L,S}$
Caspase-8
(Caspase-10)
BID
IAP
Caspase-3, -6, -7
(effector caspases)
Death substrates
Apoptosis
B
Survival signal
PI3K
BID
BAX, BIM
Bcl-2
Bcl-X$_L$
AKT
BAD
Apoptosome:
Apaf-1, Cyt c,
Pro-caspase-9
SMAC, HtrA2
Caspase-9
IAP
Caspase-3, -6, 7
(effector caspases)
Death substrates
Apoptosis

Figure 1-2. Domain structure of the mitochondrial serine protease HtrA2 and comparison to its homologues.

(A) Domain structure of HtrA2 showing the MTS (amino acids 1-31), the TM (amino acids 105-125), the trypsin-like serine protease domain (amino acids 166-342) and the C-terminal PDZ domain (amino acids 364-445). Within the protease domain is the catalytic triad, consisting of histidine 198, aspartate 228 and serine 306. Proteolytic processing reveals an IBM at the new N-terminus of mature HtrA2 which starts at amino acid 134. The positions of the amino acids are derived from the human sequence of HtrA2. **(B)** Comparison of the domain structure of *E. coli* proteases DegP and DegS, all four H. sapiens HtrA family members and *D. melanogaster* dHtrA2. Domains: SS, signal peptide; TM, transmembrane domain; IGFBP, insulin growth factor binding domain; KI, kazal protease inhibitor domain; protease, trypsin-like protease domain; PDZ, PDZ domain. The exact position of the domains cannot be taken from the diagram, only their relative position. SwissProt/TREMBL accession numbers are DegP (P09376), DegS (P31137), HtrA1 (Q92743), HtrA2 (Q43464), HtrA3 (P83110), HtrA4 (P83105), and dHtrA2 (Q9VFJ3).

Figure 1-2

A

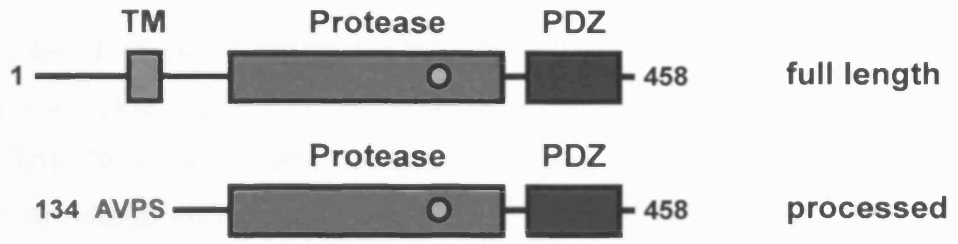

B

Protein	Species	Size (aa)	SS TM IGF BP KI Protease PDZ
DegS	*E. coli*	355	
DegP	*E. coli*	448	
HtrA1	*H. sapiens*	458	
HtrA2	*H. sapiens*	458	
HtrA3	*H. sapiens*	436	
HtrA4	*H. sapiens*	445	
dHtrA2	*D. melano.*	422	

Figure 1-3. Crystal structure of HtrA2, DegS and DegP proteases.

(A) Crystal structure of an inactive HtrA2 monomer shown as a ribbon. The PDZ domain is folded onto the protease domain. The catalytic serine 306 is indicated. The N-terminal IBM is exposed and unstructured. **(B)** Crystal structure of an HtrA2 trimer as side or top view. The PDZ domains are yellow and the catalytic serine is highlighted in red. **(C)** Crystal structure of the active DegS trimer from side or top view. The catalytic serine is highlighted in red, the PDZ domain in yellow. **(D)** Crystal structure of the proteolytically active and inactive DegP hexamer from side view. The PDZ domains are yellow. The structural information are taken from (Krojer et al. 2002; Li et al. 2002; Wilken et al. 2004).

Figure 1-3

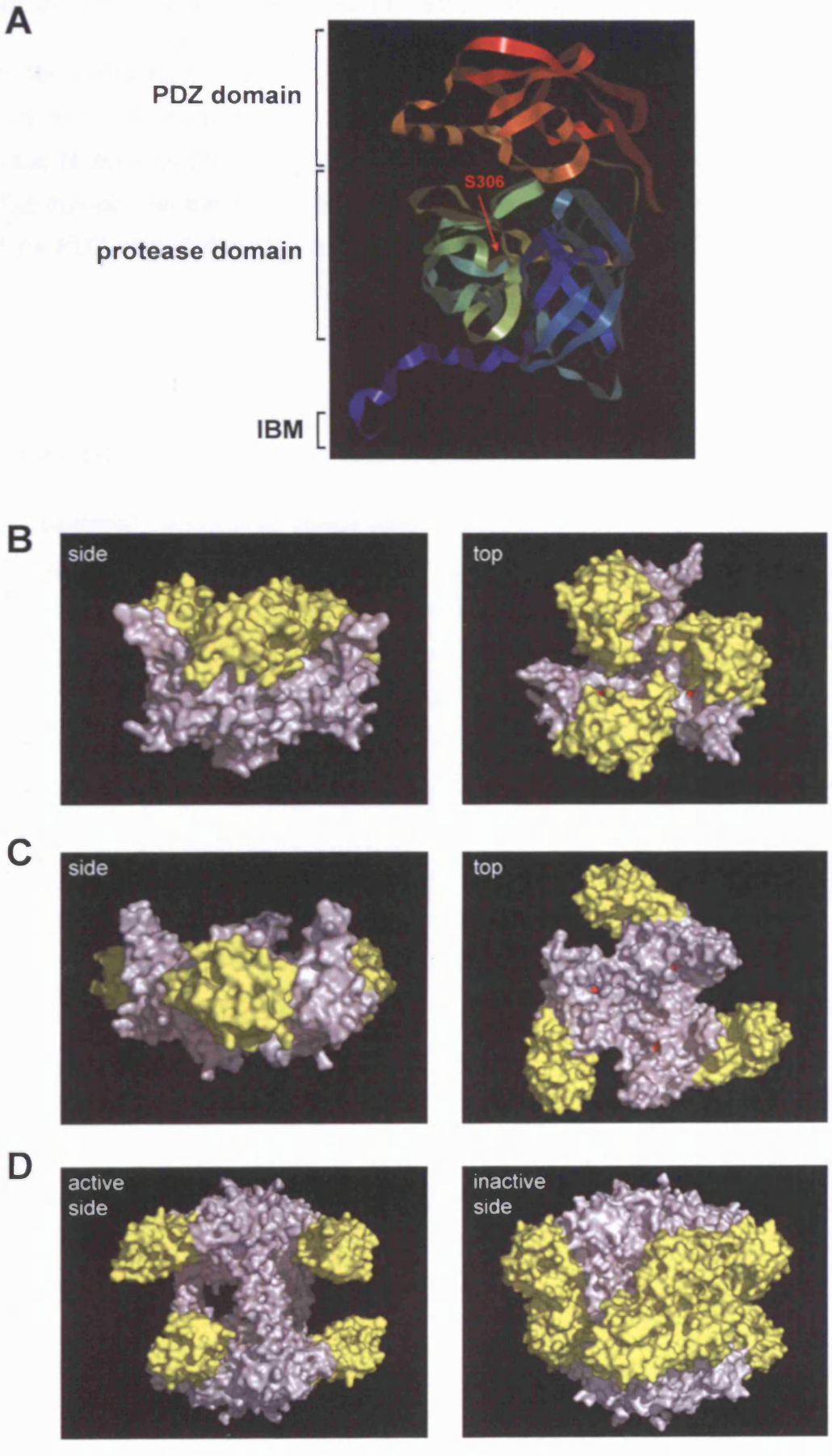
A
PDZ domain
protease domain
IBM
S306
B
side
top
C
side
top
D
active
side
inactive
side

Figure 1-4. Activation of HtrA2 proteolytic activity.

Model illustrating the activation of HtrA2 proteolytic activity. The mature inactive enzyme can be activated by heat shock (temperature increase), by IAP binding to the N-terminal IBM, or by interaction of binding partners with the C-terminal PDZ domain. All these mechanisms are proposed to lead to the displacement of the PDZ domain from the active site area. Taken from (Martins et al. 2003).

Figure 1-5. The bacterial stress response pathway involving DegS.

The bacterial periplasmic stress response involving DegS as a stress sensor. The stress signal is sensed in the periplasmic space of the bacterial envelope and the signal must cross the inner membrane, requiring a more sophisticated pathway. The transcriptional regulator of the periplasmic stress response is σ^E, which is normally held in an inactive complex bound to the cytoplasmic domains of the inner membrane proteins RseA and RseB. Upon external stress, the periplasmic DegS protease is activated by unfolded porins located in the outer membrane. The C-terminus of the porins ends in a PDZ binding motif (YXF) that binds to the PDZ domain of DegS leading to its activation. The periplasmic domain of RseA is efficiently cleaved by DegS, which allows a further proteolytic cleavage of RseA by the rhomboid-like metallo protease RseP (also known as YaeL) in the inner membrane. These proteolysis events are thought to destabilise RseA's cytoplasmic domain, releasing σ^E to activate transcription of the appropriate genes to help the bacteria to cope with the stress. One of the genes that is induced encodes for the periplasmic protease DegP which is active as a chaperone as well as a protease. Adapted from (Young and Hartl 2003).

Figure 1-4

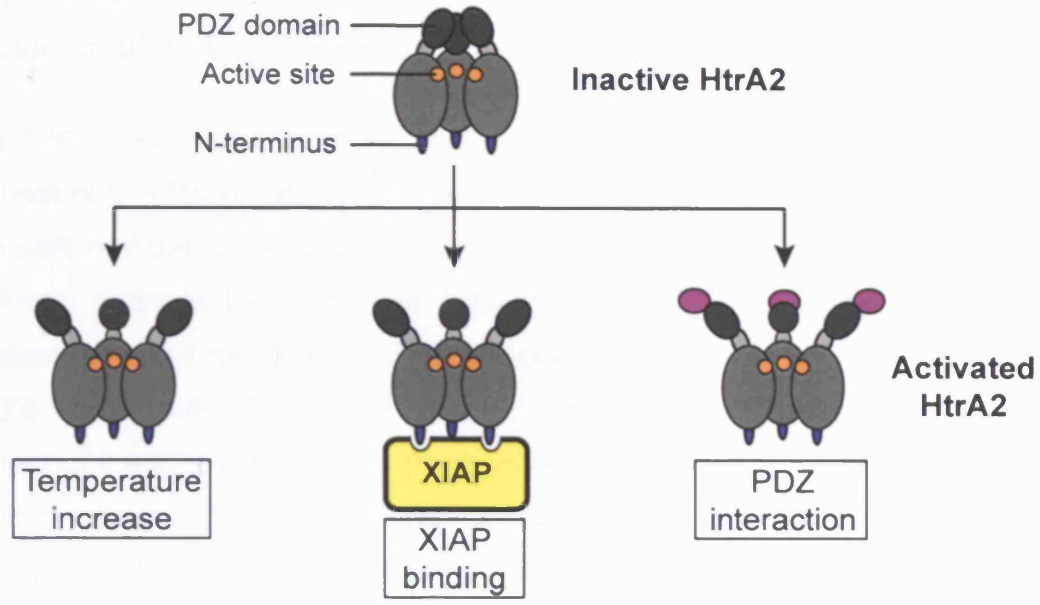

Figure 1-5

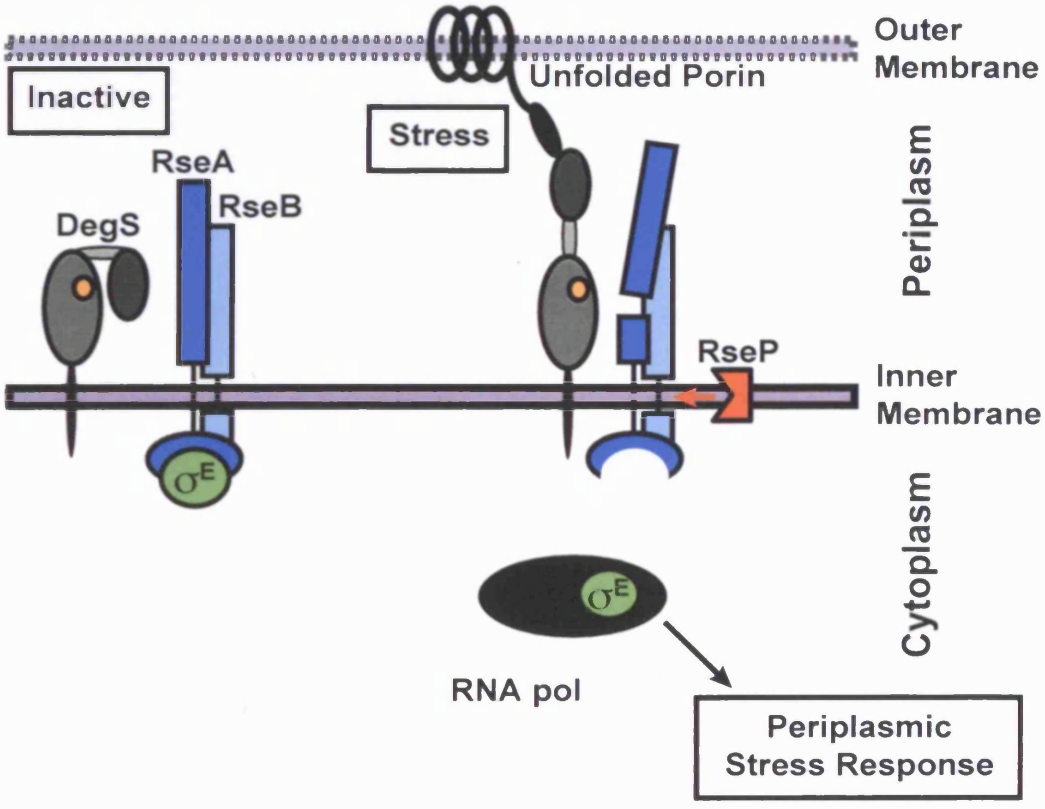

Figure 1-6. The unfolded protein response and pathways leading to activation of eIF2α kinases.

(A) The three branches of the metazoan UPR. The three types of ER stress transducers – PERK, ATF6, and IRE1 – sense the levels of unfolded protein in the lumen of the ER and communicate this information across the membrane to activate cognate bZip TFs via regulation of translational control, regulated proteolysis, and regulated mRNA splicing, respectively. In mammalian cells, ATF6 up-regulates expression of XBP-1 mRNA (indicated by plus sign). The output of the TFs is integrated through their combinatorial action on UPR target genes, whose products increase the protein folding capacity of the cell and hence help the system re-establish homeostasis. PERK also reduces general translation in cells, thereby reducing the protein influx into the ER. If homeostasis in ER protein folding cannot be reached, cells undergo apoptosis. Abbreviations: K, kinase domain; R, ribonuclease domain. Adapted from (Bernales et al. 2006). **(B)** Cellular stress pathways involving the activation of eIF2α kinases. GCN2, PKR, HRI and PERK are activated through the indicated stresses and phosphorylate the translation elongation factor eIF2α on serine 51. This leads to inhibition of general (cap-dependent translation). However, ATF4 mRNA possesses uORFs that facilitate its translation under these conditions. Therefore, ATF4 protein levels increase following eIF2α phosphorylation. ATF4 is a TF that activates transcription of ATF3, CHOP and Herp. ATF3 itself can also activate CHOP transcription. ATF4 can be phosphorylated and thereby be targeted to proteasomal degradation (Lassot et al. 2001).

Figure 1-6

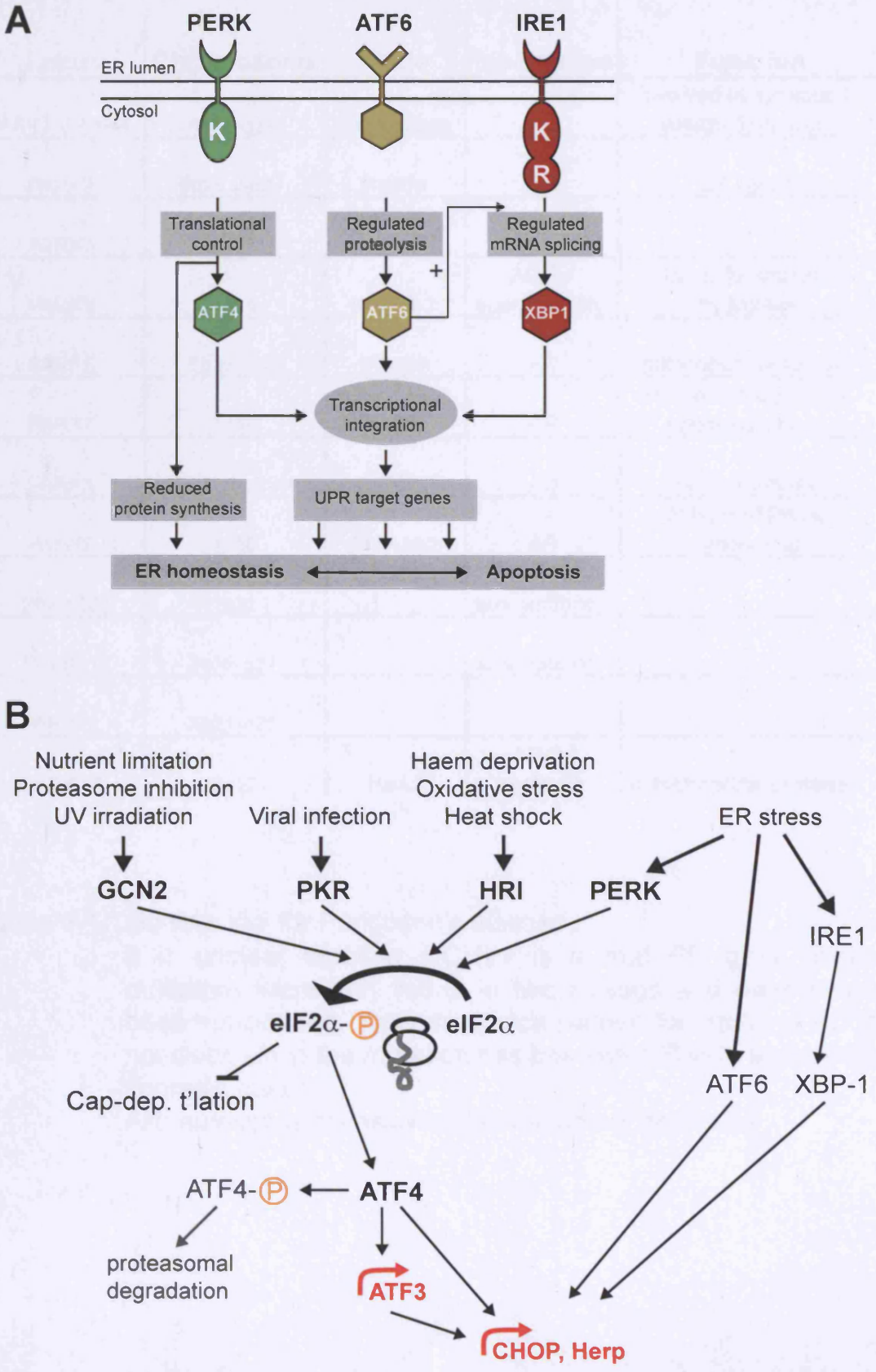
A
PERK
ATF6
IRE1
ER lumen
Cytosol
K
K
R
Translational control
Regulated proteolysis
Regulated mRNA splicing
+
ATF4
ATF6
XBP1
Transcriptional integration
Reduced protein synthesis
UPR target genes
ER homeostasis
Apoptosis
B
Nutrient limitation
Proteasome inhibition
UV irradiation
Viral infection
Haem deprivation
Oxidative stress
Heat shock
ER stress
GCN2
PKR
HRI
PERK
IRE1
eIF2α-P
eIF2α
Cap-dep. t'lation
ATF6
XBP-1
ATF4-P
ATF4
proteasomal degradation
ATF3
CHOP, Herp

Table 1-1

Locus	Chromosome	Gene	Inheritance	Function
PARK1, PARK4	4q21-q23	**α-synuclein**	AD	involved in synaptic vesicle formation
PARK2	6q25.2-q27	**Parkin**	AR	E3 ligase
PARK3	2p13		AD	
PARK5	4p14	**UCHL1 ?**	AD ? / susceptibility	ubiquitin-protein hydrolase
PARK6	1p35-p36	**PINK1**	AR	mitochondrial kinase
PARK7	1p36	**DJ-1**	AR	involved in oxidative stress response
PARK8	12p11.2-q13.1	**LRRK2**	AD	protein kinase
PARK9	1p36	**ATP13A2**	AR	P-type ATPase, lysosomal
PARK10	1p32		susceptibility	
PARK11	2q36-q37		susceptibility	
PARK12	Xq21-q25			
PARK13	2p12	**HtrA2**	AD ? / sporadic	mitochondrial protease

Table 1-1. Genetic loci for Parkinson's disease.
It is unclear whether UCHL1 is a real PD gene, since mutations were only found in two siblings and have never been reproduced. The inheritance pattern for HtrA2 in PD is not clear, since the mutation has been identified in apparently sporadic cases.
AR: autosomal recessive; AD: autosomal dominant

Figure 1-7. Domain structure of PINK1.

Domain structure of PINK1 showing the kinase domain (amino acids 156-509). The coding regions for each of the eight exons are numbered in amino acids. Mutations found in familial PD are indicated above the domain structure.

Figure 1-8. Common themes in Parkinson's disease.

Mutations in seven genes encoding α-synuclein, Parkin, UCHL1, LRRK2, PINK1, HtrA2 and DJ-1 are associated with familial forms of PD through pathogenic pathways that may commonly lead to deficits in mitochondrial and UPS function. PINK1, Parkin, HtrA2, LRRK2 and DJ-1 may play a role in normal mitochondrial function, whereas Parkin, UCHL1, and DJ-1 may be involved in normal UPS function. Parkin may protect against ER stress, whereas oxidative stress leads to activation of the UPR. α-synuclein fibrillisation and aggregation is promoted by pathogenic mutations, oxidative stress, and oxidation of cytosolic dopamine (DA), leading to impaired UPS function and possibly mitochondrial damage. α-synuclein may normally be degraded by the UPS. UPS dysfunction can activate the UPR, and activation of the UPR enhances the demand for functional UPS. Some environmental toxins and pesticides can inhibit complex I and lead to mitochondrial dysfunction, whereas alterations in mitochondrial DNA (mtDNA) may influence mitochondrial function. Impaired mitochondrial function leads to oxidative stress, deficits in ATP synthesis, and α-synuclein aggregation, which may contribute to UPS dysfunction. Oxidative stress may also influence the antioxidant function of DJ-1, can impair Parkin function through S-nitrosylation, and may promote DA oxidation. Excess DA metabolism may further promote oxidative stress. Red lines indicate inhibitory effects, green arrows depict defined relationships between components or systems, and blue dashed arrows indicate proposed or putative relationships. Adapted from (Moore et al. 2005).

Figure 1-7

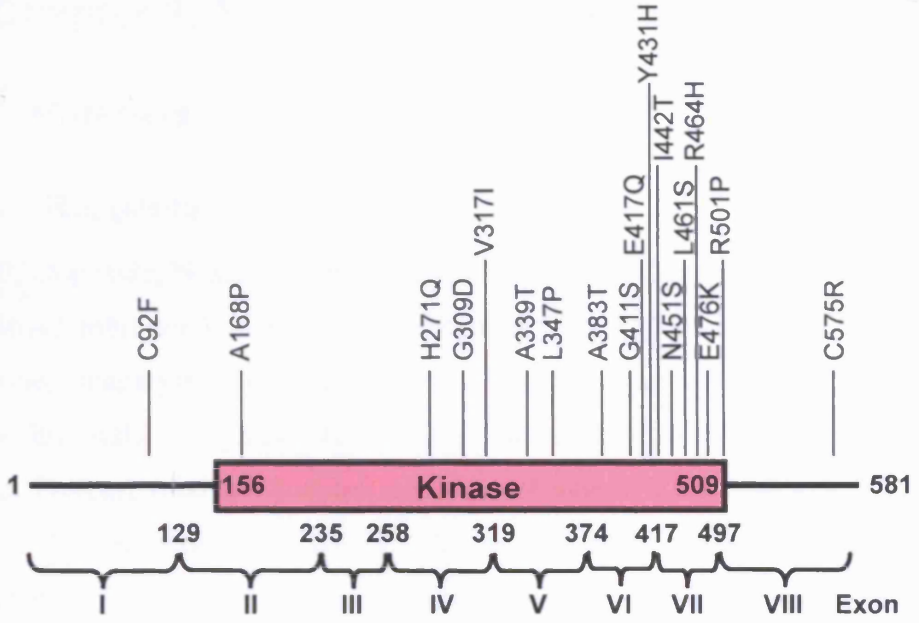

Figure 1-8

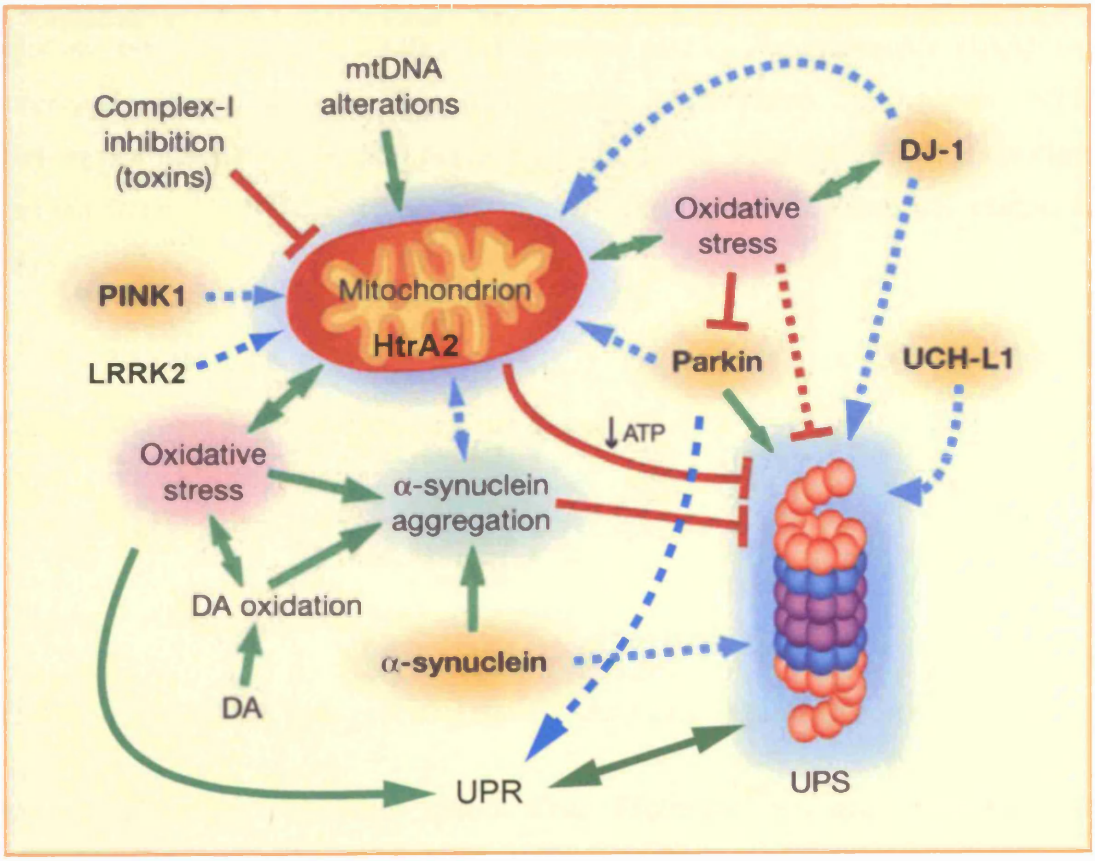

2 Chapter 2: Materials and Methods

2.1 Materials

2.1.1 Reagents

CCCP, etoposide, N-acetyl-L-cysteine (NAC), MG-132 in solution, staurosporine, and the HtrA2 inhibitor Ucf-101 were purchased from Calbiochem. ATP, NADH, H_2O_2, rotenone, thapsigargin, tunicamycin, 6-hydroxydopamine (6-OHDA), 4-hydroxy-tamoxifen (4OH-Tx), glutamate, CHAPS, Percoll and Proteinase K were obtained from Sigma. Protease inhibitor cocktail tablets (complete, EDTA-free) were purchased from Roche. Protein phospatase 2A (PP2A) was obtained from Upstate, and λ protein phosphatase (λ PPase) was purchased from New England Biolabs (NEB). Redivue™ L-[^{35}S] methionine was from Amersham. Active tobacco etch virus protease (TEV) was from Invitrogen, recombinant full length XIAP from R&D Systems. The p38 inhibitor BIRB796 was from Ana Cuenda (Kuma et al. 2005). For the 2D DIGE, CyDye DIGE Fluors, Immobiline DryStrips, Pharmalytes (IPG buffer), DeStreak rehydration solution, urea, thiourea, CHAPS, dithiothreitol (DTT), iodoacetamide (IAA) were purchased from GE Healthcare (formerly Amersham). Anhydrous 99.8% Dimethylformamide (DMF) was purchased from Sigma. Millipore purified, autoclaved distilled water (ddH_2O), and PBS was prepared by Cancer Research UK central cell services.

2.1.2 Antibodies

Actin, C-11, goat polyclonal (Santa Cruz Biotechnology)

P-Akt (Ser473), rabbit polyclonal (Cell Signaling)

Annexin V Alexa Fluor 647 (Molecular Probes)

ANT, N-19 and Q-18, both goat polyclonal (Santa Cruz Biotechnology)

BAD, C-20 rabbit polyclonal (Santa Cruz Biotechnology) and clone-48 mouse monoclonal (BD Transduction Laboratories)

Bak, clone2-14 rabbit polyclonal (Stressgen) and Ab-1 (Calbiochem)

Bax, clone YTH-6A7 mouse monoclonal (Mito Science) and rabbit polyclonal (Imgenex)

Bcl-2, N-19 rabbit polyclonal (Santa Cruz Biotechnology) and 4D7 mouse monoclonal (Pharmingen)

Bcl-XL, clone64 rabbit polyclonal (BD Transduction Laboratories)

Bif1, 30A882.1.1 mouse monoclonal (Abcam)

Bik, FL-160 rabbit and N-19 goat polyclonal (Santa Cruz Biotechnology)

Bim, N-20, goat polyclonal (Santa Cruz Biotechnology)

Bnip3L, clone 77-92 rabbit polyclonal (Calbiochem)

Cathepsin D, C-20, goat polyclonal (Santa Cruz Biotechnology), lysosomal marker

Complex I 17kD subunit, clone 21C11, mouse monoclonal (Molecular Probes)

Complex III UQCRC1, 2E3, mouse monoclonal (Molecular Probes)

ComplexV subunit alpha, 7H10, mouse monoclonal (Molecular Probes)

ComplexV subunit beta, 3D5, mouse monoclonal (Molecular Probes)

ComplexV subunit d, 7F9, mouse monoclonal (Molecular Probes)

ComplexV subunit OSCP, 4C11, mouse monoclonal (Molecular Probes)

ComplexV inhibitory Protein, 5E2, mouse monoclonal (Molecular Probes)

Complex V, 12F4AD8AF8, mouse monoclonal (Mito Science)

CPS1, rabbit polyclonal (Abcam)

Cytochome c, 7H8.2C12, mouse monoclonal (Pharmingen)

DJ-1, gift from Valina Dawson, rabbit polyclonal, 1:5000 dilution for Western blotting

P-eIF2α (Ser51), rabbit polyclonal (Cell Signaling)

P-ERK1/2 (Thr202/Tyr204), E10, mouse monoclonal (Cell Signaling)

FLAG, M2 antibody and affinity gel, mouse monoclonal (Sigma)

Grp75, clone 30A5, mouse monoclonal (Stressgen), 1:5000 dilution for Western blotting

HA-HRP, 3F10, rat (Roche), 1:1000 dilution for Western blotting

HAX-1, clone52, mouse monoclonal (BD Transduction Laboratories), 1:300 dilution for Western blotting

Hrk, N-20, goat polyclonal (Santa Cruz Biotechnology)

Hsp60, clone Mab11-13, monoclonal (Stressgen), 1:1000 dilution for Western blotting

HtrA2, rabbit polyclonal (Alexis), which is raised against recombinant mature HtrA2 and was used at 1:2000 to 1:5000 for Western blotting

P-S142 HtrA2, rabbit polyclonal, 1:1000 for Western blotting. This antibody was raised against the phosphorylated peptide SPPPASPRSQYC of human HtrA2 by coupling an additional N-terminal C to keyhole limpet hemacyanin (KLH) using malemeide and injection into a rabbit at Harlan Bioproducts for Science, UK. The P-HtrA2 antibody was characterised by Western blotting cellular lysates where either WT or S142A HtrA2 was over-expressed, verifying that this antibody does not detect HtrA2 that cannot be phosphorylated on S142 (Figure 5-3C and D).

IκBα, C-21, rabbit polyclonal (Santa Cruz Biotechnology)

P-IκBα (Ser32/36), 5A5, mouse monoclonal (Cell Signaling)

P-JNK (Thr183/Tyr185), rabbit polyclonal (Cell Signaling)

KDEL, clone 10C3, mouse monoclonal (Stressgen), endoplasmic reticulum marker

Lamin B1, C-20, goat polyclonal (Santa Cruz Biotechnology)

Myc, 9E10, mouse monoclonal (Evan et al. 1985)

P-p38 (Thr180/Tyr182), rabbit polyclonal (Cell Signaling)

PINK1, rabbit polyclonal, 1:1000 dilution for Western blotting. This antibody was raised against peptide KSKPGPDPLDTRRLQ of human PINK1 by coupling an additional N-terminal C to KLH using malemeide and injection into a rabbit at Harlan Bioproducts for Science, UK. The PINK1 antibody was biotinylated using the EZ-linkR NHS-PEO Biotinylation kit (Pierce). The PINK1 antibody was characterised by Western blotting cellular lysates where PINK1 had been down-regulated using siRNA (Figure 5-3A) or where PINK1 was over-expressed (Figure 5-1D).

Prohibitin, II-14-10, mouse monoclonal (Abcam)

Smac, rabbit polyclonal, generated against the C-terminal sequence of human Smac (EQEAYLRED) (Vyas et al. 2004)

VDAC / Porin, clone 31HL, mouse monoclonal (Calbiochem)

VDAC2, C-17, goat polyclonal (Santa Cruz Biotechnology)

XIAP, clone-48, mouse monoclonal (BD Transduction Laboratories)

All primary antibodies were used at dilutions recommended by the manufacturer's, unless otherwise indicated. Secondary anti-mouse and rabbit antibodies (Amersham) coupled to horseradish peroxidase (HRP) were used at dilution 1:4000. 1:30,000

dilution of streptavidin conjugated to peroxidase (DAKO) was required for the detection of biotinylated antibodies.

2.1.3 Plasmids

The expression construct pCMV-SPORT HtrA2 was from GlaxoSmithKline, and HtrA2 S306A was generated by introduction of a single point mutation by site-directed mutagenesis using the QuickChange kit (Stratagene) and confirmed by DNA sequencing. HtrA2-Flag was cloned by PCR into pcDNA3 (Invitrogen), inserting an KpnI site at the 5' end and a XhoI site after the Flag at the 3' end. All of this was done from a plasmid of HtrA2 which had the EcoRI and BamHI sites within the HtrA2 cDNA removed. The expression construct encoding S306A HtrA2-TAP was generated by sub-cloning into pZOME1C (Cellzome) using BamHI restriction sites to fuse HtrA2 to a C-terminal TAP tag. S142A, S142A/ S400A, and S400D HtrA2-Flag were generated by introduction of a single point mutation by site-directed mutagenesis using the QuickChange kit (Stratagene) and confirmed by DNA sequencing. Full length untagged HtrA2 was cloned into the lentiviral vector pRRLsin-cPPT-PGK-GFP-W (Tronolab, Ecole Polytechnique Federale de Lausanne) (Klages et al. 2000), where the GFP was removed and replaced with HtrA2.

The pEGFP-2 expression vector encoding enhanced green fluorescence protein and pcDNA3 (both Invitrogen) were used as control vectors. The pEGFP-F vector was obtained from Invitrogen. The pRK5 vector encoding Myc-PINK1 were a gift from Robert Harvey (University College London) and pcDNA3 PINK1 came from the Institute of Neurology. The pBabe Puro SV40LT was from Miguel Martins. The pBP3:hbER* vector encoding human ΔMEKK3:ER* was a gift from Simon Cook (Garner et al. 2002). The HA-ETHE1 and ETHE1-Flag constructs were generous gifts of Jun Fujita, Kyoto University, Japan (Higashitsuji et al. 2002). The pCAGGS rat OTC plasmid was contributed by Nicholas Hoogenraad, La Trobe University, Melbourne, Australia (Zhao et al. 2002) and PCR cloned into pcDNA3. A full length clone for Riken2410005O16 was ordered from RZPD (German Resource Center for Genome Research) and verified by DNA sequencing.

2.1.4 Primers

All primers are 5'-3'.

2.1.4.1 Cloning primers

To generate HtrA2 with BamHI restriction sites 5' and 3' to sub-clone into pZOME1C
Fwd: TTTAAGGATCCATGGCCTGCGCCGAGGGCGGG
Rev: AATTGGATCCGCCCAAGCTTACGCGT

To generate HtrA2-Flag by PCR,
5' end, Fwd: (random, KpnI site, Kozak, HtrA2 sequence)
CGAGCCGGTACCACCACCATGGCTGCGCCGAGGGCGGG
3' end, Rev: (random, XhoI site, Stop codon, Flag tag, HtrA2 sequence)
GGCTCGCTCGAGTCATTGTCGTCATCGTCTTTGTAGTCTTCTGTGACCTCAG
GG

QuickChange primer to silence EcoRI site in HtrA2 coding sequence,
Fwd: GGGGAAAAGAAGAACTCCTCCTCCGG
Rev: CCGGAGGAGGAGTTCTTCTTTTCCCC

QuickChange primer to silence BamHI site in HtrA2 coding sequence,
Fwd: GGTCACAGCTGTGGACCCCGTGGCAG
Rev: CTGCCACGGGTCCACAGCTGTGACC

QuickChange primer to mutate A306S of HtrA2,
Fwd: GCTATTGATTTTGGAAACTCTGGAGGTCCCC
Rev: GGGGACCTCCAGAGTTTCCAAAATCAATAGC

QuickChange primer to mutate S142A of HtrA2,
Fwd: GCCCGCCGCCCGCTGCTCCCCGGAGTCAG
Rev: CTGACTCCGGGGAGCAGCGGGCGGCGGGC

QuickChange primer to mutate S400A of HtrA2,
Fwd: GTCATCCTGGGCGCCCCTGCACACCGG
Rev: CCGGTGTGCAGGGGCGCCCAGGATGAC

To PCR OTC out of pCAGGS and insert into pcDNA3,

5' end, Fwd: (random, EcoRI site, Kozak, OTC sequence)

TGACAGAATTCGCCACCATGCTGTCTAATTTGAGGATCCTGCTCAACAATG

C

3' end, Rev: (random, NotI site, Stop codon, OTC sequence)

ACTGTGCGGCCGCTCAAAACTTTGGCTTCTGGAGCACAGGTG

2.1.4.2 Genotyping primer

Neo-Fwd, CCGGCCGCTTGGGTGGAGAGG,

Neo-Rev TCGGCAGGAGCAAGGTGAGATGACA

HtrA2-Fwd CCCCGGATCTCTGGGCACGATTGAAT,

HtrA2-Rev ATCCCCGCTAGGCAGCCTCACTCGTA

2.1.4.3 Real-time PCR primer

Mouse Actin γ, Fwd: CTCTTCCAGCCTTCCTTCCT,

Rev: TGCTAGGGCTGTGATCTCCT

Human Actin γ, Fwd: AAATCGTGCGCGACATCAA,

Rev: GGAACCGCTCATTGCCAAT

Mouse and human 18S rRNA, Fwd: CGGCTTAATTTGACTCAACACG,

Rev: TTAGCATGCCAGAGTCTCGTTC

Mouse HtrA2, Fwd: CCCTGACTCCCAGCATCCTTAT,

Rev: CCCAATGGCCAAGATCACAT

Mouse HtrA1, Fwd: CCTTCGCAATTCCATCCGAT,

Rev: TGGCTTTGCTAGATGTGAGCG

Mouse HtrA3, Fwd: ATCCCCTCAGATCGCATCA,

Rev: TTCAGTTCCTCCACCAAACTTG

Mouse HtrA4, Fwd: GACGGATGCCATCATTAACCA,
Rev: TGGCGCTCATGATAGTCTTCC

Mouse CHOP, Fwd: AAAGCCCTCGCTCTCCAGATT,
Rev: CCTTCTCCTTCATGCGTTGCT

Mouse ATF3, Fwd: GCGAAGACTGGAGCAAAATGA,
Rev: ATGGCGAATCTCAGCTCTTCC

Mouse Herp, Fwd: TGCTGTTGGATCACCAGTGTC,
Rev: TGTGGATTCAGCACCCTTTG

Mouse KLF5, Fwd: CACGTACACCATGCCAAGTCA,
Rev: GGAAGCAATTGTAGCGGCATA

Mouse Hsp60, Fwd: CGCTGGTTTTGAACAGGCTAA,
Rev: TCAACCCCTCTTCTCCAAACAC

Mouse MMP9, Fwd: GCGTGTCTGGAGATTCGACTTG,
Rev: CTCACACGCCAGAAGAATTTGC

Mouse AQP1, Fwd: ATTGGCACTCTGCAGCTGGTA,
Rev: CAGTGTAGTCAATCGCCAGCA

Mouse MASP1, Fwd: CAGGTGCTGGCAACCTTTTGT,
Rev: CGTCGAAGCCTGTGAATCGTT

Mouse CAV2, Fwd: TCTGGATCCTGATGCCTTTTG,
Rev: TGCATGCTGACCGATGAGA

Mouse NPNT, Fwd: AACCCCAGAAAGGCCATCTAC,
Rev: CTGCCGTGGAATGAACACAT

Human PINK1, Fwd: TGAAAGCCGCAGCTACCAAGA,
Rev: GATGAAGCACATTTGCGGCTA

2.1.5 siRNA oligos

2.1.5.1 Ambion

Silencer Negative Control, catalogue number 4615

GFP, catalogue number 16106, 5'–3': GACCCGCGCCGAGGUGAAGtt

Human PINK1, catalogue number 51323, ID 1294, 5'–3': GGCAAUUUUUACCCAGAAAtt

2.1.5.2 Dharmacon

siGLO Lamin A/C, catalogue number 001620

siCONTROL Non-Targeting siRNA SmartPool, catalogue number 001206

Human GAPDH SmartPool, catalogue number 004253,
5'–3' oligo 1: CAACGGAUUUGGUCGUAUUUU,
oligo 2: GACCUGACCUGCCGUCUAGUU,
oligo 3: CAAUAUGAUUCCACCCAUGUU,
oligo 4: GCGAUGCUGGCGCUGAGUAUU

Mouse HtrA2 SmartPool, catalogue number 050725 (OTP),
5'–3' oligo 1: UCAGACCGAUGCAGCUAUUUU,
oligo 2: GCAGAUCUGACGUCUAGGAUU,
oligo 3: CAGCAUCCUUACCGAACUAUU,
oligo 4: AAACGGAUCAGGAUUCGUAUU

2.2 Mouse techniques

2.2.1 Generation of HtrA2 deficient mice

The HtrA2 locus was targeted in mouse E14.1 (129/Ola) embryonic stem cells using standard ES cell culture and gene targeting techniques (Hogan et al. 1994; Joyner 1999). The targeting vector was generated using DNA fragments from a 129/sv mouse Bac genomic clone (Invitrogen). The 5' arm of homology was isolated as a 2.7kb XhoI-BglII fragment and the 3' arm as a 2.1kb HindIII-XhoI fragment. Targeting the HtrA2

locus with this vector inserts the neomycin resistance gene, under the control of the PGK promoter (PGK-neo), in the first coding HtrA2 exon at a position 140bp downstream of the translational start codon. The PGK-neo gene replaces part of exon 1, exon 2-6, and part of exon 7 as well as intervening intronic sequences. This removes 83% of the mHtrA2 coding sequence including the proteolytic catalytic site of HtrA2. The targeting construct was linearised with PmeI and transfected into ES cells (Bio-Rad GenePulser; 230kV, 500μF). Transfected clones were selected in 180μg/ml G418 (Sigma). A total of 300 G418-resistant ES cell colonies were isolated and screened for homologous recombination by Southern blot analysis. Two targeted clones were injected into C57Bl6/J-derived blastocysts. High percentage male chimaeras from both clones were crossed with C57Bl6/J females to produce N1F0 offspring. Heterozygous HtrA2 offspring derived from one of the targeted ES cell clones were backcrossed for at least 5 generations onto the C57Bl6/J strain. Mutant heterozygote F1 crosses were set up to generate study populations of animals containing all three possible genotypes (wild type (WT), heterozygous (Het) and homozygous (KO) mutant). The HtrA2 mutant mice were generated by GlaxoSmithKline UK.

2.2.2 Maintenance and breeding of mice

Animal husbandry and experimental procedures were performed in full compliance with the UK Animal (Scientific Procedures) Act 1986, and were approved by the Cancer Research UK procedures panel. Genotypes of HtrA2 mutant mice were confirmed by PCR as shown in (Figure 3-1A). Primers Neo-Fwd and Neo-Rev specific for neomycin gene were used to detect the mutant allele, generating a PCR product of 300bp. Primers HtrA2-Fwd and HtrA2-Rev that located in sequences within exons 1 to 2 respectively were used to detect the HtrA2 WT allele, yielding a PCR product of 500bp. Post-natal days are abbreviated as P (post-natal day 18 is P18), as commonly accepted.

2.2.3 Inclined platform test

Mice around P30 were placed in the middle portion of a 60° inclined platform and evaluation was performed as previously described (Schaefer et al. 2000).

2.2.4 Rotarod test

The rotarod apparatus (AccuScan Instruments Inc.) was used to measure fore- and hindlimb motor coordination and balance of the mice. WT and HtrA2 Het mice were initially trained on the rotarod for four consecutive days, using the same settings as for the experiments which started one month later. During this training period, no difference between WT and HtrA2 Het mice could be detected. Then the mice were monitored every two months at 10, 12, 14, and 16 months of age and were tested on the rotarod on three consecutive days. The latency to fall was measured and is displayed in seconds in the graphs. Rotarod settings were continuous acceleration from 0 to 40rpm in 570 seconds. WT n=10, Het n=10.

2.2.5 Anti-oxidant treatment of mice

HtrA2 Het x Het breeding pairs were set up for control and NAC treatment. When the females were pregnant the males were taken out of the experiment. When the mothers gave birth they started receiving NAC at 1mg/ml in drinking water. At the same time the pups started receiving NAC from day 5 with oral administration at 200mg/kg body every day. The pups in the control litters received normal water as oral administration in similar volumes. After weaning at P20 the animals received NAC at 1mg/ml in the drinking water. Following anti-oxidant administration the animals were observed and bodyweights recorded every 3-5 days. Animals were followed until they reached 30-35 days of age. If they showed signs of distress including vocalisation, breathing difficulty or seizures they were culled by schedule 1 methods.

2.3 Pathology

2.3.1 Histology and immunohistochemistry

Brain tissues were harvested from P20 and P30 mice and fixed in 10% formalin, embedded in paraffin, cut into 3μm sections and processed for haematoxylin-eosin (H&E) staining. In addition, the following immunostains were carried out according to the manufacturer's instructions: GFAP (glial fibrillary acidic protein; rabbit polyclonal antibody, 1:300; DAKO), NeuN (anti-neuronal nuclei; mouse monoclonal antibody, 1:4000; Chemicon), MAP-2 (; microtubule-associated protein-2 mouse monoclonal antibody, 1:500; Chemicon), calbindin (Calbindin; rabbit polyclonal antiserum, 1:200;

Chemicon), TH (tyrosine hydroxylase, rabbit polyclonal antiserum, 1:1000; Chemicon).

Biotinylated secondary antibodies were used for all staining and visualisation was with a horseradish peroxidase-conjugated streptavidin complex and diaminobenzidine as a chromogen. All immunostainings were carried out using the automated Nexus staining apparatus (Ventana Medical Systems; www.ventanamed.com), following the manufacturers' guidelines. Photographs were obtained on a ColorView II digital camera (www.soft-imaging.de) mounted on a ZEISS Axioplan microscope and composed in Adobe Photoshop.

2.3.2 Stereological cell counts

Immunohistochemistry was performed on serial sections (50μm) of the striatum after the tissue had been fixed with paraformaldehyde cryoprotected in 30% (w/v) sucrose in phosphate buffer and frozen rapidly in liquid isopentane. Counts were performed by using the optical fractionator method as described previously (Xia et al. 2001). In agreement with this method, NeuN positive neurons were counted in the left striatum of every third section throughout the entire extent of the striatum. Each section was viewed at low power (x 2.5 objective), and the striatum was outlined. Then the number of NeuN positive cells were counted at high power (x 63 oil) in the various groups of animals. In another set the first and fourth section from the striatum, just lateral of the thalamus, in a relatively posterio-medial portion of the basal ganglia were outlined and cells in the lower half were counted with the stereological program (StereoInvestigator, Microbrightfield, IN). TH immunostaining was carried out on striatal and midbrain sections and the TH-stained SNpc neurons were counted by stereology using the optical fractionator method. The striatal density of TH immunoreactivity was determined as described (Teismann et al. 2003).

2.4 Mammalian cell culture

2.4.1 Cell lines and culture conditions

HEK293 and Neuro-2a, a gift from Giampietro Schiavo (Cancer Research UK), cells were cultured in Dulbecco's modified Eagle medium (DMEM) supplemented with 10% foetal bovine serum (FBS). NIH 3T3 cells were cultured in DMEM supplemented with

10% donor calf serum (DCS). SH-SY5Y cells, a gift from Samantha Loh (MRC Leicester), were cultured in DMEM and Ham's nutrient mixture F12 (1:1) supplemented with 10 % (FBS). The Phoenix ecotropic retrovirus packaging cell line is a 293-based cell line and a gift from Gary Nolan (Stanford). The HEK293 TAP control cell line was a gift from Miguel Martins (MRC Leicester) (Martins et al. 2002). The NIH 3T3 myrAkt:ER (Kohn et al. 1996) and ΔRaf-DD:ER (Woods et al. 1997) cell lines were a gift from Almut Schulze (unpublished, Cancer Research UK). All media formulations were prepared by Cancer Research UK central cell services.

2.4.2 Culture of primary cortical neurons

Primary cortical neurons were isolated from E14.5 embryos and seeded at a density of 5 x 10^5 per well in 12-well plates coated with poly-L-lysine. Cells were maintained in Neurobasal medium (Invitrogen) supplemented with B27, Glutamax and Penicillin/Streptomycin (Invitrogen). Following 3 days in culture, contamination from fibroblasts and glial cells was reduced by supplementing culture media with 10μM cytosine arabinoside (Sigma). Cells were cultured for 10 days, with exchange of 50% of the media volume with fresh media every two days before treatment with toxic stimuli.

2.4.3 Isolation and immortalisation of MEFs

Primary mouse embryo fibroblasts (MEFs) were established from E14.5 embryos according to standard procedures (Hogan et al. 1994). The cells were maintained in DMEM supplemented with 10% FBS, L-glutamine and antibiotics. To establish immortalised MEFs over-expressing SV40 large T antigen (SV40LT), primary MEFs were cultured in the presence of viral supernatants prepared by transfecting the Phoenix ecotropic retrovirus packaging cell line with pBabe Puro SV40LT. Cells that integrated the virus were selected in medium containing 2μg/ml of puromycin (Sigma). HtrA2 expression was restored in HtrA2 KO MEFs, by lentiviral infected with pRRLsin-cPPT-PGK-HtrA2 as previously described (Klages et al. 2000).

2.4.4 Transfection methods

2.4.4.1 DNA transfection

HEK293, SH-SY5Y, and MEFs were transiently transfected using Effectene (Qiagen), Lipofectamine2000 (Life Technologies), and Genejuice (Novagen), respectively, according to manufacturer's guidelines. The HEK293 HtrA2-TAP stable cell line was selected with 0.5mg/ml G418 (Calbiochem), and single colonies were then assayed for Protein A epitope expression. The ΔMEKK3:ER stable cell line was selected with 1μg/ml puromycin (Sigma).

2.4.4.2 siRNA transfection

Delivery of siRNA into Neuro-2a and immortalised MEFs was performed using Dharmafect2 according to the manufacturer's guidelines (Dharmacon). Optimisation was performed with the Dharmacon siGlo oligo and transfection efficiency was determined using FACS. Following optimisation, cells were transfected on two consecutive days (day 1 + 2) with either Non-Targeting siRNA SmartPool, GAPDH siRNA SmartPool or HtrA2 siRNA SmartPool against mouse HtrA2 (all from Dharmacon) at a final concentration of 30nM. 6hrs following transfection the medium was replaced to fresh medium. 48hrs after the 2^{nd} transfection, the cells were harvested and assayed.

SH-SY5Y cells were transfected with siRNA oligos against human PINK1, Silencer Negative Control or GFP-specific siRNA (all from Ambion) at a final concentration of 50nM using Lipofectamine2000, according to the manufacturer's instructions. After 48hrs, cells were harvested for Western blotting.

2.4.5 Proliferation assay

Primary MEFs at passage 2 and immortalised MEFs were seeded at 1 x 10^5 cells/well of a 6-well plate. Every two days a well was trypsinised and counted using a haemocytometer and the total number of cells was calculated.

2.4.6 Metabolic activity assay

Primary MEFs at passage 2 were seeded at 4000 cells/well of a 96-well plate. The next

day the cells were treated with a range of concentrations (0, 0.1, 1, 10, 25, 50μM) of rotenone, CCCP, tunicamycin for 6hrs or 24hrs. The MTT assay (Cell Proliferation Kit I, Roche) was performed according to the manufacturer's instructions. The spectrophotometric absorbance was measured at 600nm wavelength.

2.5 DNA techniques

2.5.1 Basic DNA manipulations

DNA amplification by polymerase chain reaction (PCR) was performed in a 50μl reaction according to the general scheme: 100ng DNA template, 0.5μM forward and reverse primers, 200μM of each deoxynucleoside triphosphate (dATP, dCTP, dGTP, dTTP) and 2.5U Pfu or TaqPlusPrecision polymerase (both Stratagene) in a reaction buffer appropriate for the enzyme. The TaqPlusPrecision polymerase usually worked better for difficult templates with secondary structure, such as HtrA2. 2.5μl DMSO were added to some PCR reactions to increase the efficiency. Themocycling conditions were: 95°C for 4min for initial denaturation, then denaturation at 95°C for 45sec, annealing at the appropriate temperature for the primers (between 50°C to 60°C) for 1min, extension at 72°C for 1min/1kb product (30cycles), then final extension at 72°C for 10min.

Restriction enzyme digestions were performed according to the manufacturer's protocol (NEB) and DNA fragments were excised from agarose gels and recovered using the QIAquick Gel Extraction kit (Qiagen).

DNA ligation reactions were carried at 15°C for 2hrs in a volume of 10μl using T4 DNA ligase (NEB) and 100ng/μl vector, according to the manufacturer's protocol. 5μl of the ligation reaction were transformed into competent XL-10 gold *E. coli*.

2.5.2 Plasmid mutagenesis

Plasmid DNA mutagenesis was performed by an adapted QuickChange method (Stratagene) as a 50μl reaction: 50ng parental DNA template, 3.2pmol of the appropriate forward and reverse primers, 200μM of each dNTP and 2.5U of Pfu polymerase in Pfu buffer. Themocycling conditions were: 95°C for 4min, (95°C for

30sec, 55°C for 1min, 72°C for 16min) repeated for 16 cycles. 1µl DpnI restriction enzyme (NEB) was then added to the PCR reaction and incubated for 1h at 37°C to digest methylated parental DNA strands. 1µl of the resulting reaction was used to transform competend *E. coli*. A control reaction with no Pfu polymerase was performed in parallel and colonies only picked for analysis if the control plate was clear of colonies.

2.5.3 DNA gel electrophoresis

Agarose gels were prepared by dissolving 1-2% agarose (depending on the seize of the DNA) in 1X TAE buffer (40mM Tris base, pH 8.0, 1mM EDTA, 20mM acetic acid) and heating until boiling. Ethidium bromide was added to a final concentration of 0.5µg/ml before the gel was cast. Samples were mixed with DNA loading buffer (6X buffer containing 40% (w/v) sucrose, 0.25% bromophenol blue and/or 0.25% xylene cyanol FF) and electrophoresis was at 5-10 V/cm in TAE buffer. DNA molecular weight markers (100bp or 1kb Plus ladder, Invitrogen) were included on all gels and bands were visualised on a UV transilluminator.

2.5.4 Transformation of *E. coli* by heat shock

20ng of plasmid DNA, 5µl of ligation reactions or 1µl of mutagenesis reactions was incubated with 30µl competent XL-10 gold *E. coli* bacteria (Stratagene) on ice for 30min. The bacteria were then heat shocked by transfer to a 42°C water-bath for 45sec and then returned to ice for a further 2min. 1ml fresh LB medium was added and bacteria were allowed to recover by 1h incubation at 37°C gentle shaking. Bacteria wre then pelleted in a microcentrifuge, resuspended in 100µl LB medium and spread onto LB agar plates containing the appropriate selective antibiotic. Plates were incubated o/n at 37°C and then stored at 4°C.

2.5.5 Purification of plasmid DNA

Single bacterial colonies picked from LB agar plates containing the appropriate selection antibiotic were used to inoculate 5ml cultures of LB medium also containing antibiotic and incubated o/n at 37°C with shaking. For small scale (mini prep) plasmid purification the o/n culture was pelleted by centrifugation and plasmid DNA isolated using DirectPrep 96 MiniPrep automated plasmid purification system (Qiagen)

according to the manufacturer's instructions. For large scale (maxi prep) plasmid DNA purification, a single colony picked from LB agar plates containing the appropriate selection antibiotic were used to inoculate 300ml cultures of LB medium / antibiotic and incubated o/n at 37°C with shaking. Cells were harvested by centrifugation and used for Maxi-prep plasmid purification kit (Qiagen) according to the manufacturer's instructions. Purified plasmid DNA was resuspended in ddH_2O and the concentration and purity was assessed using a NanoDrop spectrophotometer by measuring optical density at 260nm (OD_{260nm}) and 280nM (OD_{280nm}). An OD_{260nm} of 1 corresponds to 50μg/ml double stranded DNA and 33μg/ml single stranded DNA. The ratio $OD_{260/280nm}$ provides an estimate of the purity of the DNA solutions and should be ~1.8 for DNA preparations. DNA was stored at -20°C.

2.5.6 DNA sequencing

Sequencing PCR reactions were performed according to the general scheme: 8μl of Big Dye Terminator reaction mix (Perkin Elmer), 3.2pmol of primer, 150-200ng of double stranded DNA template in a total reactin volume of 20μl. Thermocycling conditions were: denaturation at 96°C for 10sec, annealing at 50°C for 5sec, extension at 60°C for 4min (25 cycles). Dye-terminator removal was achieved with DyeEx2.0 spin columns (Qiagen), according to the manufacturer's instructions. Finally samples were dried in a Speed Vac microcentrifuge and stroed at -20°C until run. Sequences were read by capillary sequencing using and ABI Prism 3730 DNA analyser (Applied Biosystems).

2.5.7 *In vitro* translation assay

In vitro coupled transcription/translation was performed following the protocol by the supplier (TNT T7 Coupled Reticulocyte Lysate System, Promega). Reactions were carried out in a total volume of 50μl containing 1μg plasmid DNA. 2μl of that reaction were run for SDS-PAGE and 5μl for mitochondria import assay.

2.6 RNA techniques

2.6.1 Isolation of RNA

Total RNA from cells was isolated using the RNeasy kit (Qiagen) according to the manufacturer's instructions. Briefly, 350μl RLT buffer was added per well of a 6-well

plate, cells were then scraped and homogenised using a QIAshredder (Qiagen) to sheer the DNA. RNA was isolated by using the RNeasy spin columns, DNA was digested using the RNase-free DNase set (Qiagen) and eluted in 30µl RNase-free water.

Total RNA from tissue was also isolated using the RNeasy kit (Qiagen), 600µl RLT buffer / 30µg of tissue were first homogenised by pipetting or using a glass dounce homogeniser, then using a QIAshredder (Qiagen), and the following steps were as detailed before.

The concentration and purity of RNA was assessed using a NanoDrop spectrophotometer by measuring optical density at 260nm (OD_{260nm}) and 280nM (OD_{280nm}). An OD_{260nm} of 1 corresponds to 40µg/ml RNA. The ratio $OD_{260/280nm}$ provides an estimate of the purity of the RNA solutions and should be ~2.0 for RNA preparations. RNA was stored at -80°C.

2.6.2 RNA gel electrophoresis

The quality of total RNA was analysed on a 1.2% formaldehyde agarose gel in FA gel buffer (20mM Mops, 2mM sodium acetate, 1mM EDTA, pH 7). Ethidium bromide was added to a final concentration of 0.5µl/ml. 1µg of RNA was mixed with loading buffer (5X buffer containing 0.25% bromophenolblue, 4mM EDTA, 7.2% (v/v) of 37% (12.3M) formaldehyde, 20% (v/v) glycerol, 40% (v/v) FA gel buffer, 30.84% (v/v) formamide), incubated at 65°C for 5min and electrophoresed at 5 V/cm in FA running buffer (20mM Mops, 5mM sodium acetate, 1mM EDTA, 2% (v/v) of 37% (12.3M) formamide). 0.24-9.5kb RNA ladder and RNA century markers (Invitrogen) were included on the gels. Alternatively, the RNA was run on a Agilent Bioanalyser. The 28S ribosomal RNA band should be present at approximately twice the amounts of the 18S rRNA.

2.6.3 Complementary (cDNA) synthesis

cDNA was synthesised from total RNA with the Superscript III kit (Invitrogen) according to the manufacturer's protocol using oligo dT_{20} primer.

2.6.4 Quantitative real-time PCR

cDNA was used as a template for quantitative PCR analysis monitoring the real-time increase in fluorescence of SYBR Green (Applied Biosystems) on a Chromo4 detector system (Bio-Rad, formerly MJ Research). Gene-specific primers were designed using PrimerExpress software (Applied Biosystems). Relative transcript levels of target genes are normalised to Actin γ RNA levels. Primer sequences are listed in 2.1.4.2. Usually, 50ng of cDNA and 300nM of each primer were used in a final reaction volume of 25µl. Thermocycling conditions were: first denaturation at 95°C for 10min, then denaturation at 95°C for 15sec, annealing and extension at 60°C for 1min (40 cycles), and a dissociation curve profile was performed at the end of each run: denaturation at 95°C for 15sec, annealing and extension at 60°C for 20sec, and then slowly increasing the temperature to 95°C and taking measurements every 1°C increase. Thereby a dissociation curve can be plotted for each primer pair, a single peak should be visible representing the generation of only one product. The comparative C_T method ($\Delta\Delta C_T$) was employed to measure relative transcript levels (Livak and Schmittgen 2001). For this calculation to be valid, the efficiency of the target amplification (eg. HtrA2, CHOP) and the efficiency of the reference amplification (eg. Actin γ, 18S rRNA) must be approximately equal. Therefore, a standard curve with dilution of the template was performed and the ΔC_T (which is C_T target – C_T reference) values were plotted against each template concentration. If the efficiencies of the two amplicons are approximately equal, the plot of log input (template) versus ΔC_T has a slope of approximately zero.

2.7 Microarray techniques

2.7.1 Microarray sample preparation

The detailed protocol for the sample preparation and microarray processing is available from Affymetrix (Santa Clara, CA, USA). Briefly, 10µg purified RNA was reverse transcribed by Superscript II reverse transcriptase (Invitrogen) using $T7(dT)_{24}$ primer containing a T7 RNA polymerase promoter (Affymetrix). After synthesis of the second cDNA strand and double stranded cDNA cleanup (GeneChip Sample Cleanup Module (Affymetrix)), this product was used in an *in vitro* transcription reaction to generate biotinylated complementary RNA (cRNA) carried out with the Enzo BioArray High Yield Transcript Labelling Kit (Affymetrix). The cRNA was cleaned using the

GeneChip Sample Cleanup Module (Affymetrix) and fragmented.

2.7.2 Hybridisation to GeneChip

MOE430A GeneChips comprise about 22,000 probe sets, representing approximately 14,000 genes, therefore some genes are represented by more than one probe set. Affymetrix Mouse Genome 2.0 GeneChips comprise about 39,000 probe sets and some genes are represented by more than one probe set.

15µg of fragmented cRNA was hybridised to MOE430A (MEF) or Mouse Genome 2.0 (brain cortex) GeneChip arrays (Affymetrix) for 16hrs at 45°C with constant rotation at 60rpm according to the Affymetrix protocol. Each microarray was used to assay a single sample. After hybridisation, the microarray was washed and stained on an Affymetrix fluidics station and scanned with an argon ion confocal laser, with a 488nm emission wavelength and detection at 570nm. The fluorescence intensity was measured for each microarray.

2.7.3 Data analysis

Probe level intensities were quantile normalised and quantified using RMA (Irizarry et al. 2003). Data analysis was performed with the Genespring software version 3.0 (Silicon Genetics, now Agilent) or Bioconductor software (Gentleman et al. 2004) for the MEF or cortex brain array, respectively.

Probe sets differentially expressed in rotenone treated WT MEFs compared to untreated WT MEFs were identified using one-way analysis of variance (ANOVA) and a false discovery rate (FDR) of 0.15. A lower FDR rate did not result in the identification of any probe sets that were differentially regulated by treatment with rotenone in WT MEFs. Similary, probe sets differentially expressed in rotenone treated HtrA2 KO MEFs compared to untreated HtrA2 KO MEFs were identified by applying a FDR of 0.15, however, even a FDR of 0.07 did return differentially regulated probe sets. In order to identify probe sets that were differentially expressed in HtrA2 KO MEFs compared to WT, the untreated samples for each genotype were subjected to one-way ANOVA using a FDR of 0.05.

Probe sets differentially expressed in HtrA2 KO cortex tissue compared to WT cortex

tissue were identified using one-way ANOVA and a FDR of 0.05, which returned 792 probe sets. Application of a FDR of 0.01 did result in the identification of 79 probe sets differentially expressed in HtrA2 KO cortex tissue.

2.8 Protein techniques

2.8.1 Determination of protein concentrations

Protein concentrations were determined using the Bio-Rad Protein Assay reagent based on the method of (Bradford 1976). Sample dilutions and BSA standards were made in 0.8ml water, incubated with 0.2ml Bio-Rad Protein Assay for 5min and the absorption was measured at 595nm in a plate reader and protein concentrations were determined in the relation to the BSA standard curve.

2.8.2 Lysis of cells

Cells were scraped on ice into lysis buffer containing 50mM Tris base, pH 8, 150mM NaCl, 2mM EGTA, 5% (v/v) Glycerol, complete protease inhibitor tablet (EDTA-free, Roche), and 1-2% CHAPS or 1% Triton X-100. Cells were lysed by vortexing and leaving on ice for 10min. The lysate was then cleared of nuclei by centrifugation at 14,000rpm for 10min at 4°C in a microcentrifuge. Protein concentration was then assessed using the Bradford assay (Bio-Rad). Cell lines were also lysed directly into 1X LDS sample buffer (Invitrogen), sonicated and heated at 70°C for 10min before resolving the samples by SDS-PAGE. Cytosol and mitochondria-enriched fractions were obtained as described previously (Rytomaa et al. 2000).

2.8.3 Human brains

Brain tissue was obtained from the Queen Square Brain Bank (where it had been donated with the informed consent of next of kin) with approval from the National Hospital for Neurology and Neurosurgery/Institute of Neurology Joint Research Ethics Committee. Two flash-frozen post-mortem brains with classical neuropathological appearances of PD, associated with heterozygous mutations in the PINK1 gene were originally identified in an extensive mutation screen (Abou-Sleiman et al. 2006). Four flash-frozen brains with idiopathic PD were used as age-matched and pH-matched controls. Frozen sections from the basal ganglia of six brains were cut using a cryostat

and the caudate nucleus (part of the striatum) was dissected. Tissue was homogenised in 10mM Tris base, pH 7.6, 5mM EDTA, 50mM NaCl, 30mM sodium pyrophosphate, 50mM sodium fluoride, 1mM sodium orthovanadate and 2% CHAPS, incubated on ice for 45min, and centrifuged at 13,000g for 15min at 4 °C. Protein concentration was determined using the Bradford assay decribed before (Bio-Rad).

2.8.4 SDS-PAGE and Western blotting

Protein samples were mixed with loading buffer (LDS sample buffer, Invitrogen), were separated by SDS-PAGE on 4-12% gradient Bis-Tris NuPAGE gels in MES buffer (Invitrogen) at 165V for 1h. Full range pre-stained molecular weight markers (Rainbow Markers, Amersham) were included on all gels. For regular 2D gel electrophoresis, samples were lysed in buffer containing 8M urea, 2% CHAPS (w/v), 5% glycerol (v/v), and 1mM DTT, resolved by isoelectric focusing on immobilised pH 3-10 gradient strips in the IPGPhor system (Amersham) according to manufacturer's guidelines. The strips were then subjected to SDS-PAGE using pre-cast 4-12% gradient Bis-Tris NuPAGE gels (Novex).

Following separation, proteins were transferred onto Immobilon™ polyvenylfluoridine (PVDF) membranes (Millipore) using mini-gel wet transfer apparatus (Bio-Rad) in a buffer containing 25mM Tris base, 250mM glycine, pH 8.3, 20% methanol) at 300mA for 1.25hrs at 4°C.

Membranes were blocked in 5% milk in TBST (20mM Tris base, pH 7.4, 150mM NaCl, 0.1% Tween20) for 1h at room temperature (RT) and then incubated with primary antibodies diluted in 3% BSA in TBST at 4°C o/n with gentle shaking. Membranes were washed three times for 10min in TBST and incubated with the secondary antibody or avidin-labelled with peroxidase diluted in 5% milk in TBST for 45min at RT. Finally membranes were washed three times for 10min in TBST. Immunoreactive proteins were visualised by enhanced chemiluminescence according to the manufacturer's instructions (ECL, Amersham) and exposed to X-ray film (FujiFilm). Where indicated, membranes were stripped in 0.1M glycine pH 2.5, and neutralised in 1M Tris base pH 7.6 before re-blotting.

2.8.5 Immunoprecipitation

For co-immunoprecipitation, cells were lysed in 10mM Tris base, pH7.6, 5mM EDTA, 50mM NaCl, 30mM sodium pyrophosphate, 50mM sodium fluoride, 1mM sodium orthovanadate and 2% CHAPS (v/v). After pelleting insoluble material by spinning at 14,000rpm for 10min at 4°C, the appropriate antibody was added for immunoprecipitation and lysates were rotated at 4°C o/n. Complexes were then isolated by adding protein A sepharose beads rotating at 4°C for 2hrs. Beads were recovered by centrifugation at 1000 x g for 2min at 4°C and washed three times with 1ml of lysis buffer. Following the final wash immunoprecipitated and co-purifying proteins were eluted by the addition of LDS sample buffer (Invitrogen) and heating for 10min at 70°C.

For immunoprecipitation of HtrA2 to assess its proteolytic activity cells were lysed in lysis buffer containing 1% CHAPS (600µl / 10cm dish), and the cleared lysate of two 10cm dishes was pooled. 3µl anti-HtrA2 antibody (Alexis) were added and immunoprecipitated for 4-6hrs at 4°C with rotation. 40µl of a 50% suspension of Protein A beads (Sigma) were added and rotated at 4°C for another 2hrs. Beads were then recovered by centrifugation at 1000 x g for 2min and washed three times (1x in lysis buffer and 2x in a buffer containing 50mM Tris base, pH8, 0.5mM EDTA, 1mM DTT). While the beads were in suspension of the third wash, they were split in two tubes (for assessing the proteolytic activity of HtrA2 with or without a further stimulus).

2.8.6 Recombinant proteins

Mature, C-terminal His6-tagged HtrA2 proteins (Δ133HtrA2 WT, S142D and S400D) in pET-20b (Novagen) were expressed in the *E. coli* strain BL21(DE3)pLysS (Novagen). The point mutations were generated by quickchange PCR mutagenesis. Protein expression was induced by culturing cells at 16°C for 16h in the presence of 0.5mM isopropyl-β-D-1-thiogalactopyranoside (IPTG). Cells were lysed by freezing and thawing in lysis buffer (50mM HEPES, pH 8.0, 300mM NaCl, 10mM imidazole, 1% (v/v) Triton X-100). Lysates were cleared by centrifugation at 10,000 x g for 15min. Supernatants were incubated with nickel-nitrilotriacetic acid beads (Qiagen) for 1h at 4°C. Bound protein was washed with wash buffer (50mM HEPES, pH 8.0,

150mM NaCl, 10mM imidazole, 20% (v/v) glycerol). Elution was performed using an imidazole gradient (20–300mM) in elution buffer (50mM HEPES, pH 8.0, 150mM NaCl, 20% (v/v) glycerol). Eluted protein was dialysed o/n against storage buffer (50mM HEPES, pH 8.0, 150mM NaCl, 20% (v/v) Glycerol, 1mM DTT) and stored in aliquots at -80 °C.

2.8.7 HtrA2 protease assay

Recombinant HtrA2 prepped from *E. coli* was further fractionated by gel filtration chromatography (Superdex 75 prep grade column, GE Healthcare) to separate aggregated proteins from natively folded. Two fractions corresponding to the peak of WT HtrA2 were selected from each of the recombinant HtrA2 proteins. Purity and concentration of recombinant proteins were controlled by SDS-PAGE analysis and Bradford assay (Bio-Rad). The HtrA2 optimal substrate peptide (Mca-IRRVSYSF(Dnp)KK (where Mca is 7-methoxycoumarin-4-acetic acid and Dnp is N-dinitrophenyldiaminopropionic acid)), and the PDZ-binding peptide PDZopt (GQYYFV) were synthesised at the Tufts University Core Facility. Usually, 50nM or 100nM HtrA2 were incubated with 10μM optimal substrate at 30°C in a buffer containing 50mM Tris base, pH8, 0.5mM EDTA, 1mM DTT. Fluorescence was monitored on a CytoFluor multi-well plate reader (PerSeptive Biosystems). In order to achieve similar activity kinetics for WT and S400D HtrA2 (Figure 5-4B), S400D HtrA2 was diluted until it displayed a similar activity curve. When Ucf-101 was used to inhibit HtrA2 activity, HtrA2 and its inhibitor were incubated on ice for 15min prior to addition of the fluorescent substrate and measurement of kinetics. Similarly, 500μM of PDZopt peptide, 150nM recombinant full length XIAP (R&D Systems) or BSA were pre-incubated for 15min with HtrA2 at RT before addition of the fluorescent peptide to determine the maximal activation. Reaction rates (velocity (V) (arbitrary fluorescence units (AFU)/min) were determined by linear regression analysis of the data points corresponding to the maximum reaction rates for each assay condition. Assays are representative of at least three independent experiments.

2.8.8 TAP-tagged protein purification

HEK293 cells expressing HtrA2-TAP or TAP were grown in 15cm culture dishes and 20 plates were used per purification column. The growth media was removed and cells

detached by addition of 2ml of 2mM EDTA in PBS for 10min. Cells were then collected in PBS and pelleted at 1300rpm in a benchtop centrifuge. Cell pellets were washed in PBS and pelleted again. Then cell pellets were lysed on ice in 10ml of 2% CHAPS lysis buffer (50mM Tris base, pH 8, 150mM NaCl, 2% CHAPS, 2mM EGTA, 5% (v/v) Glycerol, complete protease inhibitor tablet (EDTA-free, Roche)) with 10 strokes in a glass dounce homogeniser. The lysate was then cleared of nuclei and large fragments by centrifugation at 4300 x g for 20min at 4°C and then added to a 15ml tube containing 500µl of a 50% suspension of pre-washed IgG-linked agarose (Sigma) and incubated for 2hrs at 4°C with rotation. Beads were then recovered by centrifugation for 5min at 1600rpm in a benchtop centrifuge and washed 3 x 10ml 1% CHAPS lysis buffer and then 1 x 10ml TEV cleavage buffer (10mM Tris base, pH8, 150mM NaCl, 0.1% (v/v) CHAPS, 0.5mM EGTA, 1mM DTT). The bead matrix, resuspended in the second of these washes, was transferred to a 15ml Poly-prep chromatography column (Bio-Rad) to simplify further handling. After the TEV cleavage buffer wash the base of the column was capped and 1ml TEV cleavage buffer and 80U recombinant TEV protease (Invitrogen) were added. The column was then capped at the top and incubated for 2hrs at RT with rotation. Flollowing TEV cleavage the sample was eluted directly into a second column capped at the base and containing 500µl of a 50% suspension of Calmodulin-linked affinity resin (Stratagene). 3.5ml calmodulin binding buffer (10mM Tris base, pH 8, 150mM NaCl, 0.1% CHAPS, 1mM MgAcetate, 1mM imidazole, 2mM $CaCl_2$, 10mM β-mercapto-ethanol) and 3.5µl 1M $CaCl_2$ were then added, the column capped at the top and incubated for 2hrs at 4°C with rotation. Finally, the calmodulin resin was washed with 3 x 10ml calmodulin binding buffer and bound proteins were eluted in 5 x 200µl fractions of calmodulin elution buffer (10mM Tris base, pH 8, 150mM NaCl, 0.1% CHAPS, 1mM MgAcetate, 1mM imidazole, 2mM EGTA, 10mM β-mercapto-ethanol). At each step aliquots were saved for diagnostic Western blotting. Final TAP eluates were concentrated using Microcon YM-10 columns (Millipore) operating at 5000 x g and 4°C from an initial volume of 1ml to a final volume of ~30-100µl. LDS sample buffer (Invitrogen) was added and the sample run on 4-12% NuPAGE gels as previously described.

2.9 2D DIGE

2.9.1 Sample preparation

Two sets of 2D DIGE gels were run, each containing four replicates. The first set did compare WT and HtrA2 KO mitochondrial proteins (isolated from four pairs of WT and HtrA2 KO littermates), and the second set did compare WT and HtrA2 KO mitochondria from two pairs of littermates, where a subset of the mitochondria had been treated with heat shock for 30min at 42°C following 30min at 30°C. Mitochondrial pellets were lysed in 2-DE lysis buffer (7M urea, 2M thiourea, 4% (w/v) CHAPS, 65mM DTT, 1% pharmalytes pH 3-10) containing a protease inhibitor cocktail (Complete Mini, Roche) and endonuclease (Benzonase, Merck) for 1h at RT. To remove unsolubilised debris the lysates were centrifuged at 4°C for 5min at 14,000rpm in a microfuge. Prior to labeling, all protein samples were cleaned using the 2-D Clean-up kit (GE Healthcare). The resulting pellets were resolubilised in DIGE labeling buffer (7M urea, 2M thiourea, 4% (w/v) CHAPS, 30mM Tris base, pH 8.5) to give a final protein concentration between 5 and 10 mg/ml. Protein concentrations of the lysates were determined using the 2-D Quant Kit (GE Healthcare) using a BSA standard curve with replicate assays performed for each sample.

2.9.2 CyDye labelling of protein extracts

Lyophilised CyDye DIGE Fluors were reconstituted in anhydrous DMF to a final stock solution concentration of 1nmol/µl, and stored at -20°C. For labelling experiments, each CyDye was diluted in DMF to a working concentration of 400pmol/µl. Samples were labelled following the manufacturer's recommended protocol. For each sample, 50µg of protein was labelled at a ratio of 8pmole Cy3 or Cy5 CyDye fluor/µg protein, where for replicates 1 and 2 the WT samples were labelled with Cy3 and the HtrA2 KO samples were labelled with Cy5, and for replicates 3 and 4 vice versa. A pooled standard (consisting of equal amounts of each of the samples to be analysed) was labelled with the Cy2 fluor at the same ratio of 8pmole CyDye fluor/µg protein. Labelling reactions were incubated for 30min on ice in the dark and stopped by quenching with 10mM lysine, followed by a further 10min incubation on ice.

2.9.3 2D gel electrophoresis

For the first dimension IEF, 24cm pH 3-10 (linear) Immobiline DryStrip (IPG) strips (GE Healthcare) were re-hydrated with with 450ml DeStreak solution (GE Healthcare) at RT o/n in a re-swelling tray. 150µg of CyDye labelled proteins (50µg of each fluor Cy2, Cy3 and Cy5) were cuploaded onto the re-swelled IEF strips. Isoelectric focussing was performed on an Ettan IPGphor IEF System using the Ettan IPGphor Cup Loading Manifold (both GE Healthcare). Focussing was performed for a total of 55kVh at 20°C, at a maximum current of 50µA/strip, as described previously (Unlu et al. 1997). Following IEF, for the second dimension SDS-PAGE, the strips were equilibrated for 15min in equilibration buffer (6M urea, 30% (v/v) glycerol, 2% SDS, 50mM Tris base, pH 8.8, and 0.01% (w/v) bromophenol blue) containing 1% DTT, followed by a further 15min in the same buffer containing 2.5% iodoacetamide (IAA) in place of the DTT as described previously (Unlu et al. 1997). Equilibrated IPG strips were transferred onto 1mm thick 25 x 20cm 12% polyacrylamide gels without a stacking gel, cast between low-fluorescence glass plates. The IEF strips were overlaid with 0.5% low melting point agarose in 2X electrophoresis buffer (50mM Tris base, 384mM glycine, 0.2% (w/v) SDS) with bromophenol blue. Gels were electrophoresed in an Ettan Dalt six gel tank (GE Healthcare) at 20°C, at 1.5 W/gel constant power (o/n) until the bromophenol blue dye front had migrated off the bottom of the gel. A running buffer of 25mM Tris, 192mM glycine, 0.1% (w/v) SDS was used for the lower chamber. 2X running buffer was used for the upper chamber.

2.9.4 Image acquisition and analysis

Following SDS-PAGE, fluorescently labelled proteins were visualised while still between the low-fluorescence glass plates using a Typhoon 9400 Variable Mode Imager and Typhoon Scanner Control Software, Version 3.0 (GE Healthcare). For the Cy2 images a 488nm laser and an emission filter of 520nm with a band pass (BP) of 40 nm was used. Cy3 images were obtained using a 532nm laser and an emission filter of 580 nm/BP30. Cy5 images were obtained using a 633nm laser and an emission filter of 670 nm/ BP30. For each scan the photomultiplier tube (PMT) voltage was adjusted on each channel (Cy2, Cy3 and Cy5) to give a maximum pixel value of between 60,000 and 80,000 to avoid image saturation (pixel value 100,000). Low-resolution (1000µm pixel size) pre-scans were used to obtain the PMT voltage settings, which were then

used for high resolution (100μm pixel size) analytical scans of all gels. All images were cropped using ImageQuant Tools to exclude non-essential information prior to DeCyder analysis. For image analysis using DeCyder, images were exported as .gel files, together with a .ds file which links the three separate .gel files for each CyDye from one gel. Analysis of gel images was performed using DeCyder Differential Analysis Software Version 5.0 (GE Healthcare). The software was used to match all 12 protein spot maps from the 4 gels per set. The Biological Variation Analysis (BVA) module was used to compare abundance changes across the WT and HtrA2 KO mitochondrial samples. DeCyder performs Student's t-tests to determine statistically significant changes, as well as calculating mean abundance changes between the two sample populations.

2.9.5 Preparative gels

Preparative gels for spot picking were prepared by running 400 to 500μg of protein on 2D gels. Due to the higher protein load, samples were applied to the first dimension strips using an in-gel re-hydration method. Samples were diluted in re-hydration solution (8M urea, 0.5% (w/v) CHAPS, 65mM DTT, 0.5% (v/v) pharmalyte pH 3 -10). Protein spots were visualised using silver staining using a mass spectrometry compatible stain modified from (Shevchenko et al. 1996). Silver stained preparative gels were imaged on a Molecular Dynamics Personal Densitometer SI (GE Healthcare). Protein spots of interest were manually excised.

2.10 Mass spectrometry

For mass spectrometry of proteins, the protein spots of interest were excised from SDS-PAGE gels, destained, trypsinised and MALDI-TOF mass spectrometric characterisation was performed by the Protein Analysis Service of Cancer Research UK.

Lipid extraction from purified mitochondria using a Percoll gradient was accomplished as described earlier and extracts were analysed by nano-electrospray time of flight mass spectrometry using a LCT instrument (Micromass) set in positive ion mode (Sorice et al. 2004). A few microliters of the extracts were injected using capillary voltage at 2,250 V and sample cone at 35 V. Semi-quantitative evaluation of lipid peaks was

undertaken using a set of internal reference ions that maintained equivalent relationships within multiple spectra of the same sample and showed little variation between WT and HtrA2 KO samples. The data was normalised to the major phosphatidyl choline, that is PO-PC (mass-to-charge ratio *m/z* 758), which was in turn normalised to other reference ions like C-24 Ceramide (*m/z* 685) (Sandra et al. 2005).

2.11 Methods to measure cell death

2.11.1 Analysis of DNA content – sub-G1 apoptosis assay

Immortalised MEFs were plated (2 x 10^5 per well) in 6-well plates and treated 16hrs later with CCCP (Calbiochem), rotenone (Sigma), tunicamycin (Sigma) or etoposide (Calbiochem) for 27hrs or H_2O_2, (all Sigma) for 4.5hrs. Immortalised HtrA2 KO and HtrA2 KO MEFs restored to express human HtrA2 were treated for 20hrs with MG-132 (Calbiochem) and 6-OHDA (Sigma) or 3hrs with staurosporine (Calbiochem). Cells were harvested by trypsinisation and washed in PBS. Then cells were fixed with ice cold 70% ethanol added dropwise while vortexing. After fixation for at least 30min at 4°C, the cells were washed twice in phosphate-citrate buffer (0.2m Na_2HPO_4, 4mM citric acid, pH 7.8) and collected by spinning at 2000rpm in a benchtop centrifuge. Each sample was then treated with 50µl of 100µ/ml RNase followed by 200µl of 50µg/ml propidium iodide (PI). Cells were then analysed by FACS using a FACSCalibur instrument (Becton Dickinson) as previously described (Darzynkiewicz and Bedner 2000). Debris and cell doublets were excluded from the analysis and the PI staining intensity (FL-3) was recorded as a measure of DNA content. For each sample at least 10,000 events were acquired and data analysis was performed using FloJo software (TreeStar).

2.11.2 Annexin V staining

Immortalised MEFs were grown in 6-well dishes at 0.7 x 10^5 cells and transfected with 1µg vector or PINK1 expression constructs and, in order to identify the transfected cells, 0.2µg of a plasmid encoding farnesylated EGFP (pEGFP-F) using Genejuice (Novagen) according to the manufacturer's guidelines. 24hrs after transfection the cells were treated with vehicle or MG-132, and the following day for 3hrs with staurosporine before harvesting all cells and washing in PBS. Cells were then resuspended in

calcium-rich buffer (Becton Dickinson) containing 2µl Alexa 647 linked anti-Annexin V antibody (Molecular Probes) in a final volume of 200µl. Cells were stained for 15min at RT in the dark, before placing them on ice and keeping them in the dark. 3µl PI were added just before analysis to each sample. Cells were analysed by FACS using a FACSCalibur instrument (Becton Dickinson). The instrument was configured to measure GFP (FL-1) fluorescence intensity and the analysis was gated on GFP-positive cells. The transfected cells were then analysed for AnexinV Alexa 647 (FL-4) and PI (FL-2/3). The percentage of GFP-positive cells displaying characteristic features of apoptotic cell death (ie. Annexin V-positive and PI-negative) was calculated as a proportion of the total GFP-positive cells using CellQuest software (Becton Dickinson).

Immortalised MEFs were grown in 6-well dishes at 2 x 10^5 cells. The next day cells were pre-treated with vehicle or the HtrA2 inhibitor Ucf-101 (Calbiochem) for 20min before addition of vehicle or 2µM staurosporine for 4hrs. Cells were harvested, washed in PBS and stained with Annexin V Alexa 647 and PI as described previously. The percentage of Annexin V-positive and PI-negative cells was calculated as a proportion of all cells.

2.11.3 Measurement of chromatin condensation

For neuron cell death analysis, cells were incubated in the presence or absence of glutamate (Sigma) for 4hrs, fixed in 4% paraformaldehyde, stained with Hoechst 33342 (Molecular Probes) according to the manufacturer's instructions and nuclear chromatin was scored as being condensed or non-condensed by fluorescence microscopy.

2.12 Mitochondria techniques

2.12.1 Morphological analysis of mitochondria

WT and HtrA2 KO MEFs were cultivated in DMEM containing 10% FBS until confluency. Cells were then subjected to the following treatments for 30 minutes: 25µM CCCP (Calbiochem) or 25µM rotenone (Calbiochem). Following treatment, media was replaced and cells were further incubated at 37°C for 2hrs. Following incubation cells were processed for electron microscopy by gently replacing the culture

medium with fixative solution (4% paraformaldehyde, 5% glutaraldehyde and 5mM $CaCl_2$ in 0.2M cacodylate buffer at pH 7.4) and incubating for 1h at RT. Cells were post-fixed with 1% osmium tetroxide/1% potassium ferrocyanide for 1h at RT. Fixed cells were stained with 5% aqueous uranyl acetate o/n at RT and harvested by scraping. The resulting pellet was dehydrated and embedded in TAAB embedding resin. Ultra thin sections were stained with lead citrate and examined in a Jeol 100-CXII electron microscope equipped with a rotating stage/eucentric goniometer. All quantitative assessments of mitochondrial morphology were based on scoring a minimum of 25 cells for each treatment. For each treatment, the number of mitochondria showing specific changes was determined.

2.12.2 Isolation of mitochondria

Mitochondria were purified from mouse livers of WT and HtrA2 KO mice at P15 to P30 using differential centrifugation. In order to achieve high purity, a percoll gradient was employed for further purification. The entire procedure was carried out at 4°C. All equipment used (dounce homogeniser, tubes) were rinsed with ice cold buffers before using. Mice were culled and livers taken out, being careful not to take any white connective material. The liver was immediately placed in 10ml ice cold buffer HSB (0.3M sucrose, 10mM HEPES, pH 7.4). The liver was cut into small cubes using two scalpels and a petri dish cooled in an ice bucket as tray. Bring volume to 15ml HSB per liver. The material was homogenised using a 15ml cooled glass dounce homogeniser with a loose pestle for 15 strokes or until there were no tissue pieces visible any more. The material from two livers could be pooled per sample. The dounce homogeniser was washed with another 10ml of HSB and this was pooled with the homogenised material, which then was centrifuged at 600 x g for 5min at 4°C to remove cell and tissue debris. The red blood cells did pellet. The supernatant was taken and the centrifugation repeated.

For purification using a Percoll gradient, the resulting supernatant was centrifuged at 8700 x g for 10min at 4°C to precipitate the mitochondrial fraction, which should be brownish/white. The supernatant was carefully discarded, and 10ml HSB supplemented with 1mM PMSF was added. The pellet was gently detached using the tip of a teflon prestle, and resuspended using a dounce homogeniser with 4-5 gentle strokes.

Centrifugation at 8700 x g for 10min at 4°C did pellet the mitochondria. The pellet was resuspended by homogenisation as before in 2ml of buffer MMB (0.3M mannitol, 5mM Mops, pH 7.2) using a small 1.5ml dounce homogeniser. The suspension was deposited on the top of the following Percoll gradient using a pasteur pipette: 1.5ml of 70% Percoll (Sigma) in MMB, 4ml of 30% Percoll in MMB, and 2ml of 10% Percoll in MMB (from bottom to top) in Beckmann Ultra-Clear centrifuge tubes (14 x 89mm, cat no: 344059). The sample was spun in an ultracentrifuge at 13,500 x g using a swinging buckets rotor for 35min at 4°C, with the brake at the zero position. The brownish mitochondrial material at the interface of 70-30% Percoll was taken off using a pasteur pipette, these are the functional intact mitochondria and everything above is disrupted mitos. The mitochondria were washed twice in 10ml cold buffer MSB (0.4M mannitol, 10mM NaH_2PO_4, 20mM HEPES, pH 7,4, 0.5mM EGTA), by homogenisation as before using a dounce homgeniser and centrifugation at 8700 x g for 10min at 4°C. The final pellet was resuspended in 1ml of MSB, and when necessary flash frozen and stored at -80°C. For heat shock, the freshly isolated mitochondria were incubated at 42°C for 30min and for another 30min at 30°C, before flash freezing.

For isolation of mitchondria by differential centrifugation only, the livers were homogenised in HSB as before or in buffer LHM (0.2M mannitol, 50mM sucrose, 10mM KCl, 1mM EGTA, 10mM HEPES, pH 7.4). The supernatant from the initial spins at 600 x g was centrifuged at 3000 x g for 10min at 4°C to precipitate the mitochondrial fraction and avoid pelleting lysosomes. The supernatant was carefully discarded, and 10ml HSB or LHM was added. The pellet was gently detached using the tip of a teflon prestle, and resuspended using a dounce homogeniser with 4-5 gentle strokes. Centrifugation at 3000 x g for 10min at 4°C did pellet the mitochondria again. This wash was repeated, and the final mitochondrial pellet was resuspended in MSB as before or mitochondria import buffer (MIB) (0.3M mannitol, 0.1mg/ml BSA, 2mM ATP, 2mM NADH, 2mM potassium phosphate, pH 7.5, 2mM β-mercato-ethanol, 50mM HEPES, pH 7.4) when the mitochondria were used for the *in vitro* import assay of *in vitro* translated proteins into mitochondria (see 2.12.3 Mitochondria import assay). The purity of the isolated mitochondria was routinely assessed by Western blotting using anti-KDEL (endoplasmic reticulum, Stressgen), anti-Cathepsin D (lysosomal) and anti-Actin antibodies (cytosolic, both Santa Cruz Biotechnology).

2.12.3 Mitochondria import assay

5µl of *in vitro* translated protein were incubated with 50µg of mitochondria in 20µl MIB (final is 25µl) at 25°C, usually for 1h unless otherwise indicated. The import was stopped by addition of 225µl of MIB containing 50µg/ml Proteinase K to each sample to digest proteins bound to the outer surface of the mitochondria (iso-osmotic conditions). In order to achieve hypo-osmotic treatment of the mitochondria resulting in rupture of the outer mitochondrial membrane only retaining the matrix proteins (formation of mitoplasts), the Proteinase K treatment was performed in a buffer containing 20mM HEPES, pH7.4 and 50µg/ml Proteinase K. The digest was incubated on ice for 15min, then 750µl MIB containing 2.5µl PMSF were added to stop the reaction. Mitochondria were pelleted at 8000 x g for 5min at 4°C, then 25µl 1X LDS (Invitrogen) were added to the pellet. Proteins were separated on a 4-12% gradient Bis-Tris NuPAGE gel (Novex, Invitrogen), transferred onto PVDF membranes and exposed to phosphoimager screen. *In vitro* translated mature HtrA2 lacking the mitochondria import sequence was included as a negative control, and full length HtrA2 as a positive control. Hypo-osmotic treatment of the mitochondria after import of full length HtrA2 did abolish the HtrA2 signal validating its location in the intermembrane space.

2.13 Statistical analysis

Data are presented as mean values and error bars indicate either the standard deviation, the standard error or the range of two determinations (Cumming et al. 2007). The p-values in Figure 4-3C and Figure 4-8 were calculated using a two-tailed unpaired t-test. The groups in Figure 5-4A were compared by one-way ANOVA using Bonferroni's post test using Prism statistical analysis software (www.graphpad.com). The significance is indicated as *** for $P < 0.001$.

3 Chapter 3: A neuroprotective role for HtrA2 *in vivo*

3.1 Introduction

The serine protease HtrA2 is released from the mitochondrial intermembrane space following apoptotic stimuli. Once in the cytosol, HtrA2 has been implicated in promoting cell death by binding to IAPs via its N-terminal IBM, thus inducing caspase activity (Suzuki et al. 2001; Hegde et al. 2002; Martins et al. 2002; van Loo et al. 2002; Verhagen et al. 2002). In addition, HtrA2 has been described to mediate caspase-independent death through its own protease activity (Suzuki et al. 2001; Hegde et al. 2002; Martins et al. 2002; Verhagen et al. 2002). However, these studies used over-expressed HtrA2 and probably any protease, when strongly over-expressed, might be able to induce cell death. At the commencement of this work, the physiological role of HtrA2 in the mitochondrial intermembrane space was poorly understood, physiological substrates of HtrA2 had not been identified, and the importance of its role as an IAP-interacting protein in apoptosis was the subject of much debate. In this chapter, the role of HtrA2 *in vivo* is illuminated, and mitochondrial substrates of its proteolytic activity are studied. The function of HtrA2 is studied by examining the phenotype of HtrA2-deficient mice and HtrA2's involvement in cell death is tested in cells derived from these mice. Unexpectedly, HtrA2 appears not to possess a pro-apoptotic function *in vitro*, but on the contrary, HtrA2 seems to protect mitochondria from stressful insults.

3.2 Deletion of HtrA2 results in a neurological phenotype leading to death at one month post-birth

In order to address the physiological role of HtrA2 *in vivo*, HtrA2-deficient mice were generated. These mice were made by Alastair Morrison and co-workers at GlaxoSmithKline, Harlow, Essex. The HtrA2 gene was disrupted by homologous recombination in 129/sv ES cells to generate HtrA2 KO mice (Figure 3-1A). The targeting vector was designed such that 83% of the coding region, encompassing part of exon 1, all of exons 2-6, and part of exon 7 were replaced with the PGK-neo cassette. Three independent ES cell clones carrying the mutated HtrA2 allele were obtained. Two of these targeted ES cell clones were injected into C57Bl6/J-derived blastocysts and chimeric mice were born. High percentage male chimaeras from both clones were identified by their coat colour and crossed with C57Bl6/J females to

produce N1F0 offspring. HtrA2 Het offspring derived from one of the targeted ES cell clones were back-crossed for at least 5 generations onto the C57Bl6/J strain. Back-crossed HtrA2 Het animals were then inter-crossed to produce the F1 progeny. Analysis of genomic DNA prepared from tail biopsy samples by PCR confirmed the successful disruption of the HtrA2 gene (Figure 3-1B). To verify that the KO allele was a null mutation, RNA prepared from brain tissue was used to generate cDNA as template for quantitative real-time PCR (qPCR). About 50% reduction in HtrA2 mRNA in Het and no product in HtrA2 KO animals were detected (Figure 3-1C). To check the level of HtrA2 protein, MEFs were prepared from HtrA2 WT, Het and KO littermates and lysates were subjected to Western blotting to detect HtrA2 expression. This analysis revealed the absence of HtrA2 protein in cells derived from KO animals and a partial reduction of protein levels in cells derived from embryos heterozygous for the HtrA2 locus (Figure 3-1D).

Genotypic analysis of the progeny of HtrA2 Het x Het crosses by PCR revealed that out of 157 pups, 40 (25%) were WT, 85 (54%) Het for the mutation and 32 (21%) were HtrA2 KO, consistent with almost normal Mendelian inheritance and indicating that deletion of the HtrA2 gene does not result in gross embryonic lethality (Figure 3-2A). Analysis of the resulting HtrA2 KO animals revealed that from P18 they began to display striking phenotypic alterations when compared with WT or Het littermates. The most dramatic alteration observed was failure to gain weight following weaning at P18 (Figure 3-2B), whereas HtrA2 Het mice did not show a difference compared to WT mice. The phenotype of HtrA2 KO mice resulted in small runted animals at P30 (Figure 3-2C). Animals lacking HtrA2 also showed a general decrease in organ size. The degree of decrease in organ size was variable, being particularly dramatic in the case of thymus, heart and spleen (data not shown). Hair loss was also occasionally seen in the HtrA2 KO mice.

Examination of the behaviour of HtrA2 KO animals revealed several neurological abnormalities. Animals lacking HtrA2 were characterised by a progressive movement disorder beginning at P18. They displayed decreased mobility and bradykinesia (difficulty to initiate movements), bended posture and tremor, and exhibited lack of coordination. Such features are characteristic of a parkinsonian syndrome in humans and have also been described in animal models of this disease (Betarbet et al. 2002).

HtrA2 KO animals died between P30 to P40, mostly due to respiratory failure. In order to minimise their suffering, HtrA2 KO mice were routinely euthanised at P30 or earlier. All the animal husbandry and experimental procedures were carried out in full compliance with the United Kingdom Animal Act of 1986 and were approved by the Cancer Research UK procedures panel.

In order to test the movement skills of the mice, they were challenged on an inclined platform test (Schaefer et al. 2000). This test monitors the ability of the mice to reach the top of an inclined platform and has been used previously to examine the onset of ataxia in mice developing a progressive neurological disorder due to expression of mutant prion protein (Chiesa et al. 1998). HtrA2 KO mice around P30 demonstrated a decreased performance on the inclined platform test, with only half of the KO mice reaching the top of the platform (Figure 3-2D). In addition, the fact that HtrA2 KO mice that managed to reach the top of the platform took three times longer (Figure 3-2E) than WT or Het littermates, suggested that deletion of HtrA2 results in deficiencies in coordination and/or strength. However, although some of the KO animals failed to stay on the platform for the 60sec trial period, 63% of KO animals remained on the platform for the entire trial, suggesting that they were not grossly impaired in muscle strength and that disturbances in coordination were principally responsible for their poor performance.

3.3 HtrA2 deletion results in the selective loss of a population of striatal neurons

The fact that the phenotype of HtrA2 KO mice was reminiscent of Parkinson's disease (PD), prompted the investigation of whether these animals displayed histopathological deficits similar to human PD patients. At the morphological and anatomical level, PD is characterised by degeneration of the neural connection between the substantia nigra (SN) and the striatum, two brain regions essential for normal motor function (for review (Fahn 2003)). The striatum receives its dopaminergic input from neurons of the substantia nigra pars compacta (SNpc) via this nigrostriatal pathway. Progressive degeneration of the nigrostriatal dopaminergic pathway results in profound striatal dopamine deficiency, leading to the described motor deficiencies.

Brains from HtrA2 KO mice were prepared for histopathology to examine for pre-synaptic deficits by analysing the SN or post-synaptic deficits by analysing the striatum. First, the neuronal circuits in the striatum of HtrA2 KO animals were examined. P30 KO animals were analysed as they displayed the most severe phenotypes. Analysis of brains from HtrA2 KO animals revealed a selective loss of a neuronal population in the striatum, just lateral of the thalamus in a relatively posteriomedial portion of the basal ganglia (Figure 3-3A). In the haematoxylin-eosin (H&E) stained sections (Figure 3-3B) focal loss of neurons was identified, with occasional ballooned cells and concomitant reaction of the astrocytes, as highlighted in a GFAP immunostain (Figure 3-3C). This loss of neurons is more clearly seen in sections immunostained for the microtubule-associated protein MAP2, a neuronal marker (Figure 3-3D). Occasionally, apoptotic cell bodies were detected (data not shown). In order to rule out a general and widespread loss of neurons in the striatum, stereological cell counts of striatal neurons were performed. These results indicated that there is no significant change in the overall neuronal density in the striatum of HtrA2 KO animals, but only in the posterior portion of the basal ganglia (Figure 3-3E). Both at P20, where no phenotypic alterations are detectable, and at P30, a decrease of neuronal density in brains from HtrA2 KO animals was detected, suggesting that neuronal loss precedes the full development of the parkinsonian syndrome. Concomitant with the neuronal loss, a selective loss of terminals, highlighted by tyrosine hydroxylase staining, of the nigrostriatal pathway in the posterior portion was identified when compared to the whole striatum (Figure 3-3F). Analysis of tyrosine hydroxylase positive neurons in the SNpc of HtrA2 KO animals revealed no loss of dopaminergic neurons when compared with WT littermates (Figure 3-3G). At present, it is unclear if this loss of terminals is a cause or a consequence of the neuronal loss detected.

3.4 HtrA2 Het mice do not develop a late onset phenotype

In the last decade, the identification of several genes that cause rare familial forms of PD has revealed novel proteins and pathways that may be involved in the development of this disease. The human HtrA2 gene is located on Chromosome 2p13. This position is within the Parkinson's Disease-3 (PARK3) locus identified in familial PD (Gasser et al. 1998). The gene responsible for the development of PD in the PARK3 families has

not been identified yet, therefore HtrA2 could be a potential candidate. Since the inheritance pattern for the PARK3 locus is autosomal dominant in the human families, the HtrA2 Het mice were examined for the development of late-onset coordination and movement disabilities. Groups of 10 WT and 10 HtrA2 Het mice were trained to run on a rotarod, a rotating stick, and the time until they fell off was measured. The mice were tested on three consecutive days every two months at an age between 10 to 16 months. However, no difference in the movement skills between the WT and Het mice was apparent at any time (Figure 3-4). Therefore, loss of HtrA2 function, as measured by this assay, seems to be recessively inherited in mice, although it cannot be ruled out that the lifespan of inbred mice is too short to detect the development of a phenotype in HtrA2 Het animals.

3.5 Deletion of HtrA2 does not alter cell proliferation or metabolic activity, but results in mitochondrial dysfunction

The homozygous deletion of HtrA2 in mice clearly leads to a severe phenotype and therefore the effect of loss of HtrA2 at the cellular level was studied. The rate of proliferation as monitored by cell counting was determined in primary or immortalised MEFs derived from WT and HtrA2 KO mice. No differences were detected over a three day period (Figure 3-5A and B). Similarly, the metabolic activity of WT and HtrA2 KO MEFs was not demonstrably different. The MEFs were treated with either CCCP, an uncoupler of mitochondrial respiration leading to a collapse of mitochondrial membrane potential, or rotenone, an inhibitor of complex I of the respiratory chain, or tunicamycin, an inhibitor of N-linked glycosylation in the endoplasmatic reticulum (ER) causing accumulation of proteins in the ER. These drugs did impact on the metabolic activity of the MEFs, however, there was no discernible difference between the WT and HtrA2 KO MEFs (Figure 3-5C, D, and E).

Given that the serine protease HtrA2 is localised to the intermembrane space of mitochondria in healthy cells, the effect of HtrA2 loss could impinge on mitochondria without notably affecting overall cellular metabolic activity. To test this possibility, the mitochondrial morphology was examined at the ultra structural level in WT and HtrA2 KO MEFs following treatment with mitochondrial stress-inducing agents. These experiments were performed by Valentina Fedele at the MRC Toxicology Unit in

Leicester. Using transmission electron microscopy (TEM), three types of previously described mitochondrial morphologies in untreated cells were observed (Ghadially 1982): normal mitochondria, mitochondria displaying ballooning of cristae (intracristal swelling) and mitochondria with abnormal form (the latter only detected in cells from KO animals) (Figure 3-6A). When cells were subjected to mitochondrial stresses in the form of the complex I inhibitor rotenone and the mitochondrial membrane potential uncoupler CCCP, cells lacking HtrA2 contained an increased percentage of mitochondria characterised by abnormal morphological alterations (Figure 3-6B and C). Therefore, deletion of HtrA2 may confer upon mitochondria an increased sensitivity to stress.

3.6 Deletion of HtrA2 results in increased susceptibility to cell death stimuli

It is possible that the increased susceptibility of HtrA2 KO mitochondria to stress could affect cell viability. To test this, immortalised WT or HtrA2 KO MEFs were subjected to apoptosis-inducing agents and the population of sub-G1 cells was measured by FACS (Figure 3-7A). Loss of HtrA2 led to increased sensitivity to agents that perturb mitochondrial function, such as CCCP and rotenone, as well as agents that cause both oxidative stress (hydrogen peroxide) and ER stress (tunicamycin). MEFs lacking HtrA2 did not show an altered sensitivity to the DNA damaging agent etoposide.

In addition to using WT and HtrA2 KO MEFs, human HtrA2 was stably re-expressed in HtrA2 KO MEFs. These restored MEFs exhibited reduced sensitivity to agents affecting mitochondrial function, shown here for 6-hydroxydopamine which inhibits complex I of the respiratory chain and leads to oxidative stress, and accumulation of proteins through the proteasome inhibitor MG-132 (Figure 3-7B). Staurosporine, a broad-spectrum kinase inhibitor that induces apoptosis very potently, did not have a differential effect on restored and HtrA2 KO MEFs similar to etoposide. The general indication from these experiments was that cells lacking HtrA2 were predominantly sensitised to stresses that have been described in the field of PD research, namely mitochondrial and oxidative stress, disturbance of the ER, and protein accumulation.

Since neuronal cells showed clear signs of degeneration in HtrA2 KO animals, cultured neurons isolated from KO mice might be more sensitive than WT controls to excitotoxic stimuli. Primary cortical neurons were isolated and subjected to glutamate-mediated excitotoxicity. These experiments revealed a significant increase in the susceptibility of neurons obtained from HtrA2 KO animals to excitotoxic stimuli (Figure 3-7C).

Taken together, the results presented so far indicate that, rather than protecting cells from apoptosis, deletion of HtrA2 results in increased sensitivity to a specific subset of death stimuli.

3.7 Identification of differential protein levels in HtrA2 KO mitochondria

Mammalian HtrA2 has homologues in bacteria, which act to protect the bacteria from the accumulation of unfolded proteins, either by cleaving them directly as in the case for DegP (Spiess et al. 1999), or by activating a transcriptional stress response and inducing expression of chaperones as in the case for DegS (Walsh et al. 2003). In order to find out if loss of HtrA2 would impact on the mitochondrial proteome, fluorescence 2D difference gel electrophoresis (2D DIGE) was employed. 2D DIGE is a powerful method for detecting protein expression differences with high accuracy and reproducibility. It uses molecular weight- and pI-matched, spectrally resolvable dyes to label protein samples prior to 2D electrophoresis on the same gel (Unlu et al. 1997). This method has been successfully used to identify alterations in the mitochondrial proteome, both from cell culture (Lehr et al. 2005) and mouse models of stress (Douette et al. 2005).

Liver mitochondria were isolated to high purity from four pairs of WT and HtrA2 KO littermates for the first set of 2D DIGE gels with 4 replicates. In addition, half of the isolated mitochondria were subjected to heat shock at 42°C for 30 minutes to be run on a second set of 2D DIGE gels, comparing untreated with heat shocked condition between WT and HtrA2 KO mitochondria. HtrA2 proteolytic activity can be increased by heat shock (Martins et al. 2003), therefore comparing heat shocked WT and HtrA2 KO mitochondria might enhance the differences between those genotypes.

Four replicate groups were run per 2D DIGE set, but no gross overall changes in protein level were detected (Figure 3-8A) between WT and HtrA2 KO mitochondria in both untreated and heat shocked conditions. The presence and absence of HtrA2 was confirmed by Western blot (Figure 3-9A), however it could not be identified in the fluorescent 2D DIGE gel images. The DeCyder software from Amersham was used to detect and analyse the protein spots on the 2D DIGE gels. Only two areas around pH6-7 and molecular weights of 66kDa and 30kDa appeared to be differential, these areas are shown enlarged in Figure 3-8A and labelled as spots 1, 8 and 9 in Figure 3-8B. In addition within the software, all protein spots were sorted on the mean ratio of change between WT and HtrA2 KO and then manually investigated for the reproducibility across the replicate groups and examined for their behaviour in the heat shocked samples. Spots found to show a greater difference in the heat shocked samples than in the untreated were of particular interest, because these might possibly comprise HtrA2 substrates. All spots picked and analysed by mass spectrometry were labelled in Figure 3-8B and their identities are listed in Table 3-1. It is notable that, unlike in publications detecting strong differences by 2D DIGE (for example (Douette et al. 2005; Lehr et al. 2005; Henkel et al. 2006)), none of the spots identified here were very convincingly differential between WT and HtrA2 KO mitochondria.

The catalytic centre of HtrA2 is in the intermembrane space of the mitochondria. Therefore, proteins localised in the matrix were deemed to be unlikely HtrA2 substrates and not followed up (dimethylglycine dehydrogenase, DMGDH; succinyl-CoA synthase β subunit, SUCLA2; electron transfer flavoprotein α subunit, ETFA). Similarly, succinate dehydrogenase flavoprotein subunit, SDHA, belonging to complex II of the respiratory chain, which is inserted into the inner membrane and facing the mitochondrial matrix, is an improbable substrate of HtrA2.

3.7.1 Grp75, chaperone of the Hsp70 family

Grp75 belongs to the Hsp70 chaperone family and assists the re-folding of proteins translocated into the mitochondrial matrix. The spot identified as Grp75 by mass spectrometry seemed to exhibit a slightly basic shift in HtrA2 KO mitochondria. Sample pairs from the 2D DIGE replicates as well as another pair of WT and HtrA2 KO mitochondria treated in the same way, were separated on 2D SDS-PAGE and

Grp75 was detected by Western blot (Figure 3-9B). However, no differences in Grp75 level or isoelectric point could be confirmed.

3.7.2 UQCRC1, respiratory chain complex III core complex I

Ubinquinol cytochrome C reductase core complex I, UQCRC1, was identified on the 2D DIGE gels to potentially show a reduction in response to heat shock in WT, but not HtrA2 KO mitochondria. When mitochondrial samples were separated by 2D SDS-PAGE (data not shown) or 1D SDS-PAGE (Figure 3-9C), no changes in UQCRC1 levels could be determined by Western blot.

3.7.3 CPS1, urea cycle enzyme

Carbamoyl phosphate synthetase 1, CPS1, is the rate-limiting enzyme that catalyses the first committed step of the hepatic urea cycle, playing an extremely important role in removing excess of ammonia from the cells. CPS1 is primarily expressed in the liver and small intestine. The full-length enzyme is 165kDa, however, the spot detected to be CPS1 on 2D DIGE ran at 66kDa (see enlargement of the 66kDa area in Figure 3-8A) and was found to be more abundant in HtrA2 KO mitochondria. Sample pairs from the 2D DIGE replicates, as well as another pair of WT and HtrA2 KO mitochondria treated in the same way, were separated on 2D SDS-PAGE and CPS1 was detected by Western blot. No changes in full-length CPS1 could be detected (data not shown), however, two spots appeared in the 66kDa region (Figure 3-9D) as before on the 2D DIGE gels. These probably represent degradation products of CPS1, because the antibody used was raised against the full-length protein and could therefore also detect smaller fragments. The more basic spot at 66kDa was clearly more intense in HtrA2 KO mitochondria, whereas the more acidic spot at the same molecular weight increased in HtrA2 KO mitochondria upon heat shock treatment. The accumulation of a fragment of CPS1 could either be a consequence of the mitochondrial dysfunction due to absence of HtrA2 or alternatively HtrA2 could be involved in the clearance of abnormal proteins and therefore in its absence such abnormal proteins could be detected. The latter hypothesis fits with the observation that heat shock treatment enhanced the appearance of 66kDa fragments of CPS1.

3.7.4 ETHE1, mutated in Ethylmalonic Encephalopathy patients

ETHE1 was previously known as HSCO, hepatoma subtracted clone one, found to be over-expressed in human hepatoma cell cultures and shown to sequester NF-κB in the cytoplasm therefore inhibiting apoptosis (Higashitsuji et al. 2002). Subsequently, mutations in the gene encoding ETHE1 were identified in patients suffering from Ethylmalonic Encephalopathy, a devastating infantile metabolic disorder affecting the brain, gastrointestinal tract and peripheral vessels (Tiranti et al. 2004). ETHE1 was shown to localise to the mitochondrial matrix (Tiranti et al. 2004). To investigate the subcellular localisation of ETHE1, N- and C-terminally tagged ETHE1 were expressed in SH-SY5Y cells, separated by SDS-PAGE and detected by Western blot using anti-HA and anti-Flag antibodies, respectively (Figure 3-9E). HA-ETHE1 appeared as a single band, whereas ETHE1-Flag showed two bands, probably reflecting mitochondrial import and processing, which is prevented by the N-termial HA-tag. ETHE1 was slightly increased in HtrA2 KO mitochondria. A polyclonal antibody against ETHE1 was kindly provided by Jun Fujita (Kyoto University, Japan), unfortunately, detection of endogenous ETHE1 in the mitochondrial samples was never successful (data not shown). Therefore, accumulation of ETHE1 in WT versus HtrA2 KO mitochondria was monitored following import of *in vitro* translated ETHE1 into mitochondria (Figure 3-9F). Imported ETHE1 was resistant to Proteinase K treatment, verifying the mitochondrial localisation, but no differences could be detected in WT and HtrA2 KO mitochondria. Imported ETHE1 was processed similarly to ETHE1-Flag in Figure 3-9E, although this is not clearly visible in the image shown due to limited resolution on the gradient gel. Certainly, it cannot be ruled out from these experiments that endogenous ETHE1 accumulates in HtrA2 KO mitochondria. The matrix localisation of EHTE1 taken together with a similar rate of accumulation of imported ETHE1 in the mitochondria *in vitro*, however, makes it a relatively unlikely substrate for HtrA2.

3.7.5 Riken 2410005O16, unknown mitochondrial protein

Riken 2410005O16 encodes for a 35kDa protein and predicted to be mitochondrial with high probability by the pSORT II algorithm (http://psort.nibb.ac.jp). A clone for Riken 2410005O16 was obtained from RZPD (German Resource Center for Genome Research), and three mutations were discovered in the predicted DNA sequence: G to

A at base pair (bp) 70 resulting in glycine to serine at amino acid 24, and C to G at bp 91 and G to C at bp92 which is a silent mutation. The 2D DIGE spot identified as Riken 2410005O16 by mass spectrometry was found at 30kDa, which could potentially represent the processed Riken 2410005O16 protein without the mitochondrial targeting sequence. A motif for the mitochondrial processing peptidase, MPP, is found at amino acid 50 and cleavage there would result in a 30kDa protein with a pI of 5.95. To test if Riken 2410005O16 is indeed a mitochondrial protein, *in vitro* translated protein was imported into mitochondria (Figure 3-9G). Full length Riken 2410005O16, running at 35kDa, was found to a small degree inside the mitochondria, since most of it was degraded by Proteinase K treatment. However, a processed form of Riken 2410005O16 rapidly accumulated at 25kDa which was totally unaffected by Proteinase K treatment. It seems likely, therefore, that the pre-sequence that is proteolytically removed from Riken 2410005O16 in the mitochondria is longer than the one predicted by pSORT. Inevitably, the 30kDa form of Riken 2410005O16 identified in the 2D DIGE, cannot be a major isoform. No differences were detected in WT and HtrA2 KO mitochondria (data not shown).

Taken together, few significant changes could be detected in the proteome of WT and HtrA2 KO mitochondria using 2D DIGE. The accumulation of 66kDa fragments of CPS1 in HtrA2 KO mitochondria was the only reproducible change that could be validated with a subsequent approach to the 2D DIGE. CPS1 is mainly expressed in liver mitochondria (Gene Cards: http://www.genecards.org/cgi-bin/carddisp.pl?gene=CPS1&search=cps1&suff=txt) and therefore it seems an unlikely target of HtrA2 that could explain the phenotype of the KO mice. However, CPS1 represents the first piece of data supporting a DegP-like role for HtrA2 in mitochondria, namely the degradation of unwanted proteins.

3.8 Discussion

When the mammalian IBM-containing proteins Smac and HtrA2 were first identified through their ability to interact with XIAP (Du et al. 2000; Verhagen et al. 2000; Suzuki et al. 2001; Hegde et al. 2002; Martins et al. 2002; van Loo et al. 2002; Verhagen et al. 2002), it appeared likely that the pro-apoptotic function of these proteins involved release from mitochondria following apoptotic insult. Once in the

cytosol, the proteins could act together to block the caspase inhibitory function of IAPs, thus promoting caspase activation and apoptosis. While over-expression of Smac or HtrA2 certainly promotes caspase-mediated apoptotic death and also, in the case of HtrA2, caspase-independent cell death, the significance of the endogenous proteins in these pathways has been much less clear. The data presented here indicate that the complete loss of expression of HtrA2 protein, including its IBM, does not obviously perturb mouse development and health beyond the effects seen due to loss of only the serine protease activity of HtrA2 due to point mutation: the phenotype of the HtrA2 KO mouse is very similar to that of the Mnd2 mouse (Jones et al. 2003). The mouse mutant Mnd2 (motor neuron degeneration 2) was identified in 1990 as a spontaneous, recessively inherited mutation that arose on the C57BL/6J inbred background (Jones et al. 1993). Subsequently, the Mnd2 mutation was identified as the missense mutation S276C in the protease domain of HtrA2 (Jones et al. 2003). Therefore, the proteolytic activity of HtrA2 rather than the its IAP-binding activity seems to be the critical element. Similarly, total loss of Smac expression has no effect on mouse development or function (Okada et al. 2002). Mice completely lacking both HtrA2 and Smac expression display a phenotype identical to HtrA2 KO animals and cells derived from these mice fail to show enhanced resistance to apoptotic stimuli (Martins et al. 2004). Thus, loss of both major XIAP-binding proteins does not have any obvious effect on the phenotype of mice that can be detected within the limited lifespan of animals lacking HtrA2 serine protease activity. It has been reported that many mitochondrial proteins might have an N-terminal IBM (Verhagen et al. 2007). Therefore, severe mitochondrial damage would cause release of many proteins with the ability to antagonise IAPs, in addition to just Smac and HtrA2, so that loss of the IBMs of these two proteins may have little detectable impact on IAP activity.

HtrA2 KO and Mnd2 mice both die prematurely at around 30 to 40 days of age due to a progressive neurological disorder caused by death of a population of striatal neurons (Jones et al. 2003; Martins et al. 2004), no differences in their phenotypes could be found. The phenotype of these mice displays some similarity to patients with parkinsonian neurodegeneration. Indeed, in human PD patients, a polymorphism and a mutation in HtrA2 linked to the disorder have been identified and characterised. The effect of these single amino acid changes is to reduce the activation of HtrA2

proteolytic activity (Strauss et al. 2005). Initially, it was anticipated that HtrA2 is part of the PARK3 locus identified in familial PD (Gasser et al. 1998), later however, the chromosomal region harbouring the PARK3 locus in the respective families could be narrowed and does no longer include HtrA2 (West et al. 2001). Recently, the HtrA2 gene has been designated as an independent locus, the PARK13 locus (http://www.ncbi.nlm.nih.gov/entrez/dispomim.cgi?id=610297).

Neuronal cell populations isolated from HtrA2 KO mice were more sensitive than WT controls to excitotoxicity-induced death in response to glutamate (Figure 3-7C). Non-neuronal cell types such as fibroblasts and T lymphocytes from the HtrA2 KO mice also showed increased sensitivity to induction of cell death by drugs that target the mitochondria, for instance the complex I inhibitor rotenone and the uncoupler CCCP (data not shown). Primary WT or HtrA2 KO MEFs did not exhibit differences in metabolic activity when challenged with CCCP, rotenone or tunicamycin as determined by an MTT assay (Figure 3-5C-E). The principle of this assay is the cleavage of MTT in metabolically active cells only, given that NADH and NADPH are required as co-factors for this cleavage to occur. Therefore, the MTT assay could be considered as a measure of cell number and could reflect the increased sensitivity of HtrA2 KO MEFs to these drugs as seen in Figure 3-7A using FACS to determine the number of sub-G1 cells. The MTT assay already showed reduced metabolic activity after only 6hrs of incubation with the drugs, this time is probably too short to impact significantly on cell death. After 24hrs of incubation with the drugs, however, the metabolic activity and likely also the cell number of WT and HtrA2 KO cells is greatly reduced even with the lowest drug concentrations. Therefore this time-point might possibly be too long or the drug concentration still too high to record differences in cell number with this assay. In contrast, measurement of apoptotic cells by sub-G1 analysis and also AnnexinV-PI staining did reveal increased cell death in HtrA2 KO MEFs when treated with CCCP, rotenone or tunicamycin (Figure 3-7A).

The increase in cell death in animals lacking HtrA2 function and absence of protection from apoptosis suggests that HtrA2 is an essential gene required for mitochondrial function, rather than a pro-apoptotic regulator. Since the Mnd2 mice display the same phenotype as the HtrA2 KO mice, it appears that the proteolytic activity of HtrA2 is critical for correct mitochondrial function. It is likely that HtrA2 acts to protect

mitochondria from certain stresses, in a manner similar to the homologous stress-adaptive proteins DegP and DegS in bacteria. If HtrA2 acts like DegS (Walsh et al. 2003), loss of HtrA2 may result in an inability to mount an adaptive transcriptional response under stress conditions that cause protein unfolding, leaving the mitochondria of striatal neurons unable to maintain their membrane potential and rendering the cells prone to either necrotic or apoptotic death. Alternatively, if HtrA2 functions like bacterial DegP (Spiess et al. 1999), mitochondria from KO mice may be unable to degrade unfolded proteins in the intermembrane space under conditions of cell stress and these could form aggregates that would directly compromise the maintenance of the mitochondrial membrane potential. Which of these different models of HtrA2's neuroprotective function is correct may be clarified once its mitochondrial binding partners and substrates are identified and once differences in stress-induced transcriptional responses are determined.

The identification of mitochondrial substrates of HtrA2 using the 2D DIGE approach revealed few proteins that were possibly differentially expressed in WT and HtrA2 KO mitochondria (Table 3-1), however, none of the proteins held up on further investigation (Figure 3-9). This probably points to the limitations of the methodology: either incorrect protein spots were being picked on the preparative gel for identification by mass spectrometry or the differences detected were random variations. The latter is probably true for all spots except 1, 8 and 9 (Figure 3-8B), since only these spots were detected as differentially expressed by the DeCyder software across all replicates. However, picking these spots from the preparative gel was difficult, especially for spot 8 and 9, due to a number of low abundance protein spots being very close to each other.

Proteins with the highest level of expression among the mitochondrial proteome are the proteins with conserved metabolic functions, many of these are matrix proteins and inner membrane proteins. HtrA2 is located in the intermembrane space and therefore matrix proteins are unlikely to be HtrA2 substrates. It is possible that differences in WT and HtrA2 KO mitochondria in low abundance proteins do exist, although these might not be visible on 2D DIGE due to the high abundance proteins. Moreover, HtrA2 itself was not detectable by fluorescence on 2D DIGE and the presence or absence of HtrA2 could only be detected by Western blot (Figure 3-9A). Whereas hydrophilic proteins are easily resolved by 2D gel electrophoresis, membrane proteins often precipitate at

the basic end of the isolelectric focussing (IEF) strips. Thus, membrane proteins that could be potential targets of HtrA2 might be missed using conventional 2D gel electrophoresis. Performing blue native 2D gel electrophoresis would allow better separation of membrane proteins.

If HtrA2 has a DegP-like function in mammalian mitochondria and is responsible for the degradation of unfolded proteins in the intermembrane space, these should accumulate in HtrA2 KO mitochondria. However, other proteases might have a partially overlapping set of substrates to HtrA2 and, therefore, such substrates might be taken care of by other proteases in HtrA2 KO mitochondria under normal conditions. Perhaps only under particular stressful conditions would certain proteins accumulate in HtrA2 KO mitochondria, such as those conditions in the striatum that ultimately cause the neurons to die.

The results presented in this chapter reveal a protective role for HtrA2 in mitochondrial function, which, when lost, leads to neurodegeneration and development of a parkinsonian syndrome in mice. However, gross changes in the mitochondrial proteome could not be unequivocally identified.

Figure 3-1. Targeting the HtrA2 gene by homologous recombination.

(A) Schematic representation of the WT mouse HtrA2 locus, the targeting construct and the targeted HtrA2 allele. These mice were generated at GlaxoSmithKline UK (see 2.2.1 for details). **(B)** Genotyping of the WT and mutant HtrA2 locus by PCR using the primers indicated in A. **(C)** Reduced and absent HtrA2 mRNA in Het and KO mice, respectively. Reverse transcriptase (RT) qPCR was performed to measure the mRNA levels of HtrA2. RNA was isolated from brain tissue. Data shown are normalised to the relative HtrA2 mRNA level in WT. Error bars represent ± standard deviation, n=3. **(D)** Reduced and absent HtrA2 protein in Het and KO mice, respectively. Western blot analysis of protein lysates obtained from WT, Het and KO MEFs. Western blot analysis for Grp75 were used as a protein loading control.

Figure 3-1

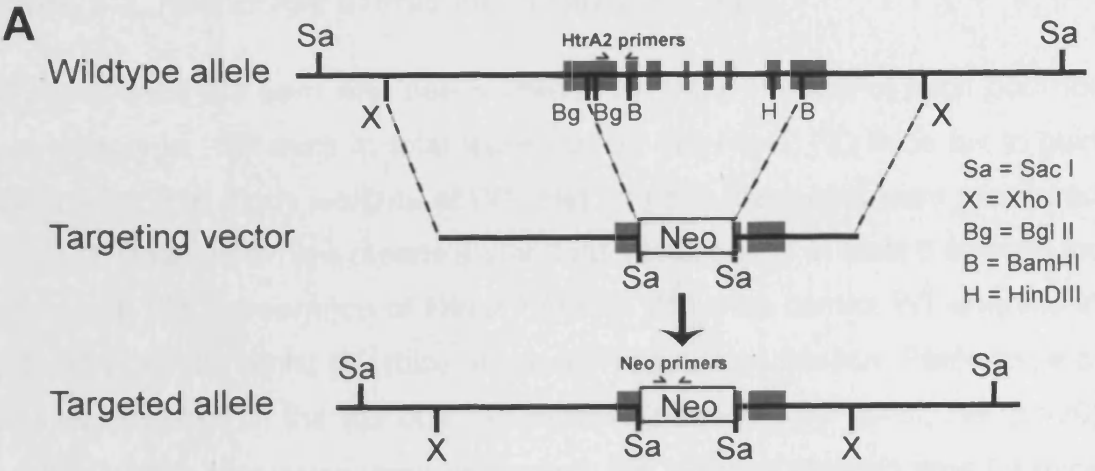
A
Wildtype allele
Sa
HtrA2 primers
Sa
X
Bg
Bg
B
H
B
X
Targeting vector
Neo
Sa
Sa
Sa = Sac I
X = Xho I
Bg = Bgl II
B = BamHI
H = HinDIII
Targeted allele
Sa
Neo primers
Neo
Sa
X
Sa
Sa
X

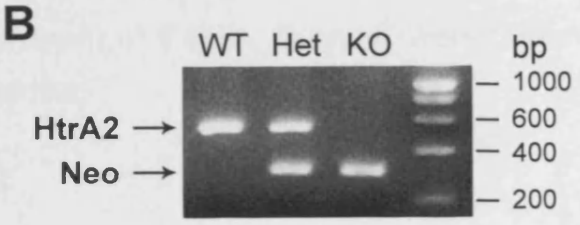
B
WT
Het
KO
bp
HtrA2
Neo
1000
600
400
200

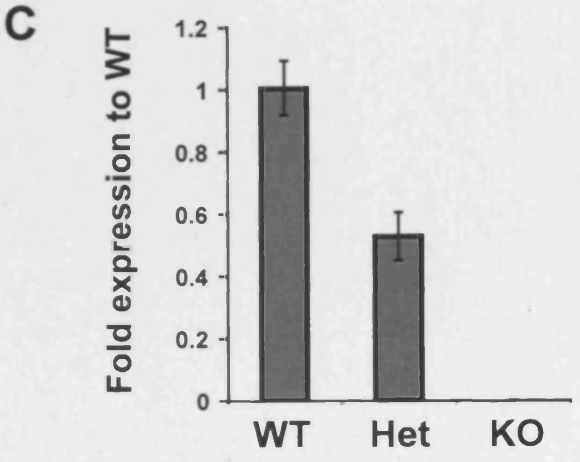
C
Fold expression to WT
1.2
1
0.8
0.6
0.4
0.2
0
WT
Het
KO

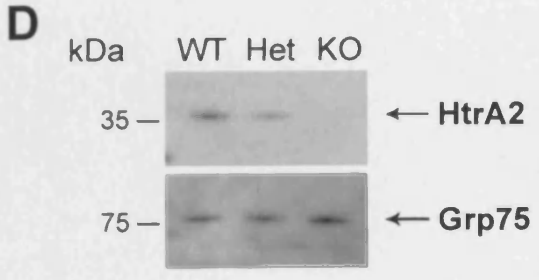
D
kDa
WT
Het
KO
35
HtrA2
75
Grp75

Figure 3-2. Phenotypic alterations of HtrA2 KO mice.

(A) HtrA2 mice are born with nearly Mendelian ratio. Percent of mice born for each genotype. 157 mice in total were scored. **(B)** HtrA2 KO mice fail to gain weight from P18. Body weights of WT, Het and KO littermates were measured until P33. Data shown are means ± standard deviations of at least 6 animals for each point. **(C)** Appearance of HtrA2 KO and littermate control WT animals at P23 and P30. **(D)** HtrA2 KO mice show decreased coordination. Percentage of mice that climbed to the top of a 60° inclined platform. WT (n=8), Het (n=20) and KO (n=16) littermates were compared. **(E)** Average elapsed time for mice to climb to the top of the platform. Data are means ± standard deviations of a minimum of 8 trials. D and E were performed by Victoria Cowling and Miguel Martins.

Figure 3-2

A

HtrA2	WT	Het	KO
%	25	54	21

B

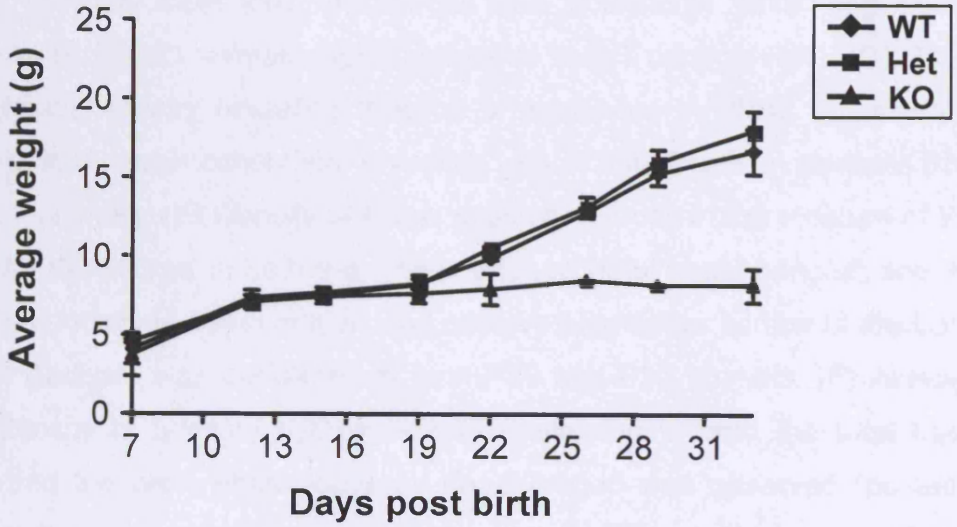

C

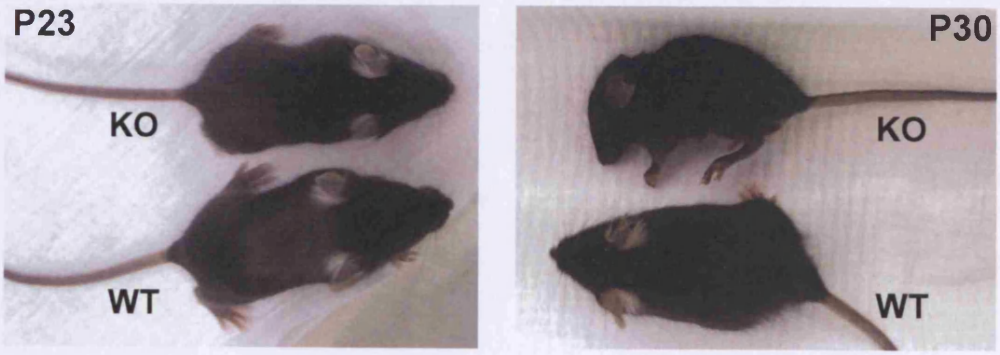

D

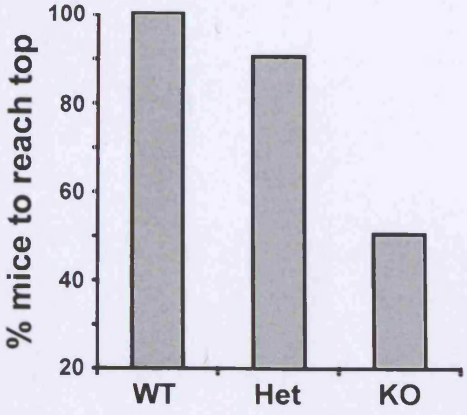

E

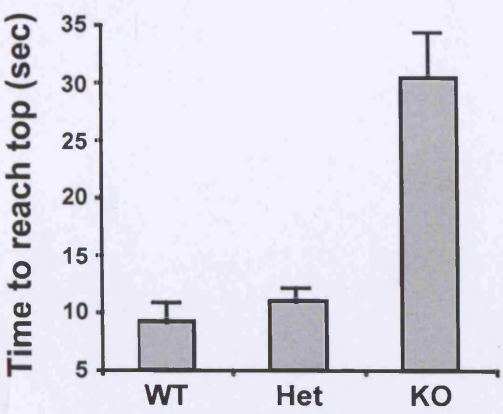

Figure 3-3. Morphological features of localised striatal degeneration in HtrA2 KO mice.

(A) Diagram of a mouse brain in sagital orientation indicating area of striatal degeneration (red box) in the striatum. **(B)** Hematoxylin and eosin (H&E) staining showing focal loss of neurons and occasional ballooning in the striatum of HtrA2 KO animals (right) compared to WT controls (left). **(C)** GFAP immunohistochemistry revealing reaction of astrocytes in HtrA2 KO animals. **(D)** MAP2 immunohistochemistry revealing loss of this protein in sections from HtrA2 KO animals. **(E)** Density of NeuN positive neurons in the striatum of WT and HtrA2 KO scored in both the whole striatum (total basal ganglia) and the area where localised degeneration was observed (posterior portion of the basal ganglia). Analysis was performed in both P20 and P30 animals. **(F)** Average optical density of tyrosine hydroxylase (TH) staining in both the total basal ganglia and the area where localised degeneration was observed (posterior portion of the basal ganglia) **(G)** Average number of TH-positive neurons in the substantia nigra pars compacta (SNpc) of WT and HtrA2 KO animals. This data was generated by Sebastian Brandner, Institute of Neurology, London.

Figure 3-3

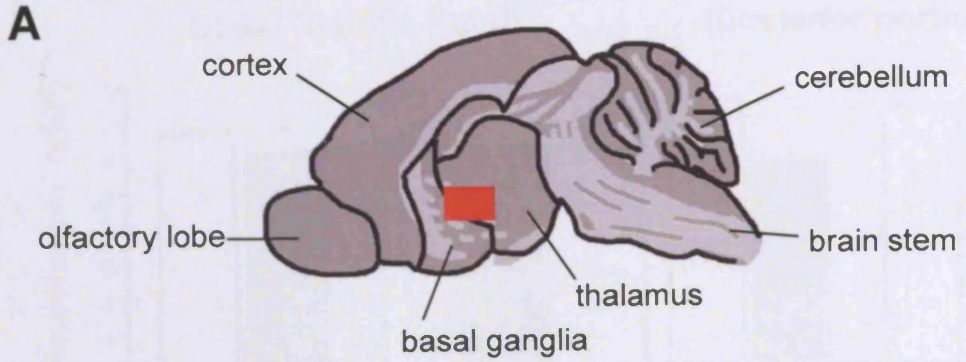
A
cortex
cerebellum
olfactory lobe
brain stem
thalamus
basal ganglia

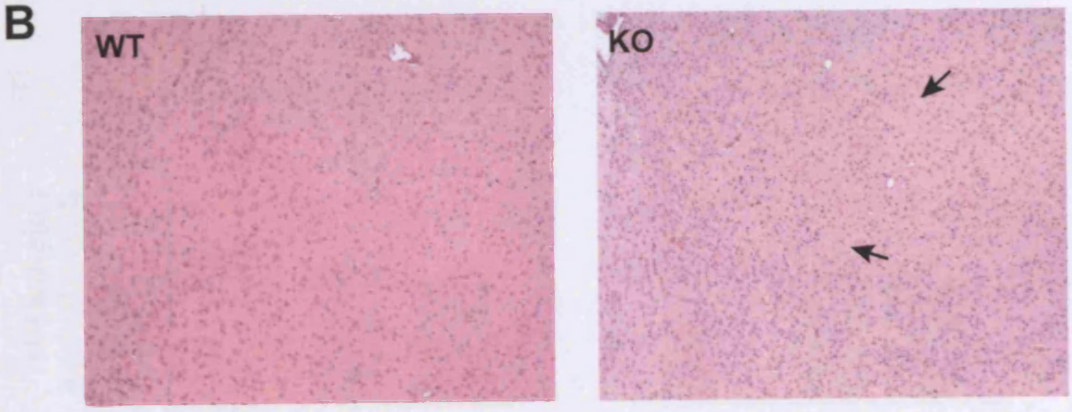
B
WT
KO

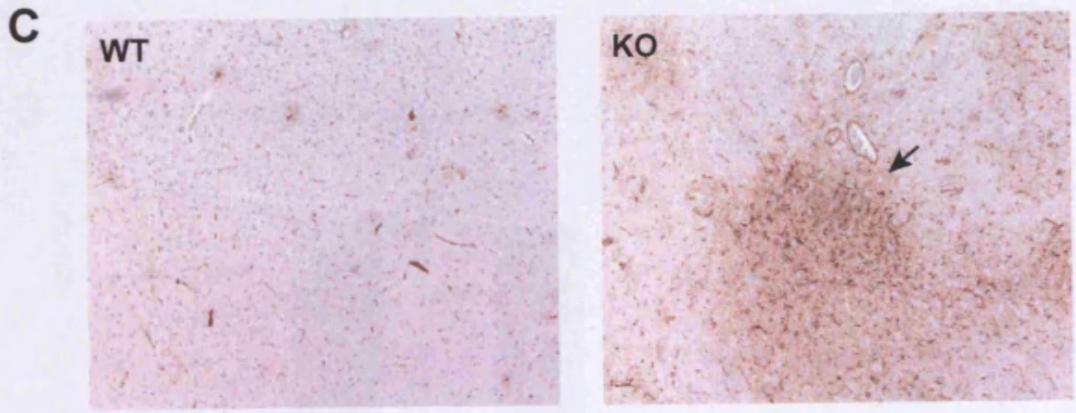
C
WT
KO

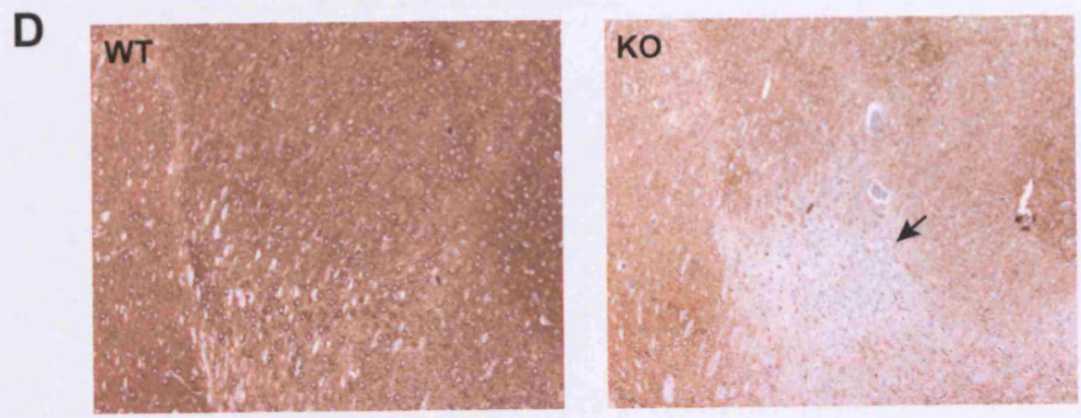
D
WT
KO

Figure 3-3

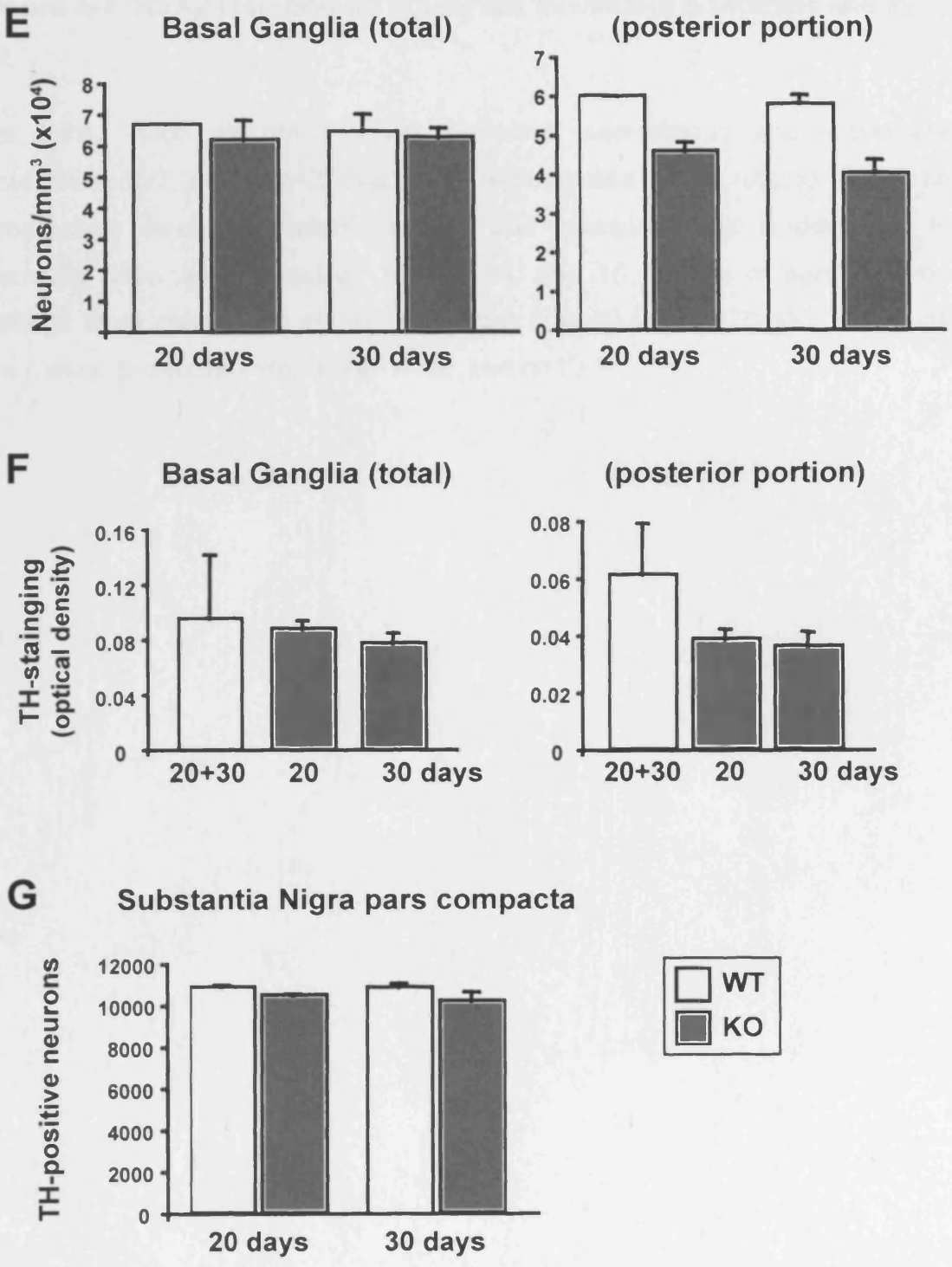
E
Basal Ganglia (total)
(posterior portion)
Neurons/mm³ (x10⁴)
20 days
30 days
20 days
30 days
F
Basal Ganglia (total)
(posterior portion)
TH-stainging (optical density)
20+30
20
30 days
20+30
20
30 days
G
Substantia Nigra pars compacta
TH-positive neurons
20 days
30 days
WT
KO

Figure 3-4. HtrA2 Het mice do not exhibit movement disabilities late in life.

Het HtrA2 mice do not develop late-onset coordination and movement disabilities. WT and HtrA2 Het mice were tested on a rotarod on three consecutive days. The latency to fall was measured and is displayed in seconds. Mice were tested at 10, 12, 14, and 16 months of age. Rotarod settings were continuous acceleration from 0 to 40rpm in 570 seconds. Data are means ± standard errors, WT n=10, Het n=10.

Figure 3-4

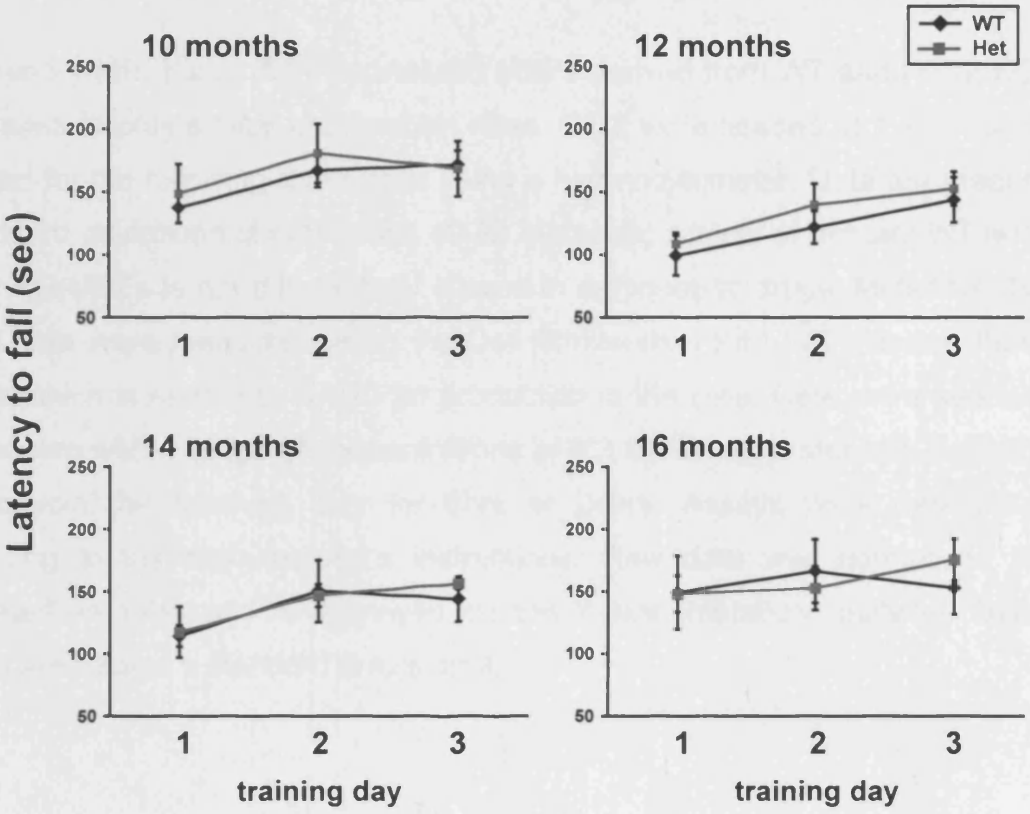
WT
Het
10 months
12 months
14 months
16 months
Latency to fall (sec)
250
200
150
100
50
1
2
3
training day

Figure 3-5. Cell proliferation and metabolic activity of HtrA2 MEFs.

(A) Primary MEFs and **(B)** immortalised MEFs derived from WT and HtrA2 KO littermates display similar proliferation rates. Cells were seeded at 1 x 10^5 and counted for the following three days using a haemocytometer. Data are means ± standard deviations of duplicates. **(C-E)** Metabolic activity of primary WT and HtrA2 KO MEFs is not differentially altered in response to drugs. Metabolically active cells were measured using the Cell Proliferation Kit I (MTT assay) from Roche which is related to NAD(P)H production in the cells. Cells were seeded and treated with a range of concentrations of **(C)** CCCP, **(D)** rotenone, and **(E)** tunicamycin the following day for 6hrs or 24hrs. Assays were performed according to the manufacturer's instructions. Raw data was normalised to untreated samples and is displayed on the Y-axis (metabolic activity). Data shown are means ± standard errors, n=3.

Figure 3-5

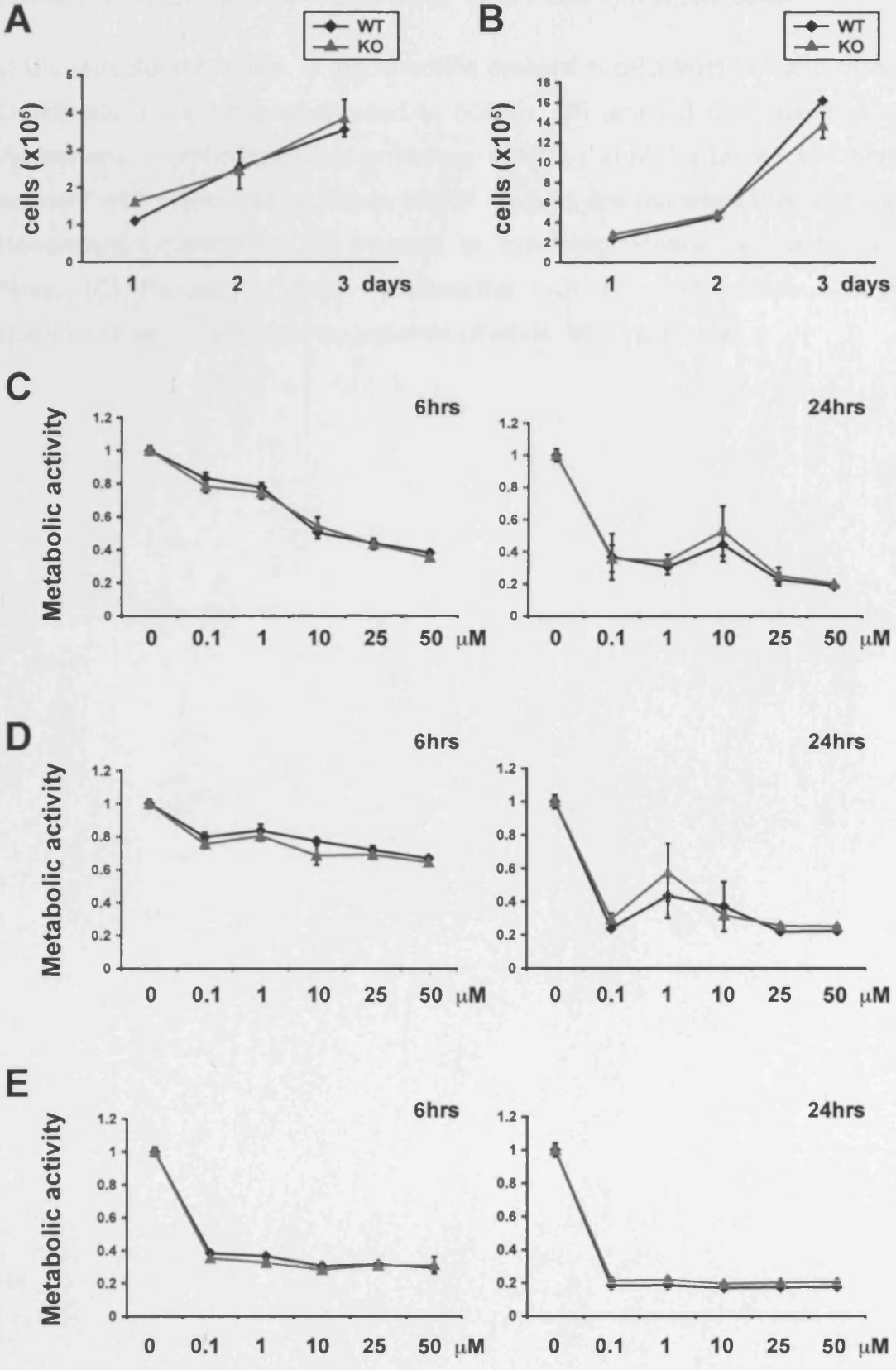
A
WT
KO
cells (x10⁵)
1
2
3 days
B
WT
KO
cells (x10⁵)
1
2
3 days
C
Metabolic activity
6hrs
24hrs
0
0.1
1
10
25
50 μM
D
Metabolic activity
6hrs
24hrs
0
0.1
1
10
25
50 μM
E
Metabolic activity
6hrs
24hrs
0
0.1
1
10
25
50 μM

Figure 3-6. Mitochondrial morphology in WT and HtrA2 KO cells.

(A) Ultrastructural features of mitochondria present in cells from WT and HtrA2 KO animals, scale bars correspond to 500nm. **(B)** and **(C)** Quantification of mitochondrial morphological abnormalities detected in MEFs before and after treatment with mitochondrial stress stimuli. Results are representative of three independent experiments. **(B)** Percent of total mitochondria with ballooned cristae. **(C)** Percent of total mitochondria with abnormal shape. These experiments were performed by Valentina Fedele, MRC Leicester.

Figure 3-6

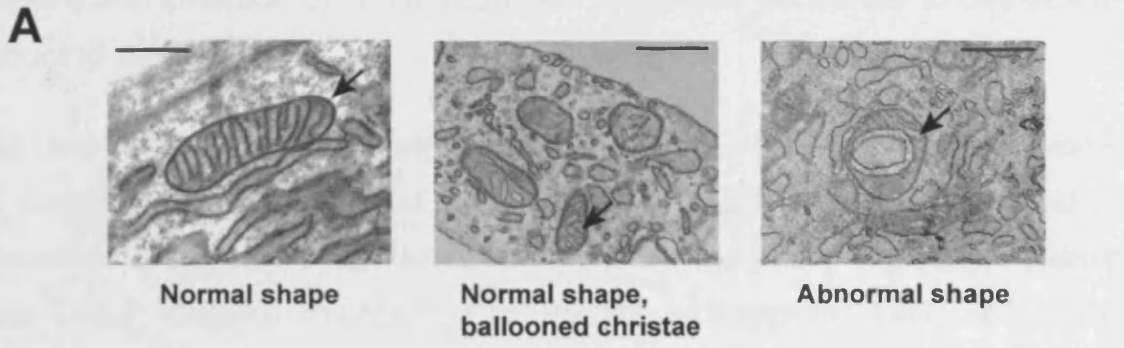
A
Normal shape
Normal shape, ballooned christae
Abnormal shape

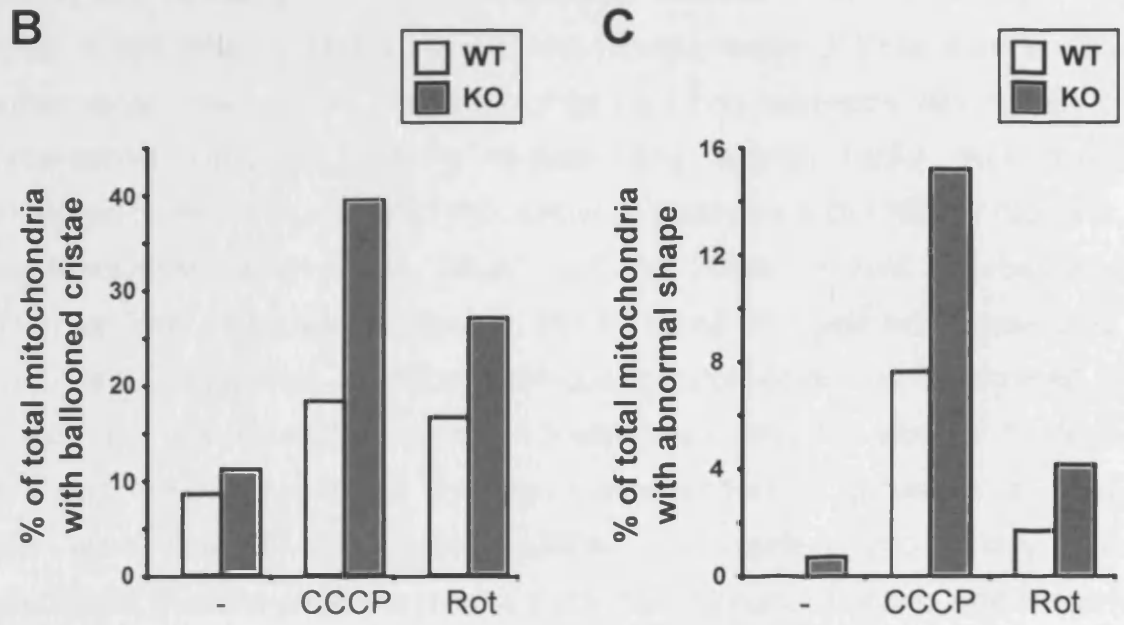
B
WT
KO
% of total mitochondria with ballooned cristae
0
10
20
30
40
-
CCCP
Rot
C
WT
KO
% of total mitochondria with abnormal shape
0
4
8
12
16
-
CCCP
Rot

Figure 3-7. Deletion of HtrA2 results in increased sensitivity to cell death-inducing agents.

(A) Loss of HtrA2 increases apoptosis in response to cell death stimuli. Viability of immortalised MEFs derived from WT and HtrA2 KO mice, determined by measurement of sub-G1 cell populations by flow-cytometry. Cells were treated with CCCP (25μM), rotenone (Rot, 25μM), tunicamycin (Tunic, 2.5μg/ml), etoposide (Etop, 170μM, all for 27hrs) or hydrogen peroxide (H_2O_2, 3μM for 4.5hrs) and compared to untreated controls. Results show the means ± the range of two determinations. Results are representative of three independent experiments. Insert shows Western blot for HtrA2 on cell lysate. **(B)** Viability of immortalised HtrA2 KO MEFs re-expressing human HtrA2 (KO+HtrA2) compared to vector alone HtrA2 KO, following treatment with MG-132 (250nM), 6-hydroxydopamine (6-OHDA, 25μM) both for 20hrs, or 2μM staurosporine (STS) for 3hrs. Insert shows Western blot for HtrA2 on lysate from these cells. **(C)** Neuronal response to glutamate-induced cytotoxicity was determined in primary neurons isolated from day 14.5 embryos cultured in vitro for 10 days. Following incubation with the indicated concentrations of glutamate for 4hrs, cells were stained with Hoechst 33342 and nuclear morphology was determined. Results show the means ± standard deviations of two independent experiments where 6 fields with at least 40 cells were scored for each data point. Experiments for C, neuronal exitotoxicity, were performed in collaboration with Miguel Martins, MRC Leicester.

Figure 3-7

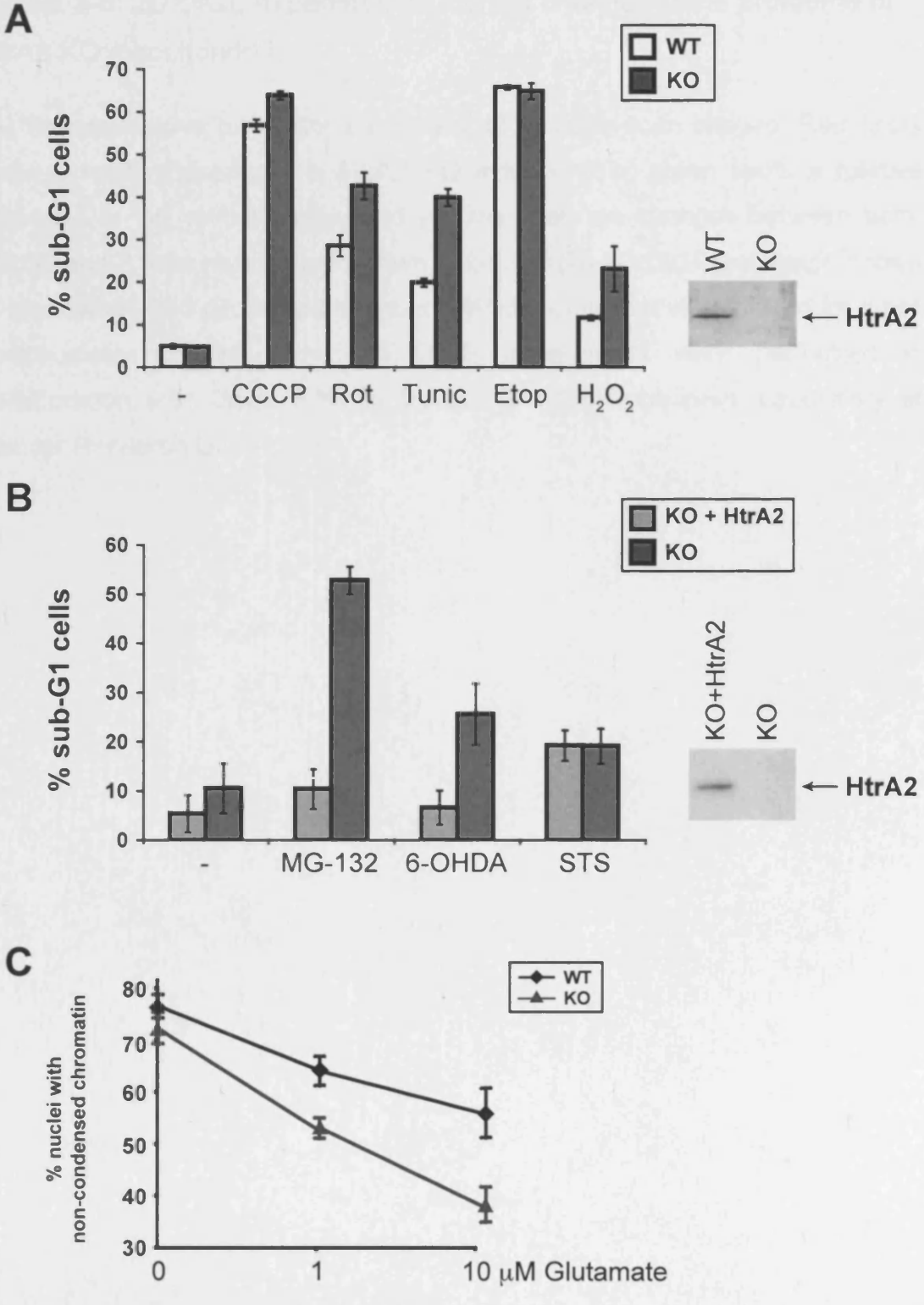
A
WT
KO
% sub-G1 cells
70
60
50
40
30
20
10
0
-
CCCP
Rot
Tunic
Etop
H_2O_2
WT
KO
HtrA2
B
KO + HtrA2
KO
% sub-G1 cells
60
50
40
30
20
10
0
-
MG-132
6-OHDA
STS
KO+HtrA2
KO
HtrA2
C
WT
KO
% nuclei with non-condensed chromatin
80
70
60
50
40
30
0
1
10 μM Glutamate

Figure 3-8. 2D DIGE experiment to identify changes in the proteome of HtrA2 KO mitochondria.

(A) Representative picture of an overlay of two dye scan images. Red spots show a relative decrease in HtrA2 KO mitochondria, green spots a relative decrease in WT mitochondria, and yellows spots no changes between both. 66kDa and 31kDa regions are shown enlarged. **(B)** 2D DIGE gel image shown in black/white, red circles and numbers denote spots that were picked for mass spectrometry analysis. The 2D DIGE experiments were performed in collaboration with David Frith in the 2D Gel Electrophoresis Laboratory at Cancer Research UK.

Figure 3-8

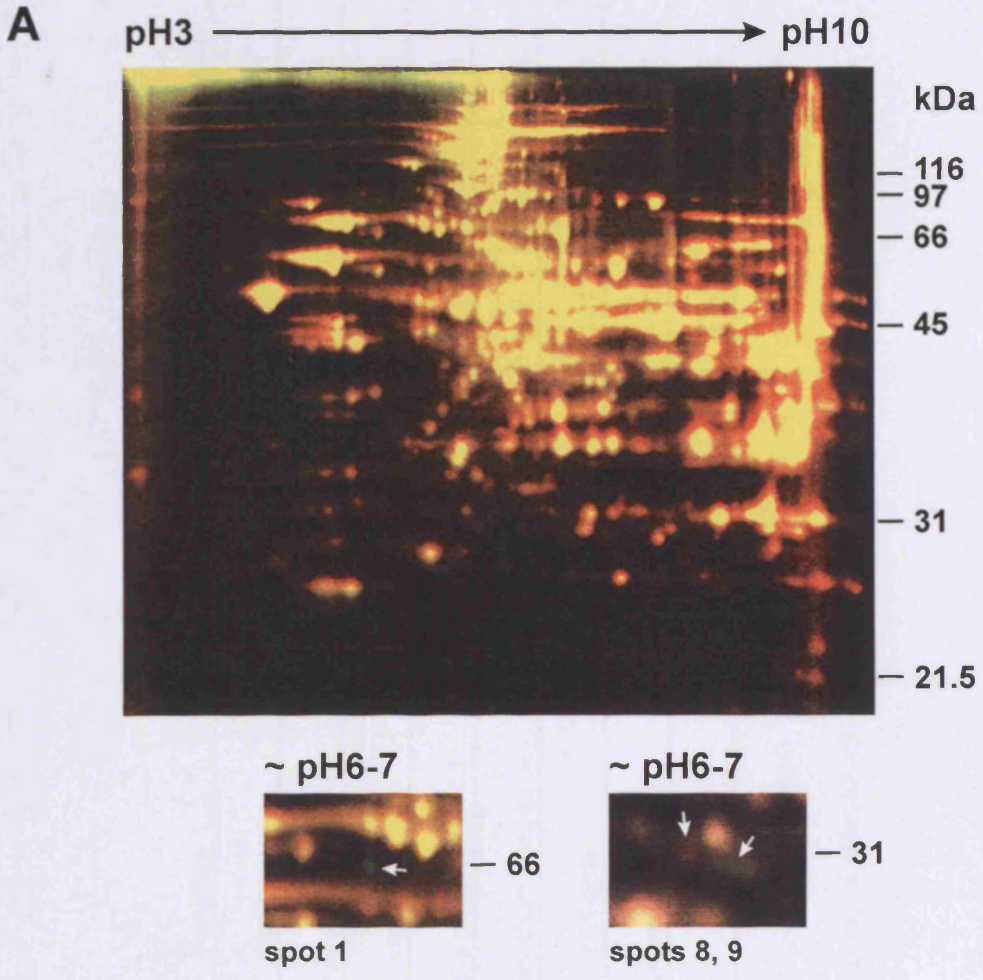
A
pH3
pH10
kDa
116
97
66
45
31
21.5
~ pH6-7
66
spot 1
~ pH6-7
31
spots 8, 9
B
pH3
pH10
kDa
116
97
66
45
31
21.5
1
2
3
4
5
6
7
8
9

		Function	Localisation	MW (kD)	pI (pH)	MW spot	number
Carboamyl-Phosphate Synthetase1	CPS1	urea cycle	mito	165	6.33	~66	**1**
DiMethylGlycine Dehydrogenase	DMGDH	AA metabolism	matrix	97	7.69	similar	**2**
Heat Shock Protein A / Grp75	Grp75	chaperone	matrix	73	5.81	similar	**3**
Succinate Dehydrogenase Fp Subu.	SDHA	respiratory chain, complex II	inner membrane	72	7.6	similar	**4**
Ubiquinol-CytC Reductase Core Complex1	UQCRC1	respiratory chain, complex III	inner membrane	53kD	5.75	similar	**5**
ATP-sp. Succinyl-CoA Synthetase b subu.	SUCLA2	TCA cycle	matrix	46	5.65	similar	**6**
Electron Transfer Flavoprotein a subu.	ETFA	electron transfer	matrix	35	8.62	~40	**7**
Riken 2410005O16		?	pSORT: mito	35	8.85	~30	**8**
Ethylmalonic-Encephalopathy1 /	ETHE1 /	mutated in AR metab. disorder /	mito /	28	6.78	similar	**9**
Hepatoma Subtracted Clone One	HSCO	inhib. p53-apoptosis, binds NF-kB	cyto / nucleus				

Table 3-1

Table 3-1. Proteins identified in 2D DIGE from wildtype and HtrA2 knock out mitochondria.

Figure 3-9. Examination of the 2D DIGE hits.

(A) Western blot for HtrA2 in WT and HtrA2 KO mitochondria verifying the presence and absence of this protein. HtrA2 runs at 35kDa with pI 6.1. **(B)** Grp75 levels and isoelectric point are not dissimilar in WT and HtrA2 KO mitochondria. Samples were separated on 2D SDS-PAGE and probed with anti-Grp75 antibody. Grp75 runs at 75kDa and pI 5.8. **(C)** UQCRC1 levels are not different in WT and HtrA2 KO mitochondria. Samples were separated on 1D SDS-PAGE and probed with anti-UQCRC1 antibody. UQCRC1 runs at 51kDa. **(D)** 66kDa fragments of CPS1 accumulate in HtrA2 KO mitochondria. Samples were separated on 2D SDS-PAGE and probed with anti-CPS1 antibody. The CPS1 fragments run at 66kDa and pI 6.6. **(E)** ETHE1 expressed in SH-SY5Y cells revealing N-terminal processing. HA-ETHE1 and ETHE1-Flag expression in cell lysates were detected by anti-HA and anti-Flag antibodies, respectively. **(F)** Mitochondrial accumulation of ETHE1 in WT and HtrA2 KO is similar. *In vitro* translated ^{35}S-labelled ETHE1-Flag was imported into mitochondria isolated from WT and HtrA2 KO mouse livers. After import mitochondria were treated with Proteinase K to remove proteins bound to the outside of the mitochondria. Lysates were separated on SDS-PAGE and visualised by exposure to PhosphorImager screen. Ornithine transcarbamylase (OTC) is a matrix protein used as control. Asterisk denotes unspecific band. **(G)** Riken 2410005O16 protein is imported into mitochondria and rapidly processed to a 25kDa form. *In vitro* translated ^{35}S-labelled Riken 2410005O16 was imported into mitochondria isolated from WT mouse livers. After import, half of the mitochondria were treated with Proteinase K. Lysates were separated on SDS-PAGE and visualised by exposure to PhosphorImager screen.

Figure 3-9

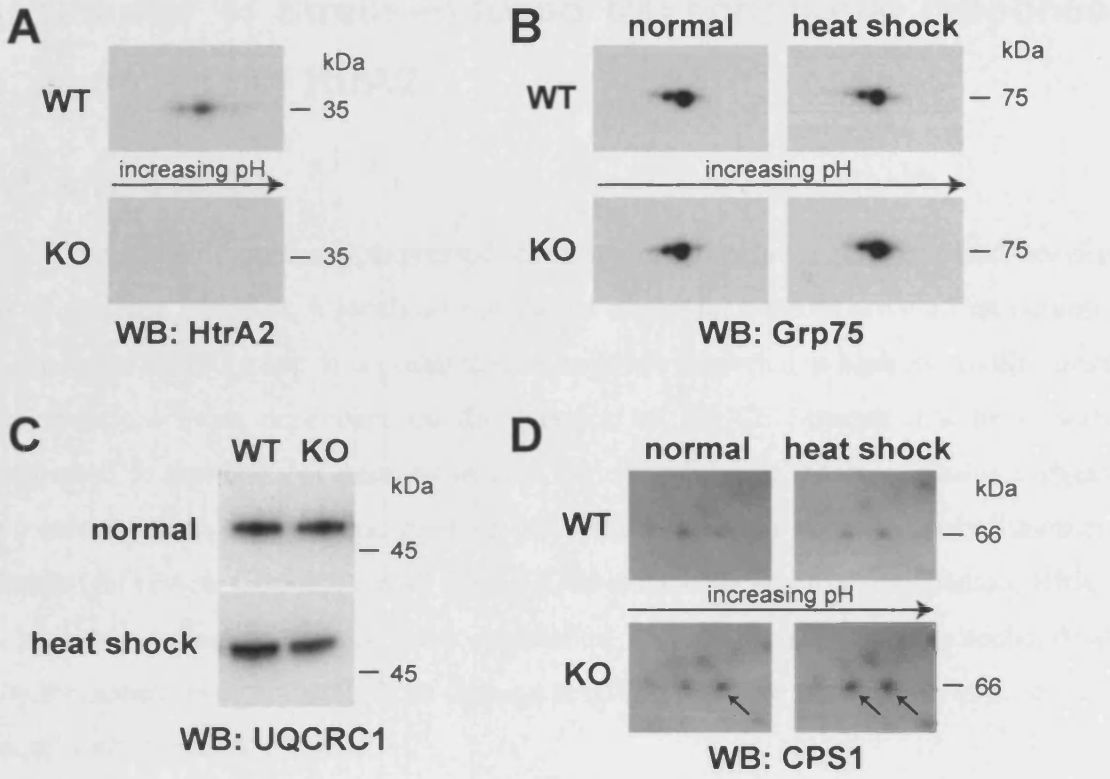
A
WT
KO
kDa
35
35
increasing pH
WB: HtrA2
B
normal
heat shock
WT
KO
kDa
75
75
increasing pH
WB: Grp75
C
WT KO
normal
heat shock
kDa
45
45
WB: UQCRC1
D
normal
heat shock
WT
KO
kDa
66
66
increasing pH
WB: CPS1
E
vector
HA-ETHE1
vector
ETHE1-Flag
kDa
45
31
21
WB: HA
WB: Flag
F
input
WT
KO
10'
30'
60'
10'
30'
60'
kDa
35
30
25
50
35
30
ETHE1
full length
mature
OTC
G
input
- Prot.K
+ Prot.K
10'
30'
60'
10'
30'
60'
kDa
50
35
30
25
full length
mature
Riken 2410005O16

4 Chapter 4: Stress-induced transcriptional response upon loss of HtrA2

4.1 Introduction

While HtrA2 is ubiquitously expressed, neurons in particular seem to depend heavily on its protease function. A localised population of striatal neurons are the first neurons to die in HtrA2 KO mice. It is possible such cells are subjected to high metabolic stress and therefore more dependent on the function of HtrA2. Stresses that have been implicated in the death of neurons *in vivo* include oxidative stress, excitotoxic stress and accumulation of denatured proteins including those with expanded polyglutamine repeats (for review (Bredesen et al. 2006)). Due to its mitochondrial localisation, HtrA2 is probably acting to protect these organelles, and in particular the mitochondrial intermembrane compartment, from damage resulting from the stresses to which striatal neurons are normally exposed.

Mitochondria operate a sensitive feedback system, which acts to calibrate and adjust their performance in the cellular context. This pathway is referred to as mitochondrial retrograde signalling or mitochondrial stress signalling, and is a mean of communication from the mitochondria to the nucleus (reviewed in (Butow and Avadhani 2004)). Originally, the pathway was discovered in yeast, however, a mitochondria-specific stress response has been reported to exist in mammalian cells (Zhao et al. 2002). In this study, the authors used a mutant version of ornithine transcarbamylase, OTC, that could not fold properly. Accumulation of the unfolded protein within the mitochondrial matrix resulted in the transcriptional up-regulation of nuclear genes encoding mitochondrial stress proteins such as Hsp60, Hsp10, mtDnaJ and ClpP, but not those encoding stress proteins of the ER. Analysis of the Hsp60/Hsp10 bidirectional promoter identified a CHOP element as the mitochondrial stress response element. The TF CHOP was shown to regulate the expression of those mitochondrial stress proteins in association with C/EBPβ (Zhao et al. 2002).

The structural similarity of mammalian HtrA2 to the bacterial DegS protease is particularly striking (see Chapter 1.3, and Figure 1-2B, Figure 1-3A-D). DegS has a domain structure similar to HtrA2 with only one PDZ domain and the crystal structure

reveals that both proteases form trimers. The catalytic centre of both proteases is distorted in the inactive conformation, and their catalytic activity can be regulated by the PDZ domains (Li et al. 2002; Wilken et al. 2004). In addition, DegS is localised in the periplasmic space between the inner and outer bacterial cell membranes, with its N-terminal region inserted into the inner membrane: this localisation is clearly analogous to that of full length HtrA2 within the mitochondria. The appearance of the exposed C-termini of unfolded porins, outer membrane channel proteins, in the periplasmic space results in activation of DegS due their binding to its PDZ domain (Figure 1-5) (Walsh et al. 2003). Similarly, engagement of the PDZ domain of HtrA2 results in activation of its protease activity (Li et al. 2002; Martins et al. 2003), although in the case of HtrA2 its natural PDZ-binding partners within the mitochondria remain to be identified. Once activated in the bacterial periplasmic space, DegS cleaves RseA, an inner membrane protein that, together with RseB, sequesters the transcriptional regulator σ^E at the cytoplasmic face of the inner membrane. It is interesting to note that DegS cleaves RseA between a valine and a serine (Walsh et al. 2003). Similarly, human and mouse HtrA2 have a preference for valine at P1 position and serine at P1' in an optimal synthetic peptide substrate (Martins et al. 2003). This suggests that conservation between DegS and HtrA2 is also present at the biochemical level. Cleavage of RseA by DegS leads to further proteolysis by the intramembrane protease RseP, resulting in the release of the transcriptional regulator σ^E into the cytosol to induce the expression of periplasmic stress response genes (Figure 1-5). While the structural and biochemical similarity between HtrA2 and DegS is evident, it has so far not been possible to identify mitochondrial mammalian homologues of other downstream components of the bacterial periplasmic stress response system.

Given these observations, it seems possible that HtrA2 is a component of a mitochondrial stress pathway. Loss of HtrA2 might have two possible outcomes: 1) If HtrA2 is actively involved in mitochondrial stress signalling, its absence might lead to down-regulation of putative signalling pathways that modulate nuclear gene expression. Or 2) Even if HtrA2 does not play a direct role in a putative mitochondrial stress signalling pathway, its loss might result in the up-regulation of stress-regulated genes as a consequence of enhanced mitochondrial stress in cells lacking this protease. This is an important question to address since it could help to understand how a

compromised mitochondrial stress responses might result in cellular dysfunction and disease.

In this chapter, differences in stress-induced mitochondrial signalling in cells derived from WT and HtrA2 KO mice are studied by transcriptional profiling using GeneChip analysis. HtrA2 KO cells are shown to exhibit greater sensitivity to the induction of a specific stress response. Moreover, this stress response seems to be activated specifically in the brains of animals lacking HtrA2 and contains a signature of genes that can be induced by the shared branch of the UPR.

4.2 Transcriptional analysis of rotenone-induced stress response in cells lacking HtrA2

In order to test the contribution of mammalian HtrA2 to the transcriptional activation of a stress response, primary MEFs derived from WT and HtrA2 KO mice were challenged with an inducer of mitochondrial stress and their transcriptional response was monitored using microarray technology (Affymetrix GeneChip array system). MEFs derived from WT and HtrA2 KO animals were chosen for these experiments, as these cells had been previously shown to display differential sensitivity to drug-induced mitochondrial stresses in terms of mitochondrial morphology as well as cell death (Figure 3-6 and Figure 3-7A). The complex I inhibitor rotenone was one of the drugs exhibiting a differential effect on WT and HtrA2 KO MEFs and therefore was used in this study to trigger mitochondrial stress. Interestingly, decreased complex I activity has been reported in biochemical and histological studies of the SN of PD patients (Schapira et al. 1990). In addition, rotenone has been shown to produce a progressive model of parkinsonism in rodents when chronically administered (Betarbet et al. 2000; Sherer et al. 2003).

Primary MEFs at passage 4 were treated with a low dose of rotenone and RNA was isolated 4hrs later. Cells were harvested 4hrs following rotenone treatment in order to minimise indirect effects of drug treatment. The purity and quality of total RNA, cRNA and fragmented cRNA for each sample were controlled by agarose gel analysis, which showed the characteristic bands of 28S and 18S rRNA of total RNA, a smear of cRNA at a range of seizes and fragmented cRNA around 150bp (Figure 4-1B). Three

experimental replicates were obtained for each condition, resulting in a total of 12 samples that were hybridised to Affymetrix MOE430A GeneChip arrays (3 untreated WT, 3 rotenone WT, 3 untreated HtrA2 KO, 3 rotenone HtrA2 KO, Figure 4-1A). MOE430A GeneChips comprise about 22,000 probe sets, representing approximately 14,000 genes, therefore some genes are represented by more than one probe set. The GeneChip array data analysis was carried out within the Genespring software (Silicon Genetics now Agilent Technologies). Probe level intensities were quantile normalised, quantified using RMA (Robust Multi-chip Average) (Irizarry et al. 2003), and a restriction on fold change of 1.2-fold was applied to select probe sets that changed in expression levels.

4.2.1 Rotenone induces a greater number of transcriptional changes in cells lacking HtrA2

First, genes that were regulated by rotenone treatment in WT and HtrA2 KO MEFs, respectively, were identified. These comparisons are highlighted in green (WT) and blue (HtrA2 KO) in Figure 4-1A. In order to determine differentially expressed probe sets, statistical analysis was performed. The false discovery rate (FDR) is a statistical method used in multiple hypothesis testing to correct for multiple comparisons. Its threshold is determined from the observed p-value distribution, and hence the FDR is adaptive to the amount of signal in the data. In WT MEFs, only 130 probe sets changed with rotenone treatment, whereas 1038 probe sets were altered in HtrA2 KO MEFs upon treatment with rotenone when applying a less stringent FDR (0.15) to both comparisons (Figure 4-2A). Choosing a more stringent FDR to identify probe sets significantly changed upon rotenone treatment did not return any probe sets for WT MEFs, whereas in HtrA2 KO MEFs probe sets could still be identified using 0.07 FDR. In both, WT and HtrA2 KO MEFs, the fold-changes upon rotenone treatment were relatively subtle with the majority of changes ranging between 1.2- to 1.5-fold. 27 probe sets in WT and 89 probe sets in HtrA2 KO MEFs were more than 1.5-fold regulated with rotenone treatment (Figure 4-2B). A subset of genes modulated by rotenone treatment in HtrA2 KO MEFs is listed in Table 4-1. Taken together the presented data indicates that the transcriptional response to treatment with rotenone was much stronger in HtrA2 KO MEFs compared to WT. Therefore, loss of HtrA2 results in an enhanced transcriptional signature in response to a mitochondrial stressor.

This is in line with previous observations showing that HtrA2 KO MEFs are more susceptible to rotenone-induced changes of mitochondrial morphology (Figure 3-6) and cell death (Figure 3-7A).

4.2.2 Rotenone results in enhanced up-regulation of CHOP in cells lacking HtrA2 *in vitro*

The TF CHOP has been previously shown to be up-regulated by mitochondrial stressors like rotenone (Ryu et al. 2002) as well as other parkinsonism-inducing drugs like 6-OHDA and MPP+ in cultured cells (Ryu et al. 2002; Holtz and O'Malley 2003). Recently, CHOP has been reported to be up-regulated in neurotoxin-induced rodent models of parkinsonism *in vivo* (Silva et al. 2005). Interestingly, the CHOP transcript was significantly induced (1.9-fold) in HtrA2 KO MEFs treated with rotenone, and not in WT MEFs treated in the same manner (Table 4-1). This induction of CHOP in cells lacking HtrA2 following rotenone treatment could point to an increased level of stress in these mitochondria, as CHOP was found to be implicated in a mitochondria-specific stress response (Zhao et al. 2002).

In order to confirm the increased induction of CHOP in HtrA2 KO MEFs, RT qPCR analysis was performed on RNA from the samples of replicate 3 of the GeneChip analysis. This revealed that rotenone treatment caused a 2-fold induction of CHOP mRNA in cells lacking HtrA2, whereas the level remained unchanged in WT cells (Figure 4-3A). Similarly, extension of this analysis to WT and HtrA2 KO MEFs immortalised with SV40LT antigen revealed that rotenone treatment resulted in an approximately 2-fold induction of CHOP in cells lacking HtrA2 while no significant change was detected in controls (Figure 4-3B). Although short incubations with rotenone failed to result in any CHOP up-regulation in WT cells, prolonged incubation with this drug led to the induction of CHOP mRNA. Nevertheless, the level of induction was consistently lower to that of HtrA2 KO cells (Figure 4-3B).

Loss of HtrA2 function renders cells more susceptible to the up-regulation of CHOP in response to rotenone. However, the cells studied so far have lost HtrA2 expression permanently. In order to test the effect of transient loss of HtrA2 function on CHOP expression, further experiments were performed in a mouse neuroblastoma cell line (Neuro-2a). In these experiments HtrA2 expression was down-regulated transiently by

siRNA and CHOP levels compared to appropriate controls. Interestingly, even in the absence of additional stress stimuli down-regulation of HtrA2 led to the up-regulation of CHOP mRNA (Figure 4-3C). It is possible, that the transfection method might provide the stress stimulus that causes induction of CHOP in cells where HtrA2 is down-regulated. In order to rule out any off-target effects by the HtrA2-specific siRNA, control experiments were performed in WT and HtrA2 KO MEFs. Such experiments showed that the up-regulation of CHOP is evident in WT MEFs following down-regulation of HtrA2 with the siRNA. However, HtrA2-specific siRNA did not significantly affect CHOP expression levels in HtrA2 KO MEFs (Figure 4-3C).

4.2.3 Brain-specific up-regulation of CHOP expression in mice lacking HtrA2

The data presented so far suggests that permanent lack of HtrA2 leads to enhanced expression of CHOP following mitochondrial stress triggered by rotenone, and that transient loss of HtrA2 itself leads to induction of CHOP without an additional stress stimulus. It is possible that tissues which are under great demand for mitochondrial function in the HtrA2 KO mice might be prone to the up-regulation of CHOP. Mitochondrial stress could be elicited through high rates of electron flow through the respiratory chain in highly metabolically active tissues. The hypothesis that only certain tissues are selectively vulnerable to mitochondrial stress is supported by the rodent model of rotenone-induced PD (Betarbet et al. 2000; Sherer et al. 2003). Systemic exposure to rotenone leads to a degenerative lesion in rats, which is selective to the nigrostriatal system, indicative of the vulnerability of this neuronal population to oxidative stress. Therefore, CHOP might be up-regulated in specific tissues whose mitochondria might be particularly vulnerable to loss of HtrA2.

To test this hypothesis, CHOP expression was measured in different tissues from HtrA2 KO mice and compared to levels in WT mice. Results from this analysis revealed that CHOP mRNA levels were found to be 5-fold greater in brains from mice lacking HtrA2 compared to controls. Interestingly, this enhanced expression of CHOP was limited to the brain but absent from other examined tissues (Figure 4-4A). Next, to determine if increased CHOP expression preceded the development of the parkinsonian syndrome of HtrA2 KO mice, the levels of CHOP mRNA were monitored in brains

isolated between P15 and P31. At every age tested, CHOP expression was higher in HtrA2 KO brains compared to controls (Figure 4-4B), proposing that up-regulation of CHOP probably precedes phenotypic alterations in mice devoid of HtrA2. Analysis of HtrA2 Het animals revealed that CHOP expression was comparable to that of WT animals, suggesting that HtrA2 is not haplosinsufficient with respect to up-regulation of CHOP (data not shown). So far, the expression of CHOP was determined using RNA prepared from whole brain homogenates. In order to determine whether CHOP up-regulation was specific to particular anatomical areas of the brain, samples were prepared from dissected cortex, cerebellum and basal ganglia (for localisation of these Figure 3-3A). This analysis revealed a widespread up-regulation of CHOP transcript in all the regions tested from HtrA2 KO mice (Figure 4-4C).

Taken together these results indicate that cells lacking HtrA2 experience a more pronounced transcriptional up-regulation of CHOP in response to treatment with rotenone than WT cells. Nevertheless, CHOP expression is also induced in WT cells, suggesting that the stress response in WT and HtrA2 KO cells might ultimately be similar. However, HtrA2 KO cells appear to be more susceptible to the induction of this stress response. Strikingly, CHOP expression is higher in brain tissue from HtrA2 KO mice, but not in any other tissue tested, suggesting that the brain is selectively vulnerable to mitochondrial stress upon loss of HtrA2 function.

4.2.4 Genes differentially expressed in cells lacking HtrA2 in the absence of any stress stimulus

In order to identify differentially transcribed genes in cells lacking HtrA2 in the absence of any stress stimulus, the untreated replicate samples for each genotype (WT and HtrA2 KO) were analysed (highlighted in orange in Figure 4-1A). The total number of probe sets differentially regulated was 298, within these, 113 were up- and 185 were down-regulated in MEFs derived from HtrA2 deficient animals compared to WT (Figure 4-5A). Similar to the changes detected in rotenone-treated cells, the majority of probe sets showed a fold-change in the range between 1.2- to 1.5-fold. Only 10 probe sets were found to differ more than 2-fold, with HtrA2 being among the strongest differential genes (Figure 4-5B). The strongest up- and down-regulated genes in the cells lacking HtrA2 are listed in Table 4-2.

Five genes were selected for further validation by RT qPCR analysis. All of the detected changes in expression were consistent with the data obtained in the GeneChip experiment (Figure 4-5C). Matrix metalloproteinase 9 (MMP9) was up-regulated in HtrA2 KO MEFs, whereas caveolin 2 (CAV2), nephronectin (NPNT), mannan-binding lectin serine peptidase (MASP1) and aquaporin 1 (AQP1) were down-regulated in the same cells. Among the list of genes differentially expressed in untreated HtrA2 KO cells compared to WT, only a small number of genes was also modulated by rotenone treatment. Most of these genes, however, were at the border of 1.2-fold difference. For example, NPNT was down-regulated in HtrA2 KO MEFs (Figure 4-5C and Table 4-2) and also induced by rotenone in HtrA2 KO MEFs (1.3-fold). However, the induction of NPNT by rotenone could not be validated by RT qPCR analysis (data not shown), suggesting, that its up-regulation by rotenone treatment is not reproducible.

4.3 Characterisation of a stress response in brain tissue from mice lacking HtrA2

The data presented so far indicates that loss of HtrA2 leads to activation of a stress response characterised by the up-regulation of CHOP. Furthermore, this up-regulation seems to occur specifically in the brains of animals lacking HtrA2. Interestingly, CHOP has not only been shown to respond to cellular stresses leading to the induction of apoptosis (Guyton et al. 1996; Matsumoto et al. 1996; Zinszner et al. 1998; Kawahara et al. 2001; Maytin et al. 2001; Gotoh et al. 2002; Mengesdorf et al. 2002), but in addition to be up-regulated in neurotoxin-induced rodent models of PD (Silva et al. 2005). Loss of HtrA2 in mice seems to elicit a similar stress response, and studying this stress response in more detail might add to understanding the molecular pathways involved in the development of PD in the HtrA2 KO mice. In order to characterise this stress response more extensively, transcriptional profiling was performed on cortex tissue from WT and HtrA2 KO mice (Figure 4-6A). Previously, an increase in the expression of CHOP was shown to occur in the basal ganglia of HtrA2 KO mice where the neurodegeneration is found, but also in the cortex and cerebellum of these mice (Figure 4-4C). Since neuronal loss does occur in the striatum (part of the basal ganglia) of the HtrA2 KO mice, this might be reflected in the transcriptional profile. Cortex tissue was chosen for the GeneChip analysis since it does not suffer from cellular loss. Therefore, the effect of the stress response could be examined rather than the impact of

the loss of cells in the transcriptome of HtrA2 KO mice brains. Affymetrix Mouse Genome 2.0 GeneChips were used in this study. These GeneChips comprise about 39,000 probe sets and some genes are represented by more than one probe set. The quality of the total RNA for each replicate was controlled on an Agilent Bioanalyser, showing the characteristic bands of 28S and 18S rRNA of total RNA (Figure 4-6B). The GeneChip array data analysis was carried out within the Bioconductor software (Gentleman et al. 2004). Probe level intensities were quantile normalised and quantified using RMA (Irizarry et al. 2003).

Probe sets differentially expressed between the WT and HtrA2 KO replicate groups were identified by applying a 0.05 FDR threshold, and these are highlighted red in the volcano plot (Figure 4-6C). In total 792 probe sets were differentially expressed and approximately equal numbers were up- and down-regulated (Figure 4-6D). When the probe sets were ranked upon their absolute fold change, only 11 were more than 3-fold different between WT and HtrA2 KO brain samples, and 70 probe sets were between 2- to 3-fold up- or down-regulated in the samples from HtrA2 KO brain. The majority of probes sets identified by the 0.05 FDR threshold were in the range of 1.2- to 2-fold differentially expressed (Figure 4-6F).

When a more stringent threshold of 0.01 FDR was applied to analyse probe sets differentially expressed between the WT and HtrA2 KO replicate groups, 79 probe sets were identified. 47 of these probe sets were up- and 32 were down-regulated (Figure 4-6E). Most of the probe sets lost by applying a 0.01 FDR compared to 0.05 FDR were regulated in the lower fold-range (Figure 4-6F). Therefore, the genes displaying a greater difference in expression between WT and HtrA2 KO cortex are more likely to withstand a more stringent statistical cut-off.

Table 4-3 shows a list of genes passing the 0.05 FDR threshold that are above 2.5-fold up- or down-regulated in the brains of mice lacking HtrA2. Genes passing the 0.01 FDR threshold are highlighted in bold and italics. Besides HtrA2, only two up-regulated genes, Shmt2 and Mthfd2, are mitochondrial proteins. Gene Ontology analysis on all genes identified by 0.05 FDR (792 probe sets, supplementary data CD), detected 36 genes that are mitochondrial proteins. Therefore, a relatively small number of genes differentially expressed in HtrA2 KO brain encode for mitochondrial proteins.

Furthermore, none of the mitochondrial proteins, Hsp60, Hsp10, mtDnaJ and ClpP, that were previously shown to be up-regulated in response to mitochondrial stress mediated by an unfolded protein (Zhao et al. 2002), were identified to be differentially expressed in HtrA2 KO brain. This observation suggests that the stress response observed in HtrA2 KO brains is probably mediated by different transcriptional elements than a CHOP element that was implicated in the up-regulation of Hsp60/Hsp10 (Zhao et al. 2002).

Next, the results for HtrA2 and CHOP, which could be viewed as negative and positive control, were examined in more detail. In Figure 4-7A and B the expression ratio for HtrA2 and CHOP, respectively, are plotted for each sample. In the GeneChip analysis, HtrA2 was 4.8-fold down-regulated in HtrA2 KO cortex and this was the strongest absolute fold change among all genes. CHOP was also among the strongest differentially expressed genes, being 3.6-fold induced in HtrA2 KO cortex (Table 4-3). The relative level of CHOP mRNA within each single sample was also measured by RT qPCR (Figure 4-7C). Although CHOP expression varied between 2.2- to 5.8-fold across the replicates when measured by RT qPCR, the average of 3.7-fold increase matched with the data obtained from the GeneChip analysis.

4.3.1 Transcripts modulated in brains lacking HtrA2: a comparative analysis with the *in vitro* stress response to rotenone treatment

In order to focus on genes that might be part of a stress response in HtrA2 KO brains similarly to CHOP, the probe sets regulated in MEFs upon rotenone treatment were tested against the expression data obtained from WT and HtrA2 KO cortex samples. The significance was tested using gene set enrichment analysis (GSEA) (Subramanian et al. 2005), which is a computational method that determines whether an *a priori* defined set of genes shows statistically significant, concordant differences between two biological conditions. When all 1099 probe sets regulated upon rotenone treatment in MEFs (WT and/or HtrA2 KO) were tested against the data acquired from the cortex tissue, the GSEA returned a p-value of 0. Therefore, a significant number of probe sets regulated by rotenone were similarly differentially expressed in HtrA2 KO cortex. In contrast, when instead a list of 1099 probe sets was randomly selected from all probe

sets on the Affymetrix Mouse Genome 2.0 GeneChip, the GSEA resulted in a p-value of 0.73, which is not significant (data not shown).

Next, the probe sets in common between the probe sets differentially expressed in HtrA2 KO brain identified by 0.05 FDR threshold and probe sets regulated in MEFs upon rotenone treatment were identified. 68 probe sets were found to be present in both conditions (Figure 4-7D). These 68 overlapping probe sets corresponded to 56 genes, however, 8 of these exhibited up-regulation in HtrA2 KO brain and down-regulation in MEFs by rotenone treatment, or vice versa, and these were therefore omitted from further analysis. 23 of the genes were up-regulated in HtrA2 KO cortex as well as upon rotenone treatment in MEFs, whereas the expression of 25 genes was down-regulated in HtrA2 KO cortex and by treatment of MEFs with rotenone (Table 4-4). Strikingly, applying a more stringent threshold of 0.01 FDR to identify genes differentially expressed in WT and HtrA2 KO cortex tissue led to the enrichment of probe sets also identified to be regulated by rotenone in MEFs (Figure 4-7E). 20 out of 79 probe sets (25.3%) were also present in the set of probe sets regulated by rotenone in MEFs, whereas the overlap was 68 probe sets out of 792 (8.6%) when using the 0.05 FDR threshold for the cortex samples. Genes passing the 0.01 FDR threshold are highlighted in bold and italics in Table 4-4.

Thus, the signature of transcripts regulated in cells treated with rotenone is similar to the genes that are differentially expressed in brains of mice lacking HtrA2. Studying the genes listed in Table 4-4 and their regulation might possibly lead to identification of common upstream signalling events that could be responsible for such transcriptional signature.

4.3.2 Heightened expression of ATF3 and Herp in brains of mice lacking HtrA2

Markedly, besides CHOP, two other genes reported to be up-regulated following ER stress and other stresses leading to activation of eIF2α kinases, were found to be expressed at higher levels in HtrA2 KO brain samples compared to WT: ATF3 and Herp (Jiang et al. 2004; Ma and Hendershot 2004) (link to figure in introduction that shows overview of this pathway). ATF3 was also induced in MEFs treated with rotenone (Table 4-4), however, Herp was not significantly induced by treatment

with rotenone. In order to validate the GeneChip results from comparision of WT and HtrA2 KO brain tissue, RT qPCR was performed on selected genes. ATF3 and Herp were included in this analysis, and in addition KLF5 and Hsp60. KLF5 is a TF that was also found induced in HtrA2 KO cortex, however, its induction has not been linked to the UPR or other stresses leading to activation of eIF2α kinases. Previously, CHOP up-regulation has been implicated in a mitochondria-specific stress response leading to increased expression of Hsp60 (Zhao et al. 2002). Although Hsp60 was not changing in the GeneChip analysis, its transcript levels were also measured by RT qPCR. CHOP, ATF3 and Herp were clearly up-regulated in brain tissue from mice lacking HtrA2 (Figure 4-8), although the increase in Herp mRNA was small compared to the high levels of CHOP and ATF3 mRNA. Herp expression in brain tissue from HtrA2 KO mice was found to be 1.5-fold above WT control levels. KLF5 expression levels did not differ between WT and HtrA2 KO brain tissue in most experiments, and Hsp60 transcript levels were never increased in HtrA2 KO tissue. Taken together, the GeneChip data could not be reproducibly validated for KLF5, however, the expression levels of CHOP, ATF3 and Herp were increased in brain tissue from mice deficient for HtrA2.

4.3.3 Genes up-regulated in brains from HtrA2 KO mice display C/EBP-ATF composite binding sites

Several of the genes found to be up-regulated in HtrA2 KO cortex and in rotenone treated MEFs have been previously described to be induced in response to ER stress dependent on the TF ATF4 (marked by an arrow next to the gene symbol in Table 4-4) (Vallejo et al. 1993; Fawcett et al. 1999; Siu et al. 2002; Harding et al. 2003; Ohoka et al. 2005). In addition, analysis of the promoter regions of several of these genes has identified C/EBP-ATF composite sites. Such genes include CHOP (Wolfgang et al. 1997), asparagine synthetase (ASNS) (Barbosa-Tessmann et al. 2000), tribbles 3 (TRB3) (Ohoka et al. 2005), Herp (Ma and Hendershot 2004), and ATF3 (Wolfgang et al. 2000). Heterodimers of C/EBP-related and ATF/CRE-related TFs can bind to this composite site, which consists of half of each, a palindromic C/EBP- and a variant ATF/CRE-binding site, and has been described for the first time in the CHOP promoter (Wolfgang et al. 1997) (Figure 4-9). Transcriptional activity is enhanced through this

site in response to amino acid starvation, ER stress and probably other stresses that result in an increase of ATF4 protein (for review (Wek et al. 2006)).

The up-regulated genes in Table 4-4 and 15 additional genes showing higher expression in HtrA2 KO brain (0.05 FDR) were selected for sequence analysis in order to identify putatitve C/EBP-ATF composite binding sites. The 15 additional genes were chosen based on their impaired induction following ER stress in ATF4 deficient cells (Harding et al. 2003). The genomic sequence of these genes and 4000bp upstream of the transcriptional start site (TSS) of each gene were screened for the presence of a C/EBP-ATF composite site with the consensus sequence: TT(G/T)CATCA. Then, the alignment of mouse and human sequence were tested and one mismatch was allowed to occur in either of the analysis steps. The analysis showed that out of the 37 genes tested only 4 (Bri3, Slc3a2, Lgals3bp, Gas5) did not contain a C/EBP-ATF composite site. 18 genes contained at least one perfect C/EBP-ATF composite site, with no mismatch from the consensus sequence or between the mouse and human alignment (Table 4-5A). Furthermore, 15 genes contained C/EBP-ATF composite sites with one mismatch to the consensus site (Table 4-5B). Of these, TRB3, H2afy3 and Sord showed one mismatch from the consensus site in the mouse sequence, but the corresponding human sequence perfectly matched the consensus sequence, suggesting that a mismatch at these positions might not influence the activity of the site. In order to rule out the possibility that the conservation of the sites between mouse and human is due to their localisation in the coding region of the genes, the locations of the C/EBP-ATF composite sites were determined. All of the sites were within the 5'UTR, the promoter or an intron of the genes, only one gene, Vps11, possessed a C/EBP-ATF composite site with one mismatch within an exon and did not contain any other sites.

Taken together, a signature of genes previously reported to be up-regulated in an ATF4-dependent manner in response to ER stress (Harding et al. 2003) was identified in brains from mice lacking HtrA2. Strikingly, sequence analysis of these genes revealed a C/EBP-ATF composite site for their transcriptional regulation in almost all of the genes.

4.3.4 Oxidative stress is implicated in the development of the HtrA2 KO phenotype

Mitochondrial dysfunction and oxidative stress have long been implicated in PD (Gandhi and Wood 2005). Neurotoxins such as MPP+, 6-OHDA and rotenone which lead to the development of PD in animal models (Jeon et al. 1995; Betarbet et al. 2000; Sedelis et al. 2001) and humans (Langston et al. 1983) are known to disturb mitochondrial function and result in enhanced oxidative stress. In addition, these neurotoxins induce changes in gene transcription associated with the UPR and apoptosis (Ryu et al. 2002; Holtz and O'Malley 2003). Recently, oxidative stress caused by 6-OHDA was shown to trigger the UPR and lead to induction of the TFs CHOP and ATF3 (Holtz et al. 2006), therefore placing generation of ROS upstream of the transcriptional changes. Intriguingly, loss of HtrA2 in cells causes mitochondrial stress and leads to increased sensitivity to specific death stimuli (Figure 3-6 and Figure 3-7A). In mice, loss of HtrA2 leads to transcriptional changes that are shared between the UPR and other cellular stresses, and the development of a parkinsonian syndrome. In addition, the bacterial HtrA2 homologues DegS and DegP appear to confer resistance to oxidative stress (Raivio 2005). Therefore, it is possible to propose that loss of HtrA2 function in mice might result in enhanced oxidative stress and generation of ROS, which would then lead to the increased expression of CHOP.

In order to address the level of oxidative stress upon loss of HtrA2, the lipid composition of WT and HtrA2 KO mitochondria was analysed by mass spectrometry (in collaboration with Mauro Degli Esposti, University of Manchester). Lipid peroxidation is the ultimate noxious product of oxygen radicals that impairs mitochondrial and cellular function, fundamentally by damaging membranes (Porter et al. 1995). The analysis revealed that mitochondria derived from HtrA2 KO mice have a greater amount of peroxidised lipids in their membranes. These could be detected in liver mitochondria (Table 4-6) as well as mitochondria isolated from brain (data not shown). Therefore, HtrA2 KO mitochondria probably suffer from increased oxidative stress. Adequately, the production of ROS in HtrA2 KO cells in response to rotenone and 6-OHDA was increased compared to WT cells (Nicoleta Moisoi, MRC Leicester; data not shown).

If HtrA2 KO mice suffer from increased oxidative stress, they might benefit from treatment with anti-oxidants. N-acetyl-L-cysteine (NAC), is widely used as an anti-oxidant in cell culture as well as animal models (Molina-Jimenez et al. 2004; Park et al. 2004), and it functions as a nucleophilic ROS scavenger as well as a precursor of intracellular cysteine and glutathione (GSH) (Weinander et al. 1994). Administration of NAC to the newborn pups was performed by oral administration (200mg/kg body weight) from P6, in addition, the nursing mother received NAC in the drinking water. After weaning at P20, the young mice continued NAC treatment by supplementing their drinking water with 1mg/ml NAC. The onset and progression of the parkinsonian syndrome was delayed in NAC treated HtrA2 KO animals, but had no detectable effect on WT or Het mice. Notably, HtrA2 KO mice treated with NAC survived longer than HtrA2 KO mice treated with vehicle (Figure 4-10). This is the first evidence that HtrA2 KO mice benefit from a reduction in oxidative stress by treatment with anti-oxidants.

Taken together these results indicate that loss of HtrA2 in mice leads to increased oxidative stress, which is implicated in the development of the parkinsonian syndrome in the HtrA2 KO mice.

4.4 The protease inhibitor Ucf-101 induces cellular responses independently of its known target HtrA2

In order to inhibit HtrA2 activity in cells many studies have used the chemical inhibitor Ucf-101, which was reported as a specific inhibitor for this protease (Cilenti et al. 2003). Ucf-101 is a cell-permeable, furfurylidine-thiobarbituric acid compound that competitively and reversibly inhibits HtrA2 protease activity ((Cilenti et al. 2003) and Figure 4-11A). It was shown to have very little activity against various other serine proteases and, when tested in caspase-9 null fibroblasts, was found to inhibit HtrA2 over-expression-induced cell death (Cilenti et al. 2003). On the assumption that it is a specific inhibitor of HtrA2, Ucf-101 has been employed to identify potential substrates of this protease (Cilenti et al. 2004; Trencia et al. 2004) and to study its role in cell death (Blink et al. 2004; Cilenti et al. 2004; Goffredo et al. 2005; Liu et al. 2005). Ucf-101 provides at least partial protection from cell death induction by cisplatin (Cilenti et al. 2004; Cilenti et al. 2004), myocardial ischemia and reperfusion (Liu et al. 2005; Bhuiyan and Fukunaga 2007), TNFα (Blink et al. 2004) and staurosporine (Figure

4-11B), leading to the assumption that HtrA2 plays a role in promoting cell death following these treatments.

Since siRNA against HtrA2 leads to an induction of CHOP mRNA level, inhibition of HtrA2 by Ucf-101 might have a similar effect. To test this, WT and as a control HtrA2 KO MEFs were incubated with Ucf-101 at different concentrations and incubation times, and the levels of CHOP mRNA were measured by RT qPCR. Tunicamycin, which inhibits N-linked glycosylation in the ER, was used as a positive control for the induction of CHOP. Surprisingly, Ucf-101 by itself induced CHOP mRNA, both in WT and HtrA2 KO MEFs (Figure 4-12A). CHOP was already induced 2-fold after only 1h incubation with 20μM Ucf-101, rising to 5-8 fold at 2hrs. In addition, the expression of the TF ATF3, known to be inducible by a variety of stresses (for review see (Hai and Hartman 2001)), was measured. ATF3 was also induced by Ucf-101 in both WT and HtrA2 KO MEFs (Figure 4-12B). The increase in CHOP and ATF3 mRNA levels in response to UCF-101 treatment did not seem to be cell type specific, because similar results were seen in the murine neuroblastoma cell line Neuro-2a (Figure 4-12C). In line with the previous results showing a stronger stress response leading to up-regulation of CHOP mRNA levels in HtrA2 KO MEFs and in brain tissue from HtrA2 KO animals, tunicamycin treatment led to 35-fold induction of CHOP in HtrA2 KO MEFs, but only 20-fold in WT MEFs.

The induction of two TFs that are known to be responsive to stress, CHOP and ATF3, suggests that Ucf-101 might trigger activation of stress pathways in cells. This action is independent of its ability to inhibit HtrA2, as the response is seen as strongly in HtrA2 KO as in WT MEFs. The activation of cellular stress and other signalling pathways by Ucf-101 in WT and HtrA2 KO cells was determined using phospho-specific antibodies (Figure 4-13A). Phosphorylation of eIF2α is a well-documented mechanism of down-regulating protein synthesis under a variety of stress conditions (Figure 1-6B) (Holcik and Sonenberg 2005). The stress-activated protein kinase/Jun-N-terminal kinase SAPK/JNK is potently and preferentially activated by diverse environmental stresses and can also be phosphorylated following stimulation of a member of the germinal centre kinase (GCK) family. p38 MAP kinase participates in a signalling cascade controlling cellular responses to cytokines and stress. Both ERK1 and ERK2 function in a protein kinase cascade that plays a critical role in the regulation of cell growth and

differentiation, and are phosphorylated in response to a wide range of extracellular signals. All of these signalling pathways were activated in a time- and concentration-dependent manner by Ucf-101 in WT and HtrA2 KO MEFs (Figure 4-13A).

Even at low concentrations, the HtrA2 inhibitor Ucf-101 seems to result in broad activation of cellular signalling pathways that is independent of its ability to inhibit HtrA2 proteolytic activity. It is not clear how Ucf-101 elicits such a pronounced overall stress response. The most important implication of these findings is that the inhibitor Ucf-101 should be used with great care and not regarded as an entirely specific inhibitor of HtrA2. Several reports have assumed that all the biological effects of Ucf-101 reflect its inhibition of HtrA2 protease activity (Blink et al. 2004; Cilenti et al. 2004; Cilenti et al. 2004; Trencia et al. 2004; Goffredo et al. 2005; Liu et al. 2005). Since Ucf-101 can induce activation of ERK (Figure 4-13A), it is possible that its survival promoting actions could be mediated via this known anti-apoptotic pathway. Alternatively, moderate activation of various stress-induced pathways has been associated with cellular adaptation, or conditioning, and protection from subsequent challenge with death stimuli, so it is possible that the ability of Ucf-101 to activate these pathways might also contribute to its reported protective effects. A number of agents that induce CHOP are also known to activate the NF-κB pathway. However, Ucf-101 is not able to activate this pathway: it fails to induce phosphorylation of IκBα under circumstances where TNFα gives a robust response (Figure 4-13B).

In addition to inhibiting HtrA2, Ucf-101 might affect other closely related proteases, such as HtrA1 (Hu et al. 1998), HtrA3 (Nie et al. 2003) or HtrA4. The mRNA levels of these proteases in HtrA2 WT and KO MEFs were measured by RT qPCR. Primer pairs for each HtrA family member were designed, so that they did not align with any of the others. HtrA1 and HtrA4 mRNA levels were similar in WT and HtrA2 KO MEFs, however, the HtrA3 mRNA level was 70% reduced in HtrA2 KO MEFs (Figure 4-14A). Therefore HtrA3 is unlikely to be the target of Ucf-101 initiating the response seen equally in WT and HtrA2 KO MEFs. The down-regulation of HtrA3 expression in HtrA2 KO MEFs seems to be an attribute of the MEF cell lines used for this experiment, since HtrA3 expression levels did not vary in tissue from WT and HtrA2 KO mice (data not shown).

While the similarity of the serine protease domains within the HtrA family would suggest that they might also be targeted by Ucf-101, it is likely that they have very distinct function from HtrA2. None of these proteins are known to be mitochondrial or to have consensus mitochondrial import signals; HtrA1 and HtrA3 are reported to be secreted from cells (Hu et al. 1998; Tocharus et al. 2004), and the same seems to be the case for HtrA4 (Figure 4-14B). Neither HtrA1 nor HtrA3 or HtrA4 have been implicated in protection from cell death or stress signalling. A single-nucleotide polymorphism has been identified in the HtrA1 promoter, which leads to an elevated level of HtrA1 expression and increases the susceptibility to Age-related Macular Degeneration causing irreversible vision loss (Dewan et al. 2006; Yang et al. 2006). Even if Ucf-101 was eliciting biological effects on cells through the inhibition of HtrA1, HtrA3 or HtrA4 in addition to inhibition of HtrA2, it seemed unlikely that it will be able to provide meaningful information about HtrA2 function, given the evident functional divergence within this family. Therefore, Ucf-101 should be used with caution to investigate HtrA2 function and its use should always be backed up by data from other approaches to the ablation of HtrA2 activity, such as gene knock out or RNA interference.

4.5 Discussion

The bacterial protease DegS is a critical mediator of a transcriptional stress response initiated in the periplasmic space (Schlieker et al. 2004). To test the attractive hypothesis that HtrA2 might be mediating a stress signalling response in mitochondria, transcriptional profiling was performed to identify HtrA2-dependent transcriptional changes. WT and HtrA2 KO MEFs were challenged with the complex I inhibitor rotenone to induce mitochondrial stress. Cells lacking HtrA2 were previously shown to be more sensitive to this complex I inhibitor when mitochondrial morphology and cell death were examined (Figure 3-6 and Figure 3-7A). A higher number of transcriptional changes were detected in HtrA2 KO MEFs in response to rotenone treatment than in WT cells (Figure 4-2), which is in line with the previous results showing that loss of HtrA2 sensitises cells and their mitochondria to stress stimuli. Although 61 probe sets were differentially expressed in rotenone treated WT cells, but not in HtrA2 KO cells treated with rotenone (Figure 4-2C), only two of these were more than 1.5-fold induced by the treatment. One of the transcripts induced only in rotenone treated WT cells is a

cDNA clone not further characterised, the other one encodes for AMP deaminase 3 (AMPD3). Moreover, no functional signature of genes could be identified that was only modulated in WT cells in response to rotenone treatment but not in HtrA2 KO cells. Therefore, an HtrA2-dependent transcriptional response similar to DegS in bacteria could not be identified. However, most of the genes modulated by rotenone were identified in HtrA2 KO cells, whereas their transcriptional regulation in WT cells was not significant. Thus, rotenone-induced transcriptional changes were more pronounced in cells lacking HtrA2.

Subsequently, the expression of the TF CHOP was shown to be induced to a greater level in HtrA2 KO cells than in WT cells when stimulated with rotenone (Figure 4-3A and B). Similarly, a greater induction of Gadd45a in HtrA2 KO than in WT cells in response to rotenone was verified by RT qPCR (data not shown). Gadd45a is the strongest up-regulated gene in rotenone treated HtrA2 KO MEFs and it is not significantly modulated in WT cells that are treated with rotenone (Table 4-1). Recently, Gadd45a has been implicated in epigenetic gene activation by inducing DNA demethylation (Barreto et al. 2007), and further investigation of its expression levels in HtrA2 KO brains might be of interest. The induction of CHOP in HtrA2 KO MEFs following rotenone treatment could point to an increased level of stress in these mitochondria, as CHOP was found to be implicated in a mitochondria-specific stress response (Zhao et al. 2002). This suggested the possibility that the function of HtrA2 was not DegS-like in a signalling cascade, but more akin to the bacterial protease DegP, which elicits its protective function by refolding or degrading unfolded accumulating proteins. The lack of HtrA2 would lead to a higher level of unfolded proteins in the mitochondrial intermembrane space and therefore the threshold for activation of the mitochondrial stress response would be lower in HtrA2 KO cells compared to the WT cells.

Interestingly, CHOP expression was higher in brain tissue from HtrA2 KO mice, but not in any other tissue tested (Figure 4-4A). This could potentially mirror a higher level of stress in brain due to an increased demand for mitochondrial function or a decreased capacity to cope with the stress elicited by loss of HtrA2 function. Furthermore, the expression of CHOP in brains from HtrA2 Het animals was comparable to that of WT mice, mirroring the fact, that no neurodegeneration or locomotor disabilities are

observed in HtrA2 Het mice. CHOP expression is already higher in brains of HtrA2 KO animals at P15 and P18, suggesting that its up-regulation probably precedes phenotypic alterations in mice devoid of HtrA2 (Figure 4-4B). However, the transcript levels of CHOP were similar in WT and HtrA2 KO brains at P8 (Nicoleta Moisoi, MRC Leicester; data not shown). Thus, the increase in CHOP expression level seems to correlate with the development of a parkinsonian syndrome in HtrA2 KO mice, and might be essential for the manifestation of this phenotype.

Transcriptional profiling of genes differentially expressed in brain tissue from HtrA2 KO mice revealed that, besides CHOP, ATF3 and Herp mRNA levels were also induced in these brains (Figure 4-8). CHOP and Herp are known to be dually regulated by the ER stress-specific and the shared branch of the UPR (Figure 1-6B) (Ma et al. 2002; Ma and Hendershot 2004). Expression of ATF3 is increased following a wide range of stress stimuli. Interestingly, the induction of ATF3 transcript in response to amino acid deprivation or ER stress was demonstrated to occur by mechanisms requiring eIF2α phosphorylation (Jiang et al. 2004). Thus, deregulation of the shared branch of the UPR or activation of other pathways that lead to phosphorylation of eIF2α, and concomitantly stimulate translation of ATF4, could possibly be implicated in the cellular events resulting from loss of HtrA2 function.

Strikingly, a substantial proportion of genes that were expressed to a higher degree in brains from HtrA2 KO mice and also up-regulated in MEFs treated with rotenone, are likely to be ATF4 target genes (Table 4-4). Harding and colleagues studied the transcriptional response of ATF4 deficient and PERK deficient cells to ER stress induced by tunicamycin, and detected an impairment of ATF4 deficient cells to up-regulate the expression of genes involved in amino acid import, resistance to oxidative stress and glutathione import (Harding et al. 2003). Additional genes have been identified in other studies that are dependent on the presence of ATF4 for their induction (Vallejo et al. 1993; Fawcett et al. 1999; Siu et al. 2002; Ohoka et al. 2005). A high proportion of the up-regulated genes listed in Table 4-4 are not or only slightly increased in ATF4 deficient cells following stimulus with tunicamycin (Harding et al. 2003). Among all genes identified to be differentially regulated in HtrA2 KO brain (792 probe sets, 0.05 FDR; list on supplementary data CD), additional genes were up-regulated that are likely to be ATF4 target genes. Therefore, from focussing on the

overlap of genes differentially regulated in HtrA2 KO brain and modulated by rotenone treatment in MEFs (Table 4-4), it was possible to identify a signature of ATF4 target genes within the up-regulated genes. Subsequently, extending the analysis to all genes differentially regulated in HtrA2 KO brain, strengthened the finding, that a signature of genes up-regulated in HtrA2 KO brain were previously reported to depend on ATF4.

Markedly, a C/EBP-ATF composite site had been characterised in the promoters of a subset of the ATF4 target genes up-regulated in HtrA2 KO brain. Transcription through this site was shown to be enhanced in response to amino acid starvation, ER stress and probably other stresses that lead to an increase of ATF4 protein (for review (Wek et al. 2006)). C/EBPβ-ATF4 and CHOP-ATF4 heterodimers were reported to enhance transcriptional activity (Ma et al. 2002; Ohoka et al. 2005), whereas C/EBPβ-ATF3 heterodimers seemed to repress this site (Chen et al. 2004; Lopez et al. 2007). Analysis of the genomic sequence of the putative ATF4 target genes that are up-regulated in HtrA2 KO brain, revealed C/EBP-ATF consensus sites in almost all of the genes (Table 4-5). These results strongly support the hypothesis that deregulation of ATF4 might contribute to the transcriptional profile in brains from mice lacking HtrA2. ATF4 protein levels are regulated through phosphorylation of eIF2α on the translational level (Figure 1-6B). Therefore, investigation of the protein level of ATF4 in WT and HtrA2 KO brain should be performed. In addition, the activity of the upstream signalling pathways (the eIF2α kinases) can be studied using phospho-specific antibodies against PERK, GCN2 and PKR. Very preliminary results indicated, that ATF4 protein levels might possibly be increased in HtrA2 KO brain (data not shown), however, no phosphorylation of PERK could be detected.

Gene expression profiling cannot differentiate between primary and secondary events and, therefore, the GeneChip analysis of brain tissue from HtrA2 mice at P29 may only provide a molecular fingerprint of late-stage processes due to loss of HtrA2. In order to avoid transcriptional differences due to cellular loss in the HtrA2 KO mice brains, cortex tissue was chosen for this analysis. In HtrA2 KO mice, the neurodegeneration can be detected in the posterior portion of the striatum which is part of the basal ganglia (Figure 3-3). It is not clear why these particular neurons die, but it is possible that these cells rely heavily on mitochondrial function, by having a high metabolic rate for

example, and are therefore very susceptible to any disturbance in the mitochondria. Up-regulation of CHOP was detected in all brain regions but not in other tissues of the HtrA2 KO mice that were tested (Figure 4-4). The signature of ATF4 target genes up-regulated in HtrA2 KO brain has been reported to be induced following stimulation with neurotoxins *in vitro* (Ryu et al. 2002; Holtz and O'Malley 2003) and for CHOP also *in vivo* (Silva et al. 2005). Therefore, a transient stimulus with neurotoxins such as 6-OHDA and MPP+ modulates the same genes found up-regulated in HtrA2 KO brains, suggesting that the identified genes are potentially important in the development of PD. Interestingly, the genes modulated by 6-OHDA and MPP+ treatment, but none of the genes induced by treatment with 6-OHDA only, were up-regulated in brains from mice lacking HtrA2 (Holtz and O'Malley 2003). Thus, genes that can be regulated through the shared branch of the UPR are induced in models of PD as diverse as neuronal cells stimulated with neurotoxins *in vitro* and HtrA2 KO mice *in vivo*.

Loss of HtrA2 in combination with cellular stress appears to modulate at least a subset of the genes differentially expressed in HtrA2 KO brain, since a signature of genes is similarly regulated in cells treated with rotenone (Table 4-4). Therefore, it is possible that the region where the neuronal loss is detected is more sensitive to the transcriptional changes or that these commence earlier and consequently lead to cellular demise. The transcriptional profile detected in the cortex tissue of HtrA2 KO mice might indicate that this region could suffer from loss of cells at a later stage, if the animals lived longer. Similarly, if the HtrA2 KO mice survived longer, other tissues could be affected from the stress leading to induction of CHOP. For example, high metabolic activity in skeletal muscle resulting from intense training of the mice might cause up-regulation of CHOP transcript.

Transcriptional profiling from human post-mortem brain tissue of PD patients and normal controls has been performed ((Papapetropoulos and McCorquodale 2007) and references therein). None of these studies identified a signature of genes that had previously been reported from the use of neurotoxin-induced cellular models of PD. However, the human studies used mostly tissue from the SN, suggesting that transcriptional differences detected might be due to loss of cells in the SN from PD patients. In addition, the results seem to vary between different studies and none of the top candidate genes were identified in another study. Therefore, transcriptional

profiling performed on brain regions other than the SN might be necessary to identify candidate genes and pathways that are deregulated in human PD patients before cellular demise occurs.

The induction of CHOP expression has previously been implicated in a mitochondrial stress response (Zhao et al. 2002). Zhao and colleagues used a mutant version of a mitochondrial matrix enzyme that could not fold properly and accumulated in the mitochondria. In their study, the authors noted the transcriptional up-regulation of nuclear genes encoding mitochondrial stress proteins such as Hsp60, Hsp10, mtDnaJ and ClpP. CHOP in association with C/EBPβ did regulate the expression of those mitochondrial stress proteins via a CHOP element in their promoters (Zhao et al. 2002). None of the mitochondrial stress proteins was differentially expressed in HtrA2 KO brain, suggesting that the type of stress in cells that lack HtrA2 might be different. Thus, loss of HtrA2 seems to elicit a different sort of stress than accumulation of unfolded proteins.

HtrA2 KO mice probably suffer from enhanced levels of oxidative stress since mitochondrial lipids from HtrA2 KO mice show a higher content of peroxidised lipids than WT mitochondria (Table 4-6). Also, HtrA2 KO cells produce more ROS than WT cells in response to rotenone and 6-OHDA (data not shown). In addition, the phenotype of HtrA2 KO mice is delayed by treatment with anti-oxidants (Figure 4-10). Oxidative stress had been placed upstream of the induction of CHOP and ATF3 in response to 6-OHDA (Holtz et al. 2006). Therefore, loss of HtrA2 might lead to the production of ROS itself or might diminish the capacity of the cells to counteract ROS, which subsequently causes induction of CHOP and potentially other stress-induced genes.

How could loss of HtrA2 lead to increased production of ROS? In light of the homology of HtrA2 to the bacterial proteases DegP and DegS, two scenarios can be proposed. By assuming a DegP-like function for HtrA2 it could be postulated that HtrA2 would be involved in clearance of unfolded proteins in the intermembrane space of the mitochondria. Therefore, loss of HtrA2 proteolytic function would result in the accumulation of unfolded proteins, possibly members of the respiratory complexes, which would lead to impaired electron transport and generation of ROS. Analogous to a DegS-like function, mammalian HtrA2 could be responsible for transducing a signal

from the mitochondria to the nucleus resulting in increased expression of other proteases or chaperones, that would help to maintain the mitochondria free from misfolded proteins. Loss of HtrA2 would therefore decrease the availability of proteases and folding catalysts in the mitochondria and in turn lead to accumulation of aberrant proteins, impaired electron transport and generation of ROS. A DegS-like function for HtrA2 would be predicted from the similarity of their domain and more importantly their closely related crystal structures (Li et al. 2002; Martins et al. 2003) and would be favoured over a DegP-like model. Furthermore, bacterial DegS is known to induce expression of DegP (Erickson and Gross 1989), supporting the idea that HtrA2 would normally lead to the expression of other proteases involved in mitochondrial maintenance.

An increased content of peroxidised lipids was identified in mitochondria isolated from liver and brain tissue of HtrA2 KO mice, however, an increase in CHOP expression level was only detected in brain tissue. This observation could certainly indicate that the increased expression of CHOP is not connected to the generation of ROS in HtrA2 KO mice, however, a more favourable explanation is that liver cells are less susceptible to the oxidative stress and therefore up-regulation of CHOP in liver or other organs cannot be detected within the life-span of the HtrA2 KO animals. Similar to CHOP expression being exclusively up-regulated in brain tissue although all cells are exposed to loss of HtrA2, the systemic treatment of rats with low doses of rotenone leads selectively to lesions in the nigrostriatal system (Betarbet et al. 2000; Sherer et al. 2003).

Treatment of HtrA2 KO mice with anti-oxidants results in prolonged life-span (Figure 4-10) and is also beneficial for the locomotor activity of the HtrA2 KO mice (Nicoleta Moisoi, Miguel Martins, MRC Leicester). It will be interesting to measure CHOP expression levels in HtrA2 KO mice treated with anti-oxidants. Preliminary analysis was performed on P30 animals, however, the level of CHOP expression was only slightly reduced in HtrA2 KO mice treated with NAC compared to vehicle treated HtrA2 KO mice. These analyses need to be repeated and more importantly extended over a time course. It is possible that measuring CHOP expression levels at P30 is too late in the development of the parkinsonian syndrome, even in HtrA2 KO mice treated with anti-oxidants. HtrA2 KO mice as young as P15 did show increased levels of

CHOP transcript, however, P8 mice did not. Therefore, CHOP expression levels should be monitored between P10 and P20 in HtrA2 KO mice treated with anti-oxidants or vehicle.

Taken together the data indicates that HtrA2 deficient cells are more susceptible to the induction of the TF CHOP in response to rotenone treatment. Moreover, transcriptional profiling of brain tissue from mice lacking HtrA2 validated the increased expression of CHOP and revealed up-regulation of a signature of genes known to be regulated through the shared branch of the UPR, namely the stabilisation of the TF ATF4. These genes appear to be characterised by C/EBP-ATF composite sites for transcriptional regulation. A similar signature of genes was reported to be up-regulated in neuronal cells following stimulation with neurotoxins. Therefore, different models used for studying PD, such as *in vitro* cell systems challenged with neurotoxins and *in vivo* the HtrA2 KO mice, share up-regulation of a specific signature of genes. Interestingly, another pathway often deregulated in PD, proteasome inhibition, was reported to result in activation of one of the eIF2α kinases, GCN2, and increased phosphorylation of eIF2α (Jiang and Wek 2005), which would possibly also lead to induction of an ATF4-dependent signature of genes. Thus, the induction of this signature of genes might be a common underlying theme in PD and the study of the upstream pathways should provide meaningful insight into the cellular mechanisms involved in the development of PD.

Figure 4-1. Transcriptional analysis of rotenone-induced stress response in cells lacking HtrA2 using microarray technology.

(A) Schematic outline of the samples processed for microarray analysis. Primary MEFs were isolated and at passage 4 subjected to treatment with vehicle or 1μM rotenone for 4hrs. 3 replicates were performed. RNA was isolated and samples were processed for hybridisation to Affymetrix MOE430A GeneChips (12 samples in total). Raw data was normalised using RMA and analysed using Genespring software. A restriction on fold change of 1.2-fold was applied and probe sets that were differentially expressed were selected by statistical analysis using one-way ANOVA. Conditions that were compared are highlighted. WT ut to WT rot (green) and KO ut to KO rot (blue): Probe sets identified to be regulated by rotenone in WT or KO MEFs were then compared (dashed line). To identify basal differences between the genotypes, WT ut to KO ut were analysed (orange). Abbreviations: untreated (ut), rot (rotenone). **(B)** Quality control of isolated total RNA from the MEFs, the resulting synthesised cRNA and fragmented cRNA for hybridisation to the GeneChip. The samples from replicate 2 shown are representative of all samples.

Figure 4-1

A

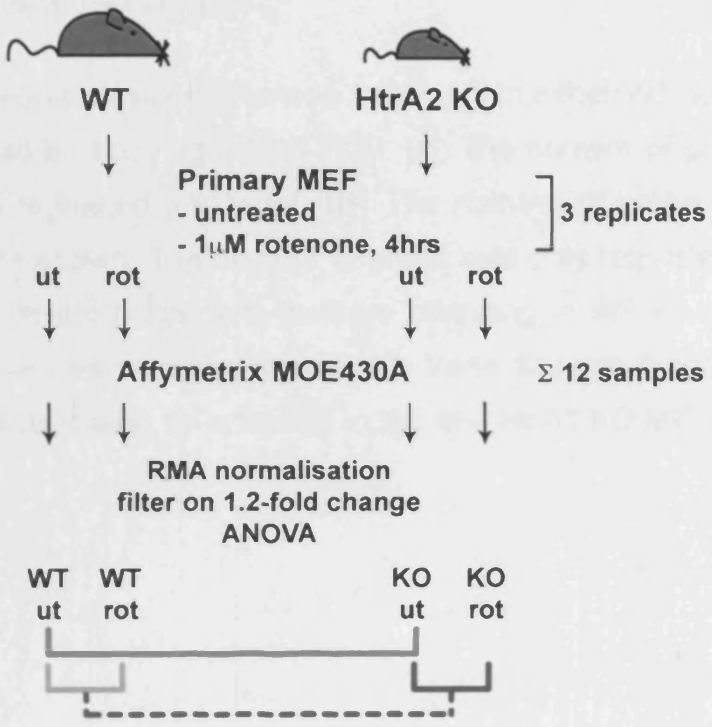
WT
HtrA2 KO
Primary MEF
- untreated
- 1μM rotenone, 4hrs
3 replicates
ut
rot
ut
rot
Affymetrix MOE430A
Σ 12 samples
RMA normalisation
filter on 1.2-fold change
ANOVA
WT ut
WT rot
KO ut
KO rot

B

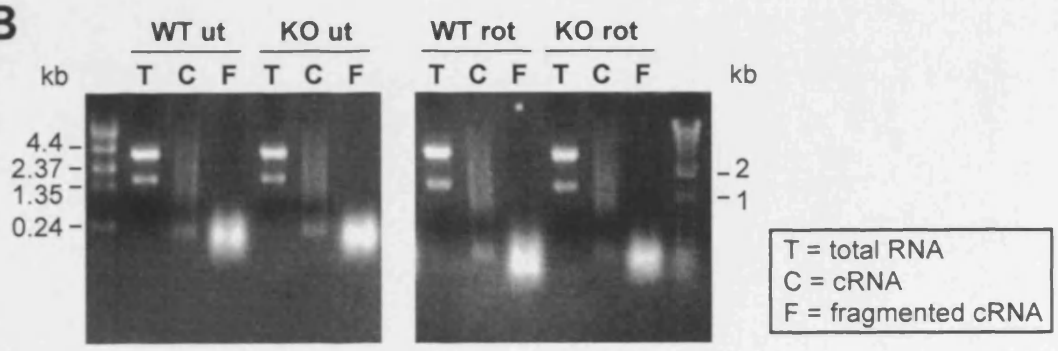
WT ut
KO ut
WT rot
KO rot
kb
T C F T C F T C F T C F
kb
4.4
2.37
1.35
0.24
2
1
T = total RNA
C = cRNA
F = fragmented cRNA

Figure 4-2. Rotenone induces a greater number of transcriptional changes in cells lacking HtrA2.

Probe sets regulated upon rotenone treatment in either WT or HtrA2 KO MEFs were identified by applying a 0.15 FDR. **(A)** The number of probe sets that are up- or down-regulated are listed. **(B)** The number of probe sets within each fold-range are shown. The number of probe sets only regulated in WT or HtrA2 KO, as well as the probe sets that are changing in WT as well as HtrA2 KO upon rotenone treatment are shown. **(C)** Venn diagram illustrating the overlap of probe sets regulated by rotenone in WT and HtrA2 KO MEFs.

Figure 4-2

A

	WT rot / WT
probe sets up	83
probe sets down	47
total	130

	KO rot / KO
probe sets up	429
probe sets down	609
total	1038

B

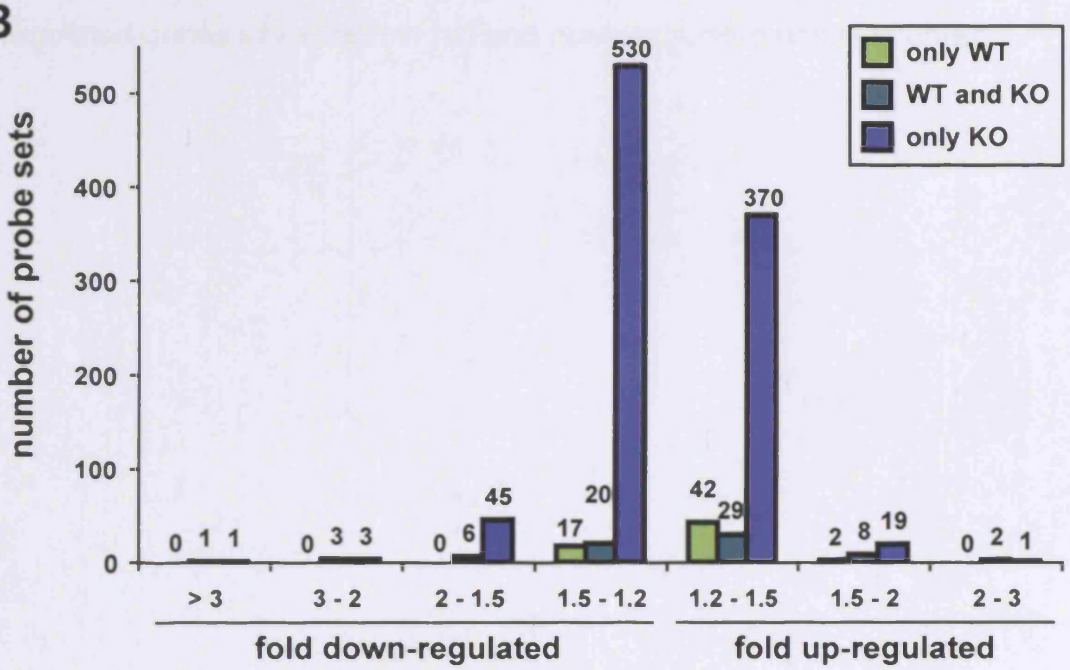

C

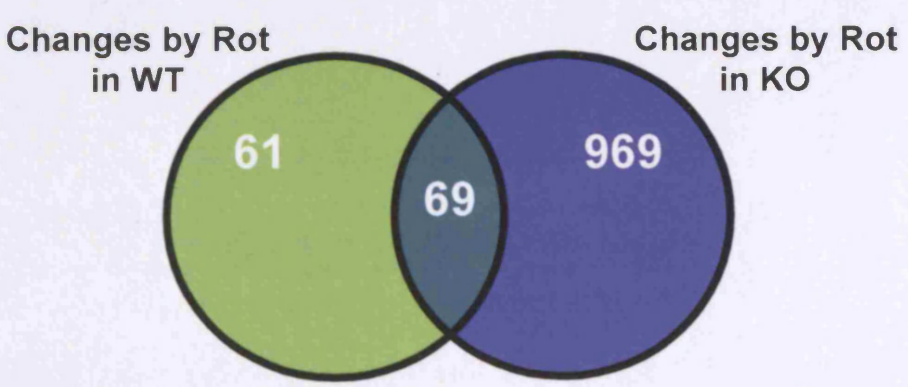

Table 4-1. Genes regulated in HtrA2 KO MEFs upon rotenone treatment.

Shown are genes that are 1.6-fold or more up- or down-regulated in HtrA2 KO MEFs following treatment with rotenone. The total list comprises 969 probe sets and can be found on the CD with supplementary data. The first column shows whether the protein is mitochondrial or not (based on the published literature as well as the prediction programme pSORT II: http://psort.nibb.ac.jp). Up-regulated genes are shown in red and down-regulated genes in green.

Table 4-1

mito	MEF KO Rot/None	Gene Title	Gene Symbol
no	2.70	Growth arrest and DNA-damage-inducible 45 alpha	Gadd45a
no	1.91	Glucosamine-6-phosphate deaminase 1	Gnpda1
no	1.91	RIKEN cDNA 1810008K03 gene	ChaC1
no	1.86	C/EBP homologous protein	CHOP
no	1.76	Stanniocalcin 2	Stc2
no	1.68	Folliculin	Flcn
no	1.68	ATPase, H+ transporting, V1 subunit B, isoform 2	Atp6v1b2
yes	1.64	Adenylate kinase 3 alpha-like 1	Ak4
no	1.63	RIKEN cDNA 4933427C19 gene	5830411G16Rik
no	1.62	Forkhead box G1	Foxg1
yes	1.62	Glutamic pyruvate transaminase (A aminotransferase) 2	Gpt2
no	1.60	Activating transcription factor 4	Atf4
no	0.63	tripartite motif protein 16	Trim16
no	0.62	Heat shock protein 2	Hspa2
no	0.62	Endothelial differentiation, sphingolipid G-protein-coupled receptor, 3	Edg3
no	0.62	Splicing factor, arginine/serine-rich 2 (SC-35)	Sfrs2
no	0.62	Protein phosphatase 1, regulatory subunit 10	Ppp1r10
no	0.62	Thioredoxin domain containing 11	Txndc11
no	0.62	Chemokine orphan receptor 1	Cmkor1
no	0.60	Insulin-like growth factor 1	Igf1
no	0.60	Platelet derived growth factor receptor, alpha polypeptide	Pdgfra
no	0.60	StAR-related lipid transfer (START) domain containing 4	Stard4
no	0.59	ELOVL family member 6, elongation of long chain fatty acids (yeast)	Elovl6
no	0.58	A disintegrin-like and metalloprotease (reprolysin type) with thrombospondin type 1 motif, 1	Adamts1
no	0.58	Tubulin, alpha 3	Tuba3
no	0.58	RIKEN cDNA 6720475J19 gene	6720475J19Rik
no	0.58	Synaptopodin	Synpo
	0.56	Expressed sequence AI448196	AI448196
no	0.55	Male sterility domain containing 2 / putative fatty acyl reductase	Mlstd2
no	0.55	Tubulin, beta 2b	Tubb2b
no	0.54	3-hydroxy-3-methylglutaryl-Coenzyme A synthase 1 (3x)	Hmgcs1
no	0.53	Sterol O-acyltransferase 1	Soat1
no	0.52	Heat shock protein 1B (2x)	Hspa1b
no	0.49	Isopentenyl-diphosphate delta isomerase (2x)	Idi1
no	0.42	Tubulin, beta 3	Tubb3
no	0.41	ADP-ribosylation factor 2	Arf2

Figure 4-3. Rotenone results in enhanced up-regulation of CHOP in cells lacking HtrA2. Transient down-regulation of HtrA2 leads to CHOP induction without further stress stimulus.

(A) CHOP is up-regulated in primary HtrA2 KO MEFs upon treatment with rotenone, but not in WT MEFs treated in the same manner. MEFs were treated with vehicle or 1μM rotenone for 4hrs, RNA was isolated and cDNA was used as a template for qPCR analysis. Transcript levels of CHOP were normalised to Actinγ RNA levels and are shown relative to vehicle treatment. **(B)** CHOP is up-regulated in immortalised HtrA2 KO MEFs by rotenone treatment. Short treatment with rotenone does not induce CHOP expression in WT cells, however it causes nearly 2-fold induction in cells lacking HtrA2. Prolonged treatment for 8hrs with rotenone leads to a 2.7-fold in WT and a 3.9-fold increase in HtrA2 KO MEFs. MEFs were treated with vehicle, 25μM for 3hrs or 10μM rotenone for 8hrs, RNA was isolated and cDNA was used as a template for qPCR analysis. Transcript levels of CHOP were normalised to Actinγ RNA levels and are shown relative to vehicle treatment. **(C)** CHOP mRNA is induced by transient down-regulation of HtrA2. HtrA2 was down-regulated using SmartPool siRNA (Dharmacon) in Neuro-2a neuroblastoma cells, and immortalised WT and HtrA2 KO MEFs. RNA was isolated and cDNA was used as a template for qPCR analysis. Transcript levels of HtrA2 and CHOP were normalised to Actinγ RNA levels and are shown relative to control siRNA. The p-value was calculated using a two-tailed unpaired t-test. The data shown in this figure represent the mean ± standard deviation, n=3.

Figure 4-3

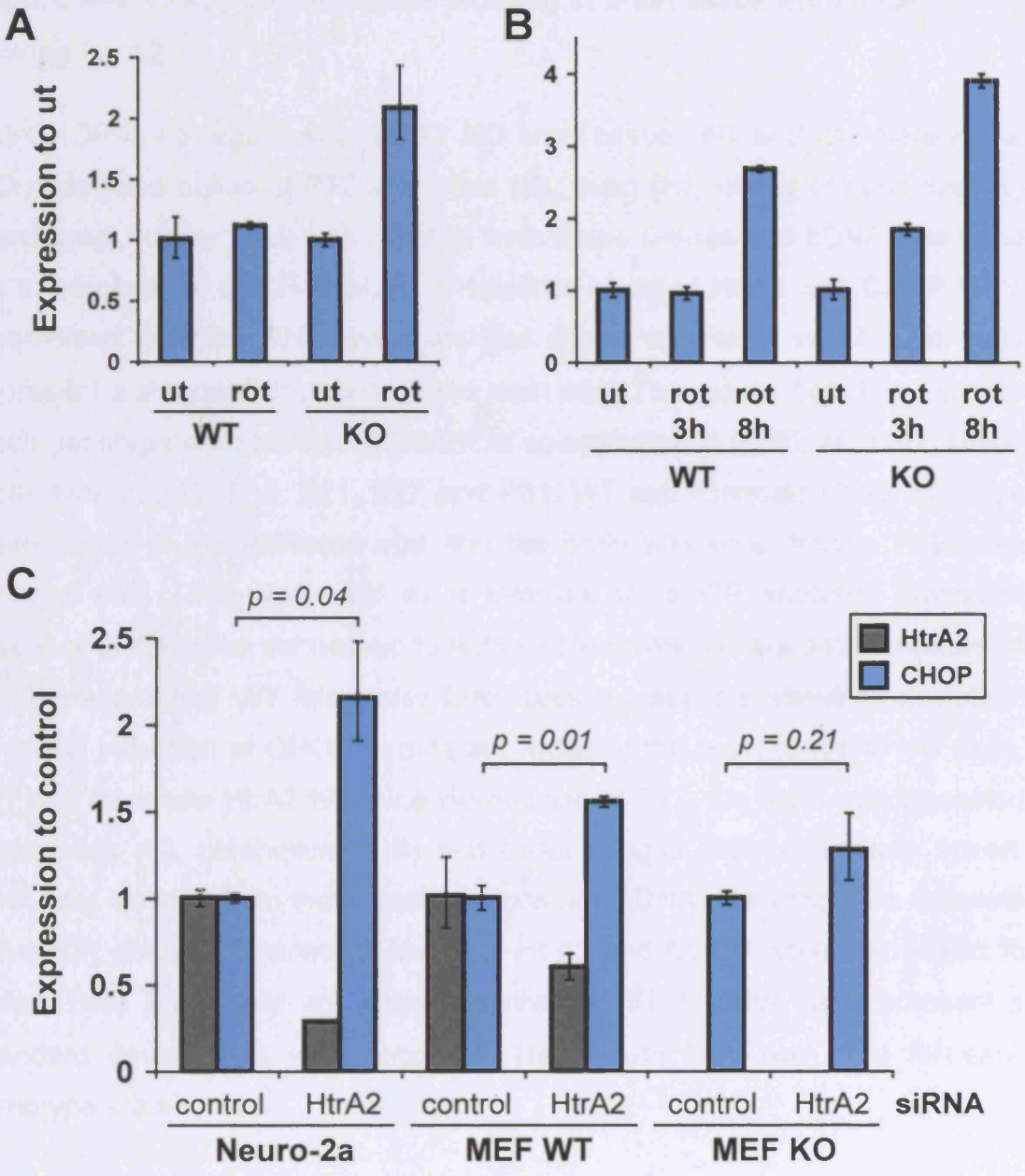
A
Expression to ut
2.5
2
1.5
1
0.5
0
ut
rot
ut
rot
WT
KO
B
4
3
2
1
0
ut
rot 3h
rot 8h
ut
rot 3h
rot 8h
WT
KO
C
Expression to control
2.5
2
1.5
1
0.5
0
p = 0.04
p = 0.01
p = 0.21
HtrA2
CHOP
control
HtrA2
control
HtrA2
control
HtrA2
siRNA
Neuro-2a
MEF WT
MEF KO

Figure 4-4. CHOP expression is induced in brain tissue from mice lacking HtrA2.

(A) CHOP is up-regulated in HtrA2 KO brain tissue. WT and littermate HtrA2 KO mice were culled at P22 and brain (B), heart (H), kidney (K) and liver (L) were snap frozen. RNA was isolated from these tissues and cDNA was used as a template for qPCR analysis. Transcript levels of HtrA2 and CHOP were normalised to Actinγ RNA levels and are shown relative to WT 2. Error bars represent ± standard deviation of two replicates. The results from two mice for each genotype are shown. **(B)** CHOP is up-regulated in HtrA2 KO brain tissue from mice at P15, P18, P21, P27 and P31. WT and littermate HtrA2 KO mice were culled at the indicated age and the brain was snap frozen. RNA was isolated and cDNA was used as a template for qPCR analysis. Transcript levels of CHOP were normalised to Actinγ RNA levels and are shown relative to the corresponding WT littermate. Error bars represent ± standard deviation, n=3. **(C)** Induction of CHOP in different areas of the brain of HtrA2 KO mice. WT and littermate HtrA2 KO mice were culled at P27, the brain was dissected and cortex (C), cerebellum (CB) and basal ganglia (BG) were snap frozen. RNA was isolated from these brain regions and cDNA was used as a template for qPCR analysis. Transcript levels of HtrA2 and CHOP were normalised to Actinγ RNA levels and are shown relative to WT 1. Error bars represent ± standard deviation of two replicates. The results from two mice for each genotype are shown.

Figure 4-4

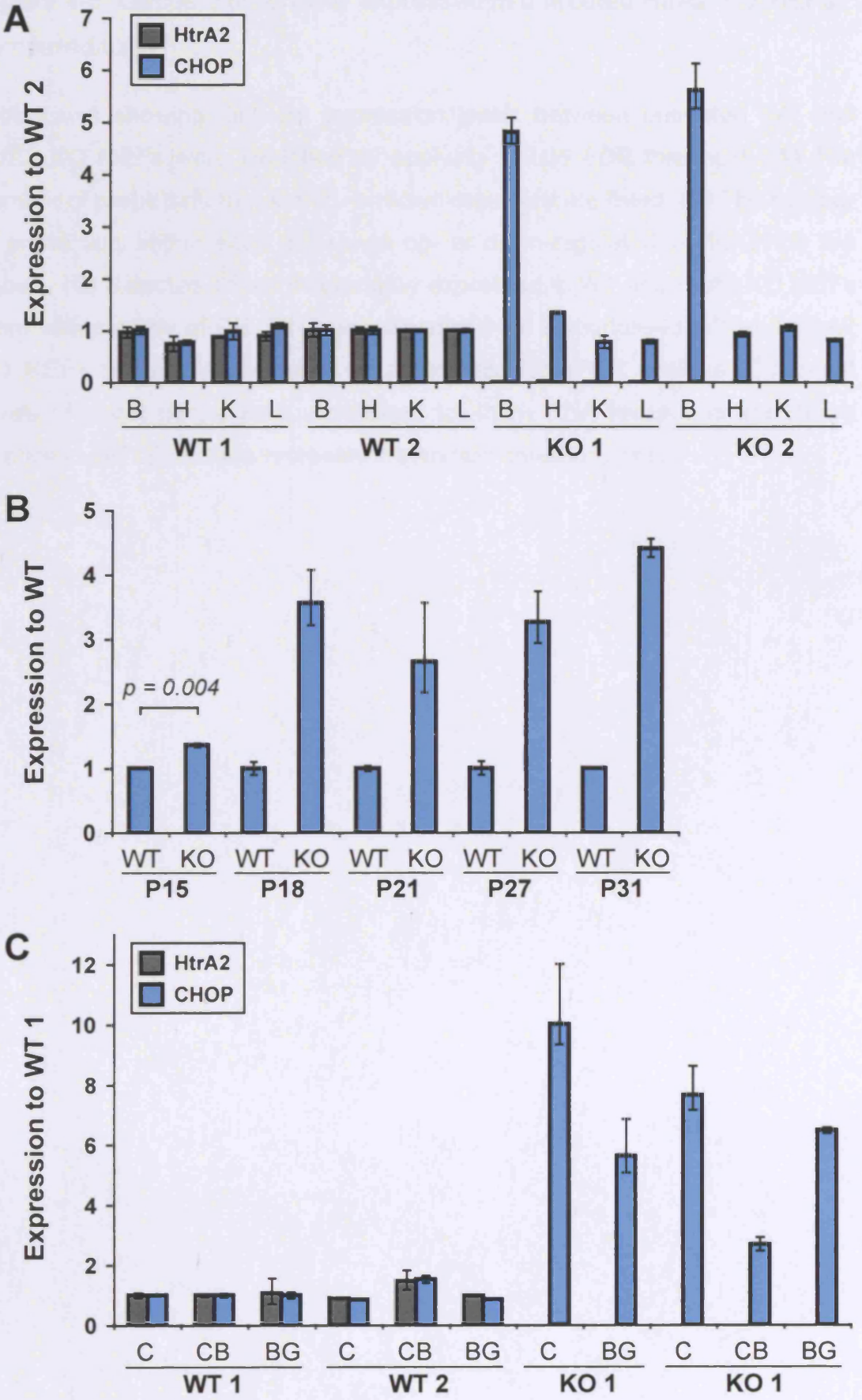
A
HtrA2
CHOP
Expression to WT 2
0
1
2
3
4
5
6
7
B H K L B H K L B H K L B H K L
WT 1
WT 2
KO 1
KO 2
B
Expression to WT
0
1
2
3
4
5
p = 0.004
WT KO WT KO WT KO WT KO WT KO
P15
P18
P21
P27
P31
C
HtrA2
CHOP
Expression to WT 1
0
2
4
6
8
10
12
C CB BG C CB BG C BG C CB BG
WT 1
WT 2
KO 1
KO 1

Figure 4-5. Genes differentially expressed in untreated HtrA2 KO MEFs compared to WT.

Probe sets showing different expression levels between untreated WT and HtrA2 KO MEFs were identified by applying a 0.05 FDR threshold. **(A)** The number of probe sets that are up- or down-regulated are listed. **(B)** The number of probe sets within each fold-range up- or down-regulated in HtrA2 KO are shown. **(C)** Selected genes differentially expressed in WT and HtrA2 KO MEFs were validated by qPCR. RNA was isolated from immortalised WT and HtrA2 KO MEFs and cDNA was used as a template for qPCR analysis. Transcript levels of target genes were normalised to Actinγ RNA levels and are shown relative to WT. Error bars represent ± standard deviation, n=3.

Figure 4-5

A

KO / WT

probe sets up	113
probe sets down	185
total	298

B

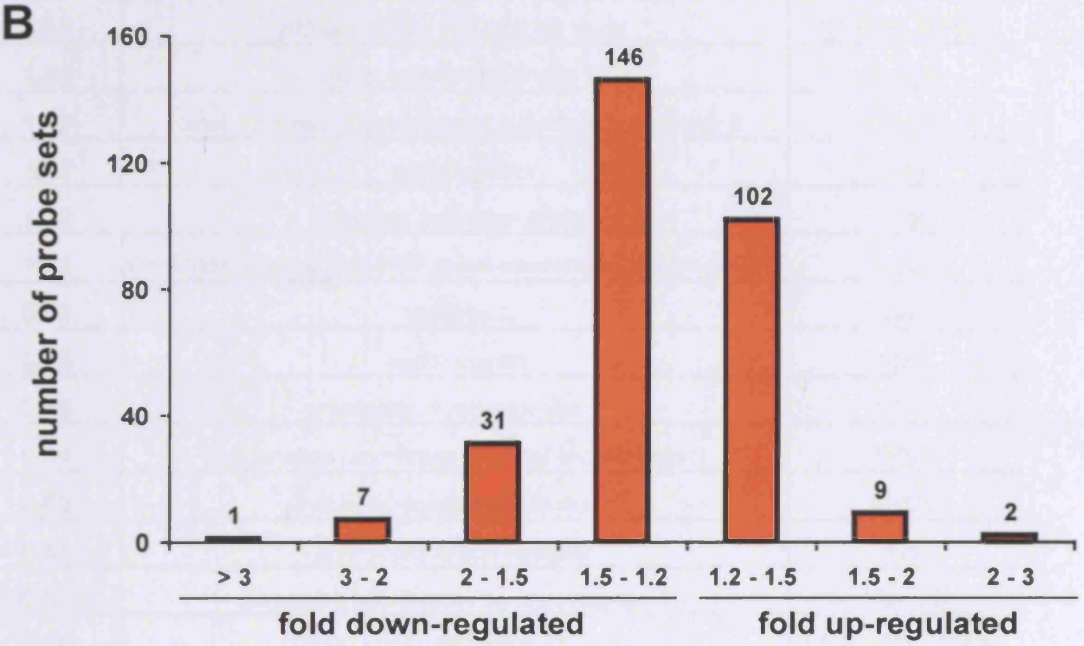

C

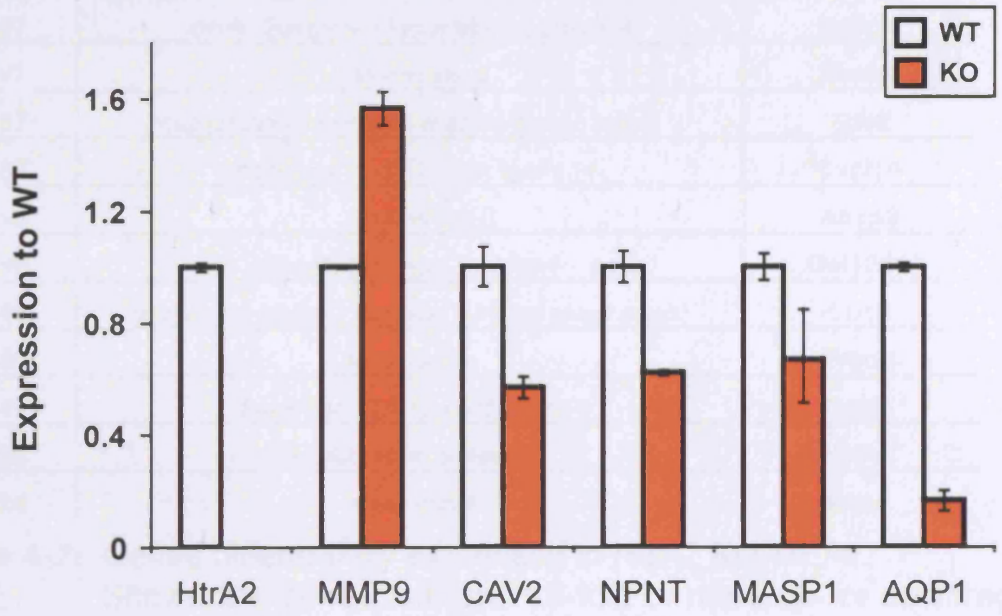

Table 4-2

MEF KO / WT	Gene Title	Gene Symbol
2.45	matrix metalloproteinase 13	Mmp13
2.14	monooxygenase, DBH-like 1	Moxd1
1.84	nephroblastoma overexpressed gene	Nov
1.74	dermatopontin	Dpt
1.61	tissue factor pathway inhibitor 2	Tfpi2
1.58	RIKEN cDNA 1110055J05 gene	1110055J05Rik
1.56	matrix metalloproteinase 9	Mmp9
1.48	tumor necrosis factor receptor superfamily, member 5	Tnfrsf5
1.57	pleiotrophin	Ptn
1.39	fibroblast activation protein	Fap
1.52	phospholipase A2, groupVII (platelet-activating factor acetylhydrolase)	Pla2g7
0.80	caveolin 2	Cav2
0.78	nephronectin	Npnt
0.65	interleukin 1 receptor-like 1	Il1rl1
0.64	gap junction membrane channel protein beta 3	Gjb3
0.62	cytokine receptor-like factor 1	Crlf1
0.61	aryl-hydrocarbon receptor	Ahr
0.61	mannan-binding lectin serine protease 1	Masp1
0.59	RIKEN cDNA A030007L17 gene	A030007L17Rik
0.56	WNT1 inducible signaling pathway protein 2	Wisp2
0.52	interleukin 1 receptor antagonist	Il1rn
0.57	insulin-like growth factor binding protein 4	Igfbp4
0.47	stathmin-like 2	Stmb2
0.53	gap junction membrane channel protein beta 2	Gjb2
0.50	chemokine (C-X-C motif) ligand 14	Cxcl14
0.46	annexin A8	Anxa8
0.49	procollagen, type X, alpha 1	Col10a1
0.46	coagulation factor C homolog (Limulus polyphemus)	Coch
0.46	fibromodulin	Fmod
0.47	chemokine (C-X-C motif) ligand 5	Cxcl5
0.38	HtrA2 serine protease	HtrA2
0.24	aquaporin 1	Aqp1

Table 4-2. Genes differentially expressed in HtrA2 KO MEFs. Shown are genes that are 1.5-fold or more up- or downregulated. The total list comprises 298 probe sets (supplementary data CD). Up-regulated genes are shown in red and downregulated genes in green.

Figure 4-6. Transcriptional profiling of brain tissue from mice lacking HtrA2.

(A) Schematic outline of the samples processed for GeneChip analysis. Brains of WT and HtrA2 KO littermates were dissected to obtain cortex tissue at P29. RNA was isolated and samples were processed for hybridisation to Affymetrix Mouse Genome 2.0 GeneChips (6 samples in total, 3 replicates for each genotype). Raw data was normalised using RMA and analysed within Bioconductor software. Probe sets that were differentially expressed were selected by statistical analysis using one-way ANOVA and a FDR threshold of 0.05 or 0.01. **(B)** Quality control of isolated total RNA for each sample run on an Agilent Bioanalyser. Numbers correspond to the replicate. **(C)** Vulcano plot showing all probe sets. Probe sets passing 0.05 FDR threshold are highlighted in red. The x-axis records the KO/WT $\log_2$ ratio for each probe set, vertical lines show 2-fold up- or down-regulation of expression. The y-axis plots the FDR in -log units, horizontal lines show 0.01, 0.05 and 0.1 FDR threshold respectively. **(D)** 0.05 FDR threshold: The number of probe sets that are up- or down-regulated in HtrA2 KO cortex are listed. **(E)** 0.01 FDR threshold: The number of probe sets that are up- or down-regulated in HtrA2 KO cortex are listed. **(F)** The number of probe sets within a certain fold-range are shown for 0.05 and 0.01 FDR threshold. The lower threshold omits probe sets that are 1.2- to 1.5-fold differentially expressed.

Figure 4-6

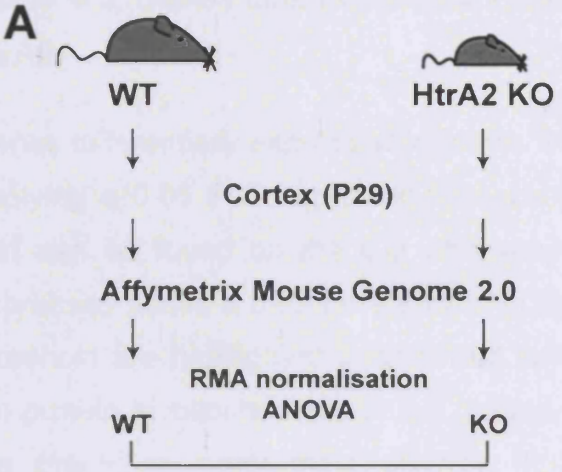

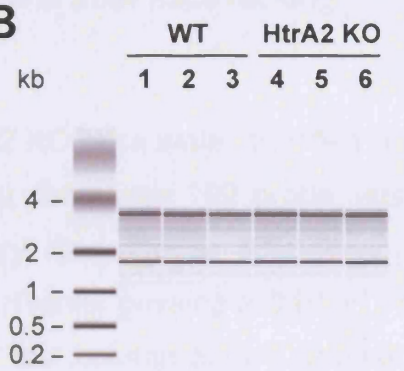

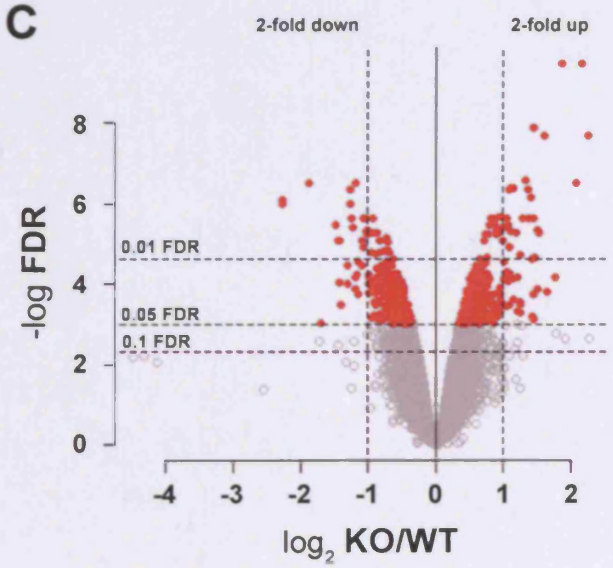

D

probe sets up	397
probe sets down	395
total	792

E

probe sets up	47
probe sets down	32
total	79

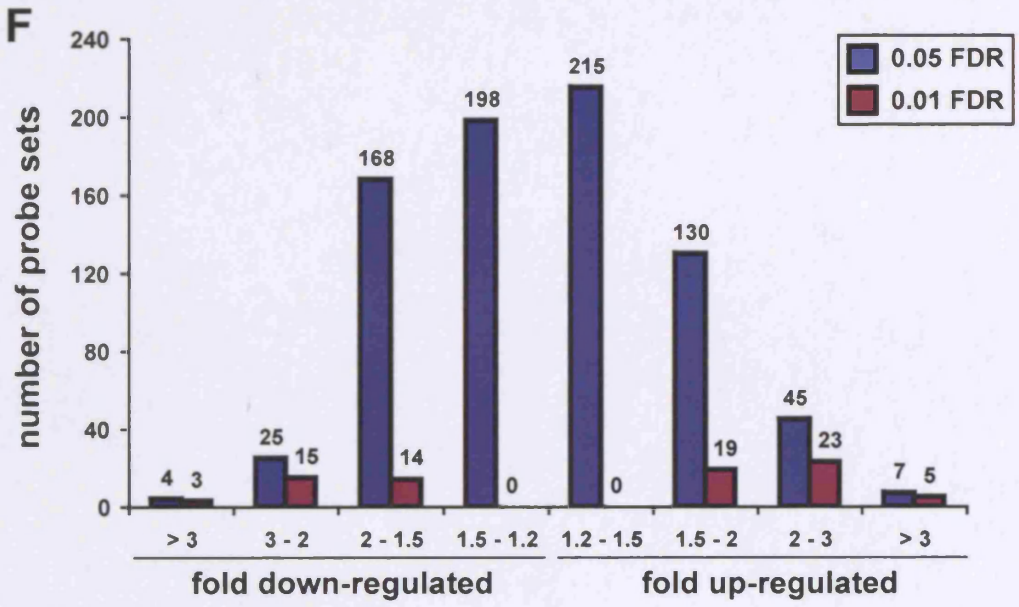

Table 4-3. Genes differentially expressed in brains from mice lacking HtrA2.

Genes differentially expressed in brains from HtrA2 KO mice were identified by applying a 0.05 FDR threshold. The complete list comprises 792 probe sets and can be found on the CD with supplementary data. Genes differentially expressed above 2.5-fold are shown in this table. Genes passing a 0.01 FDR threshold are highlighted in bold and italics. The first column shows whether the protein is mitochondrial or not (based on the published literature as well as the prediction programme pSORT II: http://psort.nibb.ac.jp). Up-regulated genes are shown in red and down-regulated genes in green.

Table 4-3

mito?	Brain KO/WT	Gene Title	Gene Symbol
no	4.76	*solute carrier family 7 (cationic amino acid transporter)*	*Slc7a3 / CAT3*
no	4.44	*cytochrome b5 reductase 1*	*Cyb5r1 / Nqo3a2*
-	4.23	*cDNA clone C230029M16*	*C230029M16*
no	3.62	*C/EBP homologous protein*	*CHOP*
no	3.41	alanine-glyoxylate aminotransferase 2-like 1	Agxt2l1
-	3.10	cDNA clone UI-M-DJ2-bwb-i-13-0-UI	
yes	3.03	serine hydroxymethyl transferase 2 (mitochondrial)	Shmt2
no	2.88	inter-alpha trypsin inhibitor, heavy chain 3	Itih3
no	2.85	pyrroline-5-carboxylate reductase 1	Pycr1
no	2.84	interferon-induced protein with tetratricopeptide repeats 3	Ifit3
-	2.78	RIKEN cDNA 9330179D12 gene	9330179D12Rik
no	2.74	ubiquitin specific peptidase 18	Usp18
no	2.73	RIKEN cDNA 1810010H24 gene	1810010H24Rik
no	2.73	RIKEN cDNA 4930546H06 gene	4930546H06Rik
no	2.73	RIKEN cDNA 1110018M03 gene	1110018M03Rik
yes	2.69	methylenetetrahydrofolate dehydrogenase (NAD+ dependent)	Mthfd2
no	2.69	FEV (ETS oncogene family)	Fev
no	2.65	RIKEN cDNA 2410006H16 gene	2410006H16Rik
-	2.60	RNA, U22 small nucleolar	Rnu22
no	2.58	angiotensinogen (serpin peptidase inhibitor, clade A, member 8)	Agt
no	2.51	RIKEN cDNA 2310005L22 gene	2310005L22Rik
no	0.38	*immunoglobulin heavy chain 6 (heavy chain of IgM)*	*Igh-6*
no	0.37	prostaglandin-endoperoxide synthase 2	Ptgs2
no	0.37	*isopentenyl-diphosphate delta isomerase*	*Idi1*
no	0.36	*Dermokine*	*Dmkn*
no	0.31	activity regulated cytoskeletal-associated protein	Arc
no	0.27	*histone 2, H3c2*	*Hist2h3c2*
no	0.21	*homer homolog 1 (Drosophila) (2x)*	*Homer1*
yes	0.21	*HtrA serine peptidase 2*	*HtrA2*

Figure 4-7. Stress response in brain tissue from mice lacking HtrA2 is similar to stress response elicited by rotenone treatment in MEFs.

Expression ratio of **(A)** HtrA2 and **(B)** CHOP plotted for each of the three WT and HtrA2 KO cortex samples used for GeneChip analysis. **(C)** RT qPCR analysis of these samples. Transcript levels of HtrA2 and CHOP were normalised to Actinγ RNA levels and are shown relative to WT replicate 1. **(D)** Venn diagram showing the overlap of probe sets that were regulated in MEFs upon rotenone treatment (0.15 FDR) and probe sets differentially expressed in WT and HtrA2 KO cortex (0.05 FDR). **(E)** Venn diagram showing the overlap of probe sets that were regulated in MEFs upon rotenone treatment (0.15 FDR) and probe sets differentially expressed in WT and HtrA2 KO cortex (0.01 FDR).

Figure 4-7

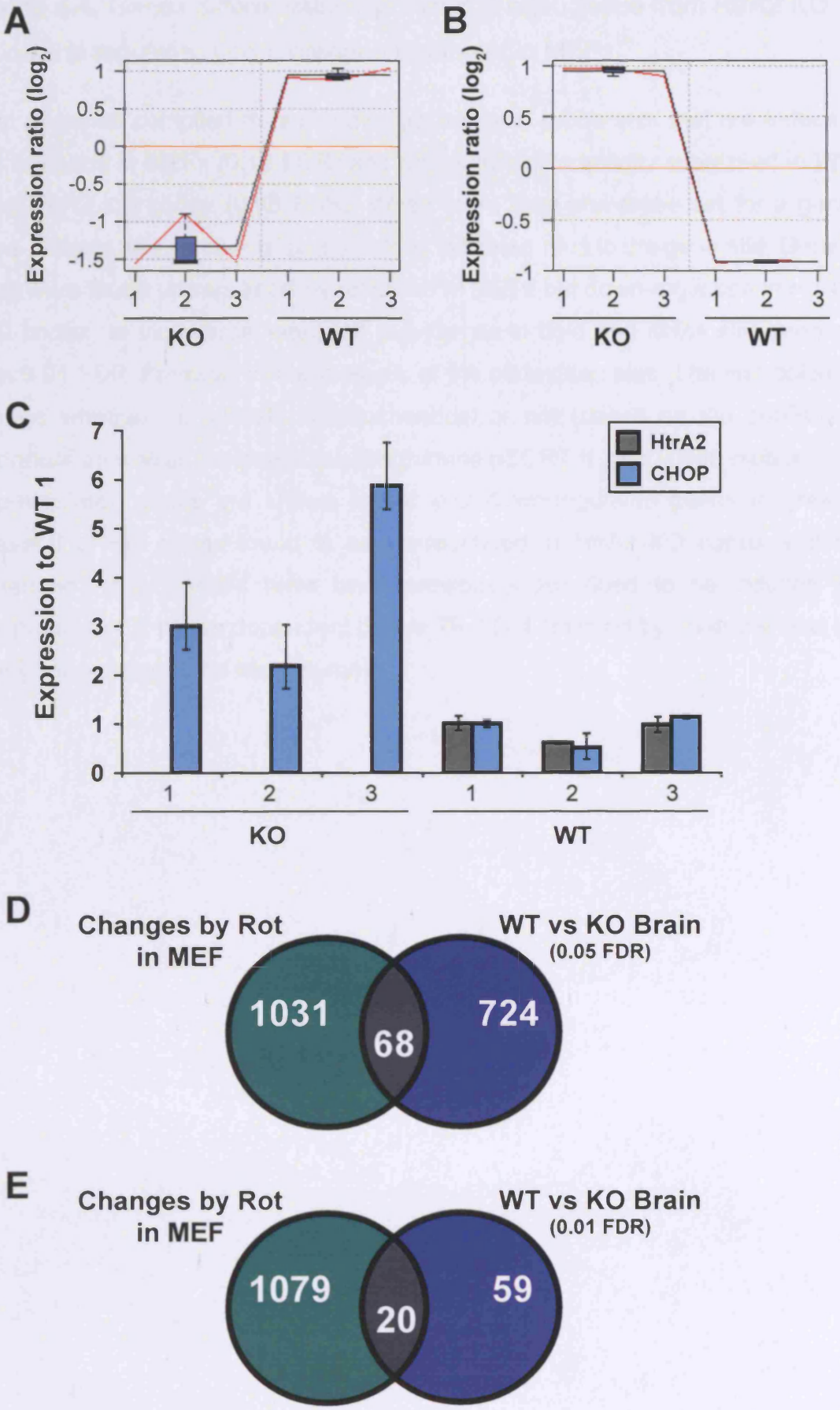
A
Expression ratio (log2)
1
0.5
0
-0.5
-1
-1.5
1 2 3 1 2 3
KO
WT
B
Expression ratio (log2)
1
0.5
0
-0.5
-1
1 2 3 1 2 3
KO
WT
C
Expression to WT 1
7
6
5
4
3
2
1
0
HtrA2
CHOP
1 2 3 1 2 3
KO
WT
D
Changes by Rot in MEF
WT vs KO Brain
(0.05 FDR)
1031
68
724
E
Changes by Rot in MEF
WT vs KO Brain
(0.01 FDR)
1079
20
59

Table 4-4. Genes differentially expressed in brain tissue from HtrA2 KO mice and regulated upon rotenone treatment in MEFs.

List of genes compiled from the overlap between probe sets that are induced by rotenone in MEFs (0.15 FDR) and probe sets differentially expressed in WT and HtrA2 KO cortex (0.05 FDR). When more than one probe set for a gene was present, the number of probe sets is indicated next to the gene title. Genes that were found up-regulated by rotenone in MEFs but down-regulated in HtrA2 KO cortex, or vice versa, were left out. Genes in bold and italics also passed the 0.01 FDR threshold in the analysis of the cortex samples. The first column shows whether the protein is mitochondrial or not (based on the published literature as well as the prediction programme pSORT II: http://psort.nibb.ac.jp). Up-regulated genes are shown in red and down-regulated genes in green. Several of the genes found to be up-regulated in HtrA2 KO cortex and in rotenone treated MEFs have been previously described to be induced in response to ER stress dependent on the TF ATF4 (marked by an arrow next to the gene symbol in the last column).

Table 4-4

mito	Brain KO/WT	MEF KO Rot/None	Gene Title	Gene Symbol
no	3.62	1.85	*C/EBP homologous protein*	*CHOP* ←
yes	3.04	1.25	*serine hydroxymethyl transferase 2 (mitochondrial)*	*Shmt2*
yes	2.70	1.32	*methylene-THF dehydrogenase (NAD+ dep), cyclohydrolase (2x)*	*Mthfd2* ←
no	2.29	1.91	*ChaC, cation transport regulator-like 1 (E. coli)*	*ChaC1*
no	2.16	1.32	plexin domain containing 1	Plxdc1
no	1.97	1.51	*D site albumin promoter binding protein (2x)*	*Dbp*
no	1.92	1.21	eukaryotic translation initiation factor 4E binding protein 1	Eif4ebp1 ←
no	1.87	1.20	solute carrier family 7 (cationic aa transporter, y+ system), member 5	Slc7a5 ←
no	1.86	1.28	*seryl-aminoacyl-tRNA synthetase (2x)*	*Sars* ←
no	1.85	1.24	*asparagine synthetase (2x)*	*Asns* ←
no	1.75	1.29	*phosphoserine phosphatase*	*Psph* ←
no	1.68	1.22	sorbitol dehydrogenase	Sord
yes	1.67	1.24	phosphoenolpyruvate carboxykinase 2 (mitochondrial)	Pck2 ←
no	1.67	1.33	Kruppel-like factor 5	Klf5
no	1.59	1.26	H2A histone family, member Y3	H2afy3
no	1.49	1.22	(glutamate/neutral aa transporter), member 4	Slc1a4
no	1.49	2.06	tribbles homolog 3 (Drosophila)	Trib3 ←
no	1.44	1.33	activating transcription factor 3	Atf3 ←
no	1.39	1.30	slc 3 (activators of dibasic and neutral aa transport), member 2	← Slc3a2 / Dnajc3
no	1.37	1.37	brain protein I3	Bri3
no	1.36	1.31	rhomboid domain containing 1	Rhbdd1
no	1.33	1.21	vacuolar protein sorting 11 (yeast)	Vps11
no	1.29	1.23	RIKEN cDNA 1810031K17 gene	1810031K17Rik

Table 4-4

mito	Brain KO/WT	MEF KO Rot/None	Gene Title	Gene Symbol
no	0.78	0.75	ubiquitin associated protein 2-like	Ubap2l
no	0.75	0.74	f-box only protein 9	Fbxo9
no	0.75	0.74	cAMP-regulated phosphoprotein 19	Arpp19
no	0.74	0.80	transmembrane protein 167	Tmem167
no	0.73	0.59	ELOVL family member 6, elongation of long chain fatty acids (yeast)	Elovl6
no	0.72	0.70	transmembrane protein 119	Tmem119
no	0.72	0.82	histone 1, H2bp	Hist1h2bp
no	0.71	0.75	regulator of G-protein signaling 4	Rgs4
no	0.70	0.80	apurinic/apyrimidinic endonuclease 2	Apex2
no	0.69	0.47	tubulin, beta 2c	Tubb2c
no	0.68	0.70	tribbles homolog 2 (Drosophila)	Trib2
no	0.68	0.82	RIKEN cDNA 1110057K04 gene	1110057K04Rik
no	0.67	0.66	tubulin, alpha 4 (2x)	Tuba4
no	0.67	0.77	7-dehydrocholesterol reductase	Dhcr7
no	0.63	0.82	cyclin D1	Ccnd1
no	0.63	1.34	poliovirus receptor	Pvr
yes?	0.59	0.68	mesoderm specific transcript	Mest / Peg1
no	0.58	0.73	histone 2, H3c1	Hist2h3c1
no	0.56	0.72	***squalene epoxidase***	***Sqle***
no	0.53	0.53	heat shock protein 1B (3x)	Hspa1b
no	0.52	0.57	***HMG-CoA synthase 1 (soluble) (4x)***	***Hmgcs1***
no	0.48	0.66	***low density lipoprotein receptor***	***Ldlr***
no	0.44	0.65	***StAR-related lipid transfer (START) domain containing 4 (2x)***	***Stard4***
no	0.41	0.72	cytochrome P450, family 51	Cyp51
no	0.37	0.50	***isopentenyl-diphosphate delta isomerase (2x)***	***Idi1***

Figure 4-8. ATF3 and Herp are induced in brain tissue from mice lacking HtrA2.

ATF3 and Herp are up-regulated in HtrA2 KO brain tissue. WT and littermate HtrA2 KO mice were culled at P27, the brain was dissected to obtain cortex and basal ganglia tissue which were snap frozen. RNA was isolated and cDNA was used as a template for qPCR analysis. Transcript levels of CHOP, ATF3, Herp, KLF5 and Hsp60 were normalised to Actinγ RNA levels and are shown relative to WT 1. Error bars represent ± standard deviation of two replicates. The results from two mice for each genotype are shown. The p-values for the increase in Herp expression in HtrA2 KO mice compared to WT were calculated using a two-tailed unpaired t-test.

Figure 4-9. C/EBP-ATF composite sites.

Alignment of C/EBP-ATF composite sites (also known as AARE, amino acid response element or NRSE, nutrient-sensing response element) with its related elements, the variant ATF/CRE and palindromic C/EBP sites. The C/EBP-ATF composite sites in the promoters of CHOP, ATF3, Herp, ASNS and TRB3 are shown, revealing the consensus sequence: TT(G/T)CATCA.

Figure 4-8

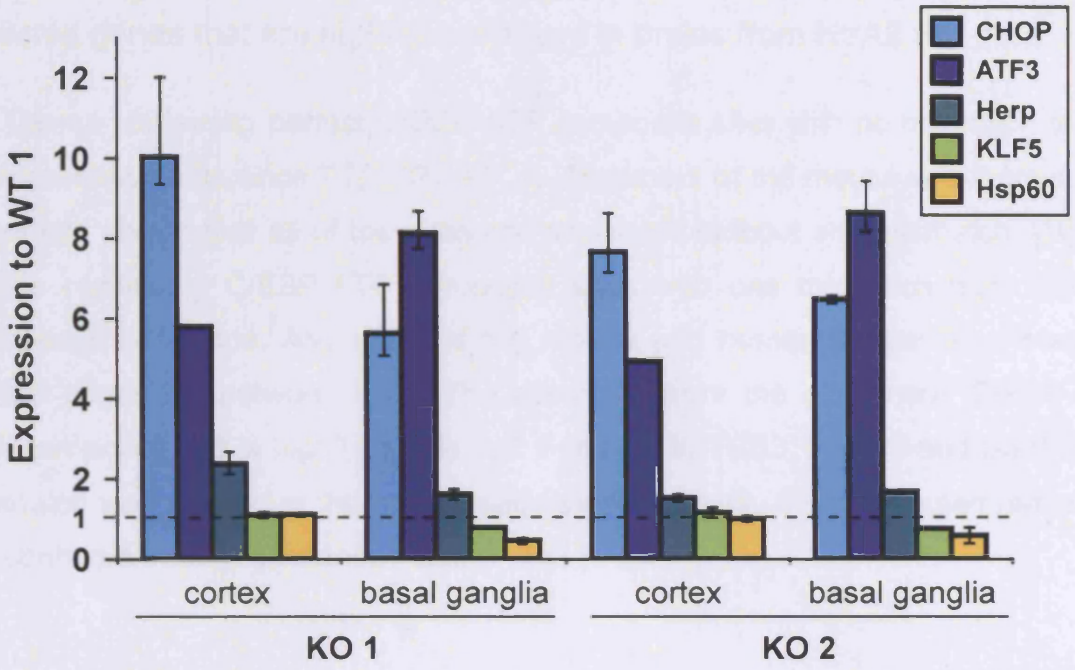

Figure 4-9

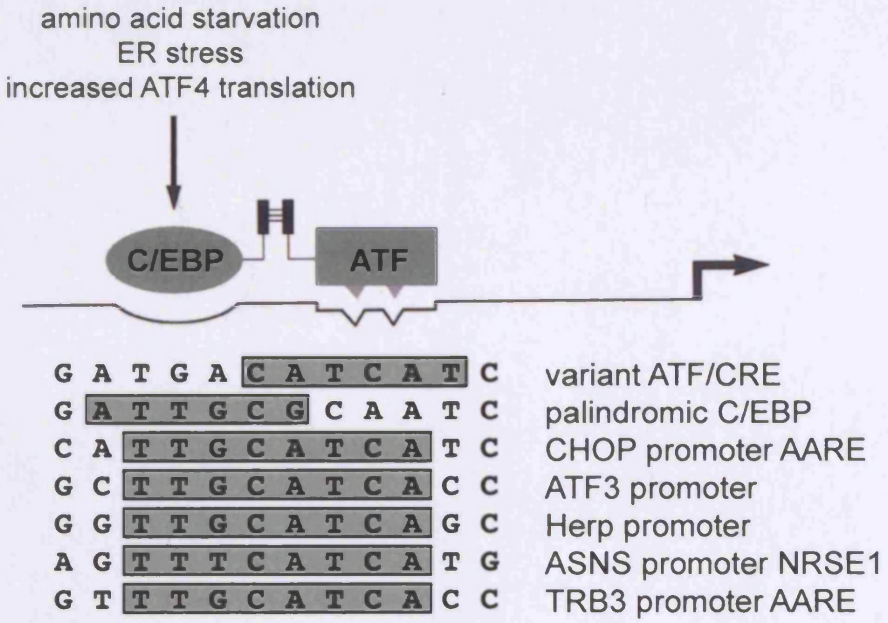

Table 4-5. Presence of C/EBP-ATF composite sites in the sequence of selected genes that are higher expressed in brains from HtrA2 KO mice.

(A) Genes containing perfect C/EBP-ATF composite sites with no mismatch to the consensus sequence TT(G/T)CATCA. Alignment of the mouse with human sequence shows that all of the sites are conserved without any mismatch. **(B)** Genes containing C/EBP-ATF composite sites with one mismatch from the consensus sequence. Alignment of the mouse and human sequence shows perfect alignment between both. The mismatch from the consensus C/EBP-ATF composite site is highlighted in red. For sites in TRB3, H2afy3 and Sord a mismatch was present in the mouse sequence, however, the human sequence did contain a perfect consensus site.

Table 4-5

A

Gene Symbol	C/EBP-ATF site (bp from TSS)	sequence	location
CHOP	-318	TTGCATCA	promoter
ASNS	-50	TTTCATCA	promoter
ATF3	60	TTGCATCA	5' UTR
Herp	-183	TTGCATCA	promoter
	1406	TTGCATCA	intron
	4174	TTGCATCA	intron
Shmt2	469	TTGCATCA	intron
Mthfd2	-417	TTTCATCA	promoter
ChaC1	-884	TTGCATCA	promoter
Slc7a5	9070	TTGCATCA	intron
Sars	961	TTGCATCA	intron
Psph	8371	TTGCATCA	5' UTR
Stc2	-1632	TTTCATCA	promoter
	-952	TTGCATCA	promoter
	562	TTTCATCA	intron
Btf3l4	-519	TTGCATCA	promoter
Klf5	2407	TTGCATCA	intron
Rhbdd1	-899	TTTCATCA	5' UTR
	61,280	TTTCATCA	intron
AARS	-237	TTGCATCA	promoter
NARS	8	TTGCATCA	5' UTR
MARS	9335	TTTCATCA	intron
Brca1	42,463	TTTCATCA	intron

B

TRB3	-22	TTACATCA	5' UTR
H2afy3	11,867	TTTTATCA	5' UTR
Sord	26,415	TTGCAGCA	intron
	6483	TTTCAGCA	intron
Klf5	2035	TTTCATTA	intron
Rhbdd1	-899	TTTCATCA	5' UTR
	35,226	TTTCTTCA	intron
Plxdc1	6466	TTTCATCT	intron
	22,222	TGTCATCA	intron
Dbp	-1893	CTTCATCA	promoter
	-1940	TTTCTTCA	promoter
Eif4ebp1	-884	TTGCATGA	promoter
Pck2	-103	TTACATCA	promoter
Slc1a4	-2584	TGTCATCA	5' UTR
	18,847	CTTCATCA	intron
	24,605	CTTCATCA	exon
Vps11	3497	GTTCATCA	exon
1810031K17Rik	-1120	TTTCTTCA	promoter
	2918	CTTCATCA	exon
YARS	-660	TTTCCTCA	promoter
	19,802	CTTCATCA	intron
MARS	-1714	TGTCATCA	promoter
CARS	3751	TTGCTTCA	intron
	40,919	TTTCATCA	intron
LARS	5,394	TTTTATCA	intron
	8,870	TTTCTTCA	intron
	9,204	TTGCCTCA	intron
	10,832	TTTCTTCA	intron
Slc6a9/Glyt1	22	TTTCACCA	5' UTR
	3364	CTTCATCA	intron
Brca1	28,463	TTTAATCA	intron
Grp75/Hspa9a	-342	TTGCGTCA	intron

Table 4-6. Amount of peroxidised lipids is increased in mitochondria from mice lacking HtrA2.

Mitochondria were isolated to high purity from WT and HtrA2 KO livers. Quantitative analysis was performed by mass spectrometry to determine the amount of peroxidised lipids. The data was normalised to the major phosphatidyl choline, that is PO-PC (*m/z* 758), which was in turn normalised to other reference ions like C-24 Ceramide (*m/z* 685). *m/z*: mass-to-charge ratio. Mass spectrometry of the lipids was performed by Mauro D Esposti, University of Manchester.

Figure 4-10. Anti-oxidant treatment of mice lacking HtrA2 delays their phenotype.

HtrA2 KO mice were treated post-birth with vehicle or NAC and their survival was monitored. Directly after birth until P6 the mothers were fed with drinking water containing 1mg/ml NAC. From P6 until weaning at P20 the pups did receive oral administration of NAC (200mg/kg body weight). From P20 onwards the young mice were fed with drinking water containing 1mg/ml NAC. Control n=13, NAC treatment n=7. These experiments were performed by Nicoleta Moisoi and Miguel Martins (MRC Leicester).

Table 4-6

m/z	peroxidised lipids	WT	KO
301	arachidonate	16.6	40.1
331	lipoxin-like	8	43
353	lipoxin-like	7.8	53.2
365	ultraperoxidised arachidonate	170	280
381	ultraperoxidised arachidonate	25	106.7

Figure 4-10

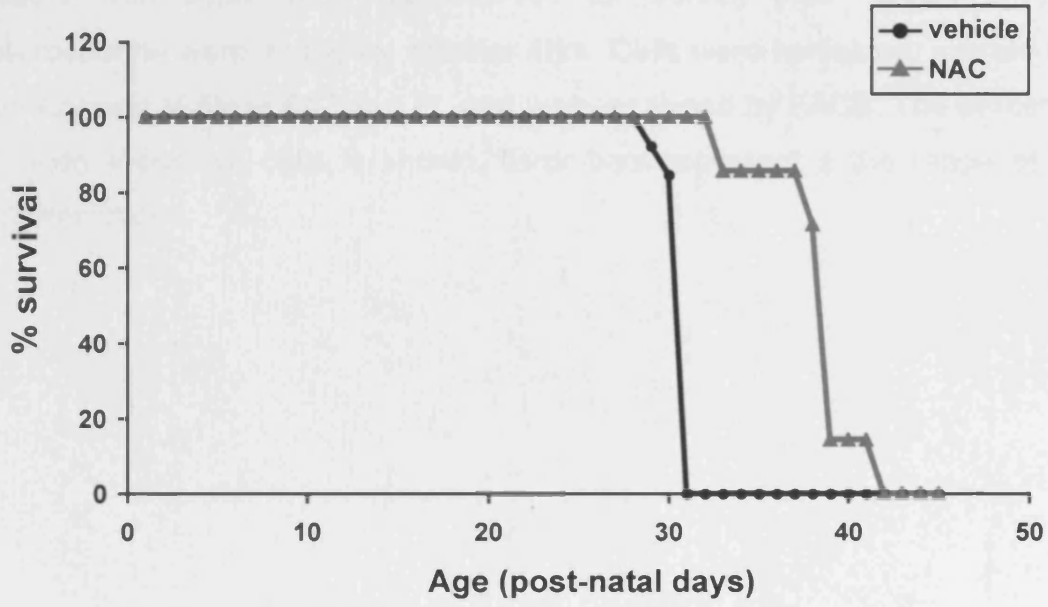

Figure 4-11. Ucf-101 inhibits HtrA2 proteolytic activity and protects cells from death stimulus.

(A) Ucf-101 inhibits HtrA2 protease activity. Recombinant HtrA2 was pre-incubated with the indicated concentrations of Ucf-101 for 15min on ice. After addition of the fluorescent substrate, the increase in fluorescence was monitored on a CytoFluor multi-well plate reader (PerSeptive Biosystems). Protease activity (arbitrary fluorescence units/min) were determined by linear regression analysis of the data points corresponding to the maximum reaction rates for each assay condition. The relative protease activity to control is shown. Error bars represent + standard deviation, n=3. **(B)** Ucf-101 protects cells from staurosporine-induced cell death. Immortalised WT MEFs were pre-treated with 50μM or 70μM Ucf-101 for 20min, then vehicle or 2μM staurosporine were added for another 4hrs. Cells were harvested, stained with anti-Annexin V Alexa 647 and PI, and were analysed by FACS. The percent of Annexin V-positive cells is shown. Error bars represent ± the range of two determinations.

Figure 4-11

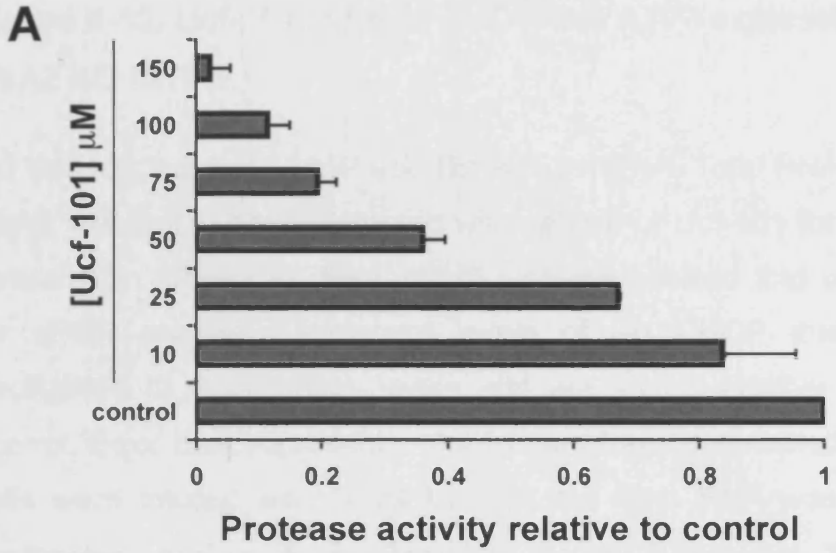
A
[Ucf-101] μM
150
100
75
50
25
10
control
0
0.2
0.4
0.6
0.8
1
Protease activity relative to control

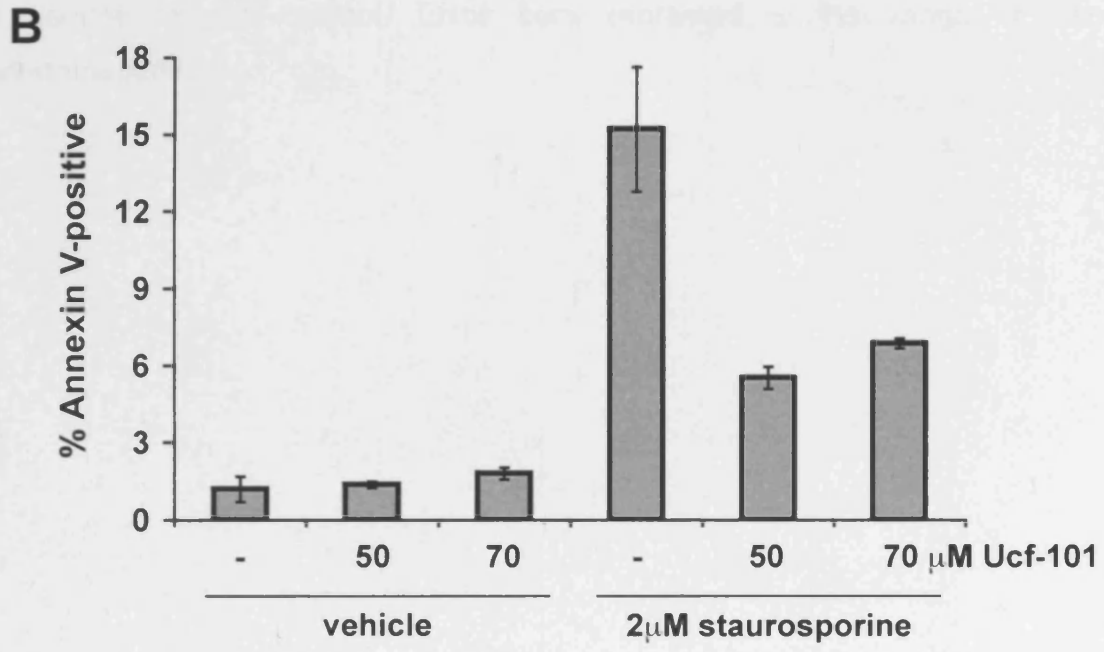
B
% Annexin V-positive
18
15
12
9
6
3
0
-
50
70
-
50
70 μM Ucf-101
vehicle
2μM staurosporine

Figure 4-12. Ucf-101 induces CHOP and ATF3 expression in WT and HtrA2 KO MEFs.

(A) Ucf-101 induces CHOP and **(B)** ATF3 mRNA. Total RNA was isolated from HtrA2 WT and KO MEFs treated with vehicle or Ucf-101 for 1h or 2hrs or with tunicamycin (Tunic) for 2hrs. cDNA was synthesised and used as a template for qPCR analysis. Transcript levels of (A) CHOP and (B) ATF3 were normalised to Actinγ RNA levels and are shown relative to vehicle treated control. Error bars represent + the range of two determinations. **(C)** Neuro-2a cells were treated with 50μM Ucf-101 for 4hrs. RNA was harvested, cDNA synthesised and used as a template for qPCR analysis. Transcript levels of CHOP and ATF3 were normalised to Actinγ RNA levels and are shown relative to vehicle treated control. Error bars represent ± the range of two determinations.

Figure 4-12

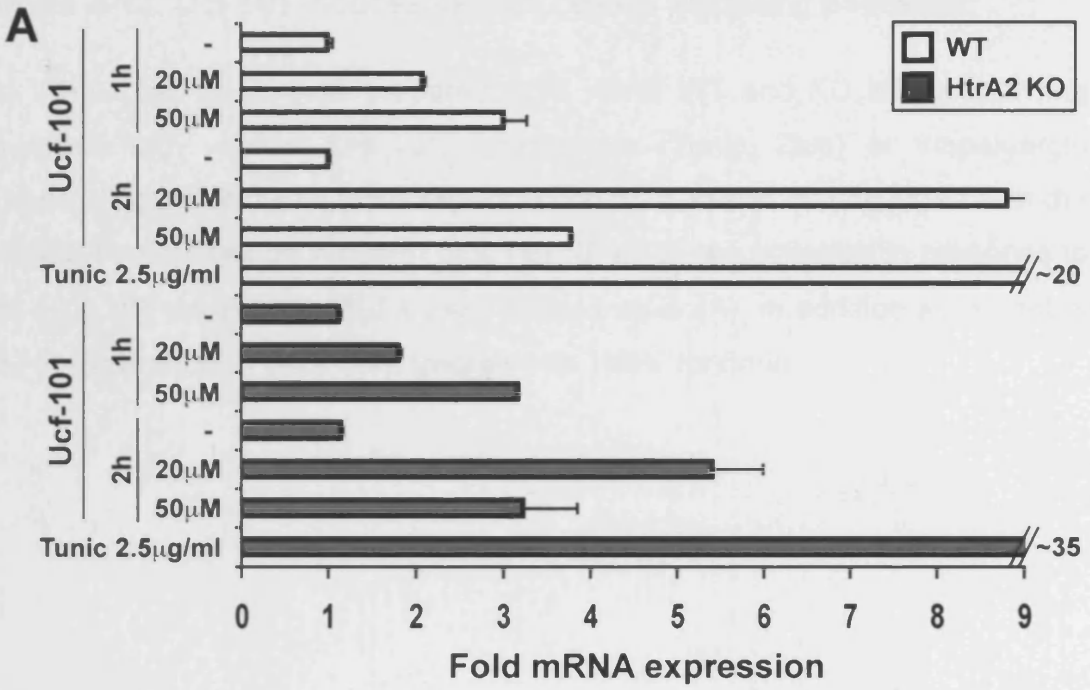
A
WT
HtrA2 KO
Ucf-101
1h
2h
-
20μM
50μM
Tunic 2.5μg/ml
~20
~35
0
1
2
3
4
5
6
7
8
9
Fold mRNA expression

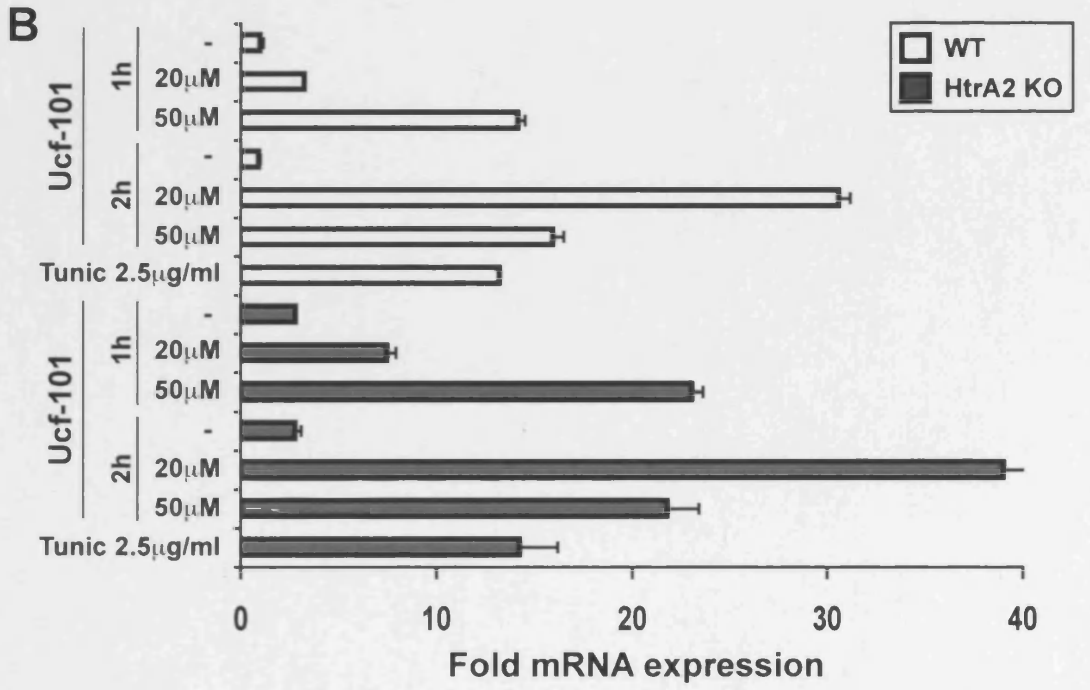
B
WT
HtrA2 KO
Ucf-101
1h
2h
-
20μM
50μM
Tunic 2.5μg/ml
0
10
20
30
40
Fold mRNA expression

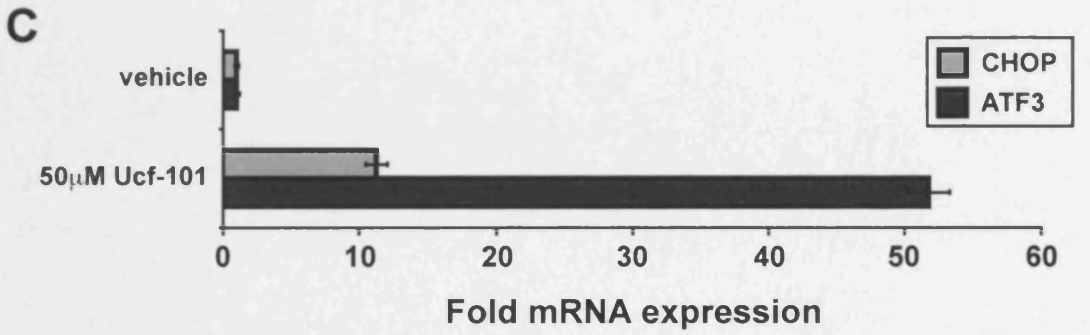
C
CHOP
ATF3
vehicle
50μM Ucf-101
0
10
20
30
40
50
60
Fold mRNA expression

Figure 4-13. Ucf-101 induces various cellular signalling pathways.

(A) Whole cell lysate was prepared from HtrA2 WT and KO MEFs following treatment with vehicle, Ucf-101, tunicamycin (Tunic, 2hrs) or thapsigargin (Thapsi, 30min). Proteins were separated on SDS-PAGE and detected with the indicated antibodies by Western blot. **(B)** NF-κB is not activated in response to Ucf-101. WT andH2 KO MEFs were treated as in (A), in addition as a control for NF-κB activation cells were treated with TNFα for 5min.

Figure 4-13

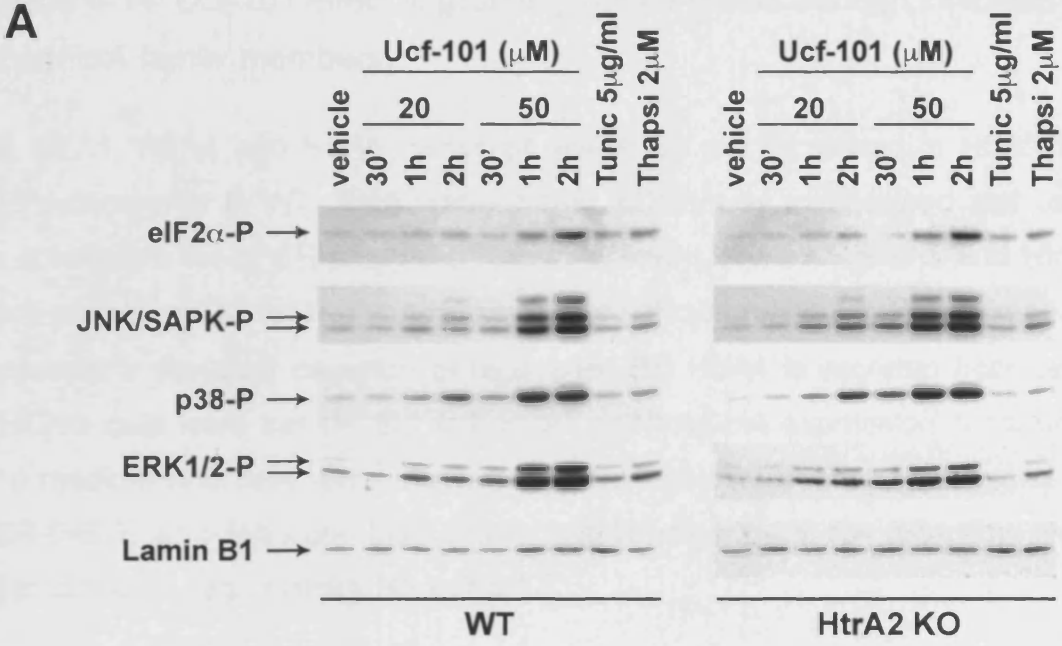
A
Ucf-101 (μM)
vehicle
20
50
30'
1h
2h
30'
1h
2h
Tunic 5μg/ml
Thapsi 2μM
eIF2α-P
JNK/SAPK-P
p38-P
ERK1/2-P
Lamin B1
WT
HtrA2 KO

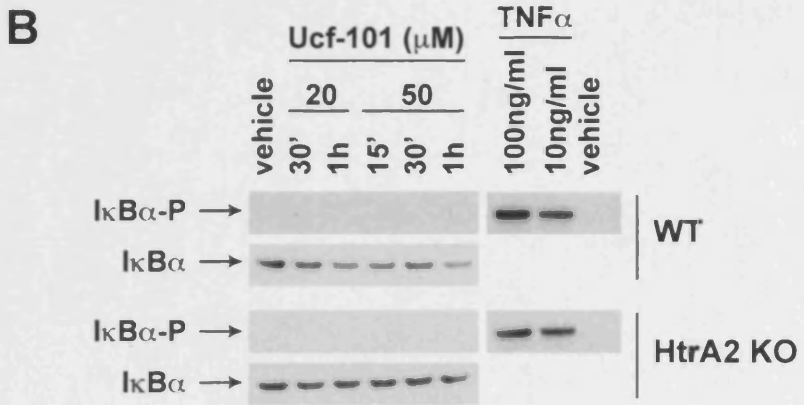
B
Ucf-101 (μM)
TNFα
vehicle
20
50
30'
1h
15'
30'
1h
100ng/ml
10ng/ml
vehicle
IκBα-P
IκBα
IκBα-P
IκBα
WT
HtrA2 KO

Figure 4-14. Ucf-101 effect is probably not mediated through inhibition of other HtrA family members.

(A) HtrA1, HtrA3 and HtrA4 transcript levels are not increased in HtrA2 KO MEFs compared to WT. RNA was isolated, cDNA was synthesised and used as a template for qPCR analysis. Transcript levels of HtrA1, HtrA3 and HtrA4 were normalised to Actinγ RNA levels and are shown relative to WT. Error bars represent ± standard deviation of replicates. **(B)** HtrA4 is secreted from cells. HEK293 cells were transfected with HtrA2 or HtrA4-HA expression constructs. The medium and cells were harvested 48hrs after transfection, processed for SDS-PAGE and Western blot. Primary antibodies used for detection were against the HA tag of HtrA4-HA or HtrA2.

Figure 4-14

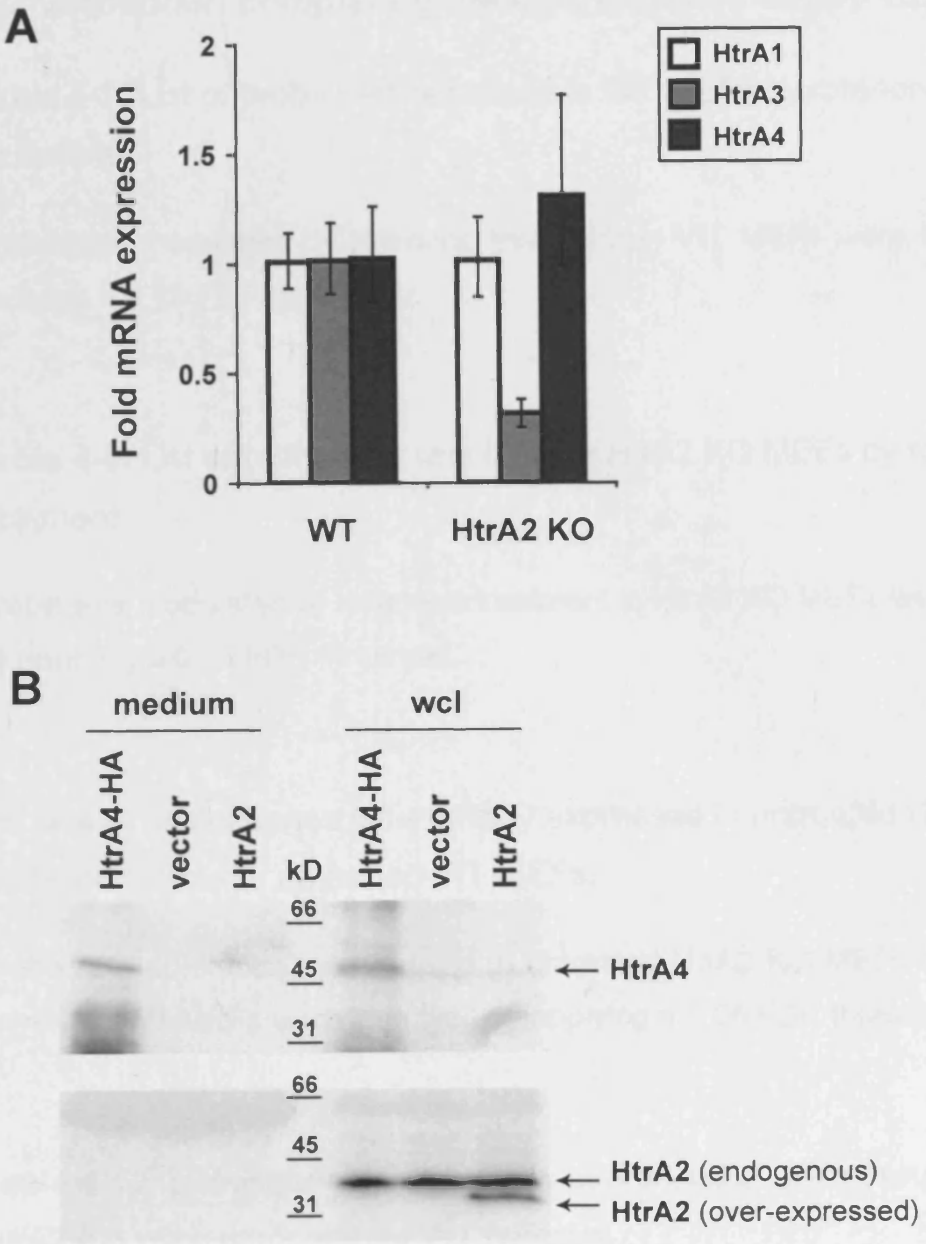
A
Fold mRNA expression
2
1.5
1
0.5
0
HtrA1
HtrA3
HtrA4
WT
HtrA2 KO
B
medium
wcl
HtrA4-HA
vector
HtrA2
kD
HtrA4-HA
vector
HtrA2
66
45
31
66
45
31
HtrA4
HtrA2 (endogenous)
HtrA2 (over-expressed)

4.6 Appendix: complete gene lists (supplementary CD)

Table 4-7. List of probe sets regulated in WT MEFs by rotenone treatment.

Probe sets modulated by rotenone treatment in WT MEFs were identified by applying a 0.15 FDR threshold.

Table 4-8. List of probe sets regulated in HtrA2 KO MEFs by rotenone treatment.

Probe sets modulated by rotenone treatment in HtrA2 KO MEFs were identified by applying a 0.15 FDR threshold.

Table 4-9. List of genes differentially expressed in untreated HtrA2 KO MEFs compared to untreated WT MEFs.

Probe sets differentially expressed in untreated HtrA2 KO MEFs compared to untreated WT MEFs were identified by applying a 0.05 FDR threshold.

Table 4-10. List of genes differentially expressed in brain tissue from HtrA2 KO mice compared to WT controls.

Probes sets differentially expressed in HtrA2 KO cortex tissue compared to WT were identified by applying a 0.05 FDR threshold. Probe sets that withstand the 0.01 FDR threshold are highlighted in bold.

Up-regulated genes are shown in red and down-regulated genes in green.

5 Chapter 5: HtrA2 is regulated by PINK1, a kinase implicated in Parkinson's disease

5.1 Introduction

Apart from HAX-1, all proteins reported to interact with or to be cleaved by HtrA2 are non-mitochondrial proteins (Suzuki et al. 2001; Cilenti et al. 2004; Gupta et al. 2004; Park et al. 2004; Trencia et al. 2004; Kuninaka et al. 2005; Sekine et al. 2005; Hong et al. 2006). However, HtrA2 function seems to be essential for protection of mitochondrial function *in vivo* (Jones et al. 2003; Martins et al. 2004), therefore identification of proteins interacting with HtrA2 in the mitochondria might elucidate the pathway in which HtrA2 is involved. Unfortunately, the unequivocal identification of mitochondrial substrates of HtrA2 using the 2D DIGE approach was not successful (see Chapter 3.7). The Tandem Affinity Purification (TAP) tag system allows the purification of protein complexes under native conditions (Rigaut et al. 1999). In this chapter, a TAP tagged version of HtrA2 is generated and purified complexes are screened for the presence of mitochondrial proteins. This leads to the identification of a novel interaction partner for HtrA2, the PD-associated putative kinase PINK1. Furthermore, HtrA2 is found to be phosphorylated and PINK1 appears to be important for this phosphorylation event to occur. Phosphorylation of HtrA2 is likely to modulate its proteolytic activity and this might contribute to increased resistance of cells to stress-induced apoptosis.

5.2 PINK1 interacts with HtrA2

In order to identify interacting proteins of HtrA2, the TAP tag system was chosen (Rigaut et al. 1999). The TAP tag consists of three components. The first element consists of tandem Protein A epitopes, which allows efficient recovery of the tagged protein and associated components by affinity purification on an IgG-linked bead matrix. This is followed by a cleavage site for the TEV protease, which allows specific elution from the matrix under native conditions. The second element in the tag consists of a calmodulin binding protein (CBP) epitope, which allows a second round of affinity purification on a calmodulin-coated bead matrix. After washing, bound material is again eluted under native conditions, this time by a chelation of Ca^{2+} ions with EGTA. The eluted tagged proteins, together with any co-purifying proteins, can then be

analysed by SDS-PAGE followed either by Western blotting or mass spectrometry.

A TAP tag was added to the C-terminus of full length HtrA2, and the catalytic serine was mutated to alanine (S306A) in order to abolish the proteolytic activity of HtrA2 which could interfere with the purification process by cleaving interacting proteins. HtrA2-TAP was stably expressed in HEK293 cells, and HtrA2 along with interacting proteins was purified. Using 33 antibodies raised against a range of 28 mitochondrial proteins as well as an anti-XIAP antibody as a positive control, the purified fraction containing HtrA2 was analysed by Western blotting (Table 5-1). HAX-1, a protein previously shown to interact with HtrA2 (Cilenti et al. 2004) was found to be co-purified, as well as XIAP, demonstrating the validity of this approach (Figure 5-1A). From the proteins tested, one other protein was found to co-purify with HtrA2, the putative mitochondrial kinase PINK1 (Figure 5-1B). Mutations in the PINK1 gene are associated with the recessive parkinsonism locus PARK6 (Table 1-1). Initially, three pedigrees were described with identified mutations: a G309D point substitution in one family and a truncation mutation (W437X) in two additional families (Valente et al. 2004). Subsequently, several studies have described other point mutations or truncations (Figure 1-7) (Hatano et al. 2004; Rogaeva et al. 2004; Rohe et al. 2004; Bonifati et al. 2005; Li et al. 2005). Given that dysfunction in both HtrA2 and PINK1 have been associated with neuronal degeneration in mammals, the putative interaction between these two might be physiologically important. To confirm the interaction between endogenous PINK1 and HtrA2, endogenous HtrA2 was immunoprecipitated from lysates prepared from WT and HtrA2 KO MEFs. When purified HtrA2 immunoprecipitates were probed with an anti-PINK1 antibody, endogenous PINK1 could be detected in complexes purified from WT but not from HtrA2 KO MEFs, further confirming the specificity of the interaction (Figure 5-1C). Next, co-immunoprecipitation experiments from lysates prepared from cells subjected to sub-cellular fractionation were performed. Such experiments showed that the interaction between endogenous HtrA2 and exogenously expressed PINK1 is detected predominantly in mitochondria-enriched fractions indicating that the interaction is likely to occur in the mitochondria (Figure 5-1D).

5.3 HtrA2 is phosphorylated on serine 142 in response to MEKK3 activation

A mutation screen of the HtrA2 gene performed in German PD patients recently led to the identification of a heterozygous G399S mutation as well as an A141S polymorphism that was associated with the disease (Strauss et al. 2005). The identified mutations localise to domains previously shown to be important in the regulation of the proteolytic activity of HtrA2 (Martins et al. 2003), namely the PDZ domain and the N-terminal portion of the mature form of HtrA2, respectively. An analysis using the Scansite algorithm (Obenauer et al. 2003) (www.scansite.mit.edu) indicates that S142 and S400, residues that lie immediately adjacent to the mutations found in the PD patients, are putative phosphorylation sites for proline-directed serine/threonine kinases (Figure 5-2A). According to Scansite, S142 is a putative phosphorylation site for Cdc2, Cdk5, ERK1 and p38, and S400 is a putative phosphorylation site for Cdc2 and Cdk5. Alignment of HtrA2 homologues of different species shows that S142 and S400 are conserved in human, rodents and chicken, and in addition S400 is further conserved in fly and baker's yeast (Figure 5-2B).

Subsequently, antibodies that specifically recognise HtrA2 phospho-peptides were raised. Peptides surrounding S142 and S400 were synthesised incorporating a phoshporylated serine at these sites. The phospho-specific S400 HtrA2 antibody did not recognise S400, however, the phospho-specific S142 HtrA2 antibody showed an unambiguous signal when used for Western blotting. The specificity of the phospho-S142 antibody was tested on lysates from cells over-expressing WT and S142A mutant HtrA2 (Figure 5-3C), and additionally on recombinant HtrA2 that had been phosphorylated *in vitro* using p38γ (data not shown). To test if HtrA2 could be phosphorylated on S142, HEK293 and NIH 3T3 cell lines expressing 4-hydroxy-tamoxifen (4OH-Tx) inducible versions of MEKK3, Akt and Raf (ΔMEKK3:ER, myrAkt:ER, ΔRaf-DD:ER) were employed. Lysates were then prepared from cells where MEKK3, Akt and Raf had been activated with 4OH-Tx and probed with the phospho-S142 HtrA2 (P-HtrA2) antibody. These experiments showed that activation of MEKK3, but not Akt or Raf, induced efficient phosphorylation of HtrA2 on S142 (Figure 5-2C). Activation of downstream signalling pathways of MEKK3, Akt and Raf were detected by determining the phosphorylation status of Akt, ERK1/2, JNK and

p38. Induction of MEKK3 resulted in strong activation of p38 and JNK and weaker activation of ERK, whereas Raf induction led to strong activation of ERK1/2 and weaker activation of JNK and p38 (Figure 5-2C).

The compound BIRB796 is a broad-spectrum inhibitor of all p38 MAPK isoforms *in vitro* and *in vivo* (Kuma et al. 2005). To test if chemical inhibition of p38 affected MEKK3-dependent phosphorylation of HtrA2, ΔMEKK3:ER expressing cells were treated with increasing concentrations of BIRB796 and the levels of phosphorylated HtrA2 and p38 were analysed. These experiments showed that pre-treatment with BIRB796 partially decreased the levels of detected P-p38 and P-HtrA2, suggesting that p38 activity might be important for the phosphorylation of HtrA2 (Figure 5-2D).

To test whether purified HtrA2 could be phosphorylated by any of the four isoforms of p38, *in vitro* kinase assays using recombinant HtrA2 and p38 were performed. These experiments revealed that HtrA2 could be predominantly phosphorylated by p38γ and also by p38β although not by the two other p38 isoforms p38α and p38δ (data not shown, Helene Plun-Favreau). In order to determine the position of the phosphorylation sites on HtrA2 in these *in vitro* assays, mass spectrometric analysis of *in vitro* phosphorylated HtrA2 by p38γ was performed. This analysis detected a phospho-serine at positions 137 and 142 (data not shown). Since S137 is not conserved in other species than human (Figure 5-2B), this site was not analysed any further. Due to the behaviour of the S400-containing peptide in mass spectrometric analysis, the phosphorylation state of this site could not be addressed directly.

It is possible that PINK1, previously shown to interact with HtrA2 (Figure 5-1) and reported to possess kinase activity (Beilina et al. 2005; Silvestri et al. 2005; Sim et al. 2006), might phosphorylate HtrA2 directly. In order to determine if PINK1 is able to phosphorylate HtrA2, *in vitro* kinase assays using purified PINK1 produced in a baculovirus expression system were performed. However, the *in vitro* kinase activity of PINK1 was relatively weak, and a theoretically kinase inactive mutant of PINK1 (K219D, abolishing one of the catalytically active residues) exhibited similar activity towards HtrA2 (data not shown), suggesting that co-purifying proteins might exhibit this activity rather than PINK1 itself. From these assays it is not possible to conclude if

PINK1 can phosphorylate HtrA2 directly.

5.4 PINK1 modulates the levels of phosphorylated HtrA2

The data presented so far suggest that HtrA2 physically interacts with PINK1 and that activation of MEKK3 is involved in a signalling pathway that leads to HtrA2 phosphorylation. Therefore, PINK1 could modulate the phosphorylation of HtrA2 induced by MEKK3. For the purpose of down-regulating PINK1, siRNA targeting PINK1 was employed, which led to a significant decrease of both PINK1 transcript and protein levels (Figure 5-3A). Down-regulation of PINK1 also resulted in a decrease in HtrA2 phosphorylation level, suggesting that PINK1 is capable of modulating HtrA2 phosphorylation (Figure 5-3B). Over-expression of PINK1 protein together with WT or S142A HtrA2 showed loss of the P-HtrA2 signal when S142A HtrA2 was expressed (Figure 5-3C). Next, the role of PINK1 in the modulation of MEKK3-induced phosphorylation of HtrA2 was assessed. Activation of MEKK3 in cells where PINK1 was down-regulated led to a clear decrease in the level of P-HtrA2 compared to control siRNA transfected cells (Figure 5-3D), suggesting that PINK1 could be implicated in a signalling pathway leading to phosphorylation of HtrA2 that can be induced by MEKK3.

If PINK1 plays a role in phosphorylation of HtrA2 *in vivo*, the phosphorylation status of HtrA2 might be altered in PD patients carrying mutant PINK1. Initially, a range of human brain regions (cortex, striatum (caudate nucleus and putamen), SN, cerebellum) were screened for P-HtrA2, and it was detected most prominently in the caudate nucleus, which is the medial part of the striatum (data not shown). Next, the levels of phosphorylated HtrA2 in the caudate of brains with idiopathic PD and brains with PD associated with mutations in the PINK1 gene (Y431H and C575R) were compared. This analysis revealed a striking decrease in P-HtrA2 in brain tissue from PD patients with PINK1 mutations compared to idiopathic PD (Figure 5-3E).

5.5 Mutations mimicking phosphorylated HtrA2 enhance its protease activity

To determine whether HtrA2 phosphorylation might affect its proteolytic activity, S142 and S400 of HtrA2 were mutated into aspartate to mimic phosphorylation of these sites.

The activity of these phospho-mimic mutants was compared to WT HtrA2 in an *in vitro* protease assay previously described (Martins et al. 2003). Comparison of the basal activity of WT, S142D and S400D mutants, revealed that both phospho-mimic mutations induced a marked increase in the ability of HtrA2 to cleave the fluorogenic substrate peptide. The proteolytic activity of HtrA2 is increased about 2-fold in the S142D phospho-mimic mutant and 3-fold in case of the S400D mutant (Figure 5-4A). To control for the effect of introducing any mutation at residues S142 and S400 rather than an effect specific to the phospho-mimetic aspartate, these residues were additionally mutated to an alanine. Both, S142A and S400A, showed markedly lower protease activity when compared to their phospho-mimic counterparts (Figure 5-4A). Quality control on the different HtrA2 mutants was performed by SDS-PAGE analysis (Figure 5-4A) and gel filtration (data not shown). Furthermore, the proteolytic activity of HtrA2 can be activated by engagement of its PDZ domain by PDZ-binding peptides or by interaction of its mature N-terminus with XIAP (Martins et al. 2003). Therefore, the ability of these stimuli to activate the phospho-mimic mutants of HtrA2 was tested. The optimal HtrA2 PDZ domain-interacting peptide, termed PDZopt, and also XIAP both caused a major increase in the reaction rate and loss of the initial time lag for cleavage of the HtrA2 substrate peptide by WT HtrA2 (Figure 5-4B). However, the protease activity of the S400D mutant of HtrA2, and to a lesser extent the S142D mutant, is already close to its maximum rate without any stimulus and can be only minimally activated further by PDZopt or XIAP (Figure 5-4C). When the amount of the phospho-mimic mutants in this assay was titrated down, so that their activity was similar to that of a higher concentration of WT HtrA2, the PDZopt peptide or XIAP still only minimally activated their proteolytic activity (Figure 5-4B, shown only for S400D), demonstrating the sensitivity of the assay.

The PDZ domain of HtrA2 usually restrains the protease activity, possibly through restricting access to the catalytic centre (Li et al. 2002; Martins et al. 2003) or alternatively by trapping a flexible activator binding loop (L3 loop) in an inactive conformation (Wilken et al. 2004). Binding of peptides to the PDZ domain probably results in a conformational change that improves substrate access to the catalytic centre (Wilken et al. 2004). The data presented here would suggest that phosphorylation of HtrA2 in the PDZ domain might lead to a similar conformational effect. Likewise,

binding of XIAP to the N-terminus of mature HtrA2 leads to its activation (Martins et al. 2003), therefore phosphorylation on S142 close to its mature N-terminus might have a similar effect.

5.6 Establishment of ex vivo HtrA2 protease assay

In order to measure the proteolytic activity of HtrA2 *ex vivo*, the protease assay was tested on exogenously expressed or endogenous HtrA2 immunoprecipitated from HtrA2 KO MEFs or HEK293 cells. Over-expression of active or catalytically inactive (S306A) HtrA2 in cells lacking HtrA2, followed by immunoprecipitation and *in vitro* protease assay showed that this assay worked on HtrA2 *ex vivo*, albeit the assay time needed to be longer to reach maximal activity (Figure 5-5A). No unspecific background activity of co-purifying proteins was detectable, suggesting that immunoprecipitates of HtrA2 were clean. Endogenous HtrA2 immunoprecipitated from HEK293 cells could also be subjected to this assay, and its proteolytic activity could be increased by incubation with the PDZopt peptide or XIAP (Figure 5-5B). However, the activation of the proteolytic activity of immunoprecipitated HtrA2 was much smaller than the activation that could be achieved using recombinant WT HtrA2 (compare Figure 5-5B with Figure 5-4B).

Then, WT or S400D HtrA2 was over-expressed in HEK293 cells and the proteolytic activity of immunoprecipitated HtrA2 was measured subsequently. This experiment revealed that S400D HtrA2 was activated to a lesser extent by the PDZopt peptide compared to WT HtrA2 (Figure 5-5C), confirming the data obtained previously using recombinant HtrA2 proteins. Thus, *ex vivo* HtrA2 protease activity can be analysed similarly to recombinant HtrA2.

5.7 Activation of HtrA2 proteolytic activity by MEKK3 induction cannot be measured

The phosphorylation of at least S142 of HtrA2 could be induced by activation of MEKK3 (Figure 5-2C and Figure 5-3D), and phospho-mimic mutants of recombinant HtrA2 displayed higher basal activity and decreased activation by the PDZopt peptide and XIAP than WT HtrA2 (Figure 5-4). In order to test if activation of MEKK3 could activate endogenous HtrA2, HEK293 cells expressing ΔMEKK3:ER were stimulated

with vehicle or 4OH-Tx to activate this signalling pathway and induce HtrA2 phosphorylation. Half of the immunoprecipitated HtrA2 of each sample was then incubated with the PDZopt peptide or XIAP to stimulate the proteolytic activity. However, neither a difference in the proteolytic rate of HtrA2 from MEKK3 stimulated cells nor a difference in the ability of PDZopt or XIAP to activate HtrA2 could be detected (Figure 5-6A).

As previously noted, the proteolytic activity of *ex vivo* HtrA2 could not be activated by PDZ engagement or binding to XIAP to the same extent as recombinant WT HtrA2. Therefore, HtrA2 might be constitutively phosphorylated in cells. However, phosphatase treatment of immunoprecipitated HtrA2 did not lead to a reduction of its basal activity (Figure 5-6B). Nevertheless, the protease assay might reach its limit of sensitivity when assaying immunoprecipitated HtrA2, therefore, it is not possible to conclude whether phosphorylation of HtrA2 *in vivo* increases its proteolytic activity or not.

5.8 PINK1 influences HtrA2 activity in vivo

Induction of HtrA2 phosphorylation by activation of MEKK3 did not reveal an increase in HtrA2 activity *ex vivo*. Besides MEKK3 activation, the over-expression of PINK1 might induce phosphorylation of HtrA2. Therefore, WT or S142A/S400A mutant HtrA2 was immunoprecipitated from HtrA2 KO cells co-transfected with vector or a PINK1 expression construct. Immunoprecipitated samples were split and half of each was incubated with the PDZopt peptide. Interestingly, PINK1 expression did reduce the ability of PDZopt to activate WT HtrA2, but not S142A/S400A mutant HtrA2 (Figure 5-6C), suggesting that these sites could potentially be phosphorylated in response to PINK1 over-expression and therefore decrease the effect of activating stimuli on HtrA2 protease activity similar to the effect observed with the phospho-mimic mutants (Figure 5-4C and Figure 5-5C).

5.9 Over-expression of PINK1 protects WT, but not HtrA2 KO cells from toxic stimuli

The data presented so far suggests that PINK1 might modulate the activity of HtrA2 through influencing its phosphorylation status. Over-expression of PINK1 has been

reported to protect SH-SY5Y cells from apoptosis induced by the proteasome inhibitor MG-132 (Valente et al. 2004) and staurosporine (Petit et al. 2005). If PINK1 acts upstream of HtrA2 in a mitochondrial pathway responsible for resistance to stress, over-expression of this kinase in cells devoid of HtrA2 might not elicit such a significant response as in WT cells. Therefore, the effect of PINK1 over-expression in WT and HtrA2 KO MEFs on stress-induced apoptosis was studied. Although PINK1 could protect WT MEFs from MG-132 or staurosporine-induced apoptosis, its ability to protect HtrA2 KO MEFs was decreased compared to WT (Figure 5-7). In contrast, when PINK1 expression was decreased using PINK1-specific siRNA, a decrease in viability and mitochondrial membrane potential were observed in WT, but not in HtrA2 KO MEFs (data not shown, Miguel Martins, MRC Leicester), supporting the data from the over-expression of PINK1 (Figure 5-7).

Taken together, these results suggest that PINK1, possibly through phosphorylation and subsequent increased proteolytic activity of HtrA2, is able to protect cells from stress-induced mitochondrial dysfunction and stress-induced apoptosis.

5.10 Discussion

Eight nuclear genes are known to carry mutations that cause PD, encoding α-synuclein, parkin, UCHL1, PINK1, DJ-1, LRRK2, ATP13A2 and HtrA2 (Table 1-1) (Farrer 2006; Ramirez et al. 2006). Mutation or altered expression of these proteins contributes to PD pathogenesis through partly overlapping mechanisms that result in mitochondrial impairment, oxidative stress, and protein mishandling. Consistent with the development of a parkinsonian syndrome in mice lacking HtrA2 function, a polymorphism and a mutation resulting in single amino acid changes in HtrA2 that appear to dampen the activation of its proteolytic activity were identified to be associated with the PARK13 locus (Strauss et al. 2005). These studies suggest that loss of function of HtrA2 leads to neuronal cell death, possibly due to mitochondrial dysfunction, both in mice and in humans. Since then, several other mutations linked to PD have been identified in HtrA2 (personal communication, Reijko Krüger). The A141S polymorphism and G399S mutation in HtrA2 localise to domains previously shown to be important in the regulation of the proteolytic activity of HtrA2 (Martins et al. 2002). In addition, these residues are adjacent to two putative phosphorylation sites in the protein, S142 and

S400, suggesting that these sites might play a major role in the regulation of the enzymatic activity of HtrA2.

PINK1 was identified as a new binding partner of HtrA2 using the TAP tag system to affinity purify interacting proteins. Furthermore, HtrA2 could be phosphorylated *in vitro* by p38γ and p38β, and preliminary data indicates that p38γ might phosphorylate both sites, S142 and S400 *in vitro* (personal communication, Helene Plun-Favreau). Activation of the MEKK3 signalling pathway led to phosphorylation of HtrA2 at least on S142 *in vivo* (Figure 5-2C), and chemical inhibition of p38 reduced the MEKK3-induced phosphorylation of HtrA2 (Figure 5-2D). Moreover, PINK1 was required for this phosphorylation to occur (Figure 5-3D) and mutations in PINK1 decreased HtrA2 phosphorylation on S142 in human brain samples from PD patients (Figure 5-3E). Unfortunately, the sequence around S400 of HtrA2 is relatively hydrophobic and does not work well as an immunogen in rabbits. Therefore it was not possible to generate an antibody specific for phospho-S400 HtrA2 and address its phosphorylation *in vivo*. Interestingly, HtrA2 mutants mimicking phosphorylation on S142 and S400 showed an increase in their protease activity (Figure 5-4).

It has been hypothesised that PINK1 may phosphorylate mitochondrial proteins in response to cellular stress, protecting against mitochondrial dysfunction (Valente et al. 2004). It is possible that HtrA2 is a substrate for PINK1, therefore the PINK1 kinase activity towards HtrA2 in an *in vitro* assay was measured. However, the weak kinase activity of bacterially expressed PINK1 (Beilina et al. 2005; Silvestri et al. 2005; Sim et al. 2006) could not be improved by using a baculoviral system. Moreover, although an apparent autophosphorylation activity of PINK1 and activity towards HtrA2 could be detected, this was also seen with a kinase inactive K219D mutant of the protein, suggesting that the kinase activity observed most likely belonged to a contaminant of the preparation (data not shown). PINK1 could entirely lack kinase activity, despite having a strong predicted kinase domain sequence. Alternatively, PINK1 might not fold properly in the insect cell system used or some essential cofactors might be missing from the purified preparation. A relatively likely explanation would be that PINK1 needs to be activated in order to exhibit substantial kinase activity. Akt for example only exhibits kinase activity when the cells are stimulated with serum or dephosphorylation is inhibited by okadaic acid (Andjelkovic et al. 1996). However, if a

"correct" stimulus to activate PINK1 exists, it has not been identified yet. Thus, it is not possible to conclude that PINK1 phosphorylates HtrA2 directly.

Why might PINK1 expression be necessary for HtrA2 phosphorylation to occur (Figure 5-3B and D)? One possibility, suggested by the data presented, is that HtrA2 phosphorylation is mediated by a kinase activated in the MEKK3 signalling pathway (potentially p38, Figure 5-2C and D), but is dependent on the interaction of HtrA2 with PINK1, possibly reflecting the existence of a multimeric complex. Another possibility is that PINK1 is indeed a kinase, but the "correct" stimulus to activate its kinase activity *in vitro* has not been identified. In this case, PINK1 might phosphorylate HtrA2 directly and PINK1 activity could be modulated by the MEKK3 pathway. Alternatively, PINK1 might be upstream of another kinase responsible for phosphorylating HtrA2 and be involved in its activation. *In vivo*, the phosphorylation of HtrA2 might require recruitment of this kinase to the mitochondria, or alternatively could occur in the cytosol before HtrA2 is imported into the mitochondria. The interaction between PINK1 and HtrA2 was predominantly detected in mitochondria-enriched fractions. However, both over-expressed full length mitochondrial and mature cytosolic HtrA2 could be phosphorylated on S142 when MEKK3 was activated and this occurred in a PINK1-dependent manner (data not shown), suggesting that the phosphorylation might occur prior to import of HtrA2 into the mitochondria.

Being located just next to the cleavage motif site (A134 is the N-terminus of mature HtrA2), phosphorylation on S142 could also impact on the processing of HtrA2. Indeed, data from several groups have revealed that Alzheimer's amyloid precursor protein (APP) processing can be regulated by phosphorylation and phosphorylation-dependent events and it is now widely accepted that abnormal processing of APP can contribute significantly to Alzheimer's disease (for review (da Cruz e Silva et al. 2004)). In order to address the impact of S142 phosphorylation on processing of HtrA2 to its mature form, mitochondria import assays need to be performed. Preliminary experiments suggested that over-expression of WT and S142D HtrA2 in cells did not reveal a difference in the ratio of full length to mature form of HtrA2 (data not shown).

Since the notion that HtA2 is a pro-apoptotic protein analogous to *Drosophila* Reaper family proteins has been thrown into doubt by the parkinsonian phenotype of mice

lacking HtrA2 function and its protective function in cells subjected to stress (Jones et al. 2003; Martins et al. 2004), it is attractive to speculate that human HtrA2 might act more like its bacterial homologues DegS and DegP. HtrA2 could degrade unfolded proteins, performing crucial functions with regard to protein quality control in the intermembrane space of the mitochondria, in a similar manner to DegP. Alternatively, HtrA2 could transduce a stress adaptive signal, like DegS (for review, (Young and Hartl 2003)). Thus, the proteolytic activity of HtrA2 is critical for its protective function. Phosphorylation of HtrA2 appeared to regulate its proteolytic activity, since HtrA2 mutants mimicking phosphorylation on S142 and S400 showed an increase in their protease activity (Figure 5-4A), concomitant with a reduction in the ability of the PDZopt peptide and XIAP to activate HtrA2 protease activity (Figure 5-4B and C, Figure 5-5C). This suggests that phosphorylation of HtrA2 might lead to conformational changes facilitating its protease activity. However, in these experiments, HtrA2 proteins engineered with a serine to aspartate mutation, to mimic phosphorylation at the sites of interest, were used. Therefore, it is crucial to show that "real" phosphorylation can have the same impact on HtrA2 proteolytic activity. Unfortunately, although activation of the MEKK3 signalling pathway led to increase of HtrA2 phosphorylated on S142, neither the basal activity nor the induction in HtrA2 activity by activating stimuli were altered when HtrA2 was isolated from cells in which MEKK3 had been induced (Figure 5-6A). It is possible, that the protease assay is not sensitive enough to detect subtle changes in HtrA2 activity when isolated *ex vivo*. In line with this, the ability of the PDZopt peptide or XIAP to activate HtrA2 isolated from cells is much reduced compared to recombinant WT HtrA2 (compare Figure 5-5B with Figure 5-4B). The latter observation, however, might also suggest that HtrA2 could be constitutively phosphorylated in cells thereby diminishing the increase in HtrA2 activity that can be achieved by activating stimuli. Nevertheless, phosphatase treatment of HtrA2 isolated from cells did not change its basal activity (Figure 5-6B), reinforcing the hypothesis that the protease assay is not sensitive enough for immunoprecipitated HtrA2. HtrA2 isolated in this way possibly suffers from steric hindrance resulting from the binding of the antibodies, thereby fixing HtrA2 in a particular position and reducing the flexibility of structural changes to occur. Nevertheless, the first evidence that PINK1 might indeed regulate HtrA2 activity *in vivo* comes from experiments over-expressing PINK1 prior to measuring HtrA2

activity *ex vivo* (Figure 5-6C). In line with this is the observation that over-expression of PINK1 cannot protect HtrA2 KO cells to the same extent as WT cells from stress-induced apoptosis, placing HtrA2 downstream of PINK1 function (Figure 5-7).

Previously, it was reported that both A141S and G399S PD-associated mutations in HtrA2 resulted in reduced ability of the PDZopt peptide or XIAP to activate its protease activity (Strauss et al. 2005). The influence of these PD-associated mutations on the phosphorylation of the adjacent sites (S142 and S400) is clearly an area for further investigation. Mutation of A141S creates a new potential phosphorylation site for proline-directed serine/threonine kinases on this residue. However, A141 is not well conserved across different species. In rodents this residue is a threonine, already providing such a potential phosphorylation site (Figure 5-2B) and preliminary data indicates that A141S has no effect on S142 phosphorylation *in vitro*. However, the G399 sequence is well conserved and G399S mutation in HtrA2 might lead to decreased phosphorylation of this site *in vitro*. A defect in phosphorylation due to G399S mutation and therefore impaired modulation of HtrA2 proteolytic activity could explain the increased mitochondrial dysfunction and sensitivity to stress-induced cell death of this mutant when over-expressed (Strauss et al. 2005).

The PD-associated mutations in PINK1, C575R and Y431H, resulted in a robust decrease in the levels of phosphorylated HtrA2 on position S142 in human brains (Figure 5-3E). The study of these human brains is clearly important for confirming the relevance of the interaction of HtrA2 and PINK1 *in vivo* in human PD patients. The brains of patients with mutations in the PINK1 gene are morphologically indistinguishable from sporadic PD and exhibit the pathological hallmarks of dopaminergic neuronal cell loss in the SN and the presence of Lewy bodies. In addition, there is no difference in the expression of PINK1 protein in these brains compared to brains with sporadic PD (Gandhi et al. 2006). The Y431H and C575R mutations in PINK1 are thought to influence the putative kinase activity (Sim et al. 2006). Over-expression of both PINK1 mutants resulted in a significant decrease in the mitochondrial membrane potential compared to WT PINK1 on exposure of the cells to proteasomal stress (Abou-Sleiman et al. 2006), suggesting that both mutations have a major pathogenic effect on PINK1 function. Neither the C575R nor the Y431H mutant of PINK1 have lost their ability to interact with HtrA2 *in vitro* (data not shown, Helene

Plun-Favreau), thus supporting the idea that PINK1 possibly functions as a kinase *in vivo* to phosphorylate HtrA2 and that its kinase activity towards HtrA2 could be impaired by the PD mutations.

The results from the study in human brain highlight another important controversy in PD pathogenesis: it has not yet been clear whether heterozygous mutations in the recessive genes associated with PD are sufficient to cause disease. Classically, as mutations in PINK1 cause an autosomal recessive form of PD the carriage of a single heterozygous mutation would be considered to be of no phenotypic significance. However, several groups have shown that there is a higher rate of heterozygous mutations in PD patients compared to controls (Abou-Sleiman et al. 2006). Furthermore heterozygous carriers of PINK1 mutations have a demonstrable reduction in ^{18}fluorodopa uptake in the striatum, a marker for dopaminergic dysfunction (Khan et al. 2002). Therefore, there is accumulating but circumstantial evidence that single heterozygous mutations represent a significant risk factor for developing disease in the presence of particular stress. For the first time, functional data to support this hypothesis is provided: in the presence of a PD-inducing stress, a heterozygous mutation in the PINK1 gene is able to exert a significant functional effect on the phosphorylation of HtrA2, presumably via a haploinsufficiency mechanism.

The identification of PINK1 binding to HtrA2 demonstrates a direct molecular interaction between two genes implicated in PD. Uniquely, it is the only functional interaction that has been validated *in vitro*, *in vivo* and in human PD brains. In parallel to the presented data in this thesis, genetic analyses of HtrA2 and PINK1 function in *Drosophila* place HtrA2 downstream of PINK1 and Parkin (unpublished data, Ruhena Begum *et al.*, Cancer Research UK). Thus, both HtrA2 and PINK1 proteins are genetically linked, suggesting that they could be part of the same signalling pathway. The identification of HtrA2 and PINK1 being involved in a common pathway is the first step in elucidating the molecular players around the mitochondrial function of HtrA2, and in understanding how loss of HtrA2 function can lead to increased sensitivity to mitochondrial stress. Further study of this pathway might help explain how mitochondrial dysfunction leads to neuronal death in the SN of PD patients.

Table 5-1

Company	Antigen	Detected in HtrA2-TAP eluate
Santa Cruz Biotechnology	**ANT**	**No**
Santa Cruz, BD Transduction	**Bad**	**No**
Stressgen, Calbiochem	**Bak**	**No**
Mito Science, Imgenex	**Bax**	**No**
Pharmingen, Santa Cruz	**Bcl-2**	**No**
BD Transduction Laboratories	**Bcl-XL**	**No**
Abcam	**Bif-1**	**No**
Santa Cruz Biotechnology	**Bik**	**No**
Santa Cruz Biotechnology	**Bim**	**No**
Calbiochem	**Bnip3L**	**No**
Molecular Probes	**ComplexI 17kD subunit**	**No**
Molecular Probes	**ComplexIII (UQCRC1)**	**No**
Molecular Probes	**ComplexV subunit alpha**	**No**
Molecular Probes	**ComplexV subunit beta**	**No**
Molecular Probes	**ComplexV subunit d**	**No**
Molecular Probes	**ComplexV subunit OSCP**	**No**
Molecular Probes	**ComplexV inh. Protein**	**No**
Mito Science	**ComplexV**	**No**
Pharmingen	**Cytochrome c**	**No**
V. Dawson	**DJ-1**	**No**
Stressgen	**Grp-75**	**No**
BD Transduction Laboratories	**HAX-1**	**Yes**
Santa Cruz Biotechnology	**Hrk**	**No**
Stressgen	**Hsp-60**	**No**
CRUK generated	**PINK1**	**Yes**
Abcam	**Prohibitin**	**No**
CRUK generated	**Smac**	**No**
Calbiochem	**VDAC**	**No**
Santa Cruz Biotechnology	**VDAC2**	**No**
BD Transcution Laboratories	**XIAP**	**Yes**

Table 5-1. TAP epitope-tagged HtrA2 was purified from HEK293 cells stably expressing the fusion protein, resolved by SDS-PAGE and probed with antibodies raised against mitochondrial proteins.

Figure 5-1. PINK1 interacts with HtrA2.

(A) TAP purification of HtrA2 shows interaction with XIAP and HAX-1. TAP epitope-tagged HtrA2 or TAP alone were purified from stable HEK293 cell lines, resolved by SDS-PAGE and probed with anti-XIAP or anti-HAX-1 antibodies. **(B)** TAP purification of HtrA2 identifies PINK1 as a novel binding partner. Following each step of the purification, a sample was kept for Western blotting with anti-PINK1 antibody: Lane 1, lysate from HEK293 HtrA2-TAP stable cell line. Lane 2, IgG flow through (FT). Lane 3, TEV eluate. Lane 4, calmodulin flow through (CaM FT). Lane 5, final eluate. **(C)** Co-immunoprecipitation of endogenous PINK1 with endogenous HtrA2. Lysates prepared from WT and HtrA2 KO MEFs were subjected to immunoprecipitation with anti-HtrA2 antibody and purified proteins were subjected to Western blotting with biotinylated anti-PINK1 antibody. Lysates derived from HtrA2 KO MEFs demonstrate that in the absence of HtrA2, no PINK1 purification is achieved. Duplicates for the co-immunoprecipitation of PINK1 with HtrA2 are shown. Asterisks denotes IgG background band. **(D)** Co-immunoprecipitation of HtrA2 with PINK1 occurs in mitochondria-enriched fractions. PINK1-Myc was expressed in HEK293 cells. Cytosol- and mitochondria-enriched fractions were subjected to immunoprecipitation with anti-HtrA2 antibody. Detection was performed with anti-Myc or anti-HtrA2 antibody. Asterisk denotes IgG background band.

Figure 5-1

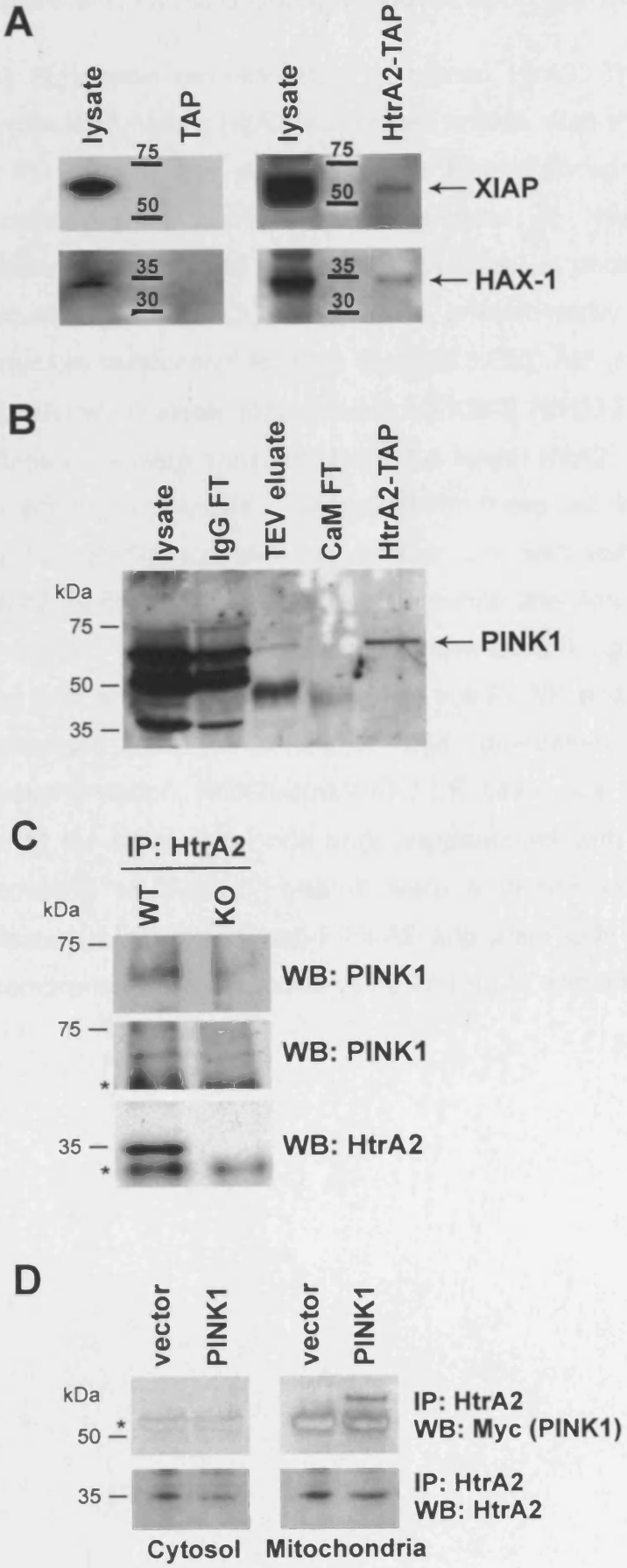
A
lysate
TAP
lysate
HtrA2-TAP
75
50
35
30
XIAP
HAX-1
B
lysate
IgG FT
TEV eluate
CaM FT
HtrA2-TAP
kDa
75
50
35
PINK1
C
IP: HtrA2
WT
KO
kDa
75
WB: PINK1
75
WB: PINK1
35
WB: HtrA2
D
vector
PINK1
vector
PINK1
kDa
50
35
IP: HtrA2
WB: Myc (PINK1)
IP: HtrA2
WB: HtrA2
Cytosol
Mitochondria

Figure 5-2. HtrA2 is phosphorylated upon MEKK3 activation.

(A) Schematic representation of human HtrA2. The IBM present in the N-terminus of mature HtrA2 is indicated in blue. Also shown are residues mutated in PD (green) and potential stress kinase phosphorylation sites (red). TM, transmembrane domain. **(B)** Alignment of HtrA2 homologues showing conservation of S142 and S400. **(C)** HtrA2 is phosphorylated on S142 upon activation of MEKK3, and p38 is predominantly activated in these cells. Inducible versions of MEKK3 (ΔMEKK3:ER), Akt (myrAkt:ER) and Raf (ΔRaf-DD:ER) were stably expressed in HEK293, NIH3T3 and NIH3T3, respectively. These cells were transfected with full length HtrA2. After over night (o/n) 4OH-Tx activation of MEKK3, Akt and Raf in these cell lines, lysates were analysed by SDS-PAGE followed by Western blot with anti-phospho-S142 HtrA2 (P-HtrA2) antibody. After stripping, the membrane was re-probed using anti-HtrA2 antibody. To assess activation of downstream signalling pathways, Western blot with anti-P-Akt, anti-P-ERK1/2, anti-P-JNK and anti-P-p38 antibodies was performed. **(D)** Inhibition of p38 decreases 4OH-Tx induced HtrA2 phosphorylation. HEK293/ΔMEKK3:ER cells were transfected with full length HtrA2 for 48hrs. After one hour pre-treatment with BIRB796 and o/n 4OH-Tx activation of MEKK3, lysates were analysed by SDS-PAGE followed by Western blotting with anti-P-HtrA2 and anti-P-p38 antibodies. After stripping, membranes were re-probed using anti-HtrA2 and anti-p38 antibodies.

Figure 5-2

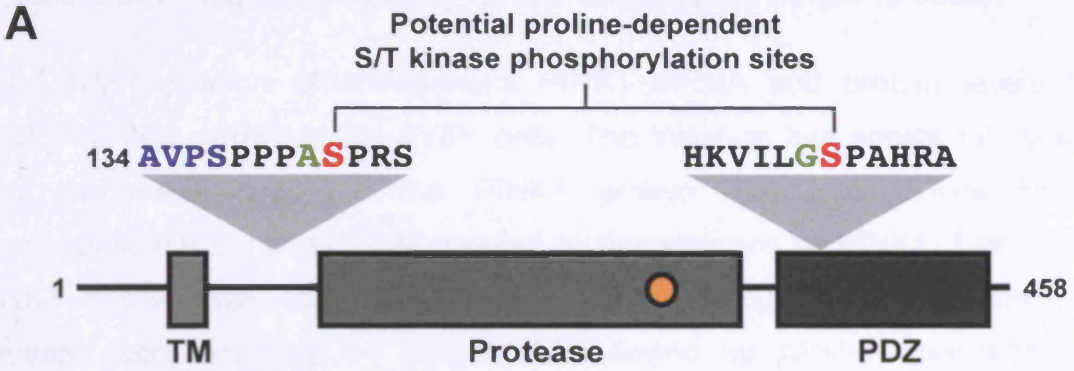

B

Protein	Species	134–148	392–406
HtrA2	*H. sapiens*	AVPSPPPASPRSQYN	LIHKVILGSPAHRAG
HtrA2	*M. musculus*	AVPAPPPTSPRSQYN	LIHKVILGSPAHRAG
HtrA2	*R. norvegicus*	AVPAPPPTSPRSQYN	LIHKVILGSPAHRAG
HtrA2	*G. gallus*	SPPAPPPGSPRAAFN	LIHKVIIGSPAHQAG
dHtrA2	*D. melano.*	KLPQPPVIVLQRGPH	LVWKVIVGSPAHSGG
YNL123W	*S. cerevisiae*	---------------	YCTFRGESSPALQYG
DegS	*E. coli*	---------------	VVNEVSPDGPAANAG
DegP	*E. coli*	---------------	VVNNVKTGTPAAQIG

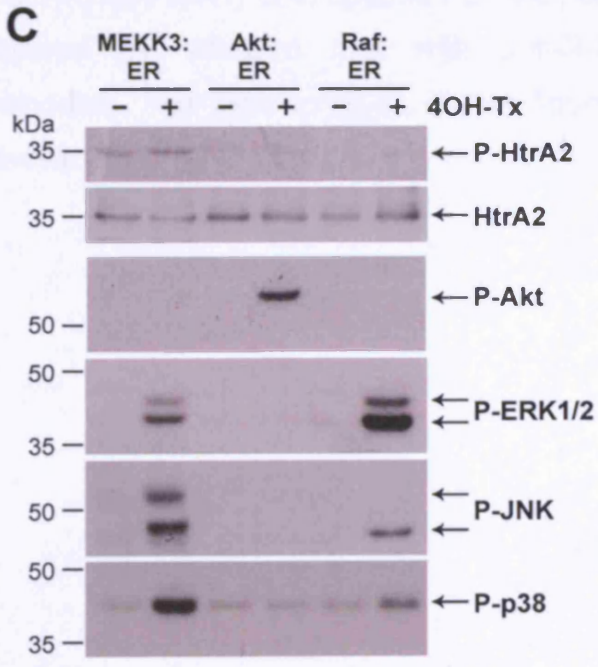

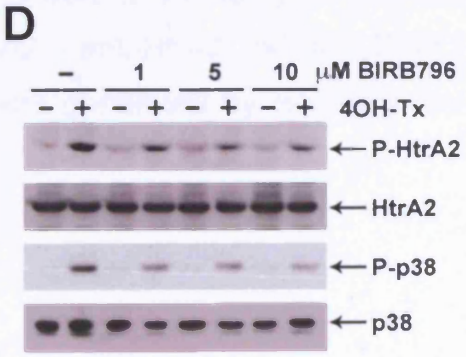

Figure 5-3. PINK1 is necessary for HtrA2 phosphorylation to occur.

(A) Down-regulation of endogenous PINK1 mRNA and protein levels by PINK1-specific siRNA in SH-SY5Y cells. The Western blot shows full length and processed forms of the PINK1 protein. **(B)** Endogenous HtrA2 phosphorylation on S142 is decreased in the absence of PINK1. Control or PINK1 siRNA was transfected into SH-SY5Y and mitochondria-enriched fractions were analysed by SDS-PAGE followed by Western blot with the antibody against P-HtrA2. After stripping, the membrane was re-probed using anti-HtrA2 antibody. **(C)** Over-expression of PINK1 reveals phosphorylation on S142 of HtrA2. Full length WT or S142A HtrA2 were co-expressed with PINK1 in SH-SY5Y cells and lysates subjected to Western blot using anti-P-HtrA2 and anti-HtrA2 antibodies. **(D)** Down-regulation of endogenous PINK1 by siRNA inhibits HtrA2 phosphorylation on S142 upon 4OH-Tx activation of MEKK3. Full length WT and S142A HtrA2 expression constructs and control or PINK1-specific siRNA were co-transfected into HEK293/ΔMEKK3:ER cells that were treated with vehicle or 4OH-Tx o/n. Cell lystates were subjected to Western blot with anti-P-HtrA2 and anti-HtrA2 antibodies. **(E)** HtrA2 is phosphorylated on S142 in PD brains. Human brain tissue samples from the caudate nucleus (which is part of the striatum) carrying a mutation in the PINK1 gene (C575R and Y431H PINK1) or idiopathic PD (IPD) brains were analysed by SDS-PAGE followed by Western blot with anti-P-HtrA2, anti-HtrA2 or anti-PINK1 antibodies. The data in (B-E) of this figure was generated by Helene Plun-Favreau.

Figure 5-3

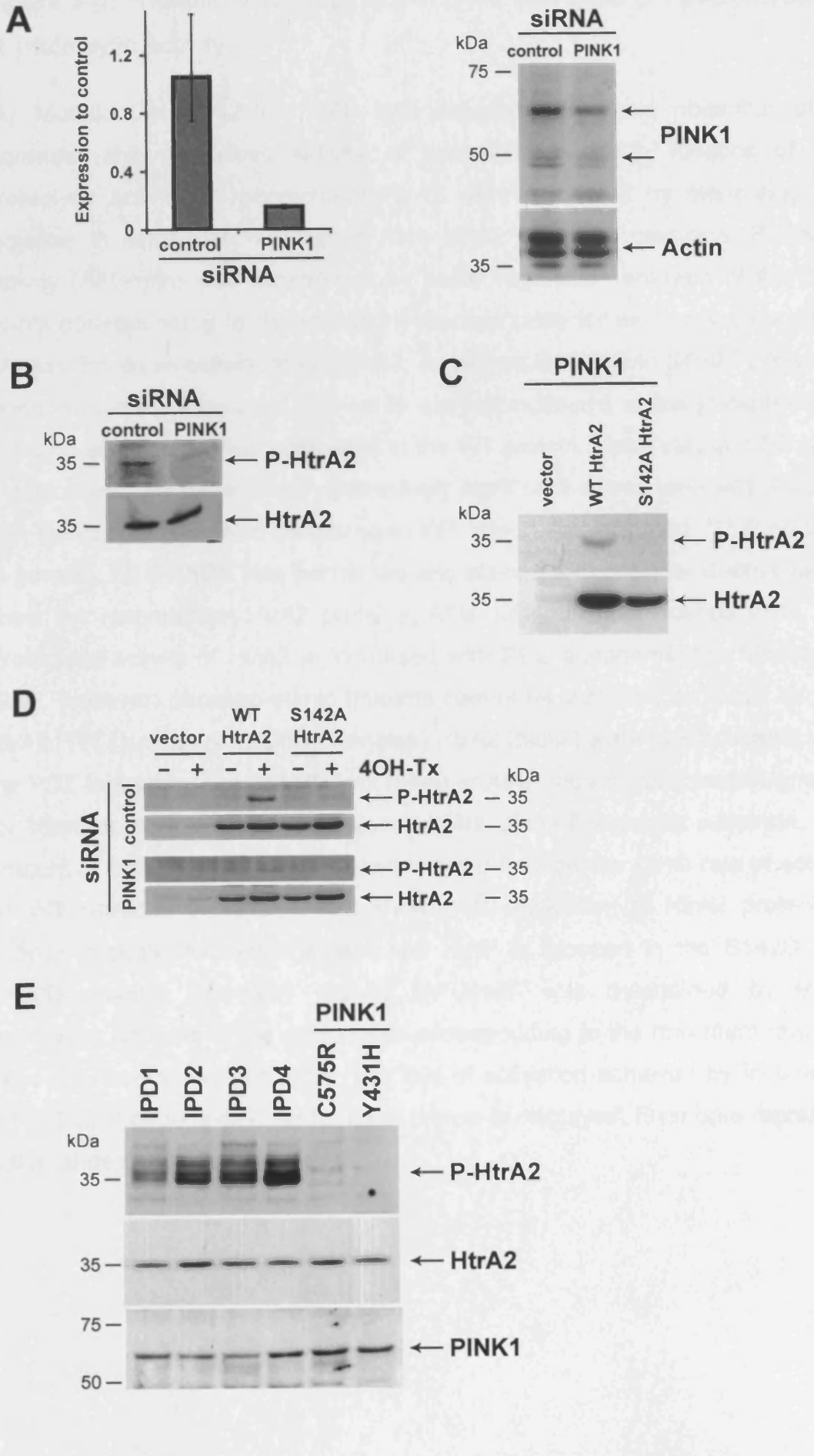
A
Expression to control
1.2
0.8
0.4
0
control
PINK1
siRNA
siRNA
kDa
control PINK1
75
50
PINK1
35
Actin
B
siRNA
kDa
control PINK1
35
P-HtrA2
35
HtrA2
C
PINK1
vector
WT HtrA2
S142A HtrA2
kDa
35
P-HtrA2
35
HtrA2
D
vector
WT HtrA2
S142A HtrA2
– + – + – +
4OH-Tx
kDa
siRNA
control
PINK1
P-HtrA2 35
HtrA2 35
P-HtrA2 35
HtrA2 35
E
PINK1
IPD1
IPD2
IPD3
IPD4
C575R
Y431H
kDa
35
P-HtrA2
35
HtrA2
75
50
PINK1

Figure 5-4. Phosphorylation-mimics of S142 and S400 of HtrA2 increase its proteolytic activity.

(A) Mutation of S142 or S400 into aspartate to mimic phosphorylation increases the proteolytic activity of recombinant HtrA2. Kinetics of the proteolytic activity of recombinant HtrA2 were monitored by measuring the increase in fluorescence resulting from HtrA2 substrate cleavage. Protease activity (AFU/min) was determined by linear regression analysis of the data points corresponding to the maximum reaction rates for each assay condition (Vmax). Protease activity of WT HtrA2, as well as S142D and S400D phospho-mimic mutants is displayed. Serine to alanine mutations at the phospho-sites show no significant effect compared to the WT protein. Mean values ± SD of 4-6 data points are represented. Statistically significant values (one-way ANOVA with Bonferroni post-test, compared to WT HtrA2) are indicated: *** $P < 0.001$. In parallel, SDS-PAGE was performed and stained with colloidal Coomassie to show the recombinant HtrA2 proteins. AFU, arbitrary fluorescence units. **(B)** Proteolytic activity of HtrA2 is increased with PDZ engagement or binding to XIAP, however, phospho-mimic mutants cannot be activated as much as WT HtrA2. WT (circles) or S400D (triangles) HtrA2 (black) were pre-incubated with the PDZ-interacting peptide PDZopt (blue) or XIAP recombinant protein (green) for 15min at room temperature before addition of the fluorescent substrate. The amount of S400D HtrA2 was reduced in order to show the same rate of activity as WT HtrA2 in the experiment shown. **(C)** Activation of HtrA2 proteolytic activity through PDZ engagement and XIAP is reduced in the S142D and S400D mutants. Protease activity (AFU/min) was determined by linear regression analysis of the data points corresponding to the maximum reaction rates for each assay condition. The fold of activation achieved by incubation with PDZopt peptide or XIAP for each protein is displayed. Error bars represent + the range of two determinations.

Figure 5-4

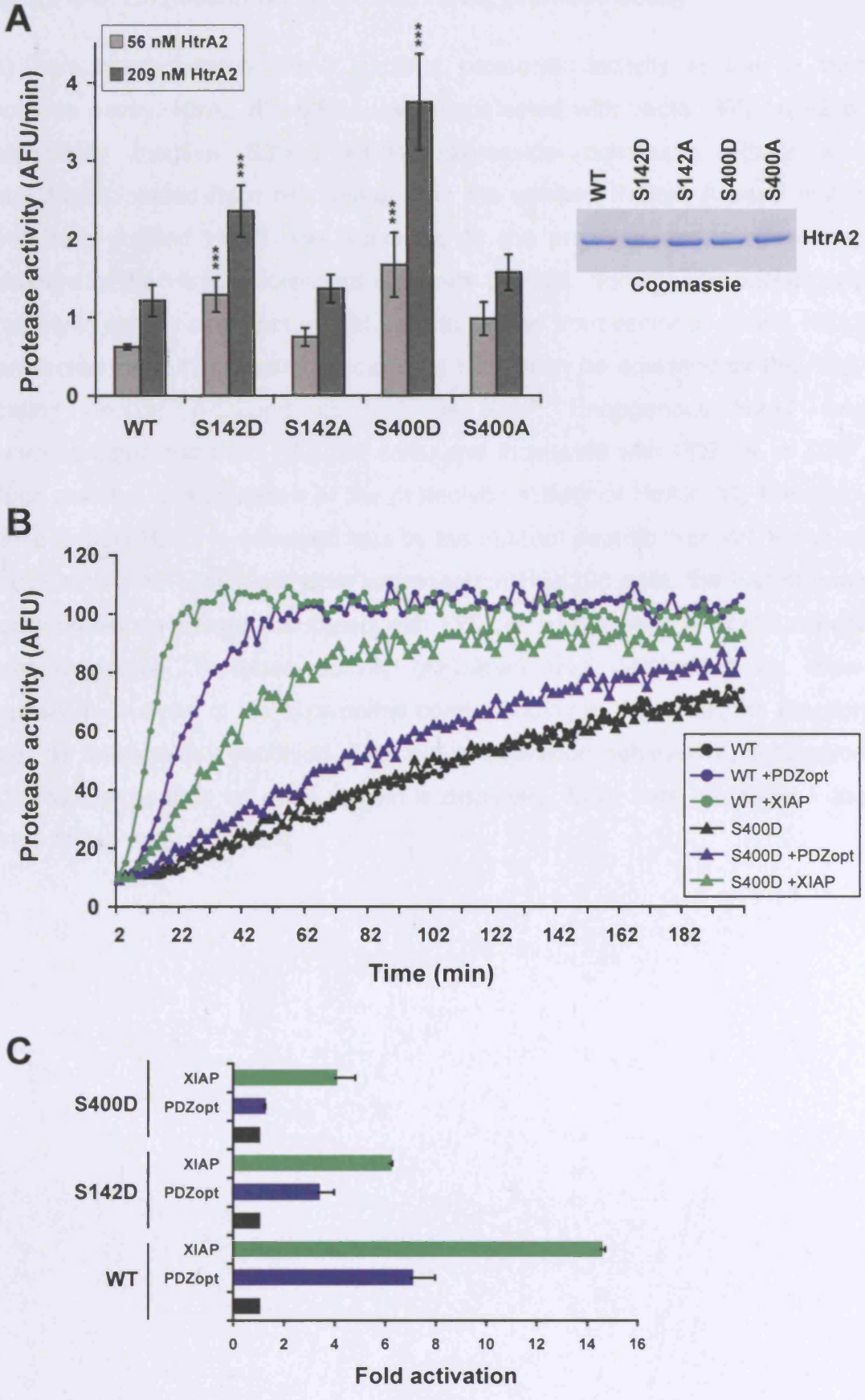
A
56 nM HtrA2
209 nM HtrA2
Protease activity (AFU/min)
0
1
2
3
4
WT
S142D
S142A
S400D
S400A
WT
S142D
S142A
S400D
S400A
HtrA2
Coomassie
B
Protease activity (AFU)
0
20
40
60
80
100
120
2
22
42
62
82
102
122
142
162
182
Time (min)
WT
WT +PDZopt
WT +XIAP
S400D
S400D +PDZopt
S400D +XIAP
C
S400D
S142D
WT
XIAP
PDZopt
0
2
4
6
8
10
12
14
16
Fold activation

Figure 5-5. Establishment of *ex vivo* HtrA2 protease assay.

(A) Immunoprecipitated HtrA2 exhibits proteolytic activity in the *in vitro* protease assay. HtrA2 KO MEFs were transfected with vector, WT HtrA2 or catalytically inactive S306A HtrA2 expression constructs. HtrA2 was immunoprecipitated from cell lysates and the washed Protein A bead matrix containing purified HtrA2 was subjected to the protease assay, measuring cleavage of the HtrA2 fluorescent substrate peptide. Non-specific background proteolytic activity could not be detected in lysates from vector or S306A HtrA2 transfected cells. **(B)** Immunoprecipitated HtrA2 can be activated by the PDZ-binding peptide (PDZopt) as well as XIAP. Endogenous HtrA2 was immunoprecipitated from HEK293 cells, and incubated with PDZopt or XIAP, which resulted in stimulation of the proteolytic activity of HtrA2. **(C)** Phospho-mimic S400D HtrA2 is activated less by the PDZopt peptide than WT HtrA2 *ex vivo*. Both HtrA2 constructs were expressed in HEK293 cells, the half of each immunoprecipitates was incubated with PDZopt and kinetics of HtrA2 activity were measured. Protease activity (AFU/min) was determined by linear regression analysis of the data points corresponding to the maximum reaction rates for each assay condition. The fold of activation achieved by incubation with PDZopt peptide for each protein is displayed. Error bars represent + the range of two determinations.

Figure 5-5

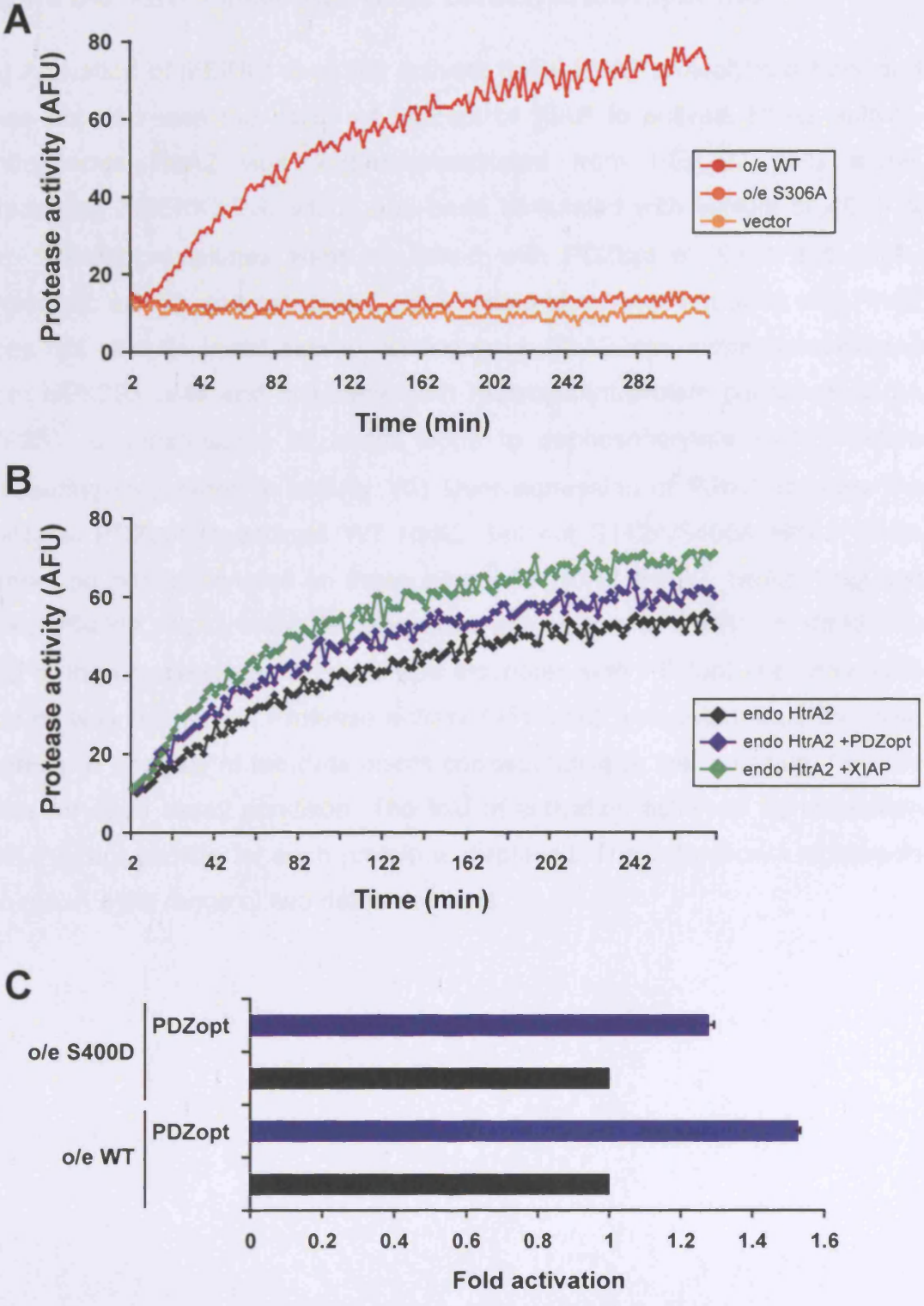
A
Protease activity (AFU)
80
60
40
20
0
2
42
82
122
162
202
242
282
Time (min)
o/e WT
o/e S306A
vector
B
Protease activity (AFU)
80
60
40
20
0
2
42
82
122
162
202
242
Time (min)
endo HtrA2
endo HtrA2 +PDZopt
endo HtrA2 +XIAP
C
o/e S400D
PDZopt
o/e WT
PDZopt
0
0.2
0.4
0.6
0.8
1
1.2
1.4
1.6
Fold activation

Figure 5-6. PINK1 influences HtrA2 proteolytic activity *in vivo*.

(A) Activation of MEKK3 does not activate basal HtrA2 proteolytic activity and does not decrease the ability of PDZopt or XIAP to activate HtrA2 activity. Endogenous HtrA2 was immunoprecipitated from HEK293 cells stably expressing ΔMEKK3:ER, which had been stimulated with vehicle or 4OH-Tx o/n. Immunoprecipitates were incubated with PDZopt or XIAP and HtrA2 proteolytic activity was measured. **(B)** Phosphatase treatment of *ex vivo* HtrA2 does not alter its basal activity. Endogenous HtrA2 was immunoprecipitated from HEK293 cells and incubated with recombinant protein phosphatase 2A (PP2A), λ phosphatase or buffer alone to dephosphorylate HtrA2, before measuring its proteolytic activity. **(C)** Over-expression of PINK1 reduces the ability of PDZopt to activate WT HtrA2, but not S142A/S400A HtrA2 which cannot be phosphorylated on these sites. WT HtrA2 (HtrA2, HtrA2-Flag) and S142A/S400A HtrA2 were co-expressed with vector or PINK1 in HtrA2 KO MEFs. Immunoprecipitated HtrA2 was incubated with PDZopt and proteolytic activity was measured. Protease activity (AFU/min) was determined by linear regression analysis of the data points corresponding to the maximum reaction rates for each assay condition. The fold of activation achieved by incubation with PDZopt peptide for each protein is displayed. The data shown represents the mean ± the range of two determinations.

Figure 5-6

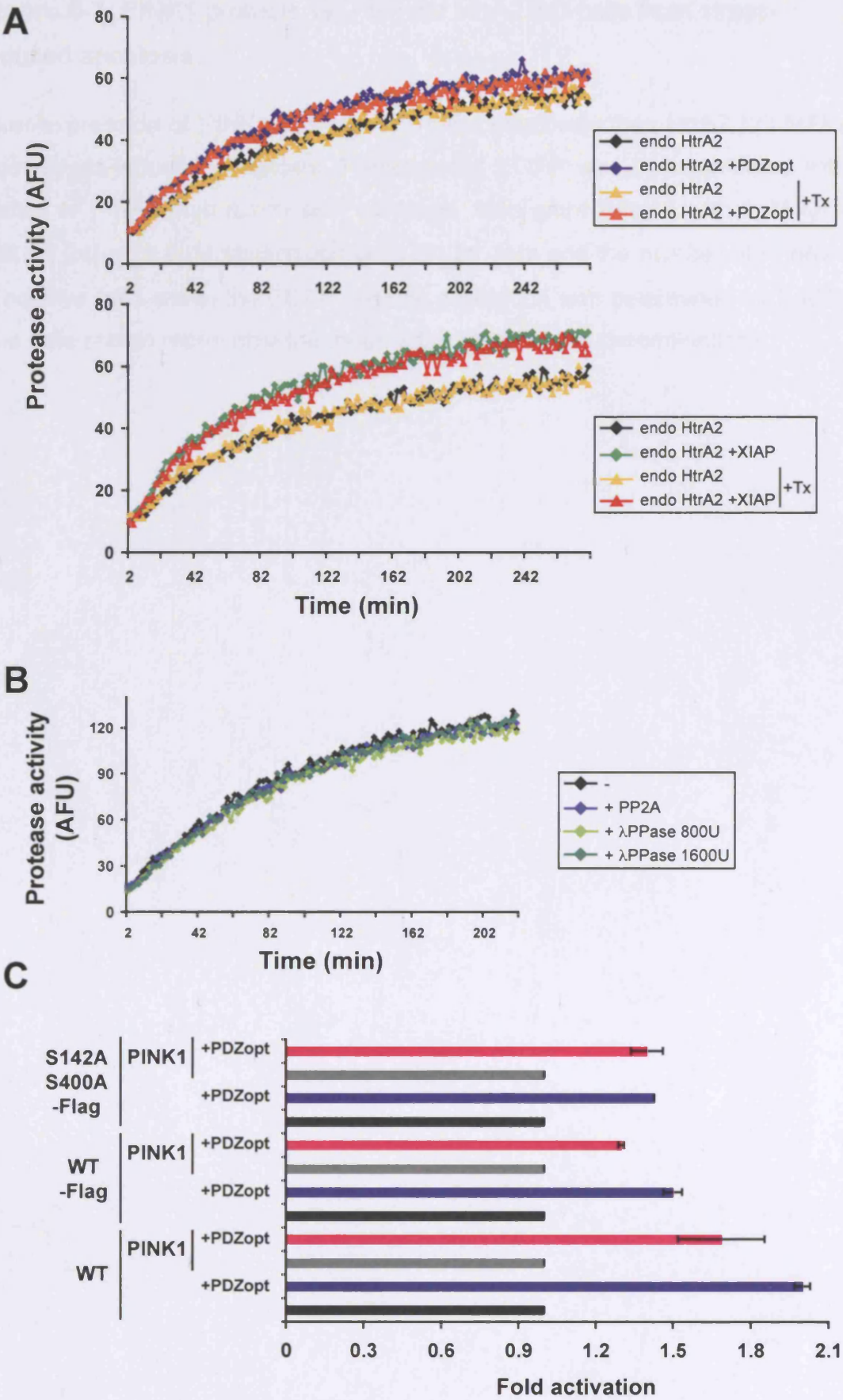
A
Protease activity (AFU)
80
60
40
20
0
2
42
82
122
162
202
242
endo HtrA2
endo HtrA2 +PDZopt
endo HtrA2
endo HtrA2 +PDZopt
+Tx
endo HtrA2
endo HtrA2 +XIAP
endo HtrA2
endo HtrA2 +XIAP
+Tx
Time (min)
B
Protease activity (AFU)
120
90
60
30
0
2
42
82
122
162
202
-
+ PP2A
+ λPPase 800U
+ λPPase 1600U
Time (min)
C
S142A
S400A
-Flag
PINK1
+PDZopt
+PDZopt
WT
-Flag
PINK1
+PDZopt
+PDZopt
WT
PINK1
+PDZopt
+PDZopt
0
0.3
0.6
0.9
1.2
1.5
1.8
2.1
Fold activation

Figure 5-7. PINK1 protects WT, but not HtrA2 KO cells from stress-induced apoptosis.

Over-expression of PINK1 protects WT more effectively than HtrA2 KO MEFs from stress-induced apoptosis. Farnesylated EGFP was co-transfected with vector or PINK1-myc expression construct, cells were treated with 1μM MG-132 for 24hrs or 2μM staurosporine (STS) for 3hrs and the number of Annexin V positive cells within the EGFP positive population was determined by FACS. The data shown represents the mean ± the range of two determinations.

Figure 5-7

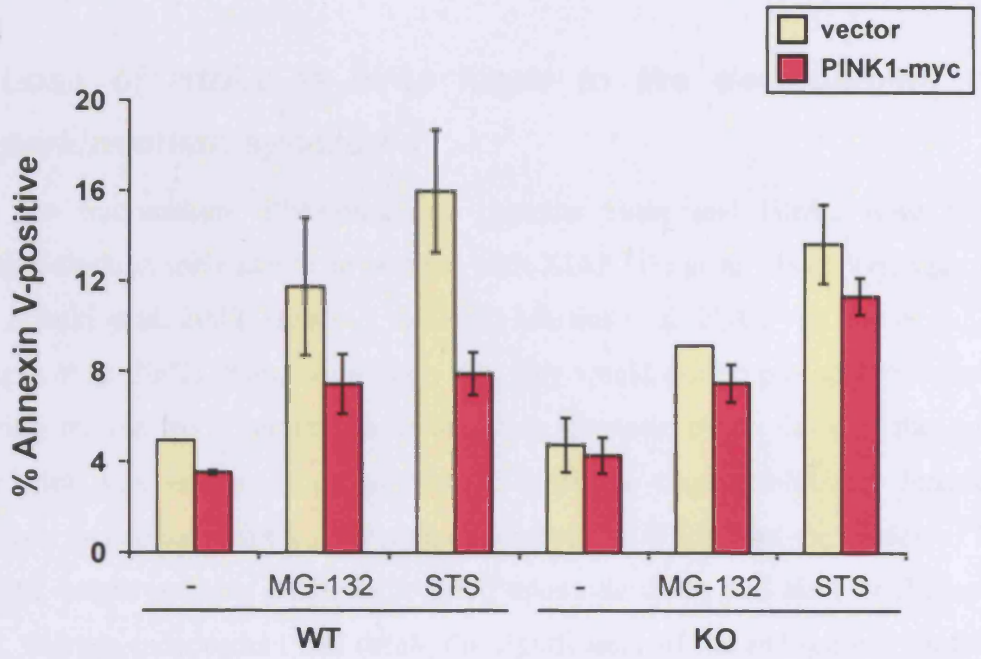
vector
PINK1-myc
% Annexin V-positive
20
16
12
8
4
0
-
MG-132
STS
-
MG-132
STS
WT
KO

6 Chapter 6: Final Discussion

6.1 *Loss of HtrA2 in mice leads to the development of a parkinsonian syndrome*

When the mammalian IBM-containing proteins Smac and HtrA2 were initially identified through their ability to interact with XIAP (Du et al. 2000; Verhagen et al. 2000; Suzuki et al. 2001; Hegde et al. 2002; Martins et al. 2002; van Loo et al. 2002; Verhagen et al. 2002), it appeared likely that they would exhibit pro-apoptotic function involving release from mitochondria following apoptotic insult. Once in the cytosol, the proteins were thought to act together to block the caspase inhibitory function of IAPs, thus promoting caspase activation and apoptosis. While over-expression of Smac or HtrA2 might promote caspase-mediated apoptotic death and also, in the case of HtrA2, caspase-independent cell death, the significance of the endogenous proteins in these pathways has been much less clear. The data presented in Chapter 3 indicate that the complete loss of expression of HtrA2 protein *in vivo*, including its IBM, does not result in resistance to cell death, as one might expect from deletion of a pro-apoptotic protein. It has been reported that many mitochondrial proteins might have an N-terminal IBM (Verhagen et al. 2007). Therefore, severe mitochondrial damage would cause release of many proteins with the ability to antagonise IAPs, in addition to just Smac and HtrA2, so that loss of the IBMs of these two proteins may have little detectable impact on IAP activity. In contrast to showing resistance to cell death, neuronal cell populations isolated from HtrA2 KO mice were more sensitive than WT controls to excitotoxicity-induced death in response to glutamate (Figure 3-7C). Similarly, non-neuronal cell types such as fibroblasts from the HtrA2 KO mice also showed increased sensitivity to induction of cell death by specific drugs, for instance the complex I inhibitor rotenone, the ER stressor tunicamycin and H_2O_2 which elicits oxidative stress (Figure 3-7A). The increase in cell death in animals lacking HtrA2 function and absence of protection from apoptosis suggests that HtrA2 is an essential gene required for mitochondrial function, rather than a pro-apoptotic regulator.

The phenotype of the HtrA2 KO mice displays some similarity to patients with parkinsonian neurodegeneration, such as resting tremor, rigidity, bradykinesia and postural instability. Moreover, complete loss of HtrA2 protein has a very similar effect

to that of only loss of HtrA2 serine protease activity: HtrA2 KO and Mnd2 mice both die prematurely at around 30 to 40 days of age due to a progressive neurological disorder caused by death of a population of striatal neurons (Jones et al. 2003; Martins et al. 2004). Since the Mnd2 mice display the same phenotype as the HtrA2 KO mice, it appears that the proteolytic activity of HtrA2 is critical for its correct mitochondrial function.

Analysis of brains from HtrA2 KO animals reveals a selective loss of a neuronal population in the striatum, concomitantly with selective loss of terminals of the nigrostriatal pathway, just lateral of the thalamus in a relatively posteriomedial portion of the basal ganglia (Figure 3-3A and F). In humans, PD is characterised by degeneration of the neural connection between the SN and the striatum. The striatum receives its dopaminergic input from neurons of the SNpc via this nigrostriatal pathway. Progressive degeneration of the nigrostriatal dopaminergic pathway results in profound striatal dopamine deficiency, leading to the described motor deficiencies (for review (Fahn 2003)). The clinical symptoms of PD arise by a threshold effect, whereby denervation of the striatum by dopaminergic neuronal loss reduces dopamine levels to below 70% of wild type (Bernheimer et al. 1973). Thus, loss of the neuronal population in the striatum of HtrA2 KO mice is likely to lead to the locomotor deficits observed in HtrA2 KO mice. Additionally, these neurons are already lost at P20, where no phenotypic alterations in the mice are detectable. This suggests that neuronal loss precedes the full development of the parkinsonian syndrome in HtrA2 KO mice, and is in line with the described threshold effect in human PD patients.

Why are certain neurons more susceptible to the loss of HtrA2? In rats systemic administration of rotenone results in mild but systemic complex I inhibition and can produce a progressive model of parkinsonism (Betarbet et al. 2000; Sherer et al. 2003). When a degenerative lesion results, it is selective to the nigrostriatal system, indicative of the vulnerability of this neuronal population to oxidative stress. In the case of human PD patients, there is circumstantial evidence that SN dopamine neurons are under greater metabolic stress, and this potentially provides an explanation for why these neurons are selectively susceptible to mitochondrial toxins and why they are more likely to degenerate in PD (Greene et al. 2005). In line with these observations are the results in Chapter 3, which show that a population of striatal neurons in mice appears to

be specifically sensitive to the loss of HtrA2. Therefore, neurons and in particular these striatal neurons might push their mitochondria to the limit of energy generation with the concomitant enhanced ROS production and stress.

6.1.1 Rodent models of PD

Rodent models of parkinsonism aim to reproduce key pathogenic features of the syndrome including movement disorder induced by the progressive loss of dopminergic neurons in the SN, accompanied by the formation of α-synuclein containing Lewy body inclusions. Despite the creation of many chemically induced and genetically engineered models, there is none that accurately demonstrates these features.

One of the first acute models was created using 6-OHDA administration in rats which causes depletion of striatal and SN neurons through oxidative stress, providing fundamental insights into basal ganglia physiology. Bilateral injection into both hemispheres of the striatum results in akinesia (absence of movement) and unilateral injection in asymmetric circling motor behavior. Lewy body formation was not observed in the 6-OHDA model (Jeon et al. 1995).

Mitochondrial complex I inhibitors such as MPTP and rotenone have provided more progressive models of disease when chronically administered at low dose, resulting in degeneration of the nigrostriatal pathway. MPTP administration in mice results in symptoms of akinesia and rigidity (Sedelis et al. 2001), and transgenic mice over-expressing α-synuclein have increased sensitivity to MPTP, suggesting that genetic and environmental causes may converge (Song et al. 2004).

Chronic administration of rotenone in rats results not only in degeneration of the nigrostriatal pathway, but also in the appearance of Lewy body-like inclusions. The animals show symptoms of akinesia, rigidity and tremor, thus recapitulating most of the mechanisms thought to be important in PD pathogenesis (Betarbet et al. 2000; Sherer et al. 2003).

Genetic mutations identified in familial parkinsonism have provided new tools to implicate and understand the molecular pathways affected.

α-synuclein mutations and multiplications are dominantly inherited and gain-of-function. A vast number of mice over-expressing WT or mutant α-synuclein have been

generated. Some of these show pathological and behavioural impairments that worsen with age and are reminiscent of PD patients. These impairments include a reduction in dopaminergic nerve terminals in the striatum, neuronal inclusions containing α-synuclein, and motor abnormalities (for review (Fleming et al. 2005)).

PD mutations in Parkin, DJ-1 and PINK1 are recessively inherited and loss-of-function. Parkin deficient mice show no overt loss of neurons in the SN or striatum, but relatively subtle alterations were identified, including increased extracellular dopamine concentration and reduced excitability of neurons in the striatum. Interestingly, these mice show a reduction in weight gain, mitochondrial respiration and antioxidant capacity, and increased oxidative damage in the ventral midbrain (Palacino et al. 2004). The behavioural phenotype of the Parkin KO mice is modest by exhibiting a mild reduction in locomotor activity and ability. Therefore, Parkin deficient mice are useful to identify the early effects of a PD-causing mutation *in vivo* (for review (Fleming et al. 2005)).

Similar to Parkin KO mice, DJ-1 deficient mice show no loss of nigrostriatal dopaminergic neurons, but they exhibit increased striatal dopamine levels and up-take rates. Behaviourally, DJ-1 KO mice display subtle deficits such as decreased locomotor activity.

Mice deficient for PINK1 are being characterised, and they show no overt neuronal loss or behavioural phenotype. However, a decrease in dopamine release has been identified that appears to result in impairment of long-term potentiation and depression in striatal neurons (Jie Shen, Keystone Symposium "Molecular Mechanisms of Neurodegeneration 2007").

The HtrA2 KO mice exhibit a very strong phenotype with reduction in weight gain (Figure 3-2B) and the progressive development of motor deficits such as tremor, rigidity, postural instability and bradykinesia or akinesia. This phenotype develops over a short period of only 10 days and thereby allows the study of the late stages of the disease. Pathologically, the HtrA2 KO mice suffer from loss of a population of striatal neurons (Figure 3-3E) concomitant with a reduction in nerve terminals of the nigrostriatal pathway in the posterior portion of the striatum (Figure 3-3F). Neither neuronal loss in the SNpc (Figure 3-3G) nor Lewy body-like aggregates could be detected. In human PD, non-motor symptoms clearly precede the onset of

parkinsonism, and this is also the case in the HtrA2 KO animals since the striatal neuron loss is evident already at P20. Therefore, further study of the HtrA2 KO mice at earlier time points would be needed to determine when the neuronal loss occurs. None of the mice deleted for one of the recessive PD genes, Parkin, DJ-1 and PINK1, exhibits neuronal loss in the SNpc or striatum and severe motor deficits such as the HtrA2 KO mice. Some of the α-synuclein transgenic mice show a reduction in dopaminergic nerve terminals in the striatum similar to HtrA2 KO mice, however their motor deficits are not as severe as the deficits of the HtrA2 KO mice. Therefore, loss of HtrA2 in mice results in a relatively strong model of parkinsonism compared to the other genetic mouse models of PD, and they represent a useful model for further studies because they have pathology and behavioural impairments reminiscent of the pathology and symptoms observed in patients with PD.

6.2 Loss of HtrA2 leads to a stress-induced transcriptional response

Transcriptional profiling was performed to identify HtrA2-dependent transcriptional changes. WT and HtrA2 KO MEFs were challenged with the complex I inhibitor rotenone to induce mitochondrial stress. A higher number of transcriptional changes were detected in HtrA2 KO MEFs in response to rotenone treatment than in WT cells (Figure 4-2C). Although a subset of genes were differentially expressed in rotenone treated WT cells, but not in HtrA2 KO cells treated with rotenone, no functional signature of genes could be identified that was only modulated in WT cells in response to rotenone treatment but not in HtrA2 KO cells. Most of the genes modulated by rotenone were identified in HtrA2 KO cells, whereas their transcriptional regulation in WT cells was not significant (Figure 4-2C). The stress-inducible TF CHOP as well as Gadd45a were among those transcripts being significantly induced by rotenone treatment in HtrA2 KO cells but not in WT cells in the GeneChip analysis, and their enhanced expression in HtrA2 KO cells following rotenone treatment was confirmed by RT qPCR analysis (Figure 4-3A, B and data not shown). Recently, Gadd45a has been implicated in epigenetic gene activation by inducing DNA demethylation (Barreto et al. 2007), and further investigation of its expression levels in HtrA2 KO brains might be of interest. The induction of CHOP in HtrA2 KO MEFs following rotenone treatment could point to an increased level of stress in these mitochondria, as CHOP

was found to be implicated in a mitochondria-specific stress response (Zhao et al. 2002). Interestingly, CHOP expression was higher in brain tissue from HtrA2 KO mice, but not in any other tissue tested (Figure 4-4A), potentially mirroring a higher level of stress in brain due to an increased demand for mitochondrial function or a decreased capacity to cope with the stress elicited by loss of HtrA2 function. Furthermore, the increase in CHOP expression level seems to correlate with the development of a parkinsonian syndrome in HtrA2 KO mice (Figure 4-4B and Figure 3-2B) and might be essential for the manifestation of this phenotype.

Transcriptional profiling of genes differentially expressed in brain tissue from HtrA2 KO mice revealed that, besides CHOP, ATF3 and Herp mRNA levels were also induced in these brains (Figure 4 8). CHOP and Herp are known to be dually regulated by the ER stress-specific and the shared branch of the UPR (Figure 1 6B) (Ma et al. 2002; Ma and Hendershot 2004). Expression of ATF3 is increased following a wide range of stress stimuli. Interestingly, the induction of ATF3 transcript in response to amino acid deprivation or ER stress was demonstrated to occur by mechanisms requiring eIF2α phosphorylation (Jiang et al. 2004). Thus, deregulation of the shared branch of the UPR or activation of other pathways that lead to phosphorylation of eIF2α, and concomitantly stimulate translation of ATF4, could possibly be implicated in the cellular events resulting from loss of HtrA2 function.

The induction of CHOP expression has previously been implicated in a mitochondrial stress response (Zhao et al. 2002). Zhao and colleagues used a mutant version of a mitochondrial matrix enzyme that could not fold properly and accumulated in the mitochondria. In their study, the authors noted the transcriptional up-regulation of nuclear genes encoding mitochondrial stress proteins such as Hsp60, Hsp10, mtDnaJ and ClpP. CHOP in association with C/EBPβ did regulate the expression of those mitochondrial stress proteins via a CHOP element in their promoters (Zhao et al. 2002). None of the mitochondrial stress proteins was differentially expressed in HtrA2 KO brain, suggesting that the type of stress in cells that lack HtrA2 might be different. Thus, loss of HtrA2 seems to elicit a different sort of stress than accumulation of unfolded proteins.

6.2.1 Potential deregulation of the ATF4 pathway in HtrA2 KO animals

Strikingly, a subset of genes that were expressed to a higher degree in brains from HtrA2 KO mice were previously reported to dependent on the TF ATF4 for transcriptional up-regulation (Vallejo et al. 1993; Fawcett et al. 1999; Siu et al. 2002; Harding et al. 2003; Ohoka et al. 2005). Markedly, a C/EBP-ATF composite site had been characterised in the promoters of a subset of these genes, namely CHOP, ATF3, Herp, ASNS and TRB3. Analysis of the genomic sequence of the putative ATF4 target genes that are up-regulated in HtrA2 KO brain, revealed C/EBP-ATF consensus sites in almost all of the genes (Table 4-5). These results strongly support the hypothesis that deregulation of ATF4 might contribute to the transcriptional profile in brains from mice lacking HtrA2. ATF4 protein levels are regulated through phosphorylation of eIF2α on the translational level (Figure 1-6B). Therefore, investigation of the protein level of ATF4 in WT and HtrA2 KO brain should be performed. In addition, the activity of the upstream signalling pathways (the eIF2α kinases) can be studied using phospho-specific antibodies against PERK, GCN2 and PKR. Interestingly, proteasome inhibition was reported to result in activation of GCN2 and increased phosphorylation of eIF2α (Jiang and Wek 2005), suggesting that deregulation of this pathway might not be uncommon in the cellular events leading to development of PD.

Gene expression profiling cannot differentiate between primary and secondary events and, therefore, the GeneChip analysis of brain tissue from HtrA2 mice at P29 may only provide a molecular fingerprint of late-stage processes due to loss of HtrA2. However, the signature of ATF4 target genes up-regulated in HtrA2 KO brain has been reported to be induced in cellular models of PD following stimulation with neurotoxins *in vitro* (treatment of MEFs with rotenone in this thesis, and (Ryu et al. 2002; Holtz and O'Malley 2003)) and for CHOP also *in vivo* (Silva et al. 2005). Therefore, a transient stimulus with neurotoxins such as rotenone, 6-OHDA or MPP+ modulates the same genes found up-regulated in HtrA2 KO brains, suggesting that the identified genes are potentially important in the development of PD.

Interestingly, the genes modulated by 6-OHDA and MPP+ treatment, but none of the genes induced by treatment with 6-OHDA but not MPP+, were up-regulated in brains

from mice lacking HtrA2 (Table I and II respectively in (Holtz and O'Malley 2003)). In this study, the transcriptional changes induced by MPP+ or 6-OHDA treatment in the dopaminergic cell line MN9D were measured. Whereas 6-OHDA led to the induction of ER chaperones and other genes that are associated with the ER stress-specific branch of the UPR, MPP+ did not. However, both, 6-OHDA and MPP+ caused transcriptional up-regulation of a set of genes that are induced downstream of the shared branch of the UPR, as most of these genes were described previously to be induced in response to ER stress dependent on the presence of ATF4 (Harding et al. 2003). Therefore, the authors proposed that 6-OHDA is activating all three signalling pathways of the UPR, IRE1/XBP-1, ATF6 and PERK, whereas MPP+ is only activating the PERK branch (Figure 1-6B) (Holtz and O'Malley 2003). In line with this were the observations that arsenite exposure of primary neuronal cells led to the up-regulation of CHOP expression without a concurrent activation of ER-specific signalling pathways of the UPR (Mengesdorf et al. 2002).

What are the cellular events leading to 6-OHDA- and MPP+-induced toxicity? Both MPP+ and 6-OHDA can inhibit complex I of the respiratory chain, however, the cellular events and the type of cell death induced by these toxins appear to be different. MPP+ accumulates in mitochondria due to the energy-dependent electrical gradient that is maintained across the mitochondria membrane. Once accumulated in mitochondria, MPP+ inhibits complex I of the electron transport chain, at or near the rotenone sensitive site. Blockade of mitochondrial respiration has two cytotoxic consequences. First, it impairs mitochondrial energy supply resulting in decreased intracellular ATP and NAD+ contents and ATP/ADP ratio (Storch et al. 2000). In line with this are the observations, that glucose or fructose decrease MPP+-mediated toxicity by providing energy for anaerobic metabolism via glycolysis, and inhibition of glycolysis increases MPP+-induced cell death (Wu et al. 1996; Mazzio and Soliman 2003). A recent study suggests that inhibition of complex I is not solely involved in eliciting cell death. Indeed, disruption of Ca^{2+} homeostasis appears to play an additional role in MPP+ toxicity. This results in an elevation of intracellular Ca^{2+}, leading to the activation of Ca^{2+}-dependent enzymes, for example, protein kinase and calpains I and II, which disturbs the normal cell function, resulting in cellular damage (Lee et al. 2006). Second, MPP+ appears to support the occurrence of oxidative stress. This notion is

demonstrated by the generation of ROS and free iron. Any process that affects the mitochondrial respiratory chain and energy production will probably cause leakage or generation of oxyradicals and subsequent oxidative stress, so that the two processes are probably inexorably linked. However, a series of experiments comparing 6-OHDA and MPP+ toxicity showed, that generation of ROS seemed to play an essential role in 6-OHDA-mediated apoptosis, but there was no evidence of this in the setting of MPP+-induced cell death (Wu et al. 1996; Fonck and Baudry 2001; Han et al. 2003). Thus, MPP+-induced toxicity has been primarily attributed to its effect on mitochondrial energy metabolism, rather than increased oxidative stress. The neurotoxicity of 6-OHDA is believed to be related primarily to production of ROS since, in contrast to MPP+, anti-oxidants can attenuate 6-OHDA-induced cell death (Han et al. 2003) and inhibition of glycolysis has not adverse effect (Wu et al. 1996). Only 6-OHDA, but not MPP+, treatment results in activation of caspases and morphological changes associated with apoptosis, probably because MPP+ more effectively depletes cellular energy than 6-OHDA, therefore, only 6-OHDA-treated cells retain sufficient energy to execute apoptosis (Choi et al. 1999; Lotharius et al. 1999).

Transcriptional up-regulated genes in the dopaminergic cell line MN9D that were in common to treatment with both MPP+ and 6-OHDA (Table I (Holtz and O'Malley 2003)) were found to be induced in brains from HtrA2 KO mice. None of the genes associated with the ER stress-specific branch of the UPR that were induced only by 6-OHDA treatment (Table II (Holtz and O'Malley 2003)) were up-regulated in brains from HtrA2 KO mice. Which conclusions about HtrA2 could be drawn from the knowledge about the cellular events that lead to 6-OHDA- and MPP+-induced toxicity? Loss of HtrA2 causes mitochondrial dysfunction, potentially leading to impaired respiration and concomitant energy deficits as well as generation of ROS. In addition, intracellular Ca^{2+} homeostasis might be deregulated upon loss of HtrA2. It is possible that loss of HtrA2, similar to MPP+, primarily leads to impaired mitochondrial energy supply resulting in decreased intracellular ATP content. Primary WT or HtrA2 KO MEFs did not exhibit differences in metabolic activity when challenged with CCCP, rotenone or tunicamycin as determined by an MTT assay (Figure 3-5C-E), suggesting that loss of HtrA2 in MEFs might not result in metabolic defects. Analysis of the mitochondrial electron transport chain at the biochemical level in extracts prepared

from the basal ganglia of WT and HtrA2 KO animals failed to reveal any significant compromise of the function of complexes I, II, III or IV when enzymatic activities were normalised against the activity of the mitochondrial matrix enzyme citrate synthase, to account for differences in mitochondrial density in the samples. However, extracts prepared from the basal ganglia of HtrA2 KO animals showed a decrease of the yield of mitochondrial citrate synthase, indicating that mitochondrial density might be reduced in these tissue samples (Martins et al. 2004). Preliminary data using an oxygen electrode to measure oxygen consumption in brain revealed that the oxygen consumption going through complexes II, III and IV is reduced in HtrA2 KO tissue compared to WT (Nicoleta Moisoi, MRC Leicester). Thus, mitochondrial respiration might be impaired in brains from HtrA2 KO mice. Disruption of the Ca^{2+} homeostasis appears to play an additional role in MPP+ toxicity. Mitochondrial Ca^{2+} homeostasis seems to be similar in WT and HtrA2 KO cells (Nicoleta Moisoi, MRC Leicester), however, the study of intracellular and ER Ca^{2+} homeostasis needs to be extended. Both toxins, MPP+ and 6-OHDA, will cause oxidative stress albeit 6-OHDA might be more potent to induce ROS. Therefore, a lower level of ROS generation could result in activation of only the shared branch of the UPR (PERK, eIF2α), as in the case for MPP+, and higher levels of ROS might lead to signalling through all branches of the UPR as in the case for 6-OHDA (IRE1/XBP-1, ATF6, PERK). Thus, loss of HtrA2 might result in relatively mild ROS generation, thereby inducing genes that can be regulated through the shared branch of the UPR.

6.2.2 Loss of HtrA2 leads to oxidative stress

HtrA2 KO mice probably suffer from enhanced levels of oxidative stress since mitochondrial lipids from HtrA2 KO mice show a higher content of peroxidised lipids than WT mitochondria (Table 4-6). Also, HtrA2 KO cells produce more ROS than WT cells in response to rotenone and 6-OHDA (data not shown). In addition, the phenotype of HtrA2 KO mice can be delayed by treatment with an anti-oxidant (Figure 4-10). Oxidative stress had been placed upstream of the induction of CHOP and ATF3 in response to 6-OHDA (Holtz et al. 2006). Therefore, loss of HtrA2 might lead to the production of ROS itself or might diminish the capacity of the cells to counteract ROS, which subsequently causes induction of CHOP and other stress-induced genes.

An increased content of peroxidised lipids was identified in mitochondria isolated from liver and brain tissue of HtrA2 KO mice, however, an increase in CHOP expression level was only detected in brain tissue. This observation could certainly indicate that the increased expression of CHOP is not connected to the generation of ROS in HtrA2 KO mice, however, a more favourable explanation is that liver cells are less susceptible to the oxidative stress and therefore up-regulation of CHOP in liver or other organs cannot be detected within the life-span of the HtrA2 KO animals. Similar to CHOP expression being exclusively up-regulated in brain tissue although all cells are exposed to loss of HtrA2, the systemic treatment of rats with low doses of rotenone leads selectively to lesions in the nigrostriatal system (Betarbet et al. 2000; Sherer et al. 2003). In line with the observation that CHOP expression is selectively induced in the brain of HtrA2 KO mice, mitochondria isolated from the brains of WT and HtrA2 KO mice rather than liver mitochondria might result in the unambiguous identification of HtrA2 substrates in the 2D DIGE approach.

Treatment of HtrA2 KO mice with anti-oxidants results in prolonged life-span (Figure 4-10) and is also beneficial for the locomotor activity of the HtrA2 KO mice (Nicoleta Moisoi, Miguel Martins, MRC Leicester). It will be interesting to measure CHOP expression levels in HtrA2 KO mice treated with anti-oxidants. Preliminary analysis was performed on P30 animals, however, the level of CHOP expression was only slightly reduced in HtrA2 KO mice treated with NAC compared to vehicle treated HtrA2 KO mice (data not shown). These analyses need to be repeated and more importantly extended over a time course. It is possible that measuring CHOP expression levels at P30 is too late in the development of the parkinsonian syndrome, even in HtrA2 KO mice treated with anti-oxidants. HtrA2 KO mice as young as P15 did show increased levels of CHOP transcript, however, P8 mice did not. Therefore, CHOP expression levels should be monitored between P10 and P20 in HtrA2 KO mice treated with anti-oxidants or vehicle.

Taken together expression profiling of brains from HtrA2 deficient mice identified a signature of genes that appear to be characterised by C/EBP-ATF composite sites for transcriptional regulation. These genes are up-regulated in cells stimulated with neurotoxins and thought to be regulated through phosphorylation of eIF2α leading to an increase of ATF4 protein. Therefore, different models used for studying PD, such as

in vitro cell systems challenged with neurotoxins and *in vivo* the HtrA2 KO mice, share up-regulation of a specific signature of genes, suggesting that their up-regulation might be a common underlying theme in PD.

6.3 HtrA2 and Parkinson's disease

Eight nuclear genes are known to carry mutations that cause PD, encoding α-synuclein, parkin, UCHL1, PINK1, DJ-1, LRRK2, ATP13A2 and HtrA2 (Table 1-1) (Farrer 2006; Ramirez et al. 2006). Mutation or altered expression of these proteins contributes to PD pathogenesis through partly overlapping mechanisms that result in mitochondrial impairment, oxidative stress, and protein mishandling. Consistent with the development of a parkinsonian syndrome in mice lacking HtrA2 function, a polymorphism and a mutation resulting in single amino acid changes in HtrA2 that appear to dampen the activation of its proteolytic activity were identified to be associated with the PARK13 locus (Strauss et al. 2005). These studies suggest that loss of function of HtrA2 leads to neuronal cell death, possibly due to mitochondrial dysfunction, both in mice and in humans. Since then, several other mutations linked to PD have been identified in HtrA2 (personal communication, Reijko Krüger). The A141S polymorphism and G399S mutation in HtrA2 were found to be heterozygous in sporadic PD patients, therefore it is not possible to conclude from the inheritance pattern whether the HtrA2 locus is dominant or recessive. The fact that the heterozygous mutation appears to be pathogenic would suggest that it is inherited in a dominant manner, however, the mutation seems to be loss-of-function and therefore a heterozygous mutation could act as haploinsufficiency which would suggest that it is recessive. In mice, only homozygous loss of HtrA2 results in the development of a parkinsonian syndrome suggesting that loss of HtrA2 activity is recessive in mice. Targeted knock in of the G399S mutation in mice would be needed to address the effect and inheritance pattern of this PD-associated mutation.

The A141S polymorphism and G399S mutation in HtrA2 localise to domains previously shown to be important in the regulation of the proteolytic activity of HtrA2, namely the N-terminal portion of the mature form of HtrA2 and the PDZ domain, respectively (Martins et al. 2002). Interestingly, analysis using the Scansite algorithm (Obenauer et al. 2003) (www.scansite.mit.edu) indicates that S142 and S400, residues

that lie immediately adjacent to the mutations found in the PD patients, are putative phosphorylation sites for proline-directed serine/threonine kinases (Figure 5-2A), suggesting that these sites might play a major role in the regulation of the enzymatic activity of HtrA2. Alignment of HtrA2 homologues of different species shows that S142 and S400 are conserved in human, rodents and chicken, and in addition S400 is further conserved in *Drosophila* and *Sacharomyces cerevisiae* (Figure 5-2B).

6.3.1 PINK1 is upstream of HtrA2 and regulates its activity

The mitochondrial kinase PINK1 was identified as a new binding partner of HtrA2 using the TAP tag system to affinity purify interacting proteins. Mutations in PINK1 were reported to account for the PARK6 locus of familial PD and it has been hypothesised that PINK1 may phosphorylate mitochondrial proteins in response to cellular stress, protecting against mitochondrial dysfunction (Valente et al. 2004). HtrA2 might be a direct substrate of PINK1, however, the kinase activity of PINK1 in *in vitro* kinase assays was very low, thus, it is not possible to conclude whether PINK1 phosphorylates HtrA2 directly. However, HtrA2 could be phosphorylated *in vitro* by p38γ and p38β, and preliminary data indicates that p38γ might phosphorylate both sites, S142 and S400 *in vitro* (personal communication, Helene Plun-Favreau).

Activation of the MEKK3 signalling pathway led to phosphorylation of HtrA2 at least on S142 *in vivo* (Figure 5-2C), and chemical inhibition of p38 reduced the MEKK3-induced phosphorylation of HtrA2 (Figure 5-2D). Moreover, PINK1 was required for this phosphorylation to occur (Figure 5-3D) and mutations in PINK1 decreased HtrA2 phosphorylation on S142 in human brain samples from PD patients (Figure 5-3E). Unfortunately, the sequence around S400 of HtrA2 is relatively hydrophobic and does not work well as an immunogen in rabbits. Therefore it was not possible to generate an antibody specific for phospho-S400 HtrA2 and address its phosphorylation *in vivo*. Interestingly, HtrA2 mutants mimicking phosphorylation on S142 and S400 showed an increase in their protease activity (Figure 5-4).

Why might PINK1 expression be necessary for HtrA2 phosphorylation to occur (Figure 5-3B and D)? One possibility, suggested by the data presented, is that HtrA2 phosphorylation is mediated by a kinase activated in the MEKK3 signalling pathway (potentially p38, Figure 5-2C and D), but is dependent on the interaction of HtrA2 with

PINK1, possibly reflecting the existence of a multimeric complex. Another possibility is that PINK1 is indeed a kinase, but the "correct" stimulus to activate its kinase activity *in vitro* has not been identified. In this case, PINK1 might phosphorylate HtrA2 directly and PINK1 kinase activity could be modulated by the MEKK3 pathway. Alternatively, PINK1 might be upstream of another kinase responsible for phosphorylating HtrA2 and be involved in its activation. *In vivo*, the phosphorylation of HtrA2 might require recruitment of this kinase to the mitochondria, or alternatively could occur in the cytosol before HtrA2 is imported into the mitochondrial intermembrane space. The interaction between PINK1 and HtrA2 was predominantly detected in mitochondria-enriched fractions. However, both over-expressed full length mitochondrial and mature cytosolic HtrA2 could be phosphorylated on S142 when MEKK3 was activated and this occurred in a PINK1-dependent manner (data not shown), suggesting that the phosphorylation might occur prior to import of HtrA2 into the mitochondria.

Phosphorylation of HtrA2 appears to regulate its proteolytic activity, since HtrA2 mutants mimicking phosphorylation on S142 and S400 showed an increase in their protease activity *in vitro* (Figure 5-4A), concomitant with a reduction in the ability of the PDZopt peptide and XIAP to activate HtrA2 protease activity (Figure 5-4B and C, Figure 5-5C). This suggests that phosphorylation of HtrA2 might lead to conformational changes facilitating its protease activity. However, in these experiments, HtrA2 proteins engineered with a serine to aspartate mutation, to mimic phosphorylation at the sites of interest, were used. Therefore, it is crucial to show that "real" phosphorylation can have the same impact on HtrA2 proteolytic activity. First evidence that PINK1 might indeed regulate HtrA2 activity *in vivo* comes from experiments over-expressing PINK1 prior to measuring HtrA2 activity *ex vivo* (Figure 5-6C). In line with this is the observation that over-expression of PINK1 cannot protect HtrA2 KO cells to the same extent as WT cells from stress-induced apoptosis, placing HtrA2 downstream of PINK1 function (Figure 5-7).

Previously, it was reported that both A141S and G399S PD-associated mutations in HtrA2 resulted in reduced ability of the PDZopt peptide or XIAP to activate its protease activity (Strauss et al. 2005). The influence of these PD-associated mutations on the phosphorylation of the adjacent sites (S142 and S400) is clearly an area for

further investigation. Mutation of A141S creates a new potential phosphorylation site for proline-directed serine/threonine kinases on this residue. However, A141 is not well conserved across different species. In rodents this residue is a threonine, already providing such a potential phosphorylation site (Figure 5-2B) and preliminary data indicates that A141S has no effect on S142 phosphorylation *in vitro*. However, the G399 sequence is well conserved and G399S mutation in HtrA2 might lead to decreased phosphorylation of this site *in vitro*. A defect in phosphorylation due to G399S mutation and therefore impaired modulation of HtrA2 proteolytic activity could explain the increased mitochondrial dysfunction and sensitivity to stress-induced cell death of this mutant when over-expressed (Strauss et al. 2005).

The PD-associated mutations in PINK1, C575R and Y431H, resulted in a robust decrearse in the levels of phosphorylated HtrA2 at position S142 in human brains (Figure 5-3E). The study of these human brains is clearly important for confirming the relevance of the interaction of HtrA2 and PINK1 *in vivo* in human PD patients. Neither the C575R nor the Y431H mutant of PINK1 have lost their ability to interact with HtrA2 *in vitro* (data not shown, Helene Plun-Favreau), thus supporting the idea that PINK1 possibly functions as a kinase *in vivo* to phosphorylate HtrA2 and that its kinase activity towards HtrA2 could be impaired by the PD mutations. Alternatively, through interaction with HtrA2, these PINK1 mutants might be acting as dominant negatives and therefore prevent WT PINK1 from binding and exerting its effect on HtrA2.

The identification of PINK1 binding to HtrA2 demonstrates a direct molecular interaction between two genes implicated in PD. Uniquely, it is the only functional interaction that has been validated *in vitro*, *in vivo* and in human PD brains. In parallel to the presented data in this thesis, genetic analyses of HtrA2 and PINK1 function in *Drosophila* place HtrA2 downstream of PINK1 and Parkin (unpublished data, Ruhena Begum et al., Cancer Research UK). Thus, both HtrA2 and PINK1 proteins are genetically linked, suggesting that they could be part of the same signalling pathway.

6.4 Does HtrA2 function similar to bacterial DegP or DegS?

Mammalian HtrA2 may function to protect mitochondria from certain stresses in a manner similar to the homologous stress-adaptive proteins DegP and DegS in bacteria.

6.4.1 HtrA2 function akin to bacterial DegP

DegP is localised in the periplasmic space, where it controls bacterial thermal and oxidative tolerance by acting as a chaperone at normal temperatures. At elevated temperatures, the chaperone transforms into an active endoprotease that degrades damaged and misfolded proteins (Spiess et al. 1999). If HtrA2 functions similar to DegP, mitochondria from HtrA2 KO mice may be unable to degrade unfolded proteins in the intermembrane space under conditions of cell stress and these could form aggregates that would directly compromise the maintenance of the mitochondria.

Evidence for an evolutionary conservation of this function is provided by the observation that the protein level of HtrA2 appears to be increased following heat shock of human neuroblastoma SH-SY5Y cells (Gray et al. 2000), and that the proteolytic activity of recombinant HtrA2 is significantly elevated upon heat shock *in vitro* (Martins et al. 2003). However, the data showing an increase of HtrA2 protein levels was obtained using an antibody that recognised an apparently nuclear form of HtrA2 and has subsequently not been validated. In addition, chaperone activity similar to DegP has not been identified for HtrA2.

In contrast to mammalian HtrA2, bacterial DegP protease possesses two PDZ domains and does not contain a transmembrane segment (Figure 1-2B). Whereas HtrA2 is active as a trimer, DegP forms a hexameric structure (Figure 1-3B and D). In addition, in the inactive conformation, the catalytic centre of DegP is sterically blocked by a trio of loops from the surrounding protein, and the catalytic triad is distorted away from an active configuration (Krojer et al. 2002). However, in HtrA2 the proteolytic active sites are in conformation poised for catalysis (Li et al. 2002). DegP shows substrate specificity for aliphatic amino acids at the P1 position (Kolmar et al. 1996), similar to HtrA2 and DegS. However, DegP exhibits no preference for any amino acid at the P1' position, which is in contrast to HtrA2 that favours an alanine or serine at this position (Martins et al. 2003; Walle et al. 2007). In addition, DegP cleaves substrates which are

transiently or globally denatured and exhibits relatively broad substrate specificity, whereas HtrA2 has a rather narrow cleavage site preference (Walle et al. 2007).

The induction of CHOP in HtrA2 KO MEFs following rotenone treatment and in brains of HtrA2 KO mice probably points to an increased level of stress in these mitochondria. This suggests the possibility that the function of HtrA2 is not DegS-like in a signalling cascade, but more akin to the bacterial protease DegP, which elicits its protective function by refolding or degrading unfolded accumulating proteins. The lack of HtrA2 would lead to a higher level of unfolded proteins in the mitochondrial intermembrane space and therefore the threshold for activation of the mitochondrial stress response would be lower in HtrA2 KO cells compared to the WT cells.

How could loss of HtrA2 lead to increased production of ROS if HtrA2 had DegP-like function? HtrA2 would be involved in clearance of unfolded proteins in the intermembrane space of the mitochondria. Therefore, loss of HtrA2 proteolytic function would result in the accumulation of unfolded proteins, possibly members of the respiratory complexes, which would lead to impaired electron transport and generation of ROS (Figure 6-1B).

6.4.2 HtrA2 function akin to bacterial DegS

The bacterial protease DegS is a critical mediator of a transcriptional stress response initiated in the periplasmic space (Schlieker et al. 2004). If HtrA2 acts like DegS (Walsh et al. 2003), loss of HtrA2 may result in an inability to mount an adaptive transcriptional response under stress conditions that cause protein unfolding, leaving the mitochondria unable to maintain normal function and rendering the cells prone to either necrotic or apoptotic death (Figure 6-1A).

A DegS-like function for HtrA2 would be clearly predicted from the similarity of their domain and more importantly their closely related crystal structures (Figure 1-2B and Figure 1-3B and C) (Li et al. 2002; Martins et al. 2003). The catalytic centre of both proteases is slightly distorted in the inactive conformation, and their catalytic activity can be regulated by the PDZ domains (Li et al. 2002; Wilken et al. 2004). It is interesting to note that DegS cleaves RseA between a valine and a serine (Walsh et al. 2003). Similarly, human and mouse HtrA2 have a preference for valine at P1 position

and serine at P1' in an optimal synthetic peptide substrate (Martins et al. 2003). This suggests that conservation between DegS and HtrA2 is also present at the biochemical level. Moreover, HtrA2 has a rather narrow cleavage site preference (Martins et al. 2003; Walle et al. 2007), further supporting the notion that HtrA2 cleaves substrates specifically similar to DegS.

While the structural and biochemical similarity between HtrA2 and DegS is evident, it has so far not been possible to identify mitochondrial mammalian homologues of other downstream components of the bacterial periplasmic stress response system. Bacterial RseP, a rhomboid-like metalloprotease that is responsible for the second cleavage of the transmembrane receptor RseA (Kanehara et al. 2002), is a homologue of the mammalian S2P protease in the Golgi network. S2P possesses like bacterial RseP a PDZ domain, and it is interesting to note that the residue corresponding to S400 in the PDZ domain of HtrA2 is conserved in the PDZ domain of S2P, suggesting that this residue might be important for the regulation of a number of PDZ domain-containing proteases. S2P participates in proteolytic activation of membrane-tethered TFs like SREBP in response to low cholesterol levels (Sakai et al. 1996) and ATF6 in response to unfolded proteins in the ER (see Chapter 1.5.1, (Ye et al. 2000)). Cleavage of these substrates is also preceded by cleavage through another protease, the ER localised S1P (Sakai et al. 1998; Ye et al. 2000). However, there is no apparent sequence similarity between mammalian S1P and bacterial DegS or mammalian HtrA2, although all are serine proteases. Even though S2P appears to be the mammalian homologue of bacterial RseP, the localisation of S2P in the Golgi network suggests that it cannot be the functional homologue of RseP in a putative stress response pathway downstream of HtrA2 in the mitochondria.

The rotenone-mediated induction of CHOP in HtrA2 KO MEFs and the increased expression of CHOP in brains of HtrA2 KO mice probably points to an increased level of stress in these mitochondria. An HtrA2-dependent transcriptional response following rotenone treatment could not be identified. At a first glance, this seems to suggest that the function of HtrA2 is not DegS-like in a signalling cascade, but more akin to the bacterial protease DegP. However, a role for HtrA2 in actively signalling in a mitochondrial stress response cannot be excluded from the data. It is possible that rotenone might not be the "correct" stimulus to induce HtrA2-dependent stress

signalling, even though previous results show that loss of HtrA2 sensitises cells and their mitochondria to this stress stimulus (Figure 3-6 and Figure 3-7A). Furthermore, rotenone might induce a variety of stress signalling pathways that could overlay the HtrA2-dependent signature in WT cells.

How could loss of HtrA2 lead to increased production of ROS if it had DegS-like function in the mitochondria? Analogous to a DegS-like function, mammalian HtrA2 could be responsible for transducing a signal from the mitochondria to the nucleus resulting in increased expression of other proteases or chaperones, that would help to maintain the mitochondria free from misfolded proteins. Loss of HtrA2 would therefore decrease the availability of proteases and folding catalysts in the mitochondria and in turn lead to accumulation of aberrant proteins, impaired electron transport and generation of ROS (Figure 6-1B). In addition, bacterial DegS is known to induce expression of DegP (Erickson and Gross 1989), supporting the idea that HtrA2 would normally lead to the expression of other proteases involved in mitochondrial maintenance, thereby protecting against oxidative stress.

The PINK1-dependent phosphorylation of HtrA2 seems likely to influence its proteolytic activity. This observation might support a DegS-like model for HtrA2, since DegS activity is also regulated by an upstream component, rather than an environmental stimulus, heat shock, as in the case for DegP protease activity. DegS is activated by engagement of its PDZ domain by binding to C-terminal motifs of OMPs. Phosphorylation of HtrA2 in the PDZ domain might lead to a similar conformational effect. Likewise, binding of XIAP to the N-terminus of mature HtrA2 leads to its activation (Martins et al. 2003), therefore phosphorylation on S142 close to its mature N-terminus might have a similar effect.

Taken together, whether HtrA2 has inherited a function similar to bacterial DegP or DegS in mammalian mitochondria is not clear. A DegS-like function for HtrA2 would be predicted from the similarity of their closely related crystal structures and of the regulation of their proteolytic activity (Li et al. 2002; Martins et al. 2003) and would be favoured over a DegP-like model.

6.5 Concluding remarks and future directions

During the last years, progress has been made to understand the physiological role of HtrA2 in the mitochondria. Especially, the characterisation of the phenotype of the HtrA2 KO and Mnd2 mice was important to highlight HtrA2's role as being protective rather than pro-apoptotic (see Chapter 3, (Jones et al. 2003; Martins et al. 2004)). Analogous to the bacterial protease DegS, HtrA2 was proposed to function in a putative mitochondrial stress response pathway inherited from bacteria (Figure 6-1A).

From the data presented in this thesis, it is possible to postulate that PINK1 acts upstream of HtrA2 and regulates HtrA2 activity through phosphorylation (see Chapter 5). Enhanced HtrA2 activity is thought to protect cells from stress-induced death. Decreased phosphorylation of HtrA2 in human PD patients with PINK1 mutations and potentially also in patients with HtrA2 mutation will probably lead to deregulation of HtrA2 protease activity. This could possibly impair signalling of a mitochondrial stress response pathway and/or trigger a stress response similar to the response seen in brains of HtrA2 KO animals.

In the future, it will be crucial to determine whether HtrA2 is a direct substrate for PINK1 kinase activity and/or whether other kinases could be involved in the phosphorylation of HtrA2. The activtion of the MEKK3-p38 pathway leads to an increase in HtrA2 phosphorylation on S142 *in vivo*, therefore, the activity of PINK1 in these settings should be studied.

The phosphorylation of HtrA2 on S142 has been shown to occur *in vitro* and *in vivo*, however, little is known about phosphorylation on S400, a potential phosphorylation site within the PDZ domain of HtrA2. In an *in vitro* kinase assay using a peptide surrounding S400, this site can be phosphorylated (data not shown). However, for technical reasons it has not been possible to determine phosphorylation on S400 of full length or mature HtrA2. It should be fairly interesting to find out whether phosphorylation does occur *in vivo* on S400 of HtrA2. In addition, it will be important to study the impact of the polymorphism and mutation identified in HtrA2 in PD patients, S141A and G399S (Strauss et al. 2005), on the phosphorylation and proteolytic activity of HtrA2.

Loss of HtrA2 in mice leads to stress-induced transcriptional changes in brains from these animals. In addition, loss of HtrA2 results in oxidative stress, and at least a subset of genes up-regulated in brains from HtrA2 KO animals have been reported to be induced by oxidative stress. The TF CHOP has taken a central role in cellular and animal models of PD induced by neurotoxins (Ryu et al. 2002; Holtz and O'Malley 2003; Silva et al. 2005), and it is induced in brains of HtrA2 KO mice. Thus, loss of HtrA2 is the first genetic mouse model of PD that shows up-regulation of CHOP, interestingly specifically in the brains of HtrA2 KO mice. CHOP has been implicated as a mediator of apoptosis in the context of oxidative stress (Guyton et al. 1996; Mengesdorf et al. 2002), suggesting that up-regulation of CHOP might ultimately contribute to enhanced cell death. Therefore a model can be proposed, whereby HtrA2 function decreases oxidative stress, however, upon loss of HtrA2 increased oxidative stress would result in expression of CHOP and modulation of a number of other genes leading to cell death (Figure 6-1B).

Anti-oxidant treatment of the HtrA2 KO mice alleviates their phenotype and oxidative stress has been implicated in the up-regulation of CHOP. Therefore, it will be important to monitor CHOP expression levels in anti-oxidant treated HtrA2 KO mice. This will shed light on the role of CHOP in the development of the phenotype of the HtrA2 KO mice. However, it is possible that, although sustained CHOP expression has been shown to promote apoptosis (for review (Oyadomari and Mori 2004)), initial activation of CHOP could have a protective effect (Zinszner et al. 1998) similar to moderate activation of various stress-induced signalling pathways. Therefore, the interpretation of the time course of CHOP expression in anti-oxidant treated HtrA2 KO mice could be complicated.

Furthermore, to address the role of CHOP in the development of the phenotype of the HtrA2 KO mice, the HtrA2 KO mice could be crossed to CHOP deficient mice. CHOP KO mice have already been generated, and they appear phenotypically normal, have normal fertility and reproductive behaviour, but they are defective in the development of apoptosis in response to ER stress elicited by tunicamycin (Zinszner et al. 1998). Absence of CHOP might delay the development of the parkinsonian syndrome in the HtrA2 KO mice.

CHOP can be transcriptionally induced by activation of eIF2α kinases and subsequent

induction of ATF4 protein level (Figure 1-6B). Therefore, investigation of the protein level of ATF4 and the phosphorylation status of eIF2α in WT and HtrA2 KO brain should be performed. In addition, the activity of the upstream signalling pathways (the eIF2α kinases) can be studied using phospho-specific antibodies against PERK, GCN2 and PKR.

A signature of genes was identified to be up-regulated in HtrA2 KO brain that contain C/EBP-ATF composite sites (Table 4-5). Therefore, it would be interesting to investigate whether transcription through this site is enhanced in the absence of HtrA2. In addition, immunodepletion of ATF4, CHOP, C/EBPβ and other TFs might suppress this enhanced transcriptional activity and thereby could lead to the identification of the TFs responsible for activation of the C/EBP-ATF composite site upon loss of HtrA2.

The HtrA2 KO mice and neurotoxin-induced mouse models of PD exhibit up-regulation of CHOP, however, other genetic PD mouse models have not been examined for their CHOP expression levels. Therefore, it would be interesting to obtain brain tissue from α-synuclein over-expressing, and Parkin, PINK1 and DJ-1 KO mice to determine CHOP expression levels in these. Furthermore, it would be very important to test human PD patients for CHOP expression in order to verify CHOP as a common underlying theme in the human disease. Most of the dopaminergic neurons in the SNpc are lost when the PD patients die, making the comparision with the same tissue from normal humans quite difficult. Therefore, other brain regions that do not suffer from cell loss in PD patients have to be tested as well.

The characterisation of transcriptional changes in mice lacking HtrA2 identified a signature of genes potentially representing a common underlying theme in the development of PD. The identification of HtrA2 and PINK1 being involved in a common pathway is the first step in elucidating the molecular players around the mitochondrial function of HtrA2. Thus, further study of this pathway might help explain how mitochondrial dysfunction leads to neuronal death in patients with PD.

Figure 6-1. Model for HtrA2 function.

(A) A putative mitochondrial stress signalling pathway inherited from bacteria. Model for HtrA2 in a signalling pathway akin to bacterial DegS protease. **(B)** HtrA2 activity is necessary to decrease oxidative stress, and HtrA2 activity can be regulated by PINK1. Loss of HtrA2 would cause increased oxidative stress, leading to transcriptional up-regulation of CHOP, ATF3 and modulation of other genes. Increased expression of CHOP has been reported to contribute to enhanced cell death. Model akin to DegS: HtrA2 could be involved in a signalling cascade responsible for the expression of mitochondrial chaperones and proteases, thereby decreasing the load of unfolded proteins, preventing oxidative stress and cell death. Loss of HtrA2 would lead to accumulation of aberrant proteins, which could impair electron transport of the respiratory chain and cause oxidative stress. Model akin to DegP: HtrA2 could be responsible for degrading unfolded proteins, thereby preventing their accumulation which could lead to oxidative stress.

Figure 6-1

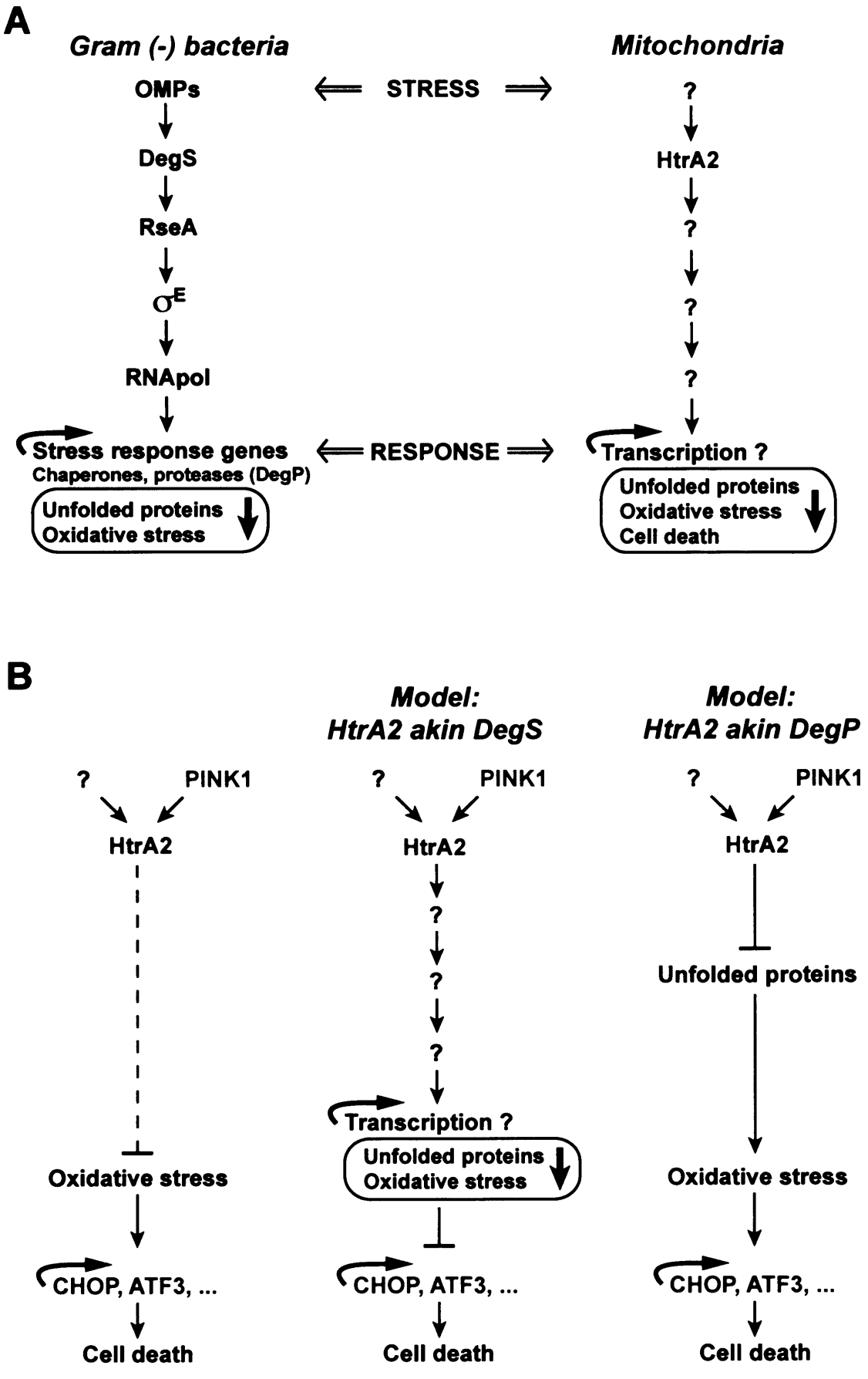
A
Gram (-) bacteria
Mitochondria
OMPs
STRESS
?
DegS
HtrA2
RseA
?
σE
?
RNApol
?
Stress response genes
Chaperones, proteases (DegP)
RESPONSE
Transcription ?
Unfolded proteins
Oxidative stress
Unfolded proteins
Oxidative stress
Cell death
B
Model:
HtrA2 akin DegS
Model:
HtrA2 akin DegP
? PINK1
HtrA2
Oxidative stress
CHOP, ATF3, ...
Cell death
? PINK1
HtrA2
?
?
?
Transcription ?
Unfolded proteins
Oxidative stress
CHOP, ATF3, ...
Cell death
? PINK1
HtrA2
Unfolded proteins
Oxidative stress
CHOP, ATF3, ...
Cell death

References

Abou-Sleiman, P. M., Muqit, M. M., McDonald, N. Q., Yang, Y. X., Gandhi, S., et al. (2006). "A heterozygous effect for PINK1 mutations in Parkinson's disease?" Ann Neurol **60**(4): 414-9.

Abrams, J. M. (1999). "An emerging blueprint for apoptosis in Drosophila." Trends Cell Biol **9**(11): 435-40.

Adams, J. M. and Cory, S. (1998). "The Bcl-2 protein family: arbiters of cell survival." Science **281**(5381): 1322-6.

Akao, Y., Otsuki, Y., Kataoka, S., Ito, Y. and Tsujimoto, Y. (1994). "Multiple subcellular localization of bcl-2: detection in nuclear outer membrane, endoplasmic reticulum membrane, and mitochondrial membranes." Cancer Res **54**(9): 2468-71.

Alba, B. M., Leeds, J. A., Onufryk, C., Lu, C. Z. and Gross, C. A. (2002). "DegS and YaeL participate sequentially in the cleavage of RseA to activate the sigma(E)-dependent extracytoplasmic stress response." Genes Dev **16**(16): 2156-68.

Andjelkovic, M., Jakubowicz, T., Cron, P., Ming, X. F., Han, J. W. and Hemmings, B. A. (1996). "Activation and phosphorylation of a pleckstrin homology domain containing protein kinase (RAC-PK/PKB) promoted by serum and protein phosphatase inhibitors." Proc Natl Acad Sci U S A **93**(12): 5699-704.

Arnoult, D., Gaume, B., Karbowski, M., Sharpe, J. C., Cecconi, F. and Youle, R. J. (2003). "Mitochondrial release of AIF and EndoG requires caspase activation downstream of Bax/Bak-mediated permeabilization." Embo J **22**(17): 4385-99.

Ashkenazi, A. and Dixit, V. M. (1998). "Death receptors: signaling and modulation." Science **281**(5381): 1305-8.

Barbosa-Tessmann, I. P., Chen, C., Zhong, C., Siu, F., Schuster, S. M., Nick, H. S. and Kilberg, M. S. (2000). "Activation of the human asparagine synthetase gene by the amino acid response and the endoplasmic reticulum stress response pathways occurs by common genomic elements." J Biol Chem **275**(35): 26976-85.

Barreto, G., Schafer, A., Marhold, J., Stach, D., Swaminathan, S. K., et al. (2007). "Gadd45a promotes epigenetic gene activation by repair-mediated DNA demethylation." Nature.

Beal, M. F. (2004). "Commentary on "Alpha-synuclein and mitochondria: a tangled skein"." Exp Neurol **186**(2): 109-11.

Beilina, A., Van Der Brug, M., Ahmad, R., Kesavapany, S., Miller, D. W., Petsko, G. A. and Cookson, M. R. (2005). "Mutations in PTEN-induced putative kinase 1 associated with recessive parkinsonism have differential effects on protein stability." Proc Natl Acad Sci U S A **102**(16): 5703-8.

Berlanga, J. J., Santoyo, J. and De Haro, C. (1999). "Characterization of a mammalian homolog of the GCN2 eukaryotic initiation factor 2alpha kinase." Eur J Biochem **265**(2): 754-62.

Berman, S. B. and Hastings, T. G. (1999). "Dopamine oxidation alters mitochondrial respiration and induces permeability transition in brain mitochondria: implications for Parkinson's disease." J Neurochem **73**(3): 1127-37.

Bernales, S., Papa, F. R. and Walter, P. (2006). "Intracellular signaling by the unfolded protein response." Annu Rev Cell Dev Biol **22**: 487-508.

Bernheimer, H., Birkmayer, W., Hornykiewicz, O., Jellinger, K. and Seitelberger, F. (1973). "Brain dopamine and the syndromes of Parkinson and Huntington. Clinical, morphological and neurochemical correlations." J Neurol Sci **20**(4): 415-55.

Bertolotti, A., Zhang, Y., Hendershot, L. M., Harding, H. P. and Ron, D. (2000). "Dynamic interaction of BiP and ER stress transducers in the unfolded-protein response." Nat Cell Biol

2(6): 326-32.

Betarbet, R., Sherer, T. B. and Greenamyre, J. T. (2002). "Animal models of Parkinson's disease." Bioessays **24**(4): 308-18.

Betarbet, R., Sherer, T. B., MacKenzie, G., Garcia-Osuna, M., Panov, A. V. and Greenamyre, J. T. (2000). "Chronic systemic pesticide exposure reproduces features of Parkinson's disease." Nat Neurosci **3**(12): 1301-6.

Bhuiyan, M. S. and Fukunaga, K. (2007). "Inhibition of HtrA2/Omi ameliorates heart dysfunction following ischemia/reperfusion injury in rat heart in vivo." Eur J Pharmacol **557**(2-3): 168-77.

Blink, E., Maianski, N. A., Alnemri, E. S., Zervos, A. S., Roos, D. and Kuijpers, T. W. (2004). "Intramitochondrial serine protease activity of Omi/HtrA2 is required for caspase-independent cell death of human neutrophils." Cell Death Differ **11**(8): 937-9.

Bonifati, V., Rizzu, P., van Baren, M. J., Schaap, O., Breedveld, G. J., et al. (2003). "Mutations in the DJ-1 gene associated with autosomal recessive early-onset parkinsonism." Science **299**(5604): 256-9.

Bonifati, V., Rohe, C. F., Breedveld, G. J., Fabrizio, E., De Mari, M., et al. (2005). "Early-onset parkinsonism associated with PINK1 mutations: frequency, genotypes, and phenotypes." Neurology **65**(1): 87-95.

Bove, J., Prou, D., Perier, C. and Przedborski, S. (2005). "Toxin-induced models of Parkinson's disease." NeuroRx **2**(3): 484-94.

Bradford, M. M. (1976). "A rapid and sensitive method for the quantitation of microgram quantities of protein utilizing the principle of protein-dye binding." Anal Biochem **72**: 248-54.

Bredesen, D. E., Rao, R. V. and Mehlen, P. (2006). "Cell death in the nervous system." Nature **443**(7113): 796-802.

Bump, N. J., Hackett, M., Hugunin, M., Seshagiri, S., Brady, K., et al. (1995). "Inhibition of ICE family proteases by baculovirus antiapoptotic protein p35." Science **269**(5232): 1885-8.

Butow, R. A. and Avadhani, N. G. (2004). "Mitochondrial signaling: the retrograde response." Mol Cell **14**(1): 1-15.

Cain, K., Brown, D. G., Langlais, C. and Cohen, G. M. (1999). "Caspase activation involves the formation of the aposome, a large (approximately 700 kDa) caspase-activating complex." J. Biol. Chem. **274**(32): 22686-22692.

Calfon, M., Zeng, H., Urano, F., Till, J. H., Hubbard, S. R., Harding, H. P., Clark, S. G. and Ron, D. (2002). "IRE1 couples endoplasmic reticulum load to secretory capacity by processing the XBP-1 mRNA." Nature **415**(6867): 92-6.

Chen, H., Pan, Y. X., Dudenhausen, E. E. and Kilberg, M. S. (2004). "Amino acid deprivation induces the transcription rate of the human asparagine synthetase gene through a timed program of expression and promoter binding of nutrient-responsive basic region/leucine zipper transcription factors as well as localized histone acetylation." J Biol Chem **279**(49): 50829-39.

Chen, J. J. and London, I. M. (1995). "Regulation of protein synthesis by heme-regulated eIF-2 alpha kinase." Trends Biochem Sci **20**(3): 105-8.

Chiesa, R., Piccardo, P., Ghetti, B. and Harris, D. A. (1998). "Neurological illness in transgenic mice expressing a prion protein with an insertional mutation." Neuron **21**(6): 1339-51.

Choi, W. S., Yoon, S. Y., Oh, T. H., Choi, E. J., O'Malley, K. L. and Oh, Y. J. (1999). "Two distinct mechanisms are involved in 6-hydroxydopamine- and MPP+-induced dopaminergic neuronal cell death: role of caspases, ROS, and JNK." J Neurosci Res **57**(1): 86-94.

Christich, A., Kauppila, S., Chen, P., Sogame, N., Ho, S. I. and Abrams, J. M. (2002). "The

damage-responsive Drosophila gene sickle encodes a novel IAP binding protein similar to but distinct from reaper, grim, and hid." Curr Biol **12**(2): 137-40.

Cilenti, L., Kyriazis, G. A., Soundarapandian, M. M., Stratico, V., Yerkes, A., et al. (2004). "Omi/HtrA2 protease mediates cisplatin-induced cell death in renal cells." Am J Physiol Renal Physiol.

Cilenti, L., Lee, Y., Hess, S., Srinivasula, S., Park, K. M., et al. (2003). "Characterization of a novel and specific inhibitor for the pro-apoptotic protease Omi/HtrA2." J Biol Chem **278**(13): 11489-94.

Cilenti, L., Soundarapandian, M. M., Kyriazis, G. A., Stratico, V., Singh, S., Gupta, S., Bonventre, J. V., Alnemri, E. S. and Zervos, A. S. (2004). "Regulation of HAX-1 anti-apoptotic protein by Omi/HtrA2 protease during cell death." J Biol Chem **279**(48): 50295-301.

Clark, I. E., Dodson, M. W., Jiang, C., Cao, J. H., Huh, J. R., Seol, J. H., Yoo, S. J., Hay, B. A. and Guo, M. (2006). "Drosophila pink1 is required for mitochondrial function and interacts genetically with parkin." Nature **441**(7097): 1162-6.

Clausen, T., Southan, C. and Ehrmann, M. (2002). "The HtrA family of proteases: implications for protein composition and cell fate." Mol Cell **10**(3): 443-55.

Clem, R. J., Fechheimer, M. and Miller, L. K. (1991). "Prevention of apoptosis by a baculovirus gene during infection of insect cells." Science **254**(5036): 1388-90.

Clemens, M. J. and Elia, A. (1997). "The double-stranded RNA-dependent protein kinase PKR: structure and function." J Interferon Cytokine Res **17**(9): 503-24.

Conway, K. A., Rochet, J. C., Bieganski, R. M. and Lansbury, P. T., Jr. (2001). "Kinetic stabilization of the alpha-synuclein protofibril by a dopamine-alpha-synuclein adduct." Science **294**(5545): 1346-9.

Cumming, G., Fidler, F. and Vaux, D. L. (2007). "Error bars in experimental biology." J Cell Biol **177**(1): 7-11.

da Cruz e Silva, O. A., Fardilha, M., Henriques, A. G., Rebelo, S., Vieira, S. and da Cruz e Silva, E. F. (2004). "Signal transduction therapeutics: relevance for Alzheimer's disease." J Mol Neurosci **23**(1-2): 123-42.

Darzynkiewicz, Z. and Bedner, E. (2000). "Analysis of apoptotic cells by flow and laser scanning cytometry." Methods Enzymol **322**: 18-39.

Deng, J., Harding, H. P., Raught, B., Gingras, A. C., Berlanga, J. J., Scheuner, D., Kaufman, R. J., Ron, D. and Sonenberg, N. (2002). "Activation of GCN2 in UV-irradiated cells inhibits translation." Curr Biol **12**(15): 1279-86.

Desagher, S. and Martinou, J. C. (2000). "Mitochondria as the central control point of apoptosis." Trends Cell Biol **10**(9): 369-77.

Deveraux, Q. L., Roy, N., Stennicke, H. R., Van Arsdale, T., Zhou, Q., Srinivasula, S. M., Alnemri, E. S., Salvesen, G. S. and Reed, J. C. (1998). "IAPs block apoptotic events induced by caspase-8 and cytochrome c by direct inhibition of distinct caspases." EMBO J. **17**(8): 2215-2223.

Deveraux, Q. L., Takahashi, R., Salvesen, G. S. and Reed, J. C. (1997). "X-linked IAP is a direct inhibitor of cell-death proteases." Nature **388**(6639): 300-4.

Dewan, A., Liu, M., Hartman, S., Zhang, S. S., Liu, D. T., et al. (2006). "HTRA1 promoter polymorphism in wet age-related macular degeneration." Science **314**(5801): 989-92.

Douette, P., Navet, R., Gerkens, P., de Pauw, E., Leprince, P., Sluse-Goffart, C. and Sluse, F. E. (2005). "Steatosis-induced proteomic changes in liver mitochondria evidenced by two-dimensional differential in-gel electrophoresis." J Proteome Res **4**(6): 2024-31.

Du, C., Fang, M., Li, Y., Li, L. and Wang, X. (2000). "Smac, a mitochondrial protein that promotes cytochrome c-dependent caspase activation by eliminating IAP inhibition." Cell **102**(1): 33-42.

Earnshaw, W. C., Martins, L. M. and Kaufmann, S. H. (1999). "Mammalian caspases: structure, activation, substrates, and functions during apoptosis." Annu Rev Biochem **68**: 383-424.

Eckelman, B. P., Salvesen, G. S. and Scott, F. L. (2006). "Human inhibitor of apoptosis proteins: why XIAP is the black sheep of the family." EMBO Rep **7**(10): 988-94.

Ekert, P. G., Silke, J., Hawkins, C. J., Verhagen, A. M. and Vaux, D. L. (2001). "DIABLO promotes apoptosis by removing MIHA/XIAP from processed caspase 9." J. Cell Biol. **152**(3): 483-490.

Ellis, H. M. and Horvitz, H. R. (1986). "Genetic control of programmed cell death in the nematode C. elegans." Cell **44**(6): 817-29.

Enari, M., Sakahira, H., Yokoyama, H., Okawa, K., Iwamatsu, A. and Nagata, S. (1998). "A caspase-activated DNase that degrades DNA during apoptosis, and its inhibitor ICAD." Nature **391**(6662): 43-50.

Erickson, J. W. and Gross, C. A. (1989). "Identification of the sigma E subunit of Escherichia coli RNA polymerase: a second alternate sigma factor involved in high-temperature gene expression." Genes Dev **3**(9): 1462-71.

Evan, G. I., Lewis, G. K., Ramsay, G. and Bishop, J. M. (1985). "Isolation of monoclonal antibodies specific for human c-myc proto-oncogene product." Mol Cell Biol **5**(12): 3610-6.

Faccio, L., Fusco, C., Chen, A., Martinotti, S., Bonventre, J. V. and Zervos, A. S. (2000). "Characterization of a novel human serine protease that has extensive homology to bacterial heat shock endoprotease HtrA and is regulated by kidney ischemia." J Biol Chem **275**(4): 2581-8.

Fahn, S. (2003). "Description of Parkinson's disease as a clinical syndrome." Ann N Y Acad Sci **991**: 1-14.

Farrer, M. J. (2006). "Genetics of Parkinson disease: paradigm shifts and future prospects." Nat Rev Genet **7**(4): 306-18.

Fawcett, T. W., Martindale, J. L., Guyton, K. Z., Hai, T. and Holbrook, N. J. (1999). "Complexes containing activating transcription factor (ATF)/cAMP-responsive-element-binding protein (CREB) interact with the CCAAT/enhancer-binding protein (C/EBP)-ATF composite site to regulate Gadd153 expression during the stress response." Biochem J **339 (Pt 1)**: 135-41.

Fleming, S. M., Fernagut, P. O. and Chesselet, M. F. (2005). "Genetic mouse models of parkinsonism: strengths and limitations." NeuroRx **2**(3): 495-503.

Fonck, C. and Baudry, M. (2001). "Toxic effects of MPP(+) and MPTP in PC12 cells independent of reactive oxygen species formation." Brain Res **905**(1-2): 199-206.

Gandhi, S., Muqit, M. M., Stanyer, L., Healy, D. G., Abou-Sleiman, P. M., et al. (2006). "PINK1 protein in normal human brain and Parkinson's disease." Brain **129**(Pt 7): 1720-31.

Gandhi, S. and Wood, N. W. (2005). "Molecular pathogenesis of Parkinson's disease." Hum Mol Genet **14**(18): 2749-55.

Garner, A. P., Weston, C. R., Todd, D. E., Balmanno, K. and Cook, S. J. (2002). "Delta MEKK3:ER* activation induces a p38 alpha/beta 2-dependent cell cycle arrest at the G2 checkpoint." Oncogene **21**(53): 8089-104.

Gasser, T., Muller-Myhsok, B., Wszolek, Z. K., Oehlmann, R., Calne, D. B., et al. (1998). "A susceptibility locus for Parkinson's disease maps to chromosome 2p13." Nat Genet **18**(3): 262-

5.

Gentleman, R. C., Carey, V. J., Bates, D. M., Bolstad, B., Dettling, M., et al. (2004). "Bioconductor: open software development for computational biology and bioinformatics." Genome Biol **5**(10): R80.

Ghadially, F. N. (1982). Ultrastructural Pathology of the Cell and Matrix, Butterworths.

Gloeckner, C. J., Kinkl, N., Schumacher, A., Braun, R. J., O'Neill, E., Meitinger, T., Kolch, W., Prokisch, H. and Ueffing, M. (2006). "The Parkinson disease causing LRRK2 mutation I2020T is associated with increased kinase activity." Hum Mol Genet **15**(2): 223-32.

Goffredo, D., Rigamonti, D., Zuccato, C., Tartari, M., Valenza, M. and Cattaneo, E. (2005). "Prevention of cytosolic IAPs degradation: a potential pharmacological target in Huntington's Disease." Pharmacol Res **52**(2): 140-50.

Gotoh, T., Oyadomari, S., Mori, K. and Mori, M. (2002). "Nitric oxide-induced apoptosis in RAW 264.7 macrophages is mediated by endoplasmic reticulum stress pathway involving ATF6 and CHOP." J Biol Chem **277**(14): 12343-50.

Goyal, L., McCall, K., Agapite, J., Hartwieg, E. and Steller, H. (2000). "Induction of apoptosis by Drosophila reaper, hid and grim through inhibition of IAP function." Embo J **19**(4): 589-97.

Gray, C. W., Ward, R. V., Karran, E., Turconi, S., Rowles, A., et al. (2000). "Characterization of human HtrA2, a novel serine protease involved in the mammalian cellular stress response." Eur J Biochem **267**(18): 5699-710.

Green, D. R. and Reed, J. C. (1998). "Mitochondria and apoptosis." Science **281**(5381): 1309-12.

Greene, J. C., Whitworth, A. J., Kuo, I., Andrews, L. A., Feany, M. B. and Pallanck, L. J. (2003). "Mitochondrial pathology and apoptotic muscle degeneration in Drosophila parkin mutants." Proc Natl Acad Sci U S A **100**(7): 4078-83.

Greene, J. G., Dingledine, R. and Greenamyre, J. T. (2005). "Gene expression profiling of rat midbrain dopamine neurons: implications for selective vulnerability in parkinsonism." Neurobiol Dis **18**(1): 19-31.

Gupta, S., Singh, R., Datta, P., Zhang, Z., Orr, C., et al. (2004). "The C-terminal tail of presenilin regulates Omi/HtrA2 protease activity." J Biol Chem **279**(44): 45844-54.

Guyton, K. Z., Xu, Q. and Holbrook, N. J. (1996). "Induction of the mammalian stress response gene GADD153 by oxidative stress: role of AP-1 element." Biochem J **314 (Pt 2)**: 547-54.

Hai, T. and Hartman, M. G. (2001). "The molecular biology and nomenclature of the activating transcription factor/cAMP responsive element binding family of transcription factors: activating transcription factor proteins and homeostasis." Gene **273**(1): 1-11.

Han, B. S., Noh, J. S., Gwag, B. J. and Oh, Y. J. (2003). "A distinct death mechanism is induced by 1-methyl-4-phenylpyridinium or by 6-hydroxydopamine in cultured rat cortical neurons: degradation and dephosphorylation of tau." Neurosci Lett **341**(2): 99-102.

Harding, H. P., Novoa, I., Zhang, Y., Zeng, H., Wek, R., Schapira, M. and Ron, D. (2000). "Regulated translation initiation controls stress-induced gene expression in mammalian cells." Mol Cell **6**(5): 1099-108.

Harding, H. P., Zhang, Y. and Ron, D. (1999). "Protein translation and folding are coupled by an endoplasmic-reticulum-resident kinase." Nature **397**(6716): 271-4.

Harding, H. P., Zhang, Y., Zeng, H., Novoa, I., Lu, P. D., et al. (2003). "An integrated stress response regulates amino acid metabolism and resistance to oxidative stress." Mol Cell **11**(3): 619-33.

Harlin, H., Reffey, S. B., Duckett, C. S., Lindsten, T. and Thompson, C. B. (2001).

"Characterization of XIAP-deficient mice." Mol Cell Biol **21**(10): 3604-8.

Hatano, Y., Li, Y., Sato, K., Asakawa, S., Yamamura, Y., et al. (2004). "Novel PINK1 mutations in early-onset parkinsonism." Ann Neurol **56**(3): 424-7.

Haze, K., Yoshida, H., Yanagi, H., Yura, T. and Mori, K. (1999). "Mammalian transcription factor ATF6 is synthesized as a transmembrane protein and activated by proteolysis in response to endoplasmic reticulum stress." Mol Biol Cell **10**(11): 3787-99.

Hegde, R., Srinivasula, S. M., Datta, P., Madesh, M., Wassell, R., et al. (2003). "The polypeptide chain-releasing factor GSPT1/eRF3 is proteolytically processed into an IAP-binding protein." J Biol Chem **278**(40): 38699-706.

Hegde, R., Srinivasula, S. M., Zhang, Z., Wassell, R., Mukattash, R., et al. (2002). "Identification of Omi/HtrA2 as a mitochondrial apoptotic serine protease that disrupts inhibitor of apoptosis protein-caspase interaction." J Biol Chem **277**(1): 432-8.

Henkel, C., Roderfeld, M., Weiskirchen, R., Berres, M. L., Hillebrandt, S., et al. (2006). "Changes of the hepatic proteome in murine models for toxically induced fibrogenesis and sclerosing cholangitis." Proteomics.

Higashitsuji, H., Higashitsuji, H., Nagao, T., Nonoguchi, K., Fujii, S., Itoh, K. and Fujita, J. (2002). "A novel protein overexpressed in hepatoma accelerates export of NF-kappa B from the nucleus and inhibits p53-dependent apoptosis." Cancer Cell **2**(4): 335-46.

Hogan, B., Beddington, R., Costantini, F. and Lacy, E. (1994). Manipulating the Mouse Embryo: A Laboratory Manual, Cold Spring Harbor Laboratory.

Holcik, M. and Sonenberg, N. (2005). "Translational control in stress and apoptosis." Nat Rev Mol Cell Biol **6**(4): 318-27.

Holtz, W. A. and O'Malley, K. L. (2003). "Parkinsonian mimetics induce aspects of unfolded protein response in death of dopaminergic neurons." J Biol Chem **278**(21): 19367-77.

Holtz, W. A., Turetzky, J. M., Jong, Y. J. and O'Malley, K. L. (2006). "Oxidative stress-triggered unfolded protein response is upstream of intrinsic cell death evoked by parkinsonian mimetics." J Neurochem **99**(1): 54-69.

Homburg, C. H., de Haas, M., von dem Borne, A. E., Verhoeven, A. J., Reutelingsperger, C. P. and Roos, D. (1995). "Human neutrophils lose their surface Fc gamma RIII and acquire Annexin V binding sites during apoptosis in vitro." Blood **85**(2): 532-40.

Hong, S. K., Cha, M. K. and Kim, I. H. (2006). "Specific protein interaction of human Pag with Omi/HtrA2 and the activation of the protease activity of Omi/HtrA2." Free Radic Biol Med **40**(2): 275-84.

Hu, S. I., Carozza, M., Klein, M., Nantermet, P., Luk, D. and Crowl, R. M. (1998). "Human HtrA, an evolutionarily conserved serine protease identified as a differentially expressed gene product in osteoarthritic cartilage." J Biol Chem **273**(51): 34406-12.

Huang, D. C. and Strasser, A. (2000). "BH3-Only proteins-essential initiators of apoptotic cell death." Cell **103**(6): 839-42.

Igney, F. H. and Krammer, P. H. (2002). "Death and anti-death: tumour resistance to apoptosis." Nat Rev Cancer **2**(4): 277-88.

Irizarry, R. A., Bolstad, B. M., Collin, F., Cope, L. M., Hobbs, B. and Speed, T. P. (2003). "Summaries of Affymetrix GeneChip probe level data." Nucleic Acids Res **31**(4): e15.

Jeon, B. S., Jackson-Lewis, V. and Burke, R. E. (1995). "6-Hydroxydopamine lesion of the rat substantia nigra: time course and morphology of cell death." Neurodegeneration **4**(2): 131-7.

Jiang, H. Y. and Wek, R. C. (2005). "Phosphorylation of the alpha-subunit of the eukaryotic initiation factor-2 (eIF2alpha) reduces protein synthesis and enhances apoptosis in response to

proteasome inhibition." J Biol Chem **280**(14): 14189-202.

Jiang, H. Y., Wek, S. A., McGrath, B. C., Lu, D., Hai, T., et al. (2004). "Activating transcription factor 3 is integral to the eukaryotic initiation factor 2 kinase stress response." Mol Cell Biol **24**(3): 1365-77.

Jones, C. H., Dexter, P., Evans, A. K., Liu, C., Hultgren, S. J. and Hruby, D. E. (2002). "Escherichia coli DegP protease cleaves between paired hydrophobic residues in a natural substrate: the PapA pilin." J Bacteriol **184**(20): 5762-71.

Jones, J. M., Albin, R. L., Feldman, E. L., Simin, K., Schuster, T. G., et al. (1993). "mnd2: a new mouse model of inherited motor neuron disease." Genomics **16**(3): 669-77.

Jones, J. M., Datta, P., Srinivasula, S. M., Ji, W., Gupta, S., et al. (2003). "Loss of Omi mitochondrial protease activity causes the neuromuscular disorder of mnd2 mutant mice." Nature **425**(6959): 721-7.

Joyner, A. L. (1999). Gene targeting: a practical approach, Oxford University Press.

Joza, N., Susin, S. A., Daugas, E., Stanford, W. L., Cho, S. K., et al. (2001). "Essential role of the mitochondrial apoptosis-inducing factor in programmed cell death." Nature **410**(6828): 549-54.

Kanehara, K., Ito, K. and Akiyama, Y. (2002). "YaeL (EcfE) activates the sigma(E) pathway of stress response through a site-2 cleavage of anti-sigma(E), RseA." Genes Dev **16**(16): 2147-55.

Kawahara, K., Oyadomari, S., Gotoh, T., Kohsaka, S., Nakayama, H. and Mori, M. (2001). "Induction of CHOP and apoptosis by nitric oxide in p53-deficient microglial cells." FEBS Lett **506**(2): 135-9.

Kerr, J. F., Wyllie, A. H. and Currie, A. R. (1972). "Apoptosis: a basic biological phenomenon with wide-ranging implications in tissue kinetics." Br J Cancer **26**(4): 239-57.

Khan, N. L., Valente, E. M., Bentivoglio, A. R., Wood, N. W., Albanese, A., Brooks, D. J. and Piccini, P. (2002). "Clinical and subclinical dopaminergic dysfunction in PARK6-linked parkinsonism: an 18F-dopa PET study." Ann Neurol **52**(6): 849-53.

Kim, D. Y., Kim, D. R., Ha, S. C., Lokanath, N. K., Lee, C. J., Hwang, H. Y. and Kim, K. K. (2003). "Crystal structure of the protease domain of a heat-shock protein HtrA from Thermotoga maritima." J Biol Chem **278**(8): 6543-51.

Kim, R. H., Smith, P. D., Aleyasin, H., Hayley, S., Mount, M. P., et al. (2005). "Hypersensitivity of DJ-1-deficient mice to 1-methyl-4-phenyl-1,2,3,6-tetrahydropyrindine (MPTP) and oxidative stress." Proc Natl Acad Sci U S A **102**(14): 5215-20.

Klages, N., Zufferey, R. and Trono, D. (2000). "A stable system for the high-titer production of multiply attenuated lentiviral vectors." Mol Ther **2**(2): 170-6.

Klein, C., Grudzien, M., Appaswamy, G., Germeshausen, M., Sandrock, I., et al. (2007). "HAX1 deficiency causes autosomal recessive severe congenital neutropenia (Kostmann disease)." Nat Genet **39**(1): 86-92.

Klein, J. A., Longo-Guess, C. M., Rossmann, M. P., Seburn, K. L., Hurd, R. E., Frankel, W. N., Bronson, R. T. and Ackerman, S. L. (2002). "The harlequin mouse mutation downregulates apoptosis-inducing factor." Nature **419**(6905): 367-74.

Klupsch, K. and Downward, J. (2006). "The protease inhibitor Ucf-101 induces cellular responses independently of its known target, HtrA2/Omi." Cell Death Differ **13**(12): 2157-9.

Kohn, A. D., Summers, S. A., Birnbaum, M. J. and Roth, R. A. (1996). "Expression of a constitutively active Akt Ser/Thr kinase in 3T3-L1 adipocytes stimulates glucose uptake and glucose transporter 4 translocation." J Biol Chem **271**(49): 31372-8.

Kokame, K., Kato, H. and Miyata, T. (2001). "Identification of ERSE-II, a new cis-acting

element responsible for the ATF6-dependent mammalian unfolded protein response." J Biol Chem **276**(12): 9199-205.

Kolmar, H., Waller, P. R. and Sauer, R. T. (1996). "The DegP and DegQ periplasmic endoproteases of Escherichia coli: specificity for cleavage sites and substrate conformation." J Bacteriol **178**(20): 5925-9.

Krajewski, S., Tanaka, S., Takayama, S., Schibler, M. J., Fenton, W. and Reed, J. C. (1993). "Investigation of the subcellular distribution of the bcl-2 oncoprotein: residence in the nuclear envelope, endoplasmic reticulum, and outer mitochondrial membranes." Cancer Res **53**(19): 4701-14.

Krojer, T., Garrido-Franco, M., Huber, R., Ehrmann, M. and Clausen, T. (2002). "Crystal structure of DegP (HtrA) reveals a new protease-chaperone machine." Nature **416**(6879): 455-459.

Kultz, D., Madhany, S. and Burg, M. B. (1998). "Hyperosmolality causes growth arrest of murine kidney cells. Induction of GADD45 and GADD153 by osmosensing via stress-activated protein kinase 2." J Biol Chem **273**(22): 13645-51.

Kuma, Y., Sabio, G., Bain, J., Shpiro, N., Marquez, R. and Cuenda, A. (2005). "BIRB796 inhibits all p38 MAPK isoforms in vitro and in vivo." J Biol Chem **280**(20): 19472-9.

Kuninaka, S., Iida, S. I., Hara, T., Nomura, M., Naoe, H., et al. (2006). "Serine protease Omi/HtrA2 targets WARTS kinase to control cell proliferation." Oncogene.

Kuninaka, S., Nomura, M., Hirota, T., Iida, S., Hara, T., et al. (2005). "The tumor suppressor WARTS activates the Omi / HtrA2-dependent pathway of cell death." Oncogene **24**(34): 5287-98.

Langston, J. W., Ballard, P., Tetrud, J. W. and Irwin, I. (1983). "Chronic Parkinsonism in humans due to a product of meperidine-analog synthesis." Science **219**(4587): 979-80.

Lashuel, H. A., Hartley, D., Petre, B. M., Walz, T. and Lansbury, P. T., Jr. (2002). "Neurodegenerative disease: amyloid pores from pathogenic mutations." Nature **418**(6895): 291.

Lassot, I., Segeral, E., Berlioz-Torrent, C., Durand, H., Groussin, L., Hai, T., Benarous, R. and Margottin-Goguet, F. (2001). "ATF4 degradation relies on a phosphorylation-dependent interaction with the SCF(betaTrCP) ubiquitin ligase." Mol Cell Biol **21**(6): 2192-202.

Lee, D. H., Han, Y. S., Han, E. S., Bang, H. and Lee, C. S. (2006). "Differential involvement of intracellular Ca2+ in 1-methyl-4-phenylpyridinium- or 6-hydroxydopamine-induced cell viability loss in PC12 cells." Neurochem Res **31**(7): 851-60.

Lehr, S., Kotzka, J., Avci, H., Knebel, B., Muller, S., et al. (2005). "Effect of sterol regulatory element binding protein-1a on the mitochondrial protein pattern in human liver cells detected by 2D-DIGE." Biochemistry **44**(13): 5117-28.

Leroy, E., Anastasopoulos, D., Konitsiotis, S., Lavedan, C. and Polymeropoulos, M. H. (1998). "Deletions in the Parkin gene and genetic heterogeneity in a Greek family with early onset Parkinson's disease." Hum Genet **103**(4): 424-7.

Li, L. Y., Luo, X. and Wang, X. (2001). "Endonuclease G is an apoptotic DNase when released from mitochondria." Nature **412**(6842): 95-9.

Li, P., Nijhawan, D., Budihardjo, I., Srinivasula, S. M., Ahmad, M., Alnemri, E. S. and Wang, X. (1997). "Cytochrome c and dATP-dependent formation of Apaf-1/caspase-9 complex initiates an apoptotic protease cascade." Cell **91**(4): 479-89.

Li, W., Srinivasula, S. M., Chai, J., Li, P., Wu, J. W., Zhang, Z., Alnemri, E. S. and Shi, Y. (2002). "Structural insights into the pro-apoptotic function of mitochondrial serine protease HtrA2/Omi." Nat Struct Biol **9**(6): 436-41.

Li, Y., Tomiyama, H., Sato, K., Hatano, Y., Yoshino, H., et al. (2005). "Clinicogenetic study of PINK1 mutations in autosomal recessive early-onset parkinsonism." Neurology **64**(11): 1955-7.

Liang, G., Wolfgang, C. D., Chen, B. P., Chen, T. H. and Hai, T. (1996). "ATF3 gene. Genomic organization, promoter, and regulation." J Biol Chem **271**(3): 1695-701.

Liao, D. I., Qian, J., Chisholm, D. A., Jordan, D. B. and Diner, B. A. (2000). "Crystal structures of the photosystem II D1 C-terminal processing protease." Nat Struct Biol **7**(9): 749-53.

Liu, H. R., Gao, E., Hu, A., Tao, L., Qu, Y., et al. (2005). "Role of Omi/HtrA2 in apoptotic cell death after myocardial ischemia and reperfusion." Circulation **111**(1): 90-6.

Liu, M. L., Liu, M. J., Kim, J. M., Kim, H. J., Kim, J. H. and Hong, S. T. (2005). "HtrA2 interacts with A beta peptide but does not directly alter its production or degradation." Mol Cells **20**(1): 83-9.

Liu, X., Zou, H., Slaughter, C. and Wang, X. (1997). "DFF, a heterodimeric protein that functions downstream of caspase-3 to trigger DNA fragmentation during apoptosis." Cell **89**(2): 175-84.

Livak, K. J. and Schmittgen, T. D. (2001). "Analysis of relative gene expression data using real-time quantitative PCR and the 2(-Delta Delta C(T)) Method." Methods **25**(4): 402-8.

Lopez, A. B., Wang, C., Huang, C. C., Yaman, I., Li, Y., et al. (2007). "A feedback transcriptional mechanism controls the level of the arginine/lysine transporter cat-1 during amino acid starvation." Biochem J **402**(1): 163-73.

Lotharius, J. and Brundin, P. (2002). "Pathogenesis of Parkinson's disease: dopamine, vesicles and alpha-synuclein." Nat Rev Neurosci **3**(12): 932-42.

Lotharius, J., Dugan, L. L. and O'Malley, K. L. (1999). "Distinct mechanisms underlie neurotoxin-mediated cell death in cultured dopaminergic neurons." J Neurosci **19**(4): 1284-93.

Lu, D., Chen, J. and Hai, T. (2007). "The regulation of ATF3 gene expression by mitogen-activated protein kinases." Biochem J **401**(2): 559-67.

Lu, L., Han, A. P. and Chen, J. J. (2001). "Translation initiation control by heme-regulated eukaryotic initiation factor 2alpha kinase in erythroid cells under cytoplasmic stresses." Mol Cell Biol **21**(23): 7971-80.

Ma, Y., Brewer, J. W., Diehl, J. A. and Hendershot, L. M. (2002). "Two distinct stress signaling pathways converge upon the CHOP promoter during the mammalian unfolded protein response." J Mol Biol **318**(5): 1351-65.

Ma, Y. and Hendershot, L. M. (2004). "Herp is dually regulated by both the endoplasmic reticulum stress-specific branch of the unfolded protein response and a branch that is shared with other cellular stress pathways." J Biol Chem **279**(14): 13792-9.

Marten, N. W., Burke, E. J., Hayden, J. M. and Straus, D. S. (1994). "Effect of amino acid limitation on the expression of 19 genes in rat hepatoma cells." Faseb J **8**(8): 538-44.

Martin, S. J., Reutelingsperger, C. P., McGahon, A. J., Rader, J. A., van Schie, R. C., LaFace, D. M. and Green, D. R. (1995). "Early redistribution of plasma membrane phosphatidylserine is a general feature of apoptosis regardless of the initiating stimulus: inhibition by overexpression of Bcl-2 and Abl." J Exp Med **182**(5): 1545-56.

Martins, L. M., Iaccarino, I., Tenev, T., Gschmeissner, S., Totty, N. F., et al. (2002). "The serine protease Omi/HtrA2 regulates apoptosis by binding XIAP through a reaper-like motif." J Biol Chem **277**(1): 439-44.

Martins, L. M., Morrison, A., Klupsch, K., Fedele, V., Moisoi, N., et al. (2004). "Neuroprotective role of the Reaper-related serine protease HtrA2/Omi revealed by targeted

deletion in mice." Mol Cell Biol **24**(22): 9848-62.

Martins, L. M., Turk, B. E., Cowling, V., Borg, A., Jarrell, E. T., Cantley, L. C. and Downward, J. (2003). "Binding specificity and regulation of the serine protease and PDZ domains of HtrA2/Omi." J Biol Chem **278**(49): 49417-27.

Matsumoto, M., Minami, M., Takeda, K., Sakao, Y. and Akira, S. (1996). "Ectopic expression of CHOP (GADD153) induces apoptosis in M1 myeloblastic leukemia cells." FEBS Lett **395**(2-3): 143-7.

Maytin, E. V., Ubeda, M., Lin, J. C. and Habener, J. F. (2001). "Stress-inducible transcription factor CHOP/gadd153 induces apoptosis in mammalian cells via p38 kinase-dependent and -independent mechanisms." Exp Cell Res **267**(2): 193-204.

Mazzio, E. and Soliman, K. F. (2003). "Pyruvic acid cytoprotection against 1-methyl-4-phenylpyridinium, 6-hydroxydopamine and hydrogen peroxide toxicities in vitro." Neurosci Lett **337**(2): 77-80.

Meier, P., Finch, A. and Evan, G. (2000). "Apoptosis in development." Nature **407**(6805): 796-801.

Mengesdorf, T., Althausen, S. and Paschen, W. (2002). "Genes associated with pro-apoptotic and protective mechanisms are affected differently on exposure of neuronal cell cultures to arsenite. No indication for endoplasmic reticulum stress despite activation of grp78 and gadd153 expression." Brain Res Mol Brain Res **104**(2): 227-39.

Meyer, T. E. and Habener, J. F. (1993). "Cyclic adenosine 3',5'-monophosphate response element binding protein (CREB) and related transcription-activating deoxyribonucleic acid-binding proteins." Endocr Rev **14**(3): 269-90.

Molina-Jimenez, M. F., Sanchez-Reus, M. I., Andres, D., Cascales, M. and Benedi, J. (2004). "Neuroprotective effect of fraxetin and myricetin against rotenone-induced apoptosis in neuroblastoma cells." Brain Res **1009**(1-2): 9-16.

Moore, D. J., West, A. B., Dawson, V. L. and Dawson, T. M. (2005). "Molecular pathophysiology of Parkinson's disease." Annu Rev Neurosci **28**: 57-87.

Moriishi, K., Huang, D. C., Cory, S. and Adams, J. M. (1999). "Bcl-2 family members do not inhibit apoptosis by binding the caspase activator Apaf-1." Proc Natl Acad Sci U S A **96**(17): 9683-8.

Nakajima, A., Kataoka, K., Hong, M., Sakaguchi, M. and Huh, N. H. (2003). "BRPK, a novel protein kinase showing increased expression in mouse cancer cell lines with higher metastatic potential." Cancer Lett **201**(2): 195-201.

Nicklas, W. J., Vyas, I. and Heikkila, R. E. (1985). "Inhibition of NADH-linked oxidation in brain mitochondria by 1-methyl-4-phenyl-pyridine, a metabolite of the neurotoxin, 1-methyl-4-phenyl-1,2,5,6-tetrahydropyridine." Life Sci **36**(26): 2503-8.

Nie, G. Y., Hampton, A., Li, Y., Findlay, J. K. and Salamonsen, L. A. (2003). "Identification and cloning of two isoforms of human high-temperature requirement factor A3 (HtrA3), characterization of its genomic structure and comparison of its tissue distribution with HtrA1 and HtrA2." Biochem J **371**(Pt 1): 39-48.

Obenauer, J. C., Cantley, L. C. and Yaffe, M. B. (2003). "Scansite 2.0: Proteome-wide prediction of cell signaling interactions using short sequence motifs." Nucleic Acids Res **31**(13): 3635-41.

Ohoka, N., Yoshii, S., Hattori, T., Onozaki, K. and Hayashi, H. (2005). "TRB3, a novel ER stress-inducible gene, is induced via ATF4-CHOP pathway and is involved in cell death." Embo J **24**(6): 1243-55.

Okada, H., Suh, W. K., Jin, J., Woo, M., Du, C., et al. (2002). "Generation and characterization

of Smac/DIABLO-deficient mice." Mol Cell Biol **22**(10): 3509-17.

Orth, M. and Schapira, A. H. (2002). "Mitochondrial involvement in Parkinson's disease." Neurochem Int **40**(6): 533-41.

Oyadomari, S. and Mori, M. (2004). "Roles of CHOP/GADD153 in endoplasmic reticulum stress." Cell Death Differ **11**(4): 381-389.

Palacino, J. J., Sagi, D., Goldberg, M. S., Krauss, S., Motz, C., Wacker, M., Klose, J. and Shen, J. (2004). "Mitochondrial dysfunction and oxidative damage in parkin-deficient mice." J Biol Chem **279**(18): 18614-22.

Pallen, M. J. and Wren, B. W. (1997). "The HtrA family of serine proteases." Mol Microbiol **26**(2): 209-21.

Pan, Y. X., Chen, H., Thiaville, M. M. and Kilberg, M. S. (2007). "Activation of the ATF3 gene through a co-ordinated amino acid-sensing response programme that controls transcriptional regulation of responsive genes following amino acid limitation." Biochem J **401**(1): 299-307.

Papapetropoulos, S. and McCorquodale, D. (2007). "Gene-expression profiling in Parkinson’s disease: discovery of valid biomarkers, molecular targets and biochemical pathways." Future Neurology **2**(1): 29-38.

Park, H. J., Kim, S. S., Seong, Y. M., Kim, K. H., Goo, H. G., Yoon, E. J., Min do, S., Kang, S. and Rhim, H. (2006). "Beta-amyloid precursor protein is a direct cleavage target of HtrA2 serine protease. Implications for the physiological function of HtrA2 in the mitochondria." J Biol Chem **281**(45): 34277-87.

Park, H. J., Seong, Y. M., Choi, J. Y., Kang, S. and Rhim, H. (2004). "Alzheimer's disease-associated amyloid beta interacts with the human serine protease HtrA2/Omi." Neurosci Lett **357**(1): 63-7.

Park, J., Lee, S. B., Lee, S., Kim, Y., Song, S., et al. (2006). "Mitochondrial dysfunction in Drosophila PINK1 mutants is complemented by parkin." Nature **441**(7097): 1157-61.

Park, S. W., Kim, S. H., Park, K. H., Kim, S. D., Kim, J. Y., Baek, S. Y., Chung, B. S. and Kang, C. D. (2004). "Preventive effect of antioxidants in MPTP-induced mouse model of Parkinson's disease." Neurosci Lett **363**(3): 243-6.

Pedersen, L. L., Radulic, M., Doric, M. and Abu Kwaik, Y. (2001). "HtrA homologue of Legionella pneumophila: an indispensable element for intracellular infection of mammalian but not protozoan cells." Infect Immun **69**(4): 2569-79.

Petit, A., Kawarai, T., Paitel, E., Sanjo, N., Maj, M., et al. (2005). "Wild-type PINK1 prevents basal and induced neuronal apoptosis, a protective effect abrogated by Parkinson disease-related mutations." J Biol Chem **280**(40): 34025-32.

Porter, N. A., Caldwell, S. E. and Mills, K. A. (1995). "Mechanisms of free radical oxidation of unsaturated lipids." Lipids **30**(4): 277-90.

Price, B. D. and Calderwood, S. K. (1992). "Gadd45 and Gadd153 messenger RNA levels are increased during hypoxia and after exposure of cells to agents which elevate the levels of the glucose-regulated proteins." Cancer Res **52**(13): 3814-7.

Raivio, T. L. (2005). "Envelope stress responses and Gram-negative bacterial pathogenesis." Mol Microbiol **56**(5): 1119-28.

Ramirez, A., Heimbach, A., Grundemann, J., Stiller, B., Hampshire, D., et al. (2006). "Hereditary parkinsonism with dementia is caused by mutations in ATP13A2, encoding a lysosomal type 5 P-type ATPase." Nat Genet **38**(10): 1184-91.

Rao, L., Perez, D. and White, E. (1996). "Lamin proteolysis facilitates nuclear events during

apoptosis." J Cell Biol **135**(6 Pt 1): 1441-55.

Rigaut, G., Shevchenko, A., Rutz, B., Wilm, M., Mann, M. and Seraphin, B. (1999). "A generic protein purification method for protein complex characterization and proteome exploration." Nat. Biotechnol. **17**(10): 1030-1032.

Rogaeva, E., Johnson, J., Lang, A. E., Gulick, C., Gwinn-Hardy, K., et al. (2004). "Analysis of the PINK1 gene in a large cohort of cases with Parkinson disease." Arch Neurol **61**(12): 1898-904.

Rohe, C. F., Montagna, P., Breedveld, G., Cortelli, P., Oostra, B. A. and Bonifati, V. (2004). "Homozygous PINK1 C-terminus mutation causing early-onset parkinsonism." Ann Neurol **56**(3): 427-31.

Ron, D. and Habener, J. F. (1992). "CHOP, a novel developmentally regulated nuclear protein that dimerizes with transcription factors C/EBP and LAP and functions as a dominant-negative inhibitor of gene transcription." Genes Dev **6**(3): 439-53.

Rytomaa, M., Lehmann, K. and Downward, J. (2000). "Matrix detachment induces caspase-dependent cytochrome c release from mitochondria: inhibition by PKB/Akt but not Raf signalling." Oncogene **19**(39): 4461-8.

Ryu, E. J., Harding, H. P., Angelastro, J. M., Vitolo, O. V., Ron, D. and Greene, L. A. (2002). "Endoplasmic reticulum stress and the unfolded protein response in cellular models of Parkinson's disease." J Neurosci **22**(24): 10690-8.

Sakai, J., Duncan, E. A., Rawson, R. B., Hua, X., Brown, M. S. and Goldstein, J. L. (1996). "Sterol-regulated release of SREBP-2 from cell membranes requires two sequential cleavages, one within a transmembrane segment." Cell **85**(7): 1037-46.

Sakai, J., Rawson, R. B., Espenshade, P. J., Cheng, D., Seegmiller, A. C., Goldstein, J. L. and Brown, M. S. (1998). "Molecular identification of the sterol-regulated luminal protease that cleaves SREBPs and controls lipid composition of animal cells." Mol Cell **2**(4): 505-14.

Salvesen, G. S. and Duckett, C. S. (2002). "IAP proteins: blocking the road to death's door." Nat Rev Mol Cell Biol **3**(6): 401-10.

Sandra, F., Degli Esposti, M., Ndebele, K., Gona, P., Knight, D., Rosenquist, M. and Khosravi-Far, R. (2005). "Tumor necrosis factor-related apoptosis-inducing ligand alters mitochondrial membrane lipids." Cancer Res **65**(18): 8286-97.

Schaefer, M. L., Wong, S. T., Wozniak, D. F., Muglia, L. M., Liauw, J. A., et al. (2000). "Altered stress-induced anxiety in adenylyl cyclase type VIII-deficient mice." J Neurosci **20**(13): 4809-20.

Schapira, A. H. (2006). "Mitochondrial disease." Lancet **368**(9529): 70-82.

Schapira, A. H., Cooper, J. M., Dexter, D., Clark, J. B., Jenner, P. and Marsden, C. D. (1990). "Mitochondrial complex I deficiency in Parkinson's disease." J Neurochem **54**(3): 823-7.

Schapira, A. H., Cooper, J. M., Dexter, D., Jenner, P., Clark, J. B. and Marsden, C. D. (1989). "Mitochondrial complex I deficiency in Parkinson's disease." Lancet **1**(8649): 1269.

Schlieker, C., Mogk, A. and Bukau, B. (2004). "A PDZ switch for a cellular stress response." Cell **117**(4): 417-9.

Schultheis, P. J., Hagen, T. T., O'Toole, K. K., Tachibana, A., Burke, C. R., McGill, D. L., Okunade, G. W. and Shull, G. E. (2004). "Characterization of the P5 subfamily of P-type transport ATPases in mice." Biochem Biophys Res Commun **323**(3): 731-8.

Sedelis, M., Schwarting, R. K. and Huston, J. P. (2001). "Behavioral phenotyping of the MPTP mouse model of Parkinson's disease." Behav Brain Res **125**(1-2): 109-25.

Sekine, K., Hao, Y., Suzuki, Y., Takahashi, R., Tsuruo, T. and Naito, M. (2005). "HtrA2

cleaves Apollon and induces cell death by IAP-binding motif in Apollon-deficient cells." Biochem Biophys Res Commun **330**(1): 279-85.

Seong, Y. M., Choi, J. Y., Park, H. J., Kim, K. J., Ahn, S. G., Seong, G. H., Kim, I. K., Kang, S. and Rhim, H. (2004). "Autocatalytic processing of HtrA2/Omi is essential for induction of caspase-dependent cell death through antagonizing XIAP." J Biol Chem **279**(36): 37588-96.

Shamoto-Nagai, M., Maruyama, W., Kato, Y., Isobe, K., Tanaka, M., Naoi, M. and Osawa, T. (2003). "An inhibitor of mitochondrial complex I, rotenone, inactivates proteasome by oxidative modification and induces aggregation of oxidized proteins in SH-SY5Y cells." J Neurosci Res **74**(4): 589-97.

Sharp, T. V., Wang, H. W., Koumi, A., Hollyman, D., Endo, Y., Ye, H., Du, M. Q. and Boshoff, C. (2002). "K15 protein of Kaposi's sarcoma-associated herpesvirus is latently expressed and binds to HAX-1, a protein with antiapoptotic function." J Virol **76**(2): 802-16.

Shen, J., Chen, X., Hendershot, L. and Prywes, R. (2002). "ER stress regulation of ATF6 localization by dissociation of BiP/GRP78 binding and unmasking of Golgi localization signals." Dev Cell **3**(1): 99-111.

Shen, X., Ellis, R. E., Lee, K., Liu, C. Y., Yang, K., et al. (2001). "Complementary signaling pathways regulate the unfolded protein response and are required for C. elegans development." Cell **107**(7): 893-903.

Sherer, T. B., Betarbet, R., Stout, A. K., Lund, S., Baptista, M., Panov, A. V., Cookson, M. R. and Greenamyre, J. T. (2002). "An in vitro model of Parkinson's disease: linking mitochondrial impairment to altered alpha-synuclein metabolism and oxidative damage." J Neurosci **22**(16): 7006-15.

Sherer, T. B., Kim, J. H., Betarbet, R. and Greenamyre, J. T. (2003). "Subcutaneous rotenone exposure causes highly selective dopaminergic degeneration and alpha-synuclein aggregation." Exp Neurol **179**(1): 9-16.

Shevchenko, A., Wilm, M., Vorm, O. and Mann, M. (1996). "Mass spectrometric sequencing of proteins silver-stained polyacrylamide gels." Anal Chem **68**(5): 850-8.

Shi, Y., Vattem, K. M., Sood, R., An, J., Liang, J., Stramm, L. and Wek, R. C. (1998). "Identification and characterization of pancreatic eukaryotic initiation factor 2 alpha-subunit kinase, PEK, involved in translational control." Mol Cell Biol **18**(12): 7499-509.

Shiozaki, E. N., Chai, J., Rigotti, D. J., Riedl, S. J., Li, P., Srinivasula, S. M., Alnemri, E. S., Fairman, R. and Shi, Y. (2003). "Mechanism of XIAP-mediated inhibition of caspase-9." Mol Cell **11**(2): 519-27.

Sidhu, A., Wersinger, C., Moussa, C. E. and Vernier, P. (2004). "The role of alpha-synuclein in both neuroprotection and neurodegeneration." Ann N Y Acad Sci **1035**: 250-70.

Silva, R. M., Ries, V., Oo, T. F., Yarygina, O., Jackson-Lewis, V., et al. (2005). "CHOP/GADD153 is a mediator of apoptotic death in substantia nigra dopamine neurons in an in vivo neurotoxin model of parkinsonism." J Neurochem **95**(4): 974-86.

Silvestri, L., Caputo, V., Bellacchio, E., Atorino, L., Dallapiccola, B., Valente, E. M. and Casari, G. (2005). "Mitochondrial import and enzymatic activity of PINK1 mutants associated to recessive parkinsonism." Hum Mol Genet **14**(22): 3477-92.

Sim, C. H., Lio, D. S., Mok, S. S., Masters, C. L., Hill, A. F., Culvenor, J. G. and Cheng, H. C. (2006). "C-terminal truncation and Parkinson's disease-associated mutations down-regulate the protein serine/threonine kinase activity of PTEN-induced kinase-1." Hum Mol Genet.

Siu, F., Bain, P. J., LeBlanc-Chaffin, R., Chen, H. and Kilberg, M. S. (2002). "ATF4 is a mediator of the nutrient-sensing response pathway that activates the human asparagine synthetase gene." J Biol Chem **277**(27): 24120-7.

Smith, W. W., Pei, Z., Jiang, H., Moore, D. J., Liang, Y., West, A. B., Dawson, V. L., Dawson, T. M. and Ross, C. A. (2005). "Leucine-rich repeat kinase 2 (LRRK2) interacts with parkin, and mutant LRRK2 induces neuronal degeneration." Proc Natl Acad Sci U S A **102**(51): 18676-81.

Sok, J., Wang, X. Z., Batchvarova, N., Kuroda, M., Harding, H. and Ron, D. (1999). "CHOP-Dependent stress-inducible expression of a novel form of carbonic anhydrase VI." Mol Cell Biol **19**(1): 495-504.

Song, D. D., Shults, C. W., Sisk, A., Rockenstein, E. and Masliah, E. (2004). "Enhanced substantia nigra mitochondrial pathology in human alpha-synuclein transgenic mice after treatment with MPTP." Exp Neurol **186**(2): 158-72.

Sood, R., Porter, A. C., Olsen, D. A., Cavener, D. R. and Wek, R. C. (2000). "A mammalian homologue of GCN2 protein kinase important for translational control by phosphorylation of eukaryotic initiation factor-2alpha." Genetics **154**(2): 787-801.

Sorice, M., Circella, A., Cristea, I. M., Garofalo, T., Di Renzo, L., Alessandri, C., Valesini, G. and Esposti, M. D. (2004). "Cardiolipin and its metabolites move from mitochondria to other cellular membranes during death receptor-mediated apoptosis." Cell Death Differ **11**(10): 1133-45.

Spiess, C., Beil, A. and Ehrmann, M. (1999). "A temperature-dependent switch from chaperone to protease in a widely conserved heat shock protein." Cell **97**(3): 339-47.

Spillantini, M. G., Crowther, R. A., Jakes, R., Hasegawa, M. and Goedert, M. (1998). "alpha-Synuclein in filamentous inclusions of Lewy bodies from Parkinson's disease and dementia with lewy bodies." Proc Natl Acad Sci U S A **95**(11): 6469-73.

Srinivasula, S. M., Datta, P., Kobayashi, M., Wu, J. W., Fujioka, M., et al. (2002). "sickle, a novel Drosophila death gene in the reaper/hid/grim region, encodes an IAP-inhibitory protein." Curr Biol **12**(2): 125-30.

Srinivasula, S. M., Gupta, S., Datta, P., Zhang, Z., Hegde, R., Cheong, N., Fernandes-Alnemri, T. and Alnemri, E. S. (2003). "Inhibitor of apoptosis proteins are substrates for the mitochondrial serine protease Omi/HtrA2." J Biol Chem.

Storch, A., Kaftan, A., Burkhardt, K. and Schwarz, J. (2000). "6-Hydroxydopamine toxicity towards human SH-SY5Y dopaminergic neuroblastoma cells: independent of mitochondrial energy metabolism." J Neural Transm **107**(3): 281-93.

Strauss, K. M., Martins, L. M., Plun-Favreau, H., Marx, F. P., Kautzmann, S., et al. (2005). "Loss of function mutations in the gene encoding Omi/HtrA2 in Parkinson's disease." Hum Mol Genet **14**(15): 2099-111.

Subramanian, A., Tamayo, P., Mootha, V. K., Mukherjee, S., Ebert, B. L., et al. (2005). "Gene set enrichment analysis: a knowledge-based approach for interpreting genome-wide expression profiles." Proc Natl Acad Sci U S A **102**(43): 15545-50.

Sun, C., Cai, M., Gunasekera, A. H., Meadows, R. P., Wang, H., et al. (1999). "NMR structure and mutagenesis of the inhibitor-of-apoptosis protein XIAP." Nature **401**(6755): 818-22.

Sun, C., Cai, M., Meadows, R. P., Xu, N., Gunasekera, A. H., Herrmann, J., Wu, J. C. and Fesik, S. W. (2000). "NMR structure and mutagenesis of the third Bir domain of the inhibitor of apoptosis protein XIAP." J. Biol. Chem. **275**(43): 33777-33781.

Susin, S. A., Lorenzo, H. K., Zamzami, N., Marzo, I., Snow, B. E., et al. (1999). "Molecular characterization of mitochondrial apoptosis-inducing factor." Nature **397**(6718): 441-6.

Susin, S. A., Zamzami, N., Castedo, M., Hirsch, T., Marchetti, P., Macho, A., Daugas, E., Geuskens, M. and Kroemer, G. (1996). "Bcl-2 inhibits the mitochondrial release of an apoptogenic protease." J Exp Med **184**(4): 1331-41.

Suzuki, Y., Demoliere, C., Kitamura, D., Takeshita, H., Deuschle, U. and Watanabe, T. (1997). "HAX-1, a novel intracellular protein, localized on mitochondria, directly associates with HS1, a substrate of Src family tyrosine kinases." J Immunol **158**(6): 2736-44.

Suzuki, Y., Imai, Y., Nakayama, H., Takahashi, K., Takio, K. and Takahashi, R. (2001). "A serine protease, HtrA2, is released from the mitochondria and interacts with XIAP, inducing cell death." Mol Cell **8**(3): 613-21.

Tabrizi, S. J., Orth, M., Wilkinson, J. M., Taanman, J. W., Warner, T. T., Cooper, J. M. and Schapira, A. H. (2000). "Expression of mutant alpha-synuclein causes increased susceptibility to dopamine toxicity." Hum Mol Genet **9**(18): 2683-9.

Takahashi, R., Imai, Y., Hattori, N. and Mizuno, Y. (2003). "Parkin and endoplasmic reticulum stress." Ann N Y Acad Sci **991**: 101-6.

Teismann, P., Tieu, K., Choi, D. K., Wu, D. C., Naini, A., Hunot, S., Vila, M., Jackson-Lewis, V. and Przedborski, S. (2003). "Cyclooxygenase-2 is instrumental in Parkinson's disease neurodegeneration." Proc Natl Acad Sci U S A **100**(9): 5473-8.

Tenev, T., Zachariou, A., Wilson, R., Paul, A. and Meier, P. (2002). "Jafrac2 is an IAP antagonist that promotes cell death by liberating Dronc from DIAP1." Embo J **21**(19): 5118-29.

Tiranti, V., D'Adamo, P., Briem, E., Ferrari, G., Mineri, R., et al. (2004). "Ethylmalonic encephalopathy is caused by mutations in ETHE1, a gene encoding a mitochondrial matrix protein." Am J Hum Genet **74**(2): 239-52.

Tirasophon, W., Welihinda, A. A. and Kaufman, R. J. (1998). "A stress response pathway from the endoplasmic reticulum to the nucleus requires a novel bifunctional protein kinase/endoribonuclease (Ire1p) in mammalian cells." Genes Dev **12**(12): 1812-24.

Tocharus, J., Tsuchiya, A., Kajikawa, M., Ueta, Y., Oka, C. and Kawaichi, M. (2004). "Developmentally regulated expression of mouse HtrA3 and its role as an inhibitor of TGF-beta signaling." Dev Growth Differ **46**(3): 257-74.

Trencia, A., Fiory, F., Maitan, M. A., Vito, P., Barbagallo, A. P., et al. (2004). "Omi/HtrA2 promotes cell death by binding and degrading the anti-apoptotic protein ped/pea-15." J Biol Chem **279**(45): 46566-72.

Ubeda, M. and Habener, J. F. (2003). "CHOP transcription factor phosphorylation by casein kinase 2 inhibits transcriptional activation." J Biol Chem **278**(42): 40514-20.

Ubeda, M., Vallejo, M. and Habener, J. F. (1999). "CHOP enhancement of gene transcription by interactions with Jun/Fos AP-1 complex proteins." Mol Cell Biol **19**(11): 7589-99.

Ubeda, M., Wang, X. Z., Zinszner, H., Wu, I., Habener, J. F. and Ron, D. (1996). "Stress-induced binding of the transcriptional factor CHOP to a novel DNA control element." Mol Cell Biol **16**(4): 1479-89.

Unlu, M., Morgan, M. E. and Minden, J. S. (1997). "Difference gel electrophoresis: a single gel method for detecting changes in protein extracts." Electrophoresis **18**(11): 2071-7.

Unoki, M. and Nakamura, Y. (2001). "Growth-suppressive effects of BPOZ and EGR2, two genes involved in the PTEN signaling pathway." Oncogene **20**(33): 4457-65.

Uren, A. G., Coulson, E. J. and Vaux, D. L. (1998). "Conservation of baculovirus inhibitor of apoptosis repeat proteins (BIRPs) in viruses, nematodes, vertebrates and yeasts." Trends Biochem. Sci. **23**(5): 159-162.

Valente, E. M., Abou-Sleiman, P. M., Caputo, V., Muqit, M. M., Harvey, K., et al. (2004). "Hereditary early-onset Parkinson's disease caused by mutations in PINK1." Science **304**(5674): 1158-60.

Vallejo, M., Ron, D., Miller, C. P. and Habener, J. F. (1993). "C/ATF, a member of the activating transcription factor family of DNA-binding proteins, dimerizes with

CAAT/enhancer-binding proteins and directs their binding to cAMP response elements." Proc Natl Acad Sci U S A **90**(10): 4679-83.

van Gurp, M., Festjens, N., van Loo, G., Saelens, X. and Vandenabeele, P. (2003). "Mitochondrial intermembrane proteins in cell death." Biochem Biophys Res Commun **304**(3): 487-97.

van Loo, G., Saelens, X., van Gurp, M., MacFarlane, M., Martin, S. J. and Vandenabeele, P. (2002). "The role of mitochondrial factors in apoptosis: a Russian roulette with more than one bullet." Cell Death Differ **9**(10): 1031-42.

van Loo, G., van Gurp, M., Depuydt, B., Srinivasula, S. M., Rodriguez, I., et al. (2002). "The serine protease Omi/HtrA2 is released from mitochondria during apoptosis. Omi interacts with caspase-inhibitor XIAP and induces enhanced caspase activity." Cell Death Differ **9**(1): 20-6.

Verhagen, A. M., Ekert, P. G., Pakusch, M., Silke, J., Connolly, L. M., Reid, G. E., Moritz, R. L., Simpson, R. J. and Vaux, D. L. (2000). "Identification of DIABLO, a mammalian protein that promotes apoptosis by binding to and antagonizing IAP proteins." Cell **102**(1): 43-53.

Verhagen, A. M., Kratina, T. K., Hawkins, C. J., Silke, J., Ekert, P. G. and Vaux, D. L. (2007). "Identification of mammalian mitochondrial proteins that interact with IAPs via N-terminal IAP binding motifs." Cell Death Differ **14**(2): 348-57.

Verhagen, A. M., Silke, J., Ekert, P. G., Pakusch, M., Kaufmann, H., et al. (2002). "HtrA2 promotes cell death through its serine protease activity and its ability to antagonize inhibitor of apoptosis proteins." J Biol Chem **277**(1): 445-54.

Vyas, S., Juin, P., Hancock, D., Suzuki, Y., Takahashi, R., Triller, A. and Evan, G. (2004). "Differentiation-dependent sensitivity to apoptogenic factors in PC12 cells." J Biol Chem **279**(30): 30983-93.

Walle, L. V., Damme, P. V., Lamkanfi, M., Saelens, X., Vandekerckhove, J., Gevaert, K. and Vandenabeele, P. (2007). "Proteome-wide Identification of HtrA2/Omi Substrates." J Proteome Res.

Walsh, N. P., Alba, B. M., Bose, B., Gross, C. A. and Sauer, R. T. (2003). "OMP peptide signals initiate the envelope-stress response by activating DegS protease via relief of inhibition mediated by its PDZ domain." Cell **113**(1): 61-71.

Wang, X. Z., Harding, H. P., Zhang, Y., Jolicoeur, E. M., Kuroda, M. and Ron, D. (1998). "Cloning of mammalian Ire1 reveals diversity in the ER stress responses." Embo J **17**(19): 5708-17.

Wang, X. Z., Kuroda, M., Sok, J., Batchvarova, N., Kimmel, R., Chung, P., Zinszner, H. and Ron, D. (1998). "Identification of novel stress-induced genes downstream of chop." Embo J **17**(13): 3619-30.

Wang, X. Z. and Ron, D. (1996). "Stress-induced phosphorylation and activation of the transcription factor CHOP (GADD153) by p38 MAP Kinase." Science **272**(5266): 1347-9.

Weinander, R., Anderson, C. and Morgenstern, R. (1994). "Identification of N-acetylcysteine as a new substrate for rat liver microsomal glutathione transferase. A study of thiol ligands." J Biol Chem **269**(1): 71-6.

Wek, R. C., Jiang, H. Y. and Anthony, T. G. (2006). "Coping with stress: eIF2 kinases and translational control." Biochem Soc Trans **34**(Pt 1): 7-11.

West, A. B., Moore, D. J., Biskup, S., Bugayenko, A., Smith, W. W., Ross, C. A., Dawson, V. L. and Dawson, T. M. (2005). "Parkinson's disease-associated mutations in leucine-rich repeat kinase 2 augment kinase activity." Proc Natl Acad Sci U S A **102**(46): 16842-7.

West, A. B., Zimprich, A., Lockhart, P. J., Farrer, M., Singleton, A., et al. (2001). "Refinement of the PARK3 locus on chromosome 2p13 and the analysis of 14 candidate genes." Eur J Hum

Genet **9**(9): 659-66.

Wilken, C., Kitzing, K., Kurzbauer, R., Ehrmann, M. and Clausen, T. (2004). "Crystal structure of the DegS stress sensor: How a PDZ domain recognizes misfolded protein and activates a protease." Cell **117**(4): 483-94.

Wing, J. P., Karres, J. S., Ogdahl, J. L., Zhou, L., Schwartz, L. M. and Nambu, J. R. (2002). "Drosophila sickle is a novel grim-reaper cell death activator." Curr Biol **12**(2): 131-5.

Wolf, B. B. and Green, D. R. (2002). "Apoptosis: letting slip the dogs of war." Curr. Biol. **12**(5): R177-179.

Wolfgang, C. D., Chen, B. P., Martindale, J. L., Holbrook, N. J. and Hai, T. (1997). "gadd153/Chop10, a potential target gene of the transcriptional repressor ATF3." Mol Cell Biol **17**(11): 6700-7.

Wolfgang, C. D., Liang, G., Okamoto, Y., Allen, A. E. and Hai, T. (2000). "Transcriptional autorepression of the stress-inducible gene ATF3." J Biol Chem **275**(22): 16865-70.

Woods, D., Parry, D., Cherwinski, H., Bosch, E., Lees, E. and McMahon, M. (1997). "Raf-induced proliferation or cell cycle arrest is determined by the level of Raf activity with arrest mediated by p21Cip1." Mol Cell Biol **17**(9): 5598-611.

Wu, Y., Blum, D., Nissou, M. F., Benabid, A. L. and Verna, J. M. (1996). "Unlike MPP+, apoptosis induced by 6-OHDA in PC12 cells is independent of mitochondrial inhibition." Neurosci Lett **221**(1): 69-71.

Xia, X. G., Harding, T., Weller, M., Bieneman, A., Uney, J. B. and Schulz, J. B. (2001). "Gene transfer of the JNK interacting protein-1 protects dopaminergic neurons in the MPTP model of Parkinson's disease." Proc Natl Acad Sci U S A **98**(18): 10433-8.

Yang, Q. H., Church-Hajduk, R., Ren, J., Newton, M. L. and Du, C. (2003). "Omi/HtrA2 catalytic cleavage of inhibitor of apoptosis (IAP) irreversibly inactivates IAPs and facilitates caspase activity in apoptosis." Genes Dev **17**(12): 1487-96.

Yang, Y., Fang, S., Jensen, J. P., Weissman, A. M. and Ashwell, J. D. (2000). "Ubiquitin protein ligase activity of IAPs and their degradation in proteasomes in response to apoptotic stimuli." Science **288**(5467): 874-7.

Yang, Y., Gehrke, S., Imai, Y., Huang, Z., Ouyang, Y., et al. (2006). "Mitochondrial pathology and muscle and dopaminergic neuron degeneration caused by inactivation of Drosophila Pink1 is rescued by Parkin." Proc Natl Acad Sci U S A **103**(28): 10793-8.

Yang, Z., Camp, N. J., Sun, H., Tong, Z., Gibbs, D., et al. (2006). "A variant of the HTRA1 gene increases susceptibility to age-related macular degeneration." Science **314**(5801): 992-3.

Ye, J., Rawson, R. B., Komuro, R., Chen, X., Dave, U. P., Prywes, R., Brown, M. S. and Goldstein, J. L. (2000). "ER stress induces cleavage of membrane-bound ATF6 by the same proteases that process SREBPs." Mol Cell **6**(6): 1355-64.

Yoshida, H., Haze, K., Yanagi, H., Yura, T. and Mori, K. (1998). "Identification of the cis-acting endoplasmic reticulum stress response element responsible for transcriptional induction of mammalian glucose-regulated proteins. Involvement of basic leucine zipper transcription factors." J Biol Chem **273**(50): 33741-9.

Yoshida, H., Matsui, T., Hosokawa, N., Kaufman, R. J., Nagata, K. and Mori, K. (2003). "A time-dependent phase shift in the mammalian unfolded protein response." Dev Cell **4**(2): 265-71.

Yoshida, H., Okada, T., Haze, K., Yanagi, H., Yura, T., Negishi, M. and Mori, K. (2000). "ATF6 activated by proteolysis binds in the presence of NF-Y (CBF) directly to the cis-acting element responsible for the mammalian unfolded protein response." Mol Cell Biol **20**(18): 6755-67.

Young, J. C. and Hartl, F. U. (2003). "A stress sensor for the bacterial periplasm." Cell **113**(1): 1-2.

Yuan, J., Shaham, S., Ledoux, S., Ellis, H. M. and Horvitz, H. R. (1993). "The C. elegans cell death gene ced-3 encodes a protein similar to mammalian interleukin-1 beta-converting enzyme." Cell **75**(4): 641-52.

Zhang, L., Shimoji, M., Thomas, B., Moore, D. J., Yu, S. W., et al. (2005). "Mitochondrial localization of the Parkinson's disease related protein DJ-1: implications for pathogenesis." Hum Mol Genet **14**(14): 2063-73.

Zhao, Q., Wang, J., Levichkin, I. V., Stasinopoulos, S., Ryan, M. T. and Hoogenraad, N. J. (2002). "A mitochondrial specific stress response in mammalian cells." Embo J **21**(17): 4411-9.

Zhaung, Z. P. and McCauley, R. (1989). "Ubiquitin is involved in the in vitro insertion of monoamine oxidase B into mitochondrial outer membranes." J Biol Chem **264**(25): 14594-6.

Zimprich, A., Biskup, S., Leitner, P., Lichtner, P., Farrer, M., et al. (2004). "Mutations in LRRK2 cause autosomal-dominant parkinsonism with pleomorphic pathology." Neuron **44**(4): 601-7.

Zinszner, H., Kuroda, M., Wang, X., Batchvarova, N., Lightfoot, R. T., Remotti, H., Stevens, J. L. and Ron, D. (1998). "CHOP is implicated in programmed cell death in response to impaired function of the endoplasmic reticulum." Genes Dev **12**(7): 982-95.

Publications

MOLECULAR AND CELLULAR BIOLOGY, Nov. 2004, p. 9848–9862 Vol. 24, No. 22
0270-7306/04/$08.00+0 DOI: 10.1128/MCB.24.22.9848–9862.2004

Neuroprotective Role of the Reaper-Related Serine Protease HtrA2/Omi Revealed by Targeted Deletion in Mice

L. Miguel Martins,[1,2] Alastair Morrison,[3] Kristina Klupsch,[1] Valentina Fedele,[2] Nicoleta Moisoi,[2] Peter Teismann,[4] Alejandro Abuin,[3] Evelyn Grau,[3] Martin Geppert,[3] George P. Livi,[5] Caretha L. Creasy,[5] Alison Martin,[1] Iain Hargreaves,[6] Simon J. Heales,[6] Hitoshi Okada,[7] Sebastian Brandner,[8] Jörg B. Schulz,[4] Tak Mak,[7] and Julian Downward[1]*

Cell Death and Differentiation (2006), 1–3

www.nature.com/cdd

Letter to the Editor

The protease inhibitor Ucf-101 induces cellular responses independently of its known target, HtrA2/Omi

Cell Death and Differentiation advance online publication, 12 May 2006; doi:10.1038/sj.cdd.4401955